

BIOLITHOGRAPHY:
SELECTIVE JOINING USING ANTIBODY-ANTIGEN REACTIONS

by

Gail Marilyn Thornton

Bachelor of Science in Mechanical Engineering with Distinction
University of Alberta; Edmonton, Alberta, Canada
1993

Submitted to the Department of Mechanical Engineering
in Partial Fulfillment of the Requirements
for the Degree of


MASTER OF SCIENCE
in Mechanical Engineering

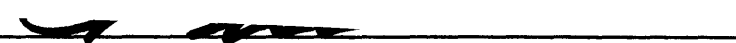
at the

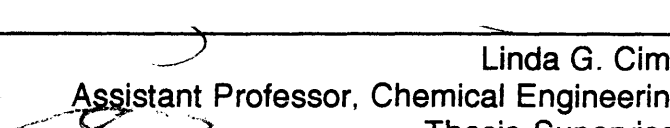
Massachusetts Institute of Technology


June 1995

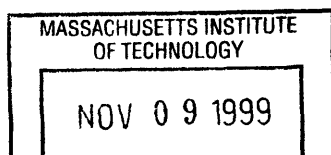
© 1995 Massachusetts Institute of Technology, All rights reserved.

Signature of author 
Department of Mechanical Engineering
May 23, 1995

Certified by 
Emanuel M. Sachs
Associate Professor, Mechanical Engineering
Thesis Supervisor

Certified by 
Linda G. Cima
Assistant Professor, Chemical Engineering
Thesis Supervisor

Accepted by 
Ain A. Sonin
Chairman, Graduate Committee



ENG

Barker Eng

**BIOLITHOGRAPHY:
SELECTIVE JOINING USING ANTIBODY-ANTIGEN REACTIONS**

by

GAIL MARILYN THORNTON

Submitted to the Department of Mechanical Engineering
on May 23, 1995 in Partial Fulfillment of the
Requirements for the Degree of
Master of Science in Mechanical Engineering

ABSTRACT

Biolithography is a contribution to the field of Solid Free Form Fabrication. Part production is based on selective joining using antibody-antigen reactions, where the selectivity is based on the thermal sensitivity of such proteins.

Antibodies and antigens can be chemically immobilized to a variety of substrate materials: polymeric, ceramic and metallic. In the present investigation, antibody coated 1 μ m polystyrene beads and antigen coated glass surface substrates, as well as, antigen solutions were used. Both antibodies and antigens were multivalent i.e. have more than one binding site for each other; thus, two antibody coated beads could be held together by one antigen.

Selective deposition was demonstrated by thermally deactivating antigen coated onto glass and precipitating antibody coated beads. Bead deposition was selective to the regions of remaining active antigens; thus, revealing the defined deactivated region. Thermal deactivation of the antigen coated substrate was first demonstrated with a 90°C water jet and improved using an argon ion laser which produced line widths on the order of tens of microns.

Selective definition of geometry was an extension of the coating process precipitating not one but two bead layers and linking beads using antigen in solution. The thermal deactivation mechanism was a modified 90°C water jet that had line width resolution on the order of millimeters. Line definition was on both antigen coated bases and bound bead bases; thus, thermal deactivation was effective on both immobilized antigen (glass) and antibody (bead).

The selective deposition of antibody coated substrate was demonstrated by thermally deactivating immobilized antigens and antibodies on surface substrates. Definition resolution was dependent on the thermal deactivation mechanism used.

Thesis supervisors : Emanuel M. Sachs
Associate Professor, Mechanical Engineering
Linda G. Cima
Assistant Professor, Chemical Engineering

DEDICATION

To my family

ACKNOWLEDGMENTS

I gratefully acknowledge the support of the National Science Foundation.

I would also thank to the many people involved in making this achievement a reality.

Ely Sachs, without your vision and risk-taking my research and education at MIT would not have been possible.

Linda Cima, for your biology and chemistry expertise and excellent guidance.

Che-Chih Tsao, for being a great resource and teacher.

Doug Lauffenburger and Suzanne Kuo, for the valued information and advice.

The members of the Three Dimensional Printing Lab:

Earl Sun, for your support and friendship.

Ed Wylonis, Christopher Shutts, Steve Michaels and Steve (Hon) Tang, for the great times spent together both in and out of the lab.

Tara Arthur, my fellow Albertan, for reminding me of home and how far we have come.

Dave Brancazio, Jim Serdy, Alain Curodeau, John Lee, Jain Charnnarong, Mike Rynerson, and Tailin Fan, for the help along the way.

The members of the Cima Lab:

Ann Park, Stephanie Lopina, Mark Powers, Philip Kuhl, Jeff Sperinde and Sue Hobbs, for all your help.

MIT support staff:

Fred Cote, Laboratory for Manufacturing and Productivity Machine Shop.
Lenny, Building 12 Scanning Electron Microscope.
Zonda, Shelley, Geoff and Kamla, Professor Sachs' Administrative Assistants.

TABLE OF CONTENTS

<u>SECTION</u>	<u>PAGE</u>
1. INTRODUCTION.....	21
1.1 MOTIVATION.....	21
1.2 CONCEPT	23
1.2.1 Agglutination Reaction.....	23
1.2.2 Thermal Deactivation.....	26
1.2.3 Coupling to Substrates.....	26
1.2.4 Two-dimensional (2D) Coating Process	26
1.2.5 Three-dimensional (3D) Layering Process.....	30
1.3 METHODOLOGY.....	33
1.3.1 Agglomeration Reaction.....	33
1.3.2 Elimination of Agglomeration Reaction	33
1.3.3 2D Coating Process	33
1.3.4 Selective Deposition.....	35
1.3.5 3D Layering Process.....	35
1.3.6 Selective Definition of Geometry	35
2. PROCESS COMPONENTS.....	37
2.1 ANTIBODIES AND ANTIGENS	37
2.1.1 Rabbit Immunoglobulin G (R-IgG).....	37
2.1.2 Goat Anti-Rabbit Immunoglobulin G (GAR-IgG).....	40
2.1.3 Protein A (SpA)	40
2.2 SUBSTRATES.....	41
2.2.1 Polystyrene Beads.....	41
2.2.1.1 Polybead® Polystyrene Microspheres.....	41
2.2.1.2 Goat Anti-Rabbit Immunoglobulin G (GAR-IgG) Beads...41	
2.2.1.3 Protein A (SpA) Carboxylate Beads	43
2.2.2 Rabbit Immunoglobulin G (R-IgG) Soda Lime Glass	45
2.3 BINDING PROPERTIES.....	53
2.3.1 Binding Affinity.....	53
2.3.2 Adhesion Strength.....	54
2.4 DEACTIVATION MECHANISMS.....	55

<u>SECTION</u>	<u>PAGE</u>
3. PROCESS DEVELOPMENT	57
3.1 AGGLOMERATION REACTION	57
3.2 ELIMINATION OF AGGLOMERATION REACTION	65
3.3 2D COATING PROCESS.....	77
3.3.1 Coating Protocol	77
3.3.1.1 Containment.....	78
3.3.1.2 Bead Volume.....	78
3.3.1.3 Washing.....	79
3.3.1.4 Protocol Optimization.....	80
3.3.1.5 Protocol	81
3.3.2 Control Deposition Standard.....	82
3.4 SELECTIVE DEPOSITION.....	93
3.4.1 Immersion.....	93
3.4.2 Continuous Hot (90°C) Water Jet	93
3.4.2.1 Apparatus.....	93
3.4.2.2 Experimental Procedure	94
3.4.2.3 Results.....	99
3.4.3 Argon Ion Laser.....	99
3.4.3.1 Apparatus.....	99
3.4.3.2 Experimental Procedure	106
3.4.3.3 Results.....	107
3.5 3D LAYERING PROCESS.....	117
3.5.1 Goat Anti-Rabbit Immunoglobulin G (GAR-IgG) Second Layer .	117
3.5.2 Protein A (SpA) Second Layer.....	120
3.6 SELECTIVE DEFINITION OF GEOMETRY.....	143
3.6.1 Soldering Iron Hot (90°C) Water Jet	143
3.6.2 Selective Definition in 3D.....	146
3.6.2.1 Predeactivated Base.....	146
3.6.2.2 Bound Bead Base	162
3.7 PROCESS ISSUES	203
3.7.1 Bulk Strength.....	203
3.7.2 Deposition Uniformity.....	205
3.7.3 Production Costs.....	205

<u>SECTION</u>	<u>PAGE</u>
4. CONCLUSIONS (EXECUTIVE SUMMARY).....	207
5. REFERENCES.....	211
APPENDIX A.....	213
APPENDIX B.....	227
APPENDIX C.....	237
APPENDIX D.....	239
APPENDIX E.....	243

LIST OF FIGURES

<u>FIGURE</u>	<u>PAGE</u>
1. BLOOD ANTIBODIES AND ANTIGENS.....	24
2. AGGLUTINATION OF RBC	25
3. THERMAL DEACTIVATION AND SHAPE CHANGE.....	27
4. DELINEATION OF SUBSTRATE COATING.....	28
5. 2D COATING PROCESS - CONCEPTUAL SCHEMATIC.....	29
6. 3D LAYERING PART CONSTRUCTION - CONCEPTUAL SCHEMATIC	31
7. BIOLITHOGRAPHY CRITICAL PATH CHART.....	34
8. TWO DIMENSIONAL SCHEMATIC OF IgG.....	38
9. DIMENSIONAL MODEL OF IgG	38
10. COUPLING PROCEDURE FOR GAR-IgG BEADS.....	42
11. COUPLING PROCEDURE SpA BEADS.....	44
12. COUPLING PROCEDURE FOR R-IgG GLASS	47
13. R-IgG CONTROL IN PBS WITH BSA; 400x.....	49
14. R-IgG CONTROL IN PBS; 400x.....	49
15. ELECTROMAGNETIC RADIATION INTERACTION MECHANISMS	56
16. GAR-IgG BEADS + R-IgG <u>1:2</u> (50µl); 100x.....	59
17. GAR-IgG BEADS + R-IgG <u>1:1</u> (50µl); 100x.....	59
18. GAR-IgG BEADS + R-IgG <u>1:0.5</u> (50µl); 100x.....	61
19. GAR-IgG BEADS + R-IgG <u>1:0.1</u> (50µl); 100x.....	61
20. GAR-IgG BEADS + R-IgG <u>1:0.05</u> (94µl); 100x	63
21. GAR-IgG BEADS NO R-IgG (25µl); 100x.....	67
BEAD HEAT TREATMENT 83°C FOR 5 MIN.	
22. GAR-IgG BEADS + R-IgG <u>1:0.1</u> (50µl); 100x.....	67
BEAD HEAT TREATMENT 83°C FOR 5 MIN.	
23. GAR-IgG BEADS + R-IgG <u>1:0.1</u> (50µl); 40x.....	71
CONTROL FOR PARTIAL HEAT TREATMENT	
24. GAR-IgG BEADS + R-IgG <u>1:0.1</u> (50µl); 100x.....	71
CONTROL FOR PARTIAL HEAT TREATMENT	
25. GAR-IgG BEADS + R-IgG <u>1:0.1</u> (50µl); 40x.....	73
HALF BEAD VOLUME HEAT TREATMENT 83°C FOR 5 MIN.	
26. GAR-IgG BEADS + R-IgG <u>1:0.1</u> (50µl); 100x.....	73
HALF BEAD VOLUME HEAT TREATMENT 83°C FOR 5 MIN.	
27. GAR-IgG BEADS + R-IgG <u>1:0.1</u> (50µl); 40x.....	75
HALF BEAD VOLUME HEAT TREATMENT 83°C FOR 10 MIN.	
28. GAR-IgG BEADS + R-IgG <u>1:0.1</u> (50µl); 100x.....	75
HALF BEAD VOLUME HEAT TREATMENT 83°C FOR 10 MIN.	
29. R-IgG CONTROL; 400x	83
30. GLASS CONTROL; 400x.....	83

<u>FIGURE</u>	<u>PAGE</u>
31. PASSIVATED Polybeads® + UNCOATED GLASS; 400x.....	87
32. PASSIVATED Polybeads® + R-IgG GLASS; 400x.....	87
33. GAR-IgG BEADS + UNCOATED GLASS; 400x.....	89
34. GAR-IgG BEADS + R-IgG GLASS; 400x.....	89
35. R-IgG CONTROL; 400x.....	91
SURFACE CONCENTRATION 17 μ g/cm ²	
36. R-IgG CONTROL; 400x.....	91
SURFACE CONCENTRATION 0.44 μ g/cm ²	
37. IMMERSION IN 98°C WATER INTERFACE; 20x.....	95
EXPOSURE TIME 30 SEC.	
38. IMMERSION IN 98°C WATER INTERFACE; 400x.....	95
EXPOSURE TIME 30 SEC.	
39. CONTINUOUS WATER JET R-IgG CONTROL; 400x.....	97
40. CONTINUOUS WATER JET AT 23°C AND 0.51m/s; 400x.....	97
EXPOSURE TIME 1 MIN.	
41. CONTINUOUS 90°C WATER JET - EXPERIMENTAL SCHEMATIC.....	100
42. CONTINUOUS 90°C WATER JET DEPOSITION INTERFACE; 20x.....	101
EXPOSURE TIME 1 MIN.	
43. CONTINUOUS 90°C WATER JET DEPOSITION INTERFACE; 400x.....	101
EXPOSURE TIME 1 MIN.	
44. CONTINUOUS 90°C WATER JET DEACTIVATED REGION; 400x.....	103
EXPOSURE TIME 1 MIN.	
45. CONTINUOUS 90°C WATER JET ACTIVE REGION; 400x.....	103
EXPOSURE TIME 1 MIN.	
46. LASER SCHEMATIC.....	105
47. 1.0W AT 3 cm/s; 200x - LINE WIDTH = 110 \pm 5 μ m.....	109
48. 1.9W AT 3 cm/s; 200x - LINE WIDTH = 97 \pm 5 μ m.....	109
49. 1.0W AT 25 cm/s; 200x - LINE WIDTH = 22 \pm 5 μ m.....	111
50. 1.0W AT 25 cm/s; 800x - LINE WIDTH = 19 \pm 1 μ m.....	111
51. 1.9W AT 25 cm/s; 200x - LINE WIDTH = 38 \pm 5 μ m.....	113
52. 1.9W AT 25 cm/s; 800x - LINE WIDTH = 34 \pm 1 μ m.....	113
53. GAR-IgG + GAR-IgG TWO LAYER PART CONSTRUCTION.....	118
54. STEP 2 ADDITION OF R-IgG - FIRST LAYER; 400x.....	121
55. STEP 2 ADDITION OF R-IgG - SECOND LAYER; 400x.....	121
56. STEP 3 ADDITION OF R-IgG - FIRST LAYER; 400x.....	123
57. STEP 3 ADDITION OF R-IgG - SECOND LAYER; 400x.....	123
58. GAR-IgG + SpA TWO LAYER PART CONSTRUCTION.....	125
59. SpA FIRST LAYER; 400x.....	129
60. GAR-IgG SECOND LAYER ON SpA FIRST LAYER; 400x.....	129
61. SpA FIRST LAYER; 200x.....	131

<u>FIGURE</u>	<u>PAGE</u>
62. SpA FIRST LAYER; 200x FLUORESCENCE	131
63. GAR-IgG SECOND LAYER ON SpA FIRST LAYER; 200x.....	133
64. GAR-IgG SECOND LAYER ON SpA FIRST LAYER; 200x.....	133
FLUORESCENCE	
65. GAR-IgG FIRST LAYER; 200x.....	135
66. GAR-IgG FIRST LAYER;200x FLUORESCENCE	135
67. SpA SECOND LAYER ON GAR-IgG FIRST LAYER; 200x.....	137
68. SpA SECOND LAYER ON GAR-IgG FIRST LAYER; 200x.....	137
FLUORESCENCE	
69. GAR-IgG FIRST LAYER; 400x.....	139
70. SpA SECOND LAYER ON GAR-IgG FIRST LAYER; 400x.....	141
71. SpA SECOND LAYER ON GAR-IgG FIRST LAYER; 400x.....	141
FLUORESCENCE	
72. SOLDERING IRON 90°C WATER JET	144
EXPERIMENTAL SCHEMATIC	
73. SOLDERING IRON WATER JET AT 23°C; 400x	147
FLOW VELOCITY 0.13m/s AND TRAVERSE SPEED 0.17mm/s	
74. SOLDERING IRON WATER JET AT 48°C; 400x	147
FLOW VELOCITY 0.24m/s AND TRAVERSE SPEED 0.33mm/s	
75. SELECTIVE DEFINITION OF GEOMETRY.....	149
3D PART REFERENCE MARKS	
76. SI JET AT 0.17mm/s; 20x - LINE WIDTH = 1.5mm.....	149
77. SI JET AT 0.17mm/s; 400x	151
DEACTIVATED REGION GAR-IgG FIRST LAYER	
78. SI JET AT 0.17mm/s; 400x	151
ACTIVE REGION GAR-IgG FIRST LAYER	
79. SI JET AT 0.33mm/s; 20x - LINE WIDTH = 1.5mm.....	153
80. SI JET AT 0.33mm/s; 400x	155
DEACTIVATED REGION GAR-IgG FIRST LAYER	
81. SI JET AT 0.33mm/s; 400x	155
ACTIVE REGION GAR-IgG FIRST LAYER	
82. SELECTIVE DEFINITION OF GEOMETRY.....	157
PREDEACTIVATED BASE	
83. PREDEACTIVATED BASE; 400x.....	159
DEACTIVATED REGION GAR-IgG FIRST LAYER	
AFTER SECOND PASS OF SI JET AT 0.33mm/s	
84. PREDEACTIVATED BASE; 400x.....	159
ACTIVE REGION GAR-IgG FIRST LAYER	
AFTER SECOND PASS OF SI JET AT 0.33mm/s	
85. PREDEACTIVATED BASE; SI JET AT 0.17mm/s; 20x.....	163
AFTER SpA SECOND LAYER - LINE WIDTH = 1.5mm	

<u>FIGURE</u>	<u>PAGE</u>
86. PREDEACTIVATED BASE; SI JET AT 0.17mm/s AFTER SpA SECOND LAYER - LINE WIDTH = 1.5mm & 7.3mm FLUORESCENCE	165
87. PREDEACTIVATED BASE; SI JET AT 0.17mm/s; 400x DEACTIVATED REGION AFTER SpA SECOND LAYER	167
88. PREDEACTIVATED BASE; SI JET AT 0.17mm/s; 400x DEACTIVATED REGION AFTER SpA SECOND LAYER FLUORESCENCE	167
89. PREDEACTIVATED BASE; SI JET AT 0.17mm/s; 400x ACTIVE REGION AFTER SpA SECOND LAYER	169
90. PREDEACTIVATED BASE; SI JET AT 0.17mm/s; 400x ACTIVE REGION AFTER SpA SECOND LAYER FLUORESCENCE	169
91. PREDEACTIVATED BASE; SI JET AT 0.33mm/s AFTER SpA SECOND LAYER - LINE WIDTH = 1.5mm	171
92. PREDEACTIVATED BASE; SI JET AT 0.33mm/s AFTER SpA SECOND LAYER - LINE WIDTHS = 1.5mm & 5.3mm FLUORESCENCE	173
93. PREDEACTIVATED BASE; SI JET AT 0.33mm/s; 400x DEACTIVATED REGION AFTER SpA SECOND LAYER	175
94. PREDEACTIVATED BASE; SI JET AT 0.33mm/s; 400x DEACTIVATED REGION AFTER SpA SECOND LAYER FLUORESCENCE	175
95. PREDEACTIVATED BASE; SI JET AT 0.33mm/s; 400x ACTIVE REGION AFTER SpA SECOND LAYER	177
96. PREDEACTIVATED BASE; SI JET AT 0.33mm/s; 400x ACTIVE REGION AFTER SpA SECOND LAYER FLUORESCENCE	177
97. SELECTIVE DEFINITION OF GEOMETRY..... BOUND BEAD BASE	179
98. BOUND BEAD BASE; SI JET AT 0.33mm/s..... AFTER SpA SECOND LAYER - LINE WIDTH = 10.6mm FLUORESCENCE	181
99. BOUND BEAD BASE; SI JET AT 0.17mm/s..... AFTER SpA SECOND LAYER - LINE WIDTH = 3.8mm - 7.6mm FLUORESCENCE	183
100. BOUND BEAD BASE; SI JET AT 0.067mm/s; 20x AFTER SpA SECOND LAYER - LINE WIDTH = 4.3 - 5.5mm FLUORESCENCE	185
101. BOUND BEAD BASE; 400x..... DEACTIVATED REGION GAR-IgG FIRST LAYER	189
102. BOUND BEAD BASE; 400x..... ACTIVE REGION GAR-IgG FIRST LAYER	189
103. BOUND BEAD BASE; 400x..... DEACTIVATED REGION GAR-IgG FIRST LAYER AFTER PASS OF SI JET AT 0.067mm/s	191

<u>FIGURE</u>	<u>PAGE</u>
104. BOUND BEAD BASE; 400x.....	191
ACTIVE REGION GAR-IgG FIRST LAYER	
AFTER PASS OF SI JET AT 0.067mm/s	
105. BOUND BEAD BASE; SI JET AT 0.067mm/s; 400x.....	193
DEACTIVATED REGION AFTER SpA SECOND LAYER	
106. BOUND BEAD BASE; SI JET AT 0.067mm/s; 400x.....	193
DEACTIVATED REGION AFTER SpA SECOND LAYER	
FLUORESCENCE	
107. BOUND BEAD BASE; SI JET AT 0.067mm/s; 400x.....	195
ACTIVE REGION AFTER SpA SECOND LAYER	
108. BOUND BEAD BASE; SI JET AT 0.067mm/s; 400x.....	195
ACTIVE REGION AFTER SpA SECOND LAYER FLUORESCENCE	
109. BOUND BEAD BASE; 400x.....	197
DEACTIVATED REGION GAR-IgG FIRST LAYER	
110. BOUND BEAD BASE; 400x.....	197
ACTIVE REGION GAR-IgG FIRST LAYER	
111. BOUND BEAD BASE; SI JET AT 0.33mm/s; 400x.....	199
DEACTIVATED REGION AFTER SpA SECOND LAYER	
112. BOUND BEAD BASE; SI JET AT 0.33mm/s; 400x.....	199
DEACTIVATED REGION AFTER SpA SECOND LAYER	
FLUORESCENCE	
113. BOUND BEAD BASE; SI JET AT 0.33mm/s; 400x.....	201
ACTIVE REGION AFTER SpA SECOND LAYER	
114. BOUND BEAD BASE; SI JET AT 0.33mm/s; 400x.....	201
ACTIVE REGION AFTER SpA SECOND LAYER FLUORESCENCE	
115. 10 μ m GLASS + 1 μ m POLYSTYRENE BEAD COMPOSITE.....	204

LIST OF TABLES

<u>TABLE</u>	<u>PAGE</u>
1. AGGLOMERATION PARAMETERS	57
2. THERMAL DEACTIVATION PARAMETERS (GAR-IgG + SpA).....	65
3. THERMAL DEACTIVATION PARAMETERS (GAR-IgG + R-IgG)	66
4. PARTIAL THERMAL DEACTIVATION PARAMETERS	69
5. BEAD VOLUMES FOR SURFACE AREA COVERAGE	78
6. LASER TEST SUMMARY	107
7. TWO LAYER GAR-IgG CONSTRUCTION OPTIONS	119
8. TWO LAYER GAR-IgG + SpA CONSTRUCTION OPTIONS.....	127
9. SELECTIVE DEFINITION LINE WIDTHS.....	162

1. INTRODUCTION

The Biolithography process is based on selective joining using antibody-antigen reactions. Motivation comes from other processes that are based on selective definition of part geometries. The Biolithography concept is described providing background on the antigen-antibody reaction and discussing how the reaction can be made selective through the use of thermal deactivation. Finally, the methodology used to develop and demonstrate the process is explained.

1.1 MOTIVATION

The Biolithography process is a contribution to the field of Solid Free Form Fabrication. Most of these processes build parts up layer by layer where layer geometry is selectively defined. The mechanism of selective definition is the fundamental feature of the process.

For large part production, the Three Dimensional Printing process uses ink jet printing of a binder into a powder layer to selectively define layer geometry and selectively join layers together. Selective Laser Sintering uses a laser to locally sinter areas of loosely compacted powder. For micron scale production, Stereolithography uses a laser to selectively solidify a photosensitive polymer. Photo-Electroforming selectively defines conductive regions in non conductive powder using a photometallization process, laser induced electroless plating.¹

Biolithography is a similar process that selectively defines regions of deposition based on the thermal sensitivity of proteins. Lithography, from which Biolithography gets its name, selectively exposes a photoresist material that has been deposited on a silicon wafer based on a pattern defined by ultraviolet radiation through a photomask. Etching of the silicon wafer in the exposed region reveals the pattern.² The basic form of Biolithography selectively deposits antibody coated beads onto an antigen coated glass substrate based on a pattern defined by thermally deactivating the immobilized antigens. The selective joining of the antibody beads to the remaining active antigens reveals

the pattern. As well, a multivalent antigen, that is, an antigen with more than one binding site for the antibody, can link together particle substrates coated with antibody. The geometry of the resulting substrate structure is defined by selectively deactivating specific antibodies and making them unable to be linked by the antigen; thus, part geometry is defined by substrate regions not subjected to thermal deactivation.

The benefits of the Biolithography process are material flexibility and potential for micron scale resolution. Attachment chemistries are available to immobilize proteins to polymeric, ceramic, and metallic substrates. The system resolution is determined by the substrate size and resolution of the thermal deactivation mechanism because the protein size is on the order of nanometers. The particle substrates can be micron and even submicron sized. The thermal deactivation mechanism providing micron scale resolution is a laser beam that can be attenuated to a micron scale spot size.

1.2 CONCEPT

The following section is provided to give background on biospecific interactions, specifically, antibody-antigen reactions. Thermal deactivation and chemical immobilization of proteins are discussed and specifically related to two dimensional and three dimensional part production processes.

1.2.1 Agglutination Reaction

The agglutination of red blood cells (RBCs) is a naturally occurring phenomenon using antigens and antibodies to create a three dimensional structure on a micron scale. Blood is typed based on the antigens expressed on the surface of RBCs.³ If the RBC has either A or B antigens, the blood is typed A or B, respectively. If the RBC has both A and B antigens, the blood is typed AB. If the RBC has neither A nor B antigens, the blood is typed O. When an antigen, for example antigen A, is not expressed on the RBC, an antibody known as anti-A develops in the plasma in response to exposure to antigen A any time after birth, Figure 1. Antibodies are multivalent, that is, have more than one binding site of their respective antigens; for example, Immunoglobulin G (IgG) has two binding sites. If blood is mismatched in a transfusion, that is, if donor type A blood (RBCs with A antigens and plasma with anti-B antibodies) is mixed with recipient type B blood (RBCs with B antigens and plasma with anti-A antibodies), the donor RBCs will be agglutinated by the recipients antibodies. Because antibodies are multivalent, a single antibody can join together two RBCs at once causing the RBCs to clump together, as seen in Figure 2.

The antibody-antigen interaction is just one example of the many types of biological interactions which can cause agglutination. Antigens may be proteins, carbohydrates or lipids and often comprise a small region of a much larger molecule. An example to illustrate the diversity of the interaction is avidin-biotin. Avidin is a protein that has four binding sites for the vitamin, biotin. In the present investigation, IgG antibodies raised by immunization of a host animal with a donor animal's IgG (antigen) were used to provoke the antibody-antigen reaction.

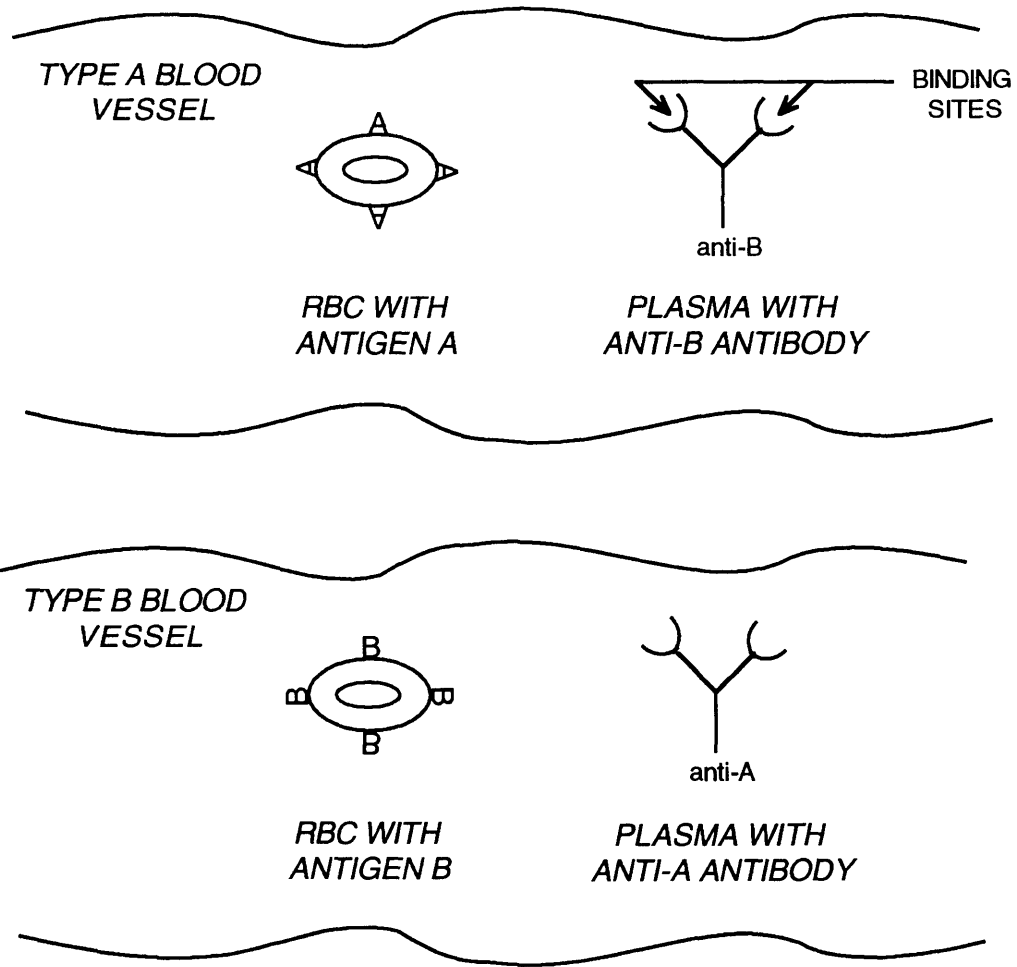
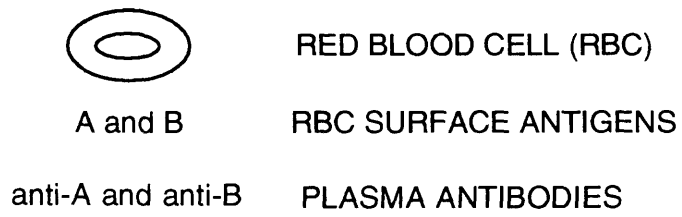
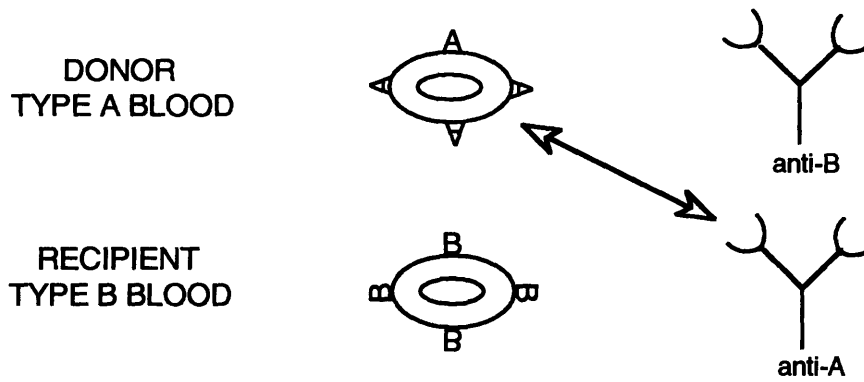
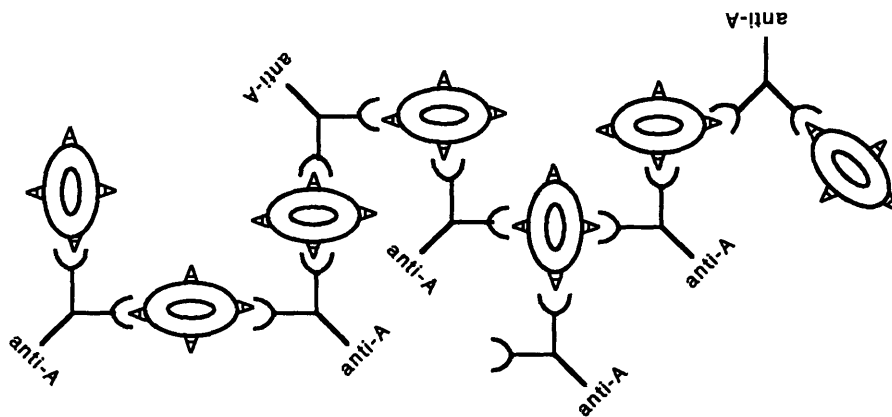


FIGURE 1 : BLOOD ANTIBODIES AND ANTIGENS

BLOOD IS MISMATCHED IN A TRANSFUSION



AGGLUTINATION OF DONOR RBC



The recipients anti-A antibodies bind to the donors antigen A coated RBC

The agglutinated complex is formed because the antibody is bivalent i.e. has two binding sites

FIGURE 2 : AGGLUTINATION OF RBC

Modified from Voet D. and Voet J.G. (1990). Biochemistry. Wiley, New York. pp. 1101.

1.2.2 Thermal Deactivation

The shape of the agglutinated structure would be altered if the antigens on a specific RBC could not bind with the antibodies. Denaturation of the antibody or antigen is a possible method of preventing antibody and antigen binding. Most proteins are denatured in the presence of high temperatures (greater than 50°C); thus, an increase in the local temperature would denature the antigen. Figure 3 shows how the shape of the agglutinated structure changed when the surface antigen A of two of the RBCs were thermally deactivated.

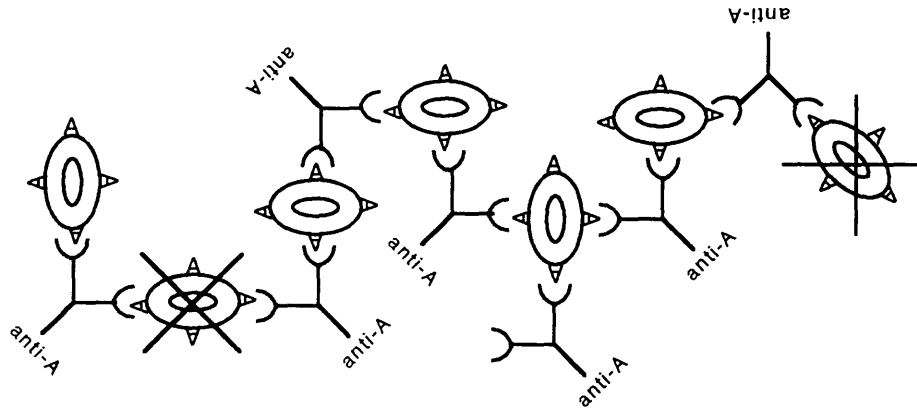
1.2.3 Coupling to Substrates

Antibodies and antigens may be attached to a variety of substrate materials. Different attachment chemistries can be performed to immobilize these proteins onto polymeric, ceramic and metallic substrates. The substrate can vary from flat substrates with size of the order of a microscope slide (microslide) to particle substrates with size of the order of microns. Figure 4 delineates substrate coating from naturally occurring blood antigens and antibodies to the chemical immobilization of proteins onto substrates.

1.2.4 Two-dimensional (2D) Coating Process

Figure 5 shows the 2D concept referring to the immobilized proteins shown in Figure 4. The antigen is coupled to the surface substrate; for example, a glass microslide, and the antibody is coupled to a particle substrate; for example, a 1 μ m diameter polystyrene bead. The antigen coated on the slide is selectively denatured to permit the selective deposition of the antibody coated substrate. A potential mechanism for thermal deactivation is to use a laser to locally heat the substrate and subsequently deactivate the antigen. Because multiple proteins are coupled to both substrates, either monovalent or multivalent antibodies and antigens may be used.

BY SOME THERMAL MECHANISM, SELECTED ANTIGEN A ARE DEACTIVATED AND CANNOT BIND



THE OVERALL SHAPE OF THE AGGLUTINATED STRUCTURE CHANGES

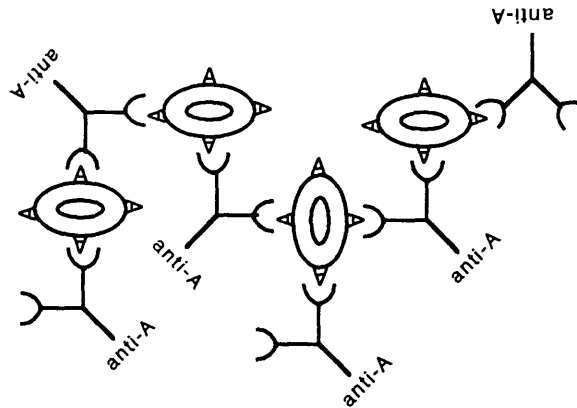


FIGURE 3: THERMAL DEACTIVATION AND SHAPE CHANGE

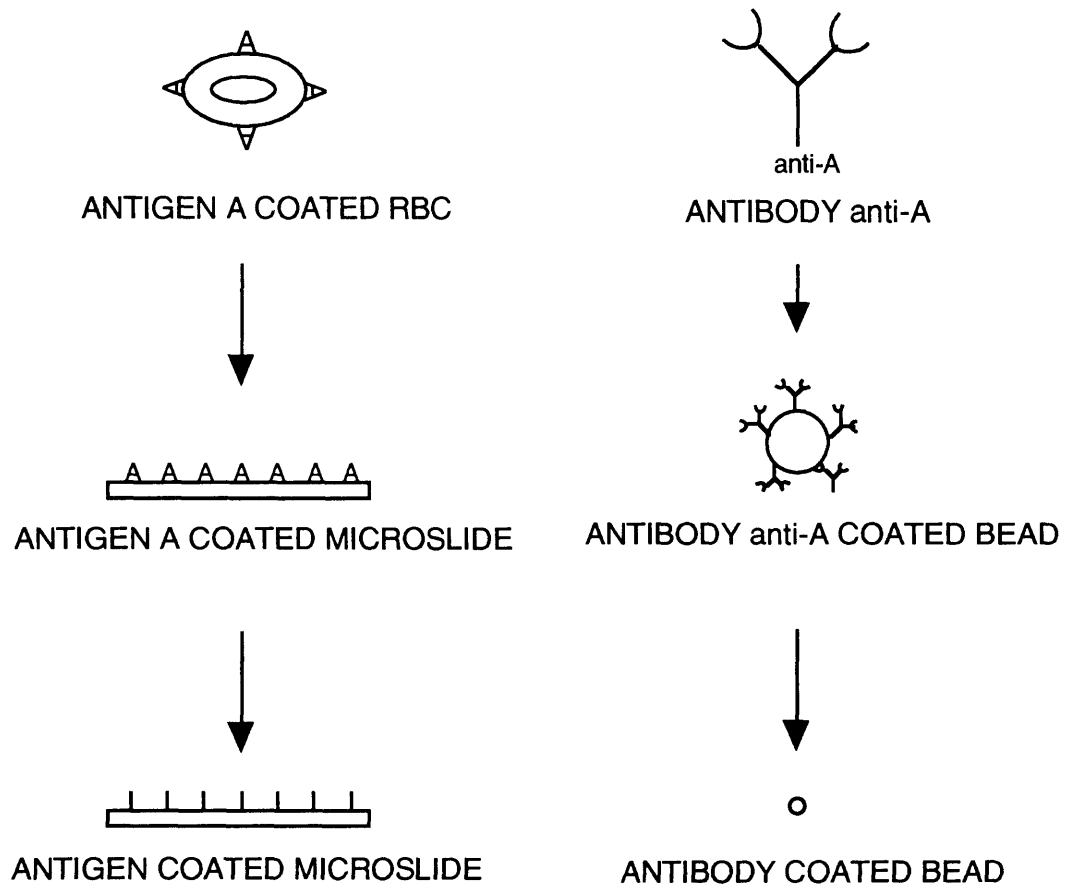
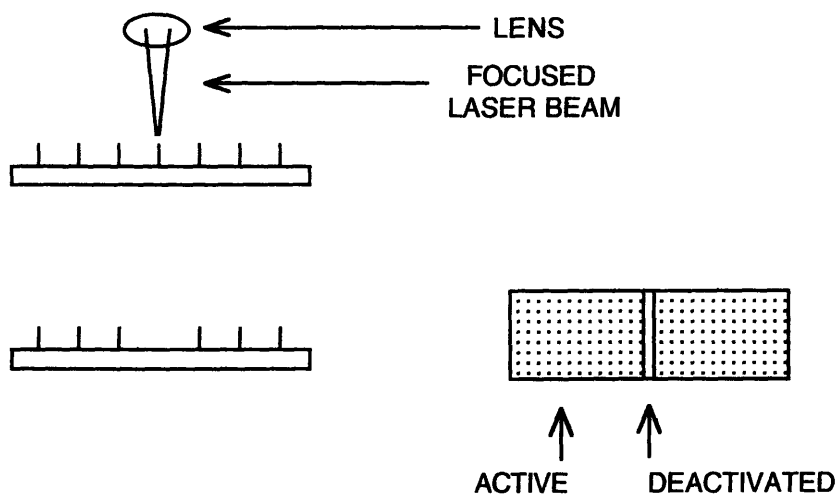


FIGURE 4 : DELINEATION OF SUBSTRATE COATING

I. ANTIGEN COATED MICROSLIDE



II. THERMALLY DEACTIVATE ANTIGEN USING LASER



III. SELECTIVE DEPOSITION OF ANTIBODY COATED BEADS

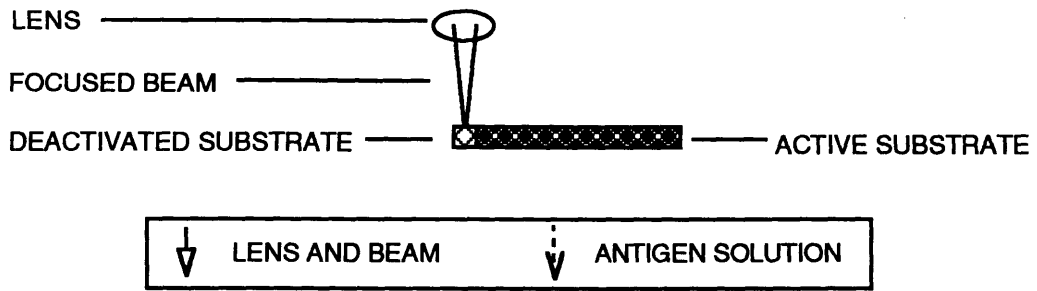


FIGURE 5 : 2D COATING PROCESS
CONCEPTUAL SCHEMATIC

1.2.5 Three-dimensional (3D) Layering Process

Stand alone part production using the 3D layering process is outlined in Figure 6. Although in the RBC agglutination reaction the antibody was used to link the antigen coated RBC together, the roles could be easily reversed and an antibody could be coupled to a micron sized substrate and an antigen used to link the substrate particles together. The 3D conceptual discussion is based on the second contingency: an antibody coupled particle substrate and an antigen in solution. After the first layer of monovalent or multivalent antibody coupled substrate is spread onto a base plate, the laser is used to selectively denature antibodies. The part geometry is defined by the area not subjected to irradiation. Subsequent layers are spread and irradiated until the part is completely defined. Then, the system is subjected to an antigen solution. Using a multivalent antigen, linkage between neighboring substrate particles is established and a network of antigen-antibody-substrate complexes results. The final step is the removal of the part from the surrounding deactivated substrate.

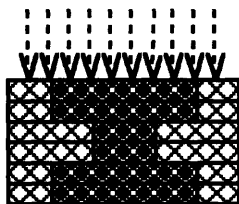
As previously mentioned, the roles of the antigen and antibody could be reversed, as long as the protein used in the flow through step was multivalent. Instead of a multivalent antigen solution, a monovalent or multivalent antigen could be coupled to a submicron substrate and used in flow through step. The antigen need not be multivalent because multiple antigens would be coupled to the submicron substrate; thus, the submicron substrate would have multiple binding sites. The resulting multivalent submicron particle would be able to link the antibody coated micron sized particles together. A network of substrate-antigen-antibody-substrate complexes would be produced. Not only would improved packing density result but two component parts could be created; for example, the antigen coated substrate could be polymeric and the antibody coated substrate could be ceramic. Another variation for the creation of two component 3D parts is the use of a multivalent antigen solution with two different substrates coupled with the same antibody. Simply, a multivalent antigen could link together an antibody coated polymer particle and an antibody



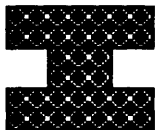
SPREAD LAYER OF ANTIBODY COUPLED SUBSTRATE
IRRADIATE TO DEACTIVATE ANTIBODY



SPREAD NEXT LAYER
IRRADIATE TO DEACTIVATE ANTIBODY



DEFINE COMPLETE PART GEOMETRY
FLOW THROUGH ANTIGEN SOLUTION
ANTIGEN BINDING TO ACTIVE ANTIBODIES



SEPARATION OF PART FROM DEACTIVATED SUBSTRATE

FIGURE 6 : 3D LAYERING PART CONSTRUCTION
CONCEPTUAL SCHEMATIC

coated ceramic or possibly metallic particle. The 2D coating and 3D layering processes could be used in tandem to add multilayered features to surfaces.

1.3 METHODOLOGY

Figure 7 is the critical path chart that details the evolution of the Biolithography process.

1.3.1 Agglomeration Reaction

A commercially available antibody coupled to a particle substrate, 1 μm polystyrene bead, and the commercially available corresponding antigen were used to test for an agglomeration reaction. The binding was similar to the agglutination of RBC except that the particle substrate was coated with the antibody (instead of antigen) and the complexes were formed by its reaction with the multivalent antigen (instead of antibody).

1.3.2 Elimination of Agglomeration Reaction

Thermal deactivation of the antibody coated beads was demonstrated using the simplest method possible, bulk heating of the beads in an oven. The elimination of the agglomeration reaction indicated that increased temperature was an effective mechanism to denature the antibody. Testing active and deactivated beads in the same sample showed the antigen bound selectively to the active antibodies.

1.3.3 2D Coating Process

In the agglomeration reaction, the antigen binding was selective to the active antibody but the active and deactivated beads became intermingled. In order to achieve localized deposition, the antigen was immobilized onto glass. The goal was to demonstrate deposition of the antibody coated beads onto the antigen coated glass. The deposition was proven to be from the antigen-antibody reaction by testing the deposition of the antibody coated beads onto uncoated glass. Deposition on the antigen coated glass was the active substrate control and on the uncoated glass was the deactivated substrate control.

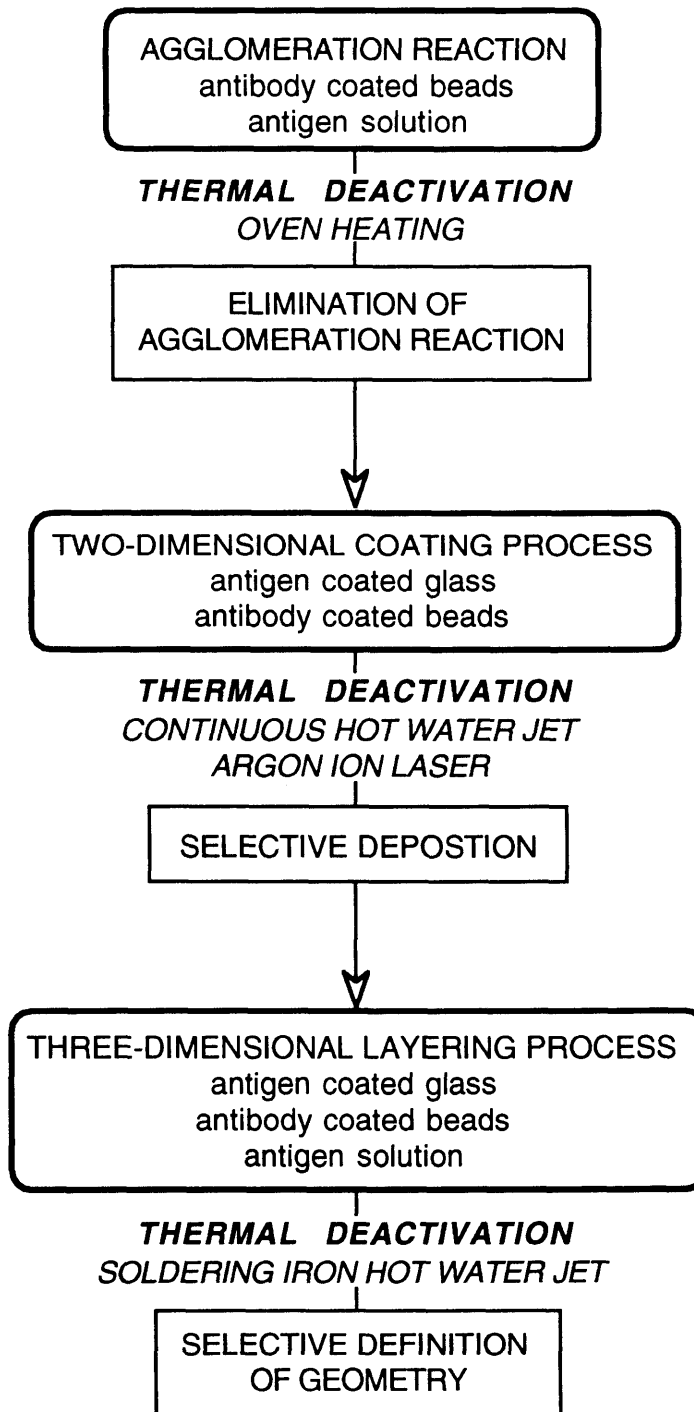


FIGURE 7 : BIOLITHOGRAPHY CRITICAL PATH CHART

1.3.4 Selective Deposition

In order to achieve selective deposition, a temperature increase in localized regions of the antigen coated substrate was required. Two methods were used: (1) continuous hot water jet and (2) argon ion laser. In the continuous hot water tests, the requirement was to demonstrate deactivation of the immobilized antigen and deposition differences of magnitudes comparable to the controls. The argon ion laser test had an additional requirement of producing micron scale resolution.

1.3.5 3D Layering Process

The layering process worked up from an antigen coated glass piece with deposited antibody beads i.e. a bound bead base. Subsequent antibody coated bead layers were bound together using antigens in solution. The goal was to demonstrate actual layering of the beads. Again deposition levels were used as controls for the thermal deactivation tests.

1.3.6 Selective Definition of Geometry

Thermal deactivation was used to define geometry in the 3D layering process. A modified soldering iron tip water nozzle system was created to achieve improved resolution over the continuous hot water jet apparatus. The goal was to use this system to produce layered parts with defined geometries starting from predeactivated and bound bead bases.

2. PROCESS COMPONENTS

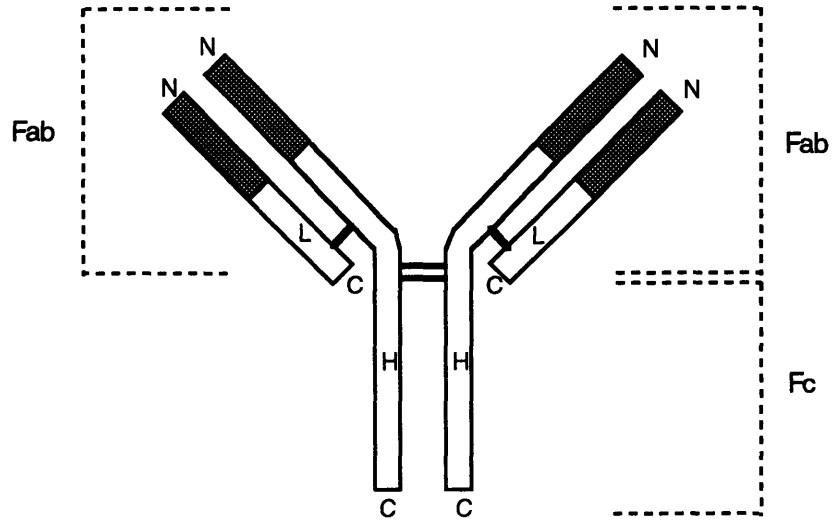
This section discusses the tested antibodies and antigens, the substrates to which they are coupled and typical binding properties of these components. Finally, the thermal deactivation mechanisms studied in this work are described.

2.1 ANTIBODIES AND ANTIGENS

Animals protect themselves from attack by disease-causing microorganisms and viruses with their immune systems. Two types of immunity are present in vertebrate systems: (1) cellular immunity that is mediated T cells so named because of their development in the thymus, and (2) humoral immunity that is mediated by an incredibly diverse array of related proteins called antibodies or immunoglobulins. Antibodies are produced by B cells so named because of their development in mammalian bone marrow.⁴ The target of the immune system is the foreign invader or antigen, for example, a bacterium or virus. Antibodies bind to the antigens to neutralize them or precipitate their destruction by scavenger cells such as macrophages.⁵ Antibody-antigen binding is the reaction that is manipulated in the Biolithography process.

2.1.1 Rabbit Immunoglobulin G (R-IgG)

Immunoglobulins are a diverse group of related proteins of which Immunoglobulin G (IgG) is the most common. Figure 8 shows a two dimensional schematic for the general structure of IgG that was reproduced based on sources detailing rabbit IgG^{6,7} and human IgG⁴, specifically, and IgG in general.^{8,9} IgG is an antibody with a characteristic Y shape. The Y shape is formed by two identical light polypeptide chains and two identical heavy polypeptide chains. The arms of the Y are the Fab fragments so labeled because they are the sites for antigen binding and the tail of the Y is Fc fragment so labeled because it is readily crystallized. The Fab fragment is composed of the light chain and the N terminal half of the heavy chain (N terminal meaning the amino or NH₂ end of the chain). Both these components



H = HEAVY CHAIN
 L = LIGHT CHAIN
 N = AMINO (NH₂) TERMINAL
 C = CARBOXYL (COOH) TERMINAL
 Fab = ANTIGEN BINDING FRAGMENT
 Fc = CRYSTALLIZABLE FRAGMENT

[Shaded Box] = VARIABLE REGION
 [White Box] = CONSTANT REGION
 [Line] = DISULFIDE BOND

FIGURE 8 : TWO DIMENSIONAL SCHEMATIC OF IgG

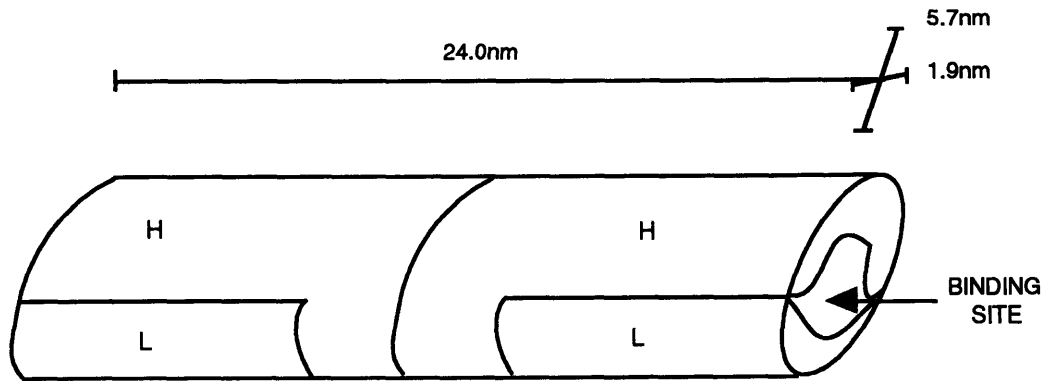


FIGURE 9 : DIMENSIONAL MODEL OF IgG
From Edelman and Gally (1964)

have variable regions, that are regions in which the amino acid sequence can be varied from one IgG to another so that different IgG can bind to different antigens. Thus, the variable regions determine the specificity of the antigen binding site.⁹ The IgG molecule has two binding sites i.e. two Fab regions and is defined as bivalent. The Fc region is composed of the C terminal halves of the heavy chain (C terminal meaning the carboxyl or COOH end of the chain)

The chains are held together by disulfide bridges. The location of these disulfide bridges is known as the hinge region because it is about this region that the Fab fragments can swing relative to one another; thus, changing the distance between the binding sites. The bivalency and flexibility of the molecule permits the linking of two particles together⁷, as observed Section 1.2, the agglutination of RBC, Figure 2.

The molecular weight (mol.wt.) of IgG is reported either in general or referring to a specific species. The values are designated for either the light chains and heavy chains or the Fab and Fc fragments or the whole molecule. For example, rabbit IgG has been reported to cleave into three fragments each of approximately 45000 to 50000mol.wt. but has been shown to have heavy chains of 50000mol.wt. and light chains of 22000mol.wt..⁶ Human IgG has a variety of weights reported; for example, light chains at 23000mol.wt. and heavy chains at 50000mol.wt.⁷ and whole molecule at 160000mol.wt..¹⁰ Goat IgG weight used by Cozens-Roberts et al (1990)⁸ was 160000mol.wt. Other times the weight is just reported in general for IgG, i.e. light chains of 22000mol.wt. and heavy chains of 50000 to 77000 mol.wt.¹¹ and whole molecule of 150000 to 160000 mol.wt..¹² The general IgG molecular weight selected for all calculations in this investigation was 160000mol.wt.

X ray low angle scattering was used to determine the dimensions of IgG. The human IgG molecule was found to be a cylindrical particle with elliptical cross-section with axes of 1.9nm and 5.7nm and with length of 23.0-24.0nm.¹³ Clausen (1981)¹⁰ reports "...Valentine and Green (1967) showed that the IgG globulin had the physical form of a Y with one very short and two very long

arms.” Figure 9 shows the IgG molecule model proposed by Edelman and Gally (1964)¹². The short tail of the Y is nested between the Fab regions. Cozens-Roberts et al (1990)⁸ used the IgG dimensions of 1.9nmx5.7nmx24.0nm for both goat and rabbit anti-goat IgG. In the present study, the dimensions were used for rabbit and goat anti-rabbit IgG.

2.1.2 Goat Anti-Rabbit Immunoglobulin G (GAR-IgG)

An anti-IgG antibody is produced when a host animal (goat) is immunized with the IgG antigen from a donor animal (rabbit). In this case, the rabbit IgG is both an antibody (against some specific unspecified target) and an antigen. Antibodies purified from the host animal will be polyclonal i.e. a mixture of anti-IgG of varying affinities will be obtained.

Given the sometimes general reporting of IgG features, such as structure, size and molecular weight, the properties of goat anti-rabbit IgG were taken to be similar to those discussed for rabbit IgG. A molecule with characteristic Y shape where the tips of the Y are the molecules two antigen binding sites. The molecule has molecular weight of 160000 and dimensions of 1.9nmx5.7nmx24.0nm.

2.1.3 Protein A (SpA)

Protein A (SpA) is isolated from the cell wall of *Staphylococcus aureus*. This 42000 molecular weight single polypeptide can be classified as having five domains: four homologous domains for Fc region binding of Immunoglobulin and one C terminal domain not suitable for Immunoglobulin binding. When SpA binds to the Fc portion of IgG, the Fab region is not affected.¹⁴ IgG and SpA binding is not defined as antibody-antigen binding because it usually involves the Fc region.¹⁵

2.2 SUBSTRATES

Attachment chemistries were used to immobilize proteins onto both polymeric and ceramic substrates. Protocols are explained and the resulting protein surface concentrations, densities and spacings are reported.

2.2.1 Polystyrene Beads

The Polysciences, Inc. (Warrington, PA) polystyrene beads used in this study were supplied in two forms: (1) plain polystyrene beads and (2) polystyrene beads with proteins attached. The polystyrene beads are specified as percent solids latex.

A latex is defined as a stable colloidal dispersion of a polymer in water. ... Polystyrene latices are in the form of microspheres, i.e. all the particles are so close to the same diameter that they may be considered one monodisperse population.¹⁶

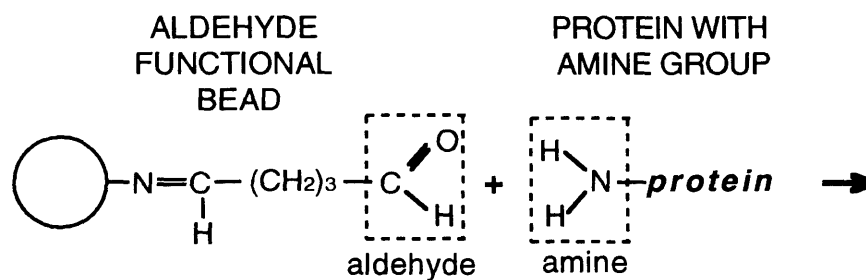
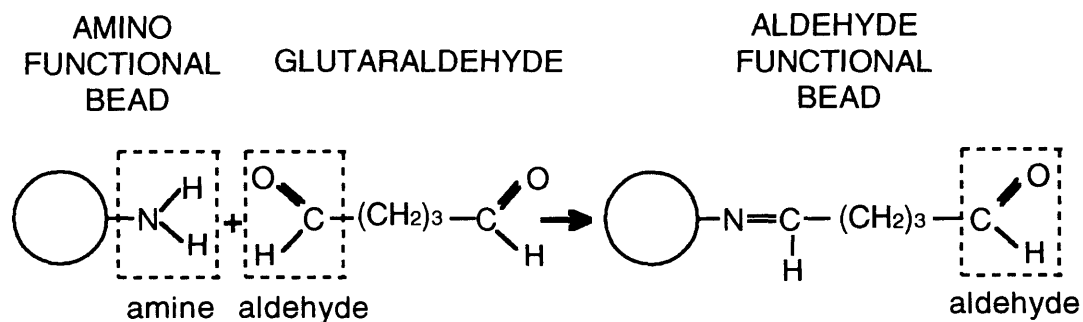
All microspheres used were 1 μ m in diameter.

2.2.1.1 Polybead[®] Polystyrene Microspheres

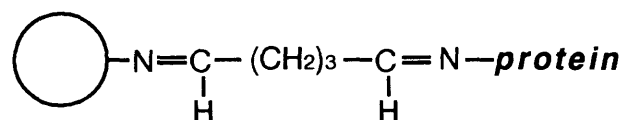
The Polybeads[®] (Polysciences product number 07310, lot 445125) were plain polystyrene beads. The beads were supplied in a 15ml vial at 2.5% solids by volume. Based on a formula provided by Polysciences,¹⁶ this converts to 4.55x10¹⁰ beads/ml (Appendix A). The Polybeads[®] were used in control tests for deposition comparisons.

2.2.1.2 Goat Anti-Rabbit Immunoglobulin G (GAR-IgG) Beads

The GAR-IgG blue dyed polystyrene beads were produced using glutaraldehyde chemistry owing to the fact that the blue dye imparts amino functionality to the polystyrene beads. Figure 10 provides chemical diagrams to aid in understanding the coating procedure. All chemical diagrams provided were modified from Weetall (1976)¹⁷. The glutaraldehyde provides an aldehyde group to which an amine group of the protein is covalently bound.⁸ The described glutaraldehyde chemistry places the coupled protein 5 carbon atoms



PROTEIN COUPLED TO BEAD



AMINO FUNCTIONAL BEAD = BLUE DYED BEAD
protein = GOAT ANTI RABBIT IgG

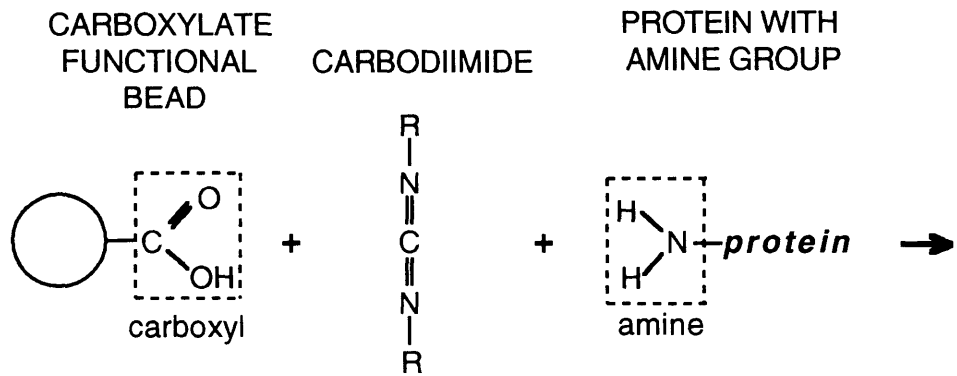
FIGURE 10 : COUPLING PROCEDURE FOR GAR-IgG BEADS

from the surface of the bead.¹⁸ Subsequent steps in the binding protocol were performed to ensure proper performance of the beads. Ethanolamine is used to block unreacted aldehyde sites and bovine serum albumin (BSA) is used to block non specific sites for protein adsorption. After these steps, the beads are placed in a storage buffer with microbicide (phosphate buffered saline (PBS), BSA, glycerol and sodium azide). Detailed protocol is provided in Appendix A.

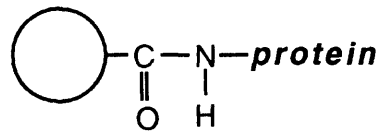
Two lots of GAR-IgG beads were used in the study (Polysciences product number 17696). These beads were provided in 1ml quantities and lot 435714 (4/94-10/94) had 1.24% solids by volume and lot 445454 (10/94-5/95) had 1.25% solids by volume. Correspondingly, there were 2.26×10^{10} beads/ml in lot 43714 and 2.27×10^{10} beads/ml in lot 445454 (Appendix A). Lot 43714 had a protein concentration of GAR-IgG of $428 \mu\text{g/ml}$. Thus, based on the surface area of a $1 \mu\text{m}$ diameter polystyrene bead ($3.14 \mu\text{m}^2$), there was $0.604 \mu\text{g/cm}^2$. Taking into account the molecular weight of the protein (160000 mol.wt.), there was 2.27×10^{12} GAR-IgG/ cm^2 and 7.14×10^4 GAR-IgG/bead. From the protein density value, 2.27×10^{12} GAR-IgG/ cm^2 , the protein spacing was calculated, 6.63nm between GAR-IgG or 6.63nm/GAR-IgG. The similar values for the lot 445454 beads that had a protein concentration of $394 \mu\text{g/ml}$ are $0.552 \mu\text{g/cm}^2$, 2.08×10^{12} GAR-IgG/ cm^2 , 6.52×10^4 GAR-IgG/bead and 6.94nm/GAR-IgG.

2.1.2.3 Protein A (SpA) Carboxylate Beads

With the SpA carboxylate beads, the SpA was attached using a carbodiimide protocol (Appendix A) because the polystyrene beads had a preattached carboxylate functionality. The use of a carbodiimide covalently binds the protein by an amine group to the carboxylate group of the bead.⁸ Figure 11 provides a diagrammatic explanation. In this situation, the protein is bound 2 to 3 carbon atoms from the surface of the bead.¹⁸ Again, ethanolamine is used to block unreacted aldehyde sites and BSA is used to block non specific sites for protein adsorption. After these steps, the beads were placed in a storage buffer with microbicide (phosphate buffered saline (PBS), BSA, glycerol and sodium azide).



PROTEIN COUPLED TO BEAD



R = organic groups

CARBOXYLATE FUNCTIONAL BEAD = WHITE AND FLUORESBRITE BEADS

protein = PROTEIN A

FIGURE 11 : COUPLING PROCEDURE FOR SpA BEADS

White SpA carboxylate beads (lot 441668) were used in preliminary agglomeration reactions with GAR-IgG beads (lot 435714). The SpA beads were supplied at 1.25% solids by volume and 95 μ g/ml. Similar to the calculation for GAR-IgG, there was 0.133 μ g/cm² and, addressing the molecular weight of the protein (42000mol.wt.), there was 1.91x10¹²SpA/cm², 5.99x10⁴SpA/bead and 7.24nm/SpA (Appendix A).

One lot (443033) of SpA Fluoresbrite™ beads (Polysciences product number 17845) was used in the study at 1.25% solids by volume and 100 μ g/ml. The characteristic values were 0.140 μ g/cm², 2.01x10¹²SpA/cm², 6.30x10⁴SpA/bead and 7.06nm/SpA. The fluorescence was achieved by introducing fluorescein isothiocyanate (FITC) dye directly into the polymer. Polysciences specifies an excitation maximum of 458nm and emission maximum of 540nm for the dye although these data have not been determined for the beads. Based on the data given for the dye, successful fluorescence microscopy was performed using a mercury lamp and fluorescence filter (Nikon DM510, B-2E) comprised of yellow, orange and red cut off glass (OG530).

2.2.2 Rabbit Immunoglobulin G (R-IgG) Soda Lime Glass

There were two types of soda lime glass used in this study: (1) Becton Dickinson Gold Seal microslides for the water studies and (2) Spectrum Black Smooth glass for the laser studies. Detailed compositions are provided in Appendix A. Coupling of proteins to the glass was performed using a silane-glutaraldehyde protocol (Appendix A). The protocol was provided by Suzanne Kuo and was used in Cozens-Roberts et al (1990)⁸ and Kuo and Lauffenburger (1993)¹⁹. Modifications made to the protocol were based on container size, glass piece size, and liquid coverage requirements.

Calculations for protein surface concentration will be discussed later in this section as they related to the various sizes of glass required for the array of experiments. First, the glass undergoes an extensive cleaning procedure. The next step exposed the glass to 3-aminopropyltriethoxysilane (3-APS) in

acetone. The 3-APS reacts with the silanol groups on the surface of the clean glass to provide an alkylamine functionality, as seen in Figure 12. With the attachment of this group the glass was transformed from a hydrophilic to a hydrophobic surface and was a check of the success of this step of the protocol. The glass was then subjected to a glutaraldehyde solution that reacts with the alkylamine to provide the glass with aldehyde functionality. The protein was covalently coupled via its amine group to the aldehyde group on the glass. Glycine was added to block any unreacted aldehyde groups. The glass was stored in PBS and sodium azide.

The protein coupling is to any amine group of the protein: the terminal amine or by lysines, glutamines, or histadines. The protein may be immobilized in different ways. The immobilization of the IgG could occupy one of the Fab fragments; thus, reducing the number of IgG binding site from two to one. However, the coupling protocol is the same as that used in Cozens-Roberts et al (1990)⁸ where they indicate that binding between the beads and glass surfaces is possible because the size and structure, especially the hinge region, of the IgG permits the alignment of the antibody's antigen binding sites to the antigen.

An optimization test was performed to determine the necessity of using BSA in the buffer solution. GAR-IgG beads were deposited onto R-IgG coated glass pieces that had been stored in two different buffer solutions: (1) PBS with sodium azide and BSA and (2) PBS with sodium azide and no BSA. Comparing Figure 13, deposition onto R-IgG glass in buffer with BSA, to Figure 14, deposition on R-IgG glass in buffer with no BSA, the deposition is not significantly different. Given that non specific binding was minimal in the absence of BSA, BSA was eliminated from the buffer solution. This result was fortunate because BSA would gel upon exposure to the laser. The elimination of BSA avoided the gelling interfering with the thermal denaturing reaction.

The R-IgG used in the protocol was SIGMA ImmunoChemicals (St. Louis, MO) product number I-8140, rabbit IgG, purified Immunoglobulin, technical grade (lot 07H8836). The stock was supplied in 50mg quantity (in PBS with

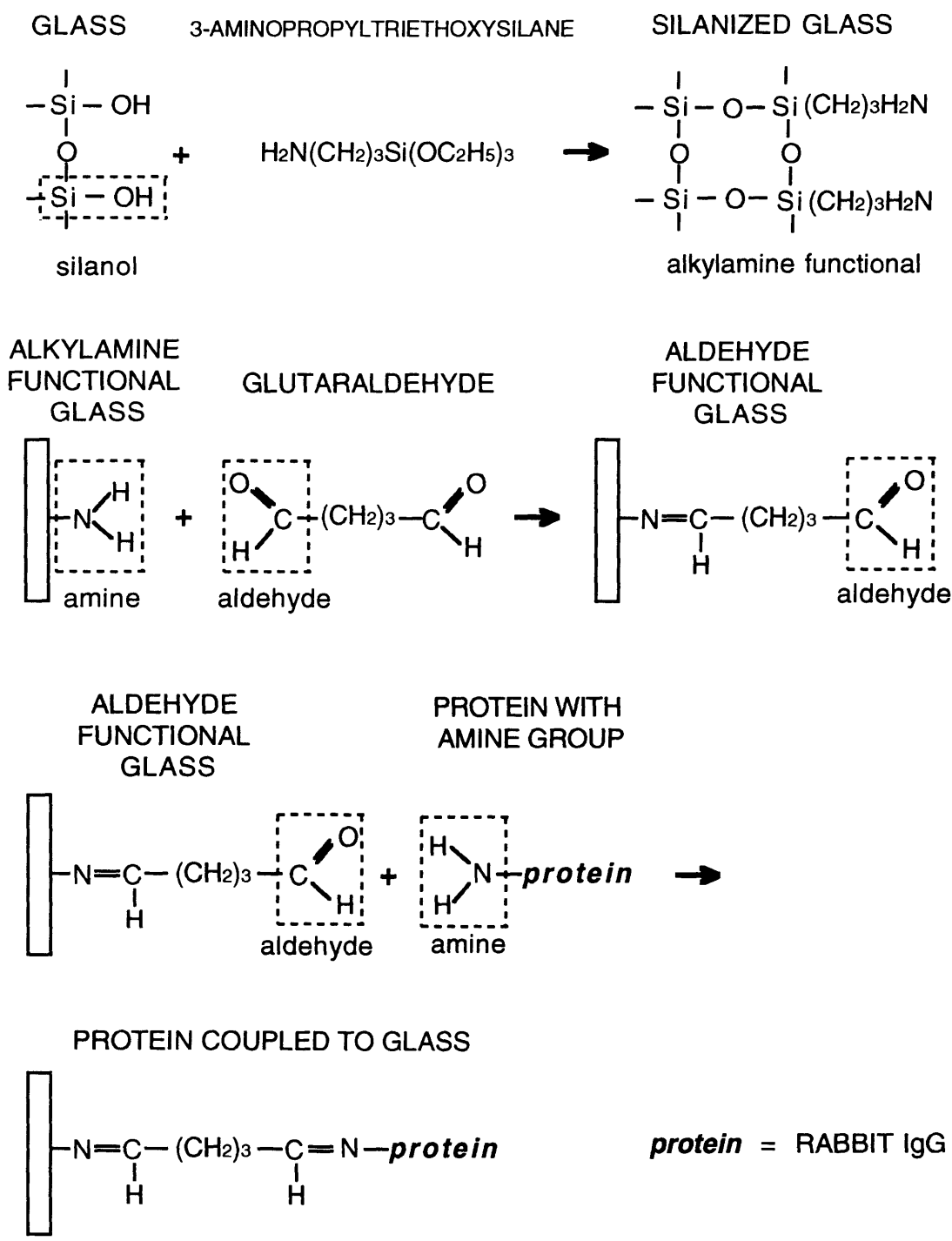


FIGURE 12 : COATING PROCEDURE FOR R-IgG GLASS

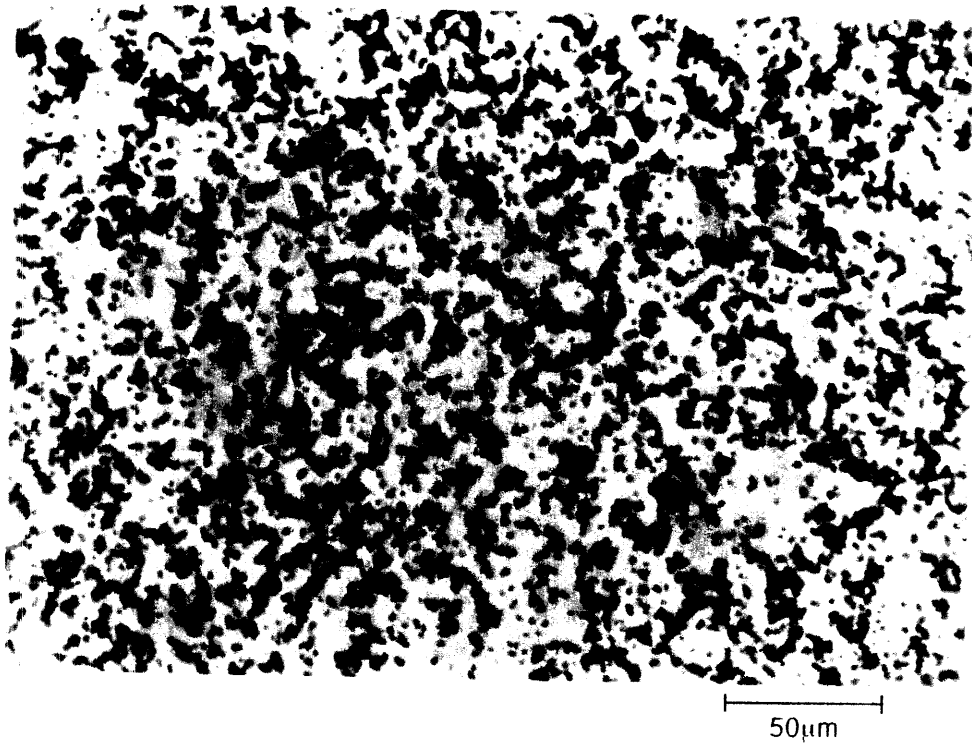


FIGURE 13 : R-IgG CONTROL IN PBS WITH BSA; 400x

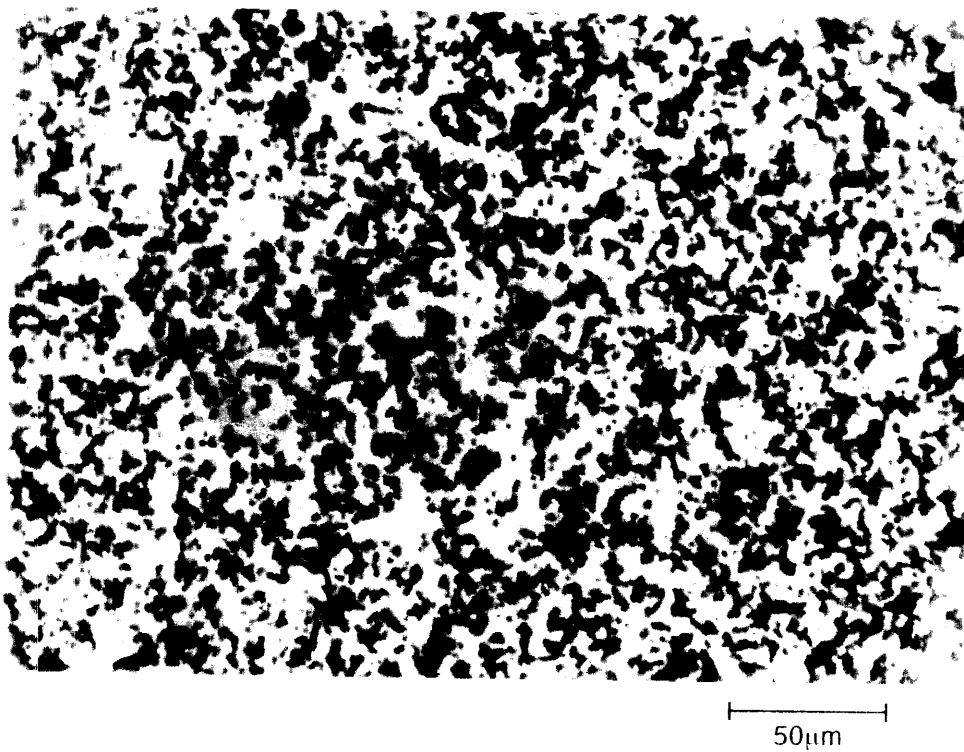


FIGURE 14 : R-IgG CONTROL IN PBS; 400x

0.1% sodium azide) with protein concentration of 11.4mg/ml. The stock was diluted into aliquots of 500µl volumes at 1 mg/ml.

For the various experiments performed various sizes of glass pieces were coated with rabbit IgG. Protein surface concentration was calculated based on a method described in Cozens-Roberts et al (1990)⁸ taking into account the amount of protein in the volume of protein coating solution above the glass surface.

$$C_{\text{glass}} \left(\frac{\mu\text{g}}{\text{cm}^2} \right) = \frac{\left[C_{\text{soln}} \left(\frac{\mu\text{g}}{\text{ml}} \right) \right] \cdot \left[V_{\text{glass}} (\text{ml}) \right]}{\left[SA_{\text{glass}} (\text{cm}^2) \right]}$$

$$\text{where } V_{\text{glass}} (\text{ml}) = \left[SA_{\text{glass}} (\text{cm}^2) \right] \cdot \left[h_{\text{soln}} (\text{cm}) \right]$$

C_{glass} = surface concentration of protein on glass

C_{soln} = concentration of protein in coating solution

V_{glass} = volume of coating solution above glass piece

SA_{glass} = surface area of glass piece

h_{soln} = height of coating solution above glass piece

The example in Appendix A details the calculation of the surface concentration for the 35mmx35mmx3mm black glass piece used in preliminary laser tests.

Using a 50µg/ml R-IgG coating solution, the surface concentration on the 35mmx35mmx3mm black glass piece was 16µg/cm². Similar to the beads, the characteristic protein density values can be calculated (Appendix A). For the 35mmx35mmx3mm piece with 16µg/cm², the protein density was 6.02x10¹³R-IgG/cm² resulting in a spacing between R-IgG of 1.29nm (1.29nm/R-IgG). For the majority of preliminary investigations and the continuous 90°C water jet tests, microslides were used. These 25mmx75mmx1mm slides had a surface concentration of protein of 19µg/cm² resulting in 7.15x10¹³R-IgG/cm² and 1.18nm/R-IgG. The black glass pieces ($SA_{\text{glass}} = 150\text{cm}^2$) used to get data observable by scanning electron

microscope (SEM) had surface concentration of $15\mu\text{g}/\text{cm}^2$. The density and spacing were $5.65 \times 10^{13} \text{R-IgG}/\text{cm}^2$ and $1.33 \text{nm}/\text{R-IgG}$. The $20\text{mm} \times 20\text{mm} \times 1\text{mm}$ microslide pieces used in the 3D layering experiments had two concentrations. Using a $50\mu\text{g}/\text{ml}$ coating solution, a $17\mu\text{g}/\text{cm}^2$ surface concentration was achieved and, using a $1.3\mu\text{g}/\text{ml}$ solution, a $0.44\mu\text{g}/\text{cm}^2$ surface concentration was achieved. The high density was $6.40 \times 10^{13} \text{R-IgG}/\text{cm}^2$ and spacing was $1.25 \text{nm}/\text{R-IgG}$; the low density was $1.66 \times 10^{12} \text{R-IgG}/\text{cm}^2$ and spacing was $7.77 \text{nm}/\text{R-IgG}$. The 15, 16, 17 and $19\mu\text{g}/\text{cm}^2$ surface concentrations were not considered significantly different.

The protein coating solution concentration used was $50\mu\text{g}/\text{ml}$ to achieve maximum protein density.²⁰ Notice that the bead concentrations were on the order of $1\mu\text{g}/\text{cm}^2$ and the glass concentrations were on the order of $10\mu\text{g}/\text{cm}^2$ except for the $0.44\mu\text{g}/\text{cm}^2$ sample. The low concentration glass sample was used to test the difference in bead deposition achieved with different R-IgG glass surface concentrations, Section 3.3.2.

2.3 BINDING PROPERTIES

Antibodies and antigens are specific types of receptors and ligands. Interactions between receptors and ligands are described in terms of affinities, a measure of the propensity of the receptor and ligand to interact. The receptor-ligand binding affinity is related to receptor-ligand adhesion strength.

2.3.1 Binding Affinity

Affinity can be explained examining the binding of a single receptor to a single ligand to form a receptor-ligand complex.



The rate constants on the arrows are for the forward, k_f , and reverse, k_r , reactions. The ratio of the reverse to forward rate constants is the equilibrium dissociation constant.

$$K_D [\text{M}] = \frac{k_r \left[\frac{1}{\text{time}} \right]}{k_f \left[\frac{1}{\text{M} \cdot \text{time}} \right]}$$

A small value of K_D , meaning the likelihood of dissociation is small, indicates a high binding affinity. "The values of K_D for various systems fall within a wide range, with 10^{-12}M near the high affinity end (the avidin/biotin bond with $K_D=10^{-15}\text{M}$ (Green, 1975) is an extreme exception) to 10^{-6}M at the low affinity end."²¹ For the present system, the binding affinity of goat anti-rabbit IgG (GAR-IgG) to rabbit IgG (R-IgG) was taken to be the same as rabbit anti-goat IgG and goat IgG which was recorded by Kuo and Lauffenburger (1993)¹⁹ to be 10^{-6}M at $\text{pH} = 7.4$. A wide variety of receptor ligand interactions have a similar binding affinity which reinforces the material flexibility of the Biolithography process.

2.3.2 Adhesion Strength

Kuo and Lauffenburger (1993)¹⁹ provided experimental evidence of the relationship between binding affinity and adhesion strength. Radial-flow detachment assay was used to measure the force required to detach 10 μ m diameter polystyrene beads coupled with IgG from glass coated with SpA. The assay imparts a shearing flow on the bead. The detachment force is determined from the shear stress required to detach the bead. A variety of animal IgG were used to provide a range of IgG-SpA binding affinities (rabbit IgG-SpA at 4.6x10⁻⁹M to goat IgG-SpA at 7.7x10⁻⁶M). The adhesion strength and detachment force were related by the number of receptors in the contact area between the bead and surface. The investigation demonstrated that the adhesion strength varied with the logarithm of the binding affinity.

Detachment force calculations are discussed in Section 3.3.1.3 where the detachment force was used as a guide to calibrate the water nozzle used to remove unbound beads from parts and in Section 3.7.1 where detachment force was used to determine the bulk strength of Biolithography parts.

2.4 DEACTIVATION MECHANISMS

Proteins denature at high temperatures. The temperature sensitivity of proteins varies depending on protein structure and chemical composition. For example, collagen denatures at 80°C²². Based on the temperature sensitivity of proteins, a variety of thermal deactivation methods were tested: (1) bulk temperature increase in an oven, (2) local temperature increase using a hot water jet and (3) local temperature increase using an argon ion laser. The temperature increases with the oven and hot water are straight forward; however, the laser method merits further discussion. As detailed in Figure 15²³, the ultraviolet (UV) and a small portion of the visible spectrum have photochemical interactions with biological materials. This interaction can stimulate cell reactions but, at high intensity, causes cell death. The infrared (IR) and the majority of the visible region have thermal interactions. In the present investigation, an argon ion laser, with visible spectrum wavelength of 488nm, was used to thermally deactivate immobilized proteins. The temperature increase was facilitated using a substrate that absorbs the laser beam and generates local heating of the substrate and the immobilized proteins. Dimensional accuracy was established with appropriate selection of lenses, scan speed and power level.

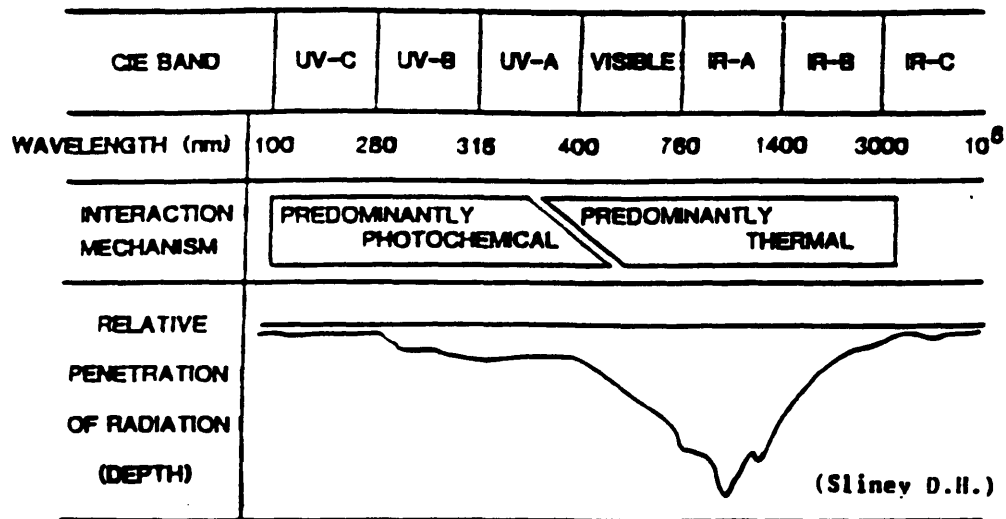


FIGURE 15 : ELECTROMAGNETIC RADIATION INTERACTION MECHANISMS

Tissue interaction mechanisms are predominantly thermal for long wavelengths and photochemical for shorter wavelengths.

From Court L.A. et al (1991). Medical Lasers and Biological Criteria and Limits of their Therapeutic Effects. In Grandolfo M. et al. Lights, Lasers and Synchrotron Radiation. Plenum Press, New York. pp. 353-371.

3. PROCESS DEVELOPMENT

Process development tested three reactions and use of thermal deactivation to make the reactions selective: (1) agglomeration reaction and the elimination of the agglomeration reaction, (2) 2D coating process and selective deposition and (3) 3D layering process and selective definition of geometry. Finally, the process issues are addressed: bulk strength, deposition uniformity and production costs.

3.1 AGGLOMERATION REACTION

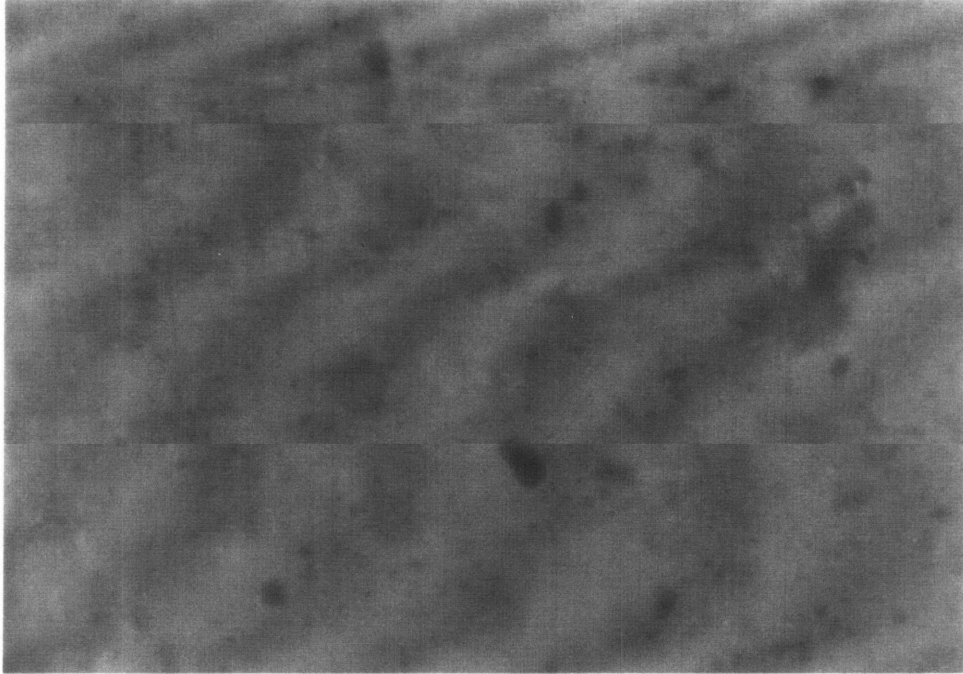
As shown in Figure 2 in Section 1.2.1, complexes of antigens and antibodies can be formed if both components are multivalent. The agglomeration experimentation combined GAR-IgG beads and R-IgG solution in various ratios of concentrations to determine at what ratios complexes were formed. The protocol was to pipette the desired volume of beads and solution into a well of a 96 well plate (well volume = 0.4ml), agitate the plate for five minutes and observe the sample ten minutes later. Agitation was performed to ensure the GAR-IgG beads and R-IgG had adequate exposure to each other and the waiting time before observation was simply time to permit the components to react. Table 1 details the sample volumes and concentrations used in the agglomeration experiments. The concentration of R-IgG was diluted from the aliquot (500 μ l at 1mg/ml) to produce the tested ratios. The protein ratio and concentration ratios were identical.

TABLE 1 : AGGLOMERATION PARAMETERS

GAR-IgG VOLUME (μ l)	GAR-IgG CONC'N (μ g/ μ l)	GAR-IgG PROTEIN (μ g)	R-IgG VOLUME (μ l)	R-IgG PROTEIN (μ g)	PBS VOLUME (μ l)	R-IgG CONC'N (μ g/ μ l)	RATIO CONC'N& PROTEIN
25	0.428	10.7	20	20	5	0.8	1:2
25	0.428	10.7	10	10	15	0.4	1:1
25	0.428	10.7	5	5	20	0.2	1:0.5
25	0.428	10.7	1	1	24	0.04	1:0.1
47	0.428	20.1	1	1	46	0.02	1:0.05

GAR-IgG beads from lot 435714 were used in all agglomeration experiments. The lot had some uncharacteristically large beads and they can be seen in all photos. A large number of the anomaly beads are present in Figure 16, which shows the 1:2 sample. Concentrating on the left side of the photo to be the representative sample, the 1:2 ratio produced negligible clustering. The 1:1 sample, Figure 17, begins to show evidence of clustering. Again the photo shows the presence of the anomaly beads (bottom left, top right and right center). Figure 18, for the 1:0.5 sample, shows evidence of clustering similar to slightly greater than the 1:1 sample. The 1:0.1 ratio produced a substantial increase in clustering with clusters on the order of 50 μ m to 100 μ m, as seen in Figure 19. The 25 μ l volume of GAR-IgG was selected to be able to accommodate the range of R-IgG concentrations required using the 1mg/ml R-IgG stock solution. However, given the success of the 1:0.1 ratio, a 1:0.05 sample was tested but the sample volume was increased to be able to achieve the 0.02 μ g/ml R-IgG concentration using 1 μ l of stock solution. Figure 20, for the 1:0.05 sample, shows slightly improved clustering, 100 μ m to 200 μ m, compared to the 1:0.1 ratio, 50 μ m to 100 μ m. For efficient use of the GAR-IgG beads (\$100/ml), the 1:0.1 ratio was selected as the control comparison of the thermal deactivation agglomeration experiments.

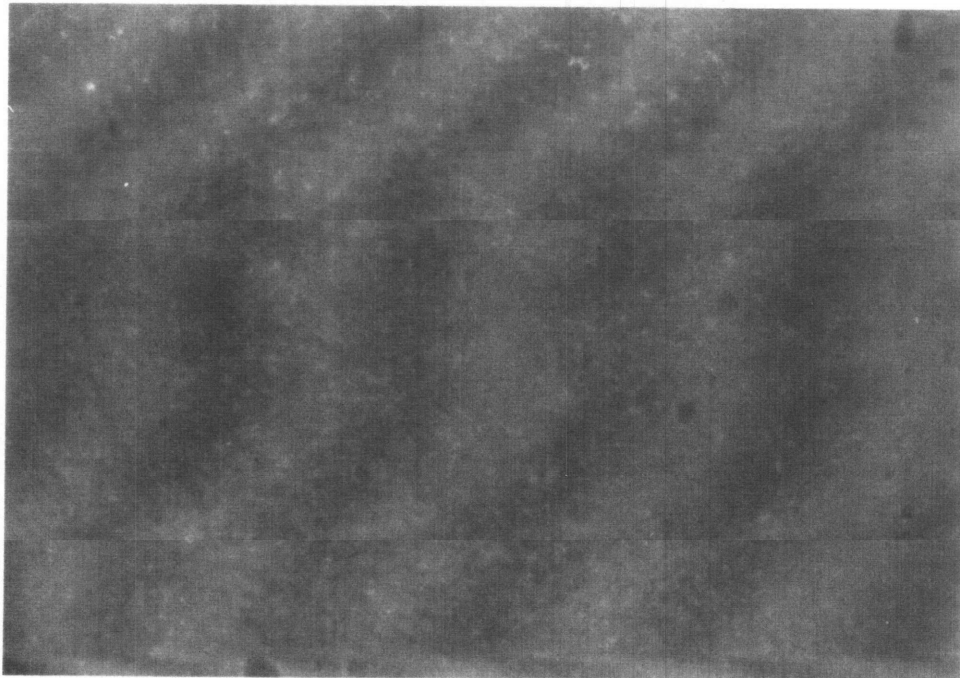
The lower concentrations of R-IgG were more effective in causing agglomeration. With higher concentrations, the R-IgG actually coats the GAR-IgG bead occupying all the binding sites. The lower concentration is required so that the R-IgG can actually have the opportunity to bind two GAR-IgG beads.



200µm

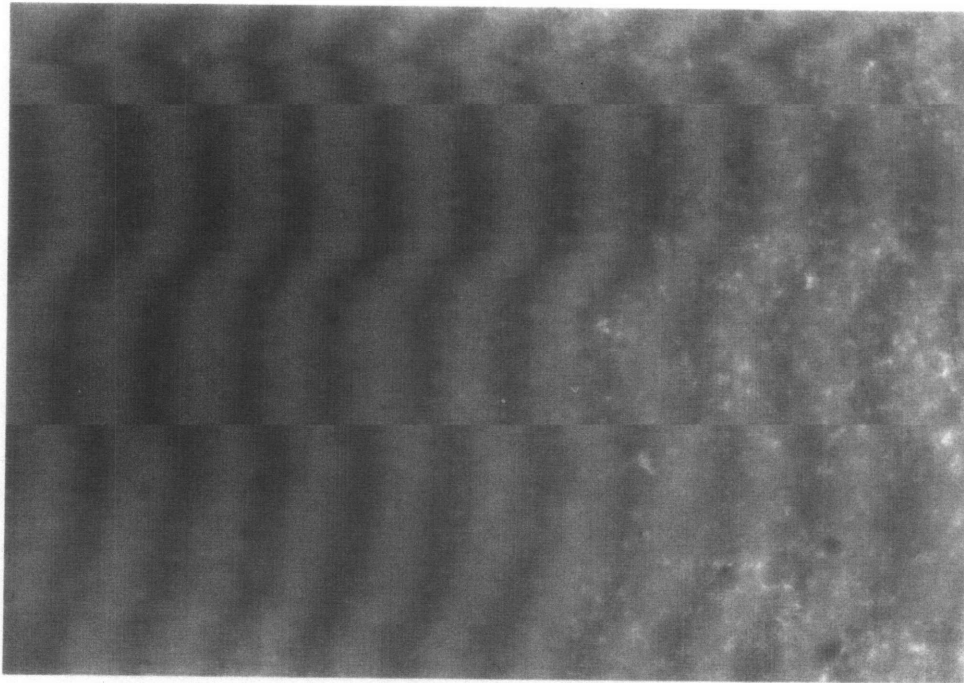
**FIGURE 16 : GAR-IgG BEADS + R-IgG 1:2 (50µl); 100x
NEGLIGIBLE CLUSTERING**

Note: Darkest regions are uncharacteristically large beads (lot 435714)



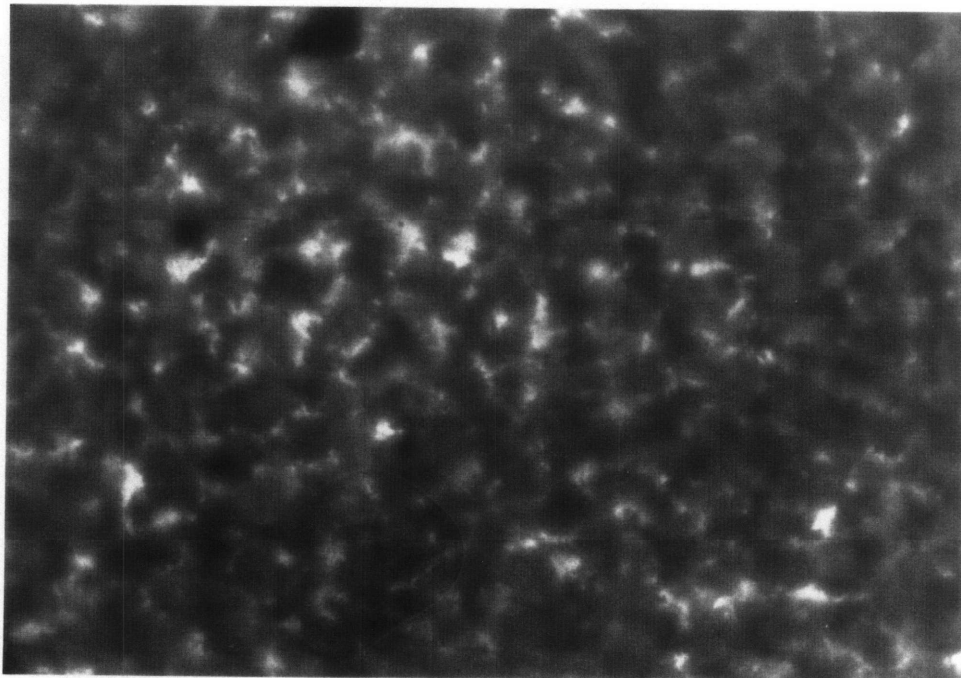
200µm

**FIGURE 17 : GAR-IgG BEADS + R-IgG 1:1 (50µl); 100x
EVIDENT CLUSTERING**



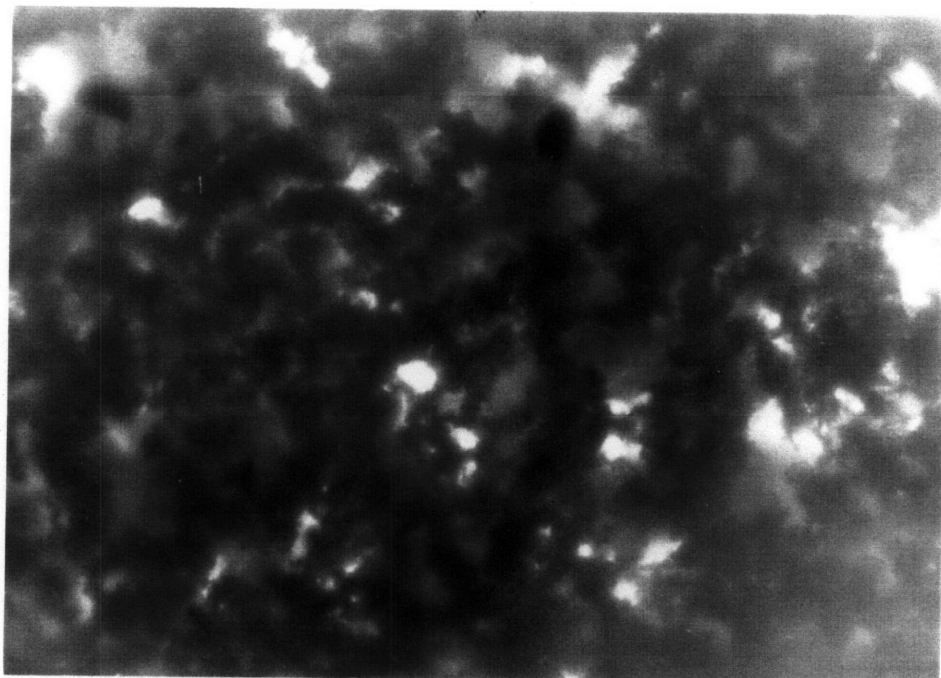
200µm

FIGURE 18 : GAR-IgG BEADS + R-IgG 1:0.5 (50µl); 100x
EVIDENT CLUSTERING



200µm

FIGURE 19 : GAR-IgG BEADS + R-IgG 1:0.1 (50µl); 100x
CLUSTER SIZE = 50 - 100µm



200 μ m

FIGURE 20 : GAR-IgG BEADS + R-IgG 1:0.05 (94 μ l); 100x
CLUSTER SIZE = 100 - 200 μ m

3.2 ELIMINATION OF AGGLOMERATION REACTION

For the thermal deactivation experimentation, GAR-IgG beads were subjected to both 60°C and 83°C oven temperatures targeting possible protein denaturing levels but avoiding the glass transition temperature of polystyrene (90°C to 100°C²⁴). The thermal deactivation protocol was similar to the agglomeration protocol except that the GAR-IgG beads received heat treatment prior to pipetting into the well of the 96 well plate. The desired volume of GAR-IgG beads (lot 435714) was pipetted into a glass vial (5ml). The volumes used were so small that they did not cover the glass base of the glass vial. The glass vial was placed in the oven at the desired temperature for the desired time. After, the beads were pipetted into the appropriate well of the 96 well plate.

Preliminary testing of the two deactivation temperatures, 60°C and 83°C, were performed using the white SpA beads to promote clustering rather than R-IgG, Table 2. Only the observation of clustering was used to judge the effectiveness of heat treatment; a simple positive-negative test.

TABLE 2 : THERMAL DEACTIVATION PARAMETERS (GAR-IgG + SpA)

GAR-IgG VOLUME (μl) @ 0.428 (μg/μl)	HEAT TREATMENT TEMPERATURE (°C)	TREATMENT TIME (minutes)	SpA VOLUME (μl) @ 0.095 (μg/μl)	CLUSTERING
25	0	0	25	+
25	60	20 ~	25	+
25	60	60 ~	25	+
25	83	5	25	-
25	83	20 *	25	-
25	83	60 *	25	-

* Rehydration required ~ Ineffective heat treatment

None of the 60°C exposures were effective in eliminating the agglomeration reaction. At the 83°C temperature, more detailed experiments were performed

with the better documented GAR-IgG beads and R-IgG in solution. Table 3 shows the tested situations.

TABLE 3 : THERMAL DEACTIVATION PARAMETERS (GAR-IgG + R-IgG)

GAR-IgG VOLUME (μ l) @ 0.428 (μ g/ μ l)	HEAT TREATMENT TEMPERATURE ($^{\circ}$ C)	TREATMENT TIME (minutes)	R-IgG VOLUME (μ l) @ 0.04 (μ g/ μ l)	RATIO
25	83	1 ~	25	1:0.1
25	83	5	25	1:0.1
25	83	20 *	25	1:0.1

* Rehydration required ~ Ineffective heat treatment

At 83 $^{\circ}$ C, any time level over 20 minutes required rehydration of the beads (addition of 25 μ l of PBS) as the original buffer had evaporated. In this situation, the bead volume would have artifacts from dehydration, such as stringy deposits possibly from the gelling of the BSA in the buffer solution. Figure 21 shows the post heat treated (83 $^{\circ}$ C for 5 minutes) GAR-IgG beads. The sample shows no sign of such artifacts because rehydration was not required at this time level. The sample was then exposed to 25 μ l of 0.04 μ g/ml R-IgG solution, to achieve the 1:0.1 ratio, and agitated for five minutes. No agglomeration reaction occurred as evident in Figure 22. Figure 21 and Figure 22 are practically identical despite the addition of R-IgG in Figure 22. There is no evidence of the reaction observed in the not heat treated sample at the 1:0.01 ratio, Figure 19. Heat treatment at 83 $^{\circ}$ C for 5 minutes was effective in eliminating the agglomeration reaction between GAR-IgG beads and R-IgG solution at a 1:0.01 ratio. Heat treatment of 1 minute was not effective in preventing the agglomeration reaction.

Thermal deactivation of GAR-IgG was demonstrated by the absence of agglomeration in Figure 22. The next set of experiments examined the effect of thermally deactivating half of the bead volume to observe specificity of binding to active, not deactivated substrates. Table 4 shows the tested parameters.

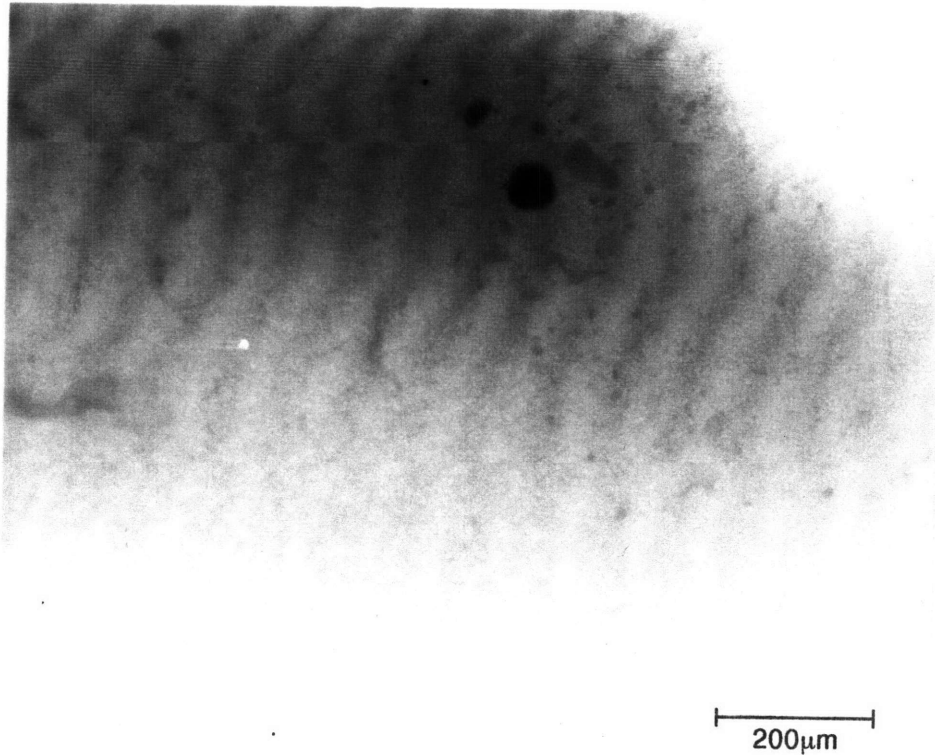


FIGURE 21: GAR-IgG BEADS NO R-IgG (25µl); 100x
BEAD HEAT TREATMENT 83°C FOR 5 MIN.

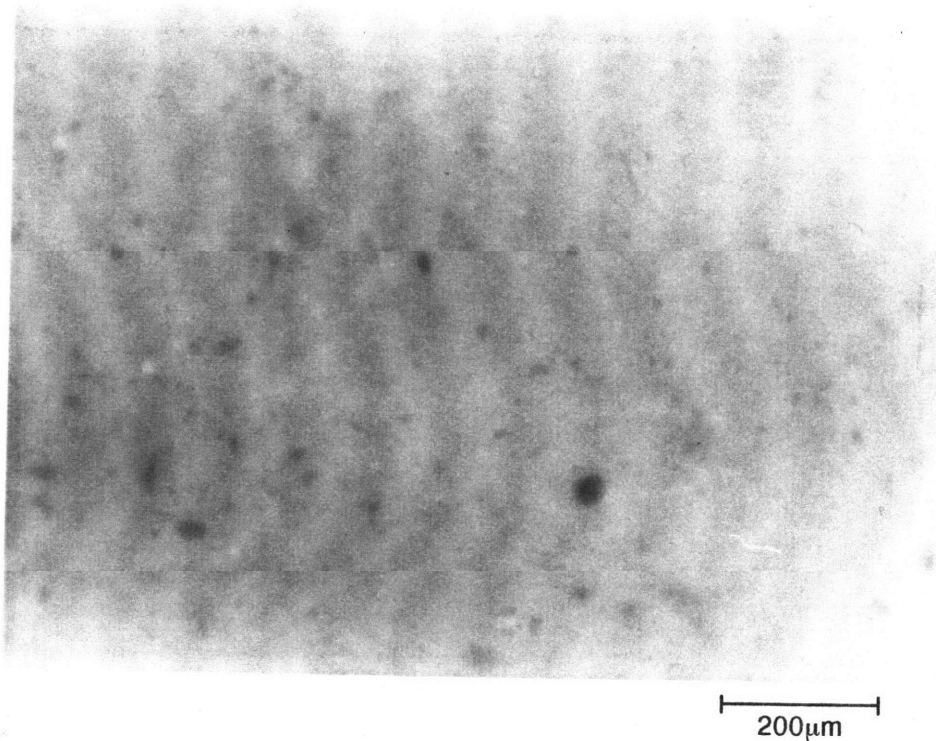
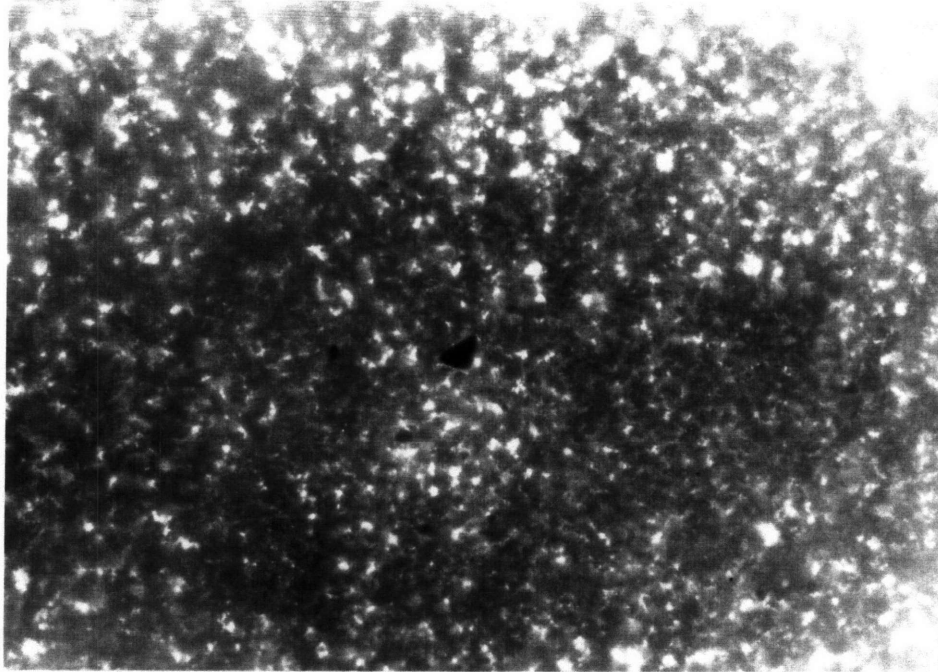


FIGURE 22 : GAR-IgG BEADS + R-IgG 1:0.1 (50µl); 100x
BEAD HEAT TREATMENT 83°C FOR 5 MIN.
NEGLIGIBLE CLUSTERING ∴ EFFECTIVE THERMAL DEACTIVATION

TABLE 4 : PARTIAL THERMAL DEACTIVATION PARAMETERS

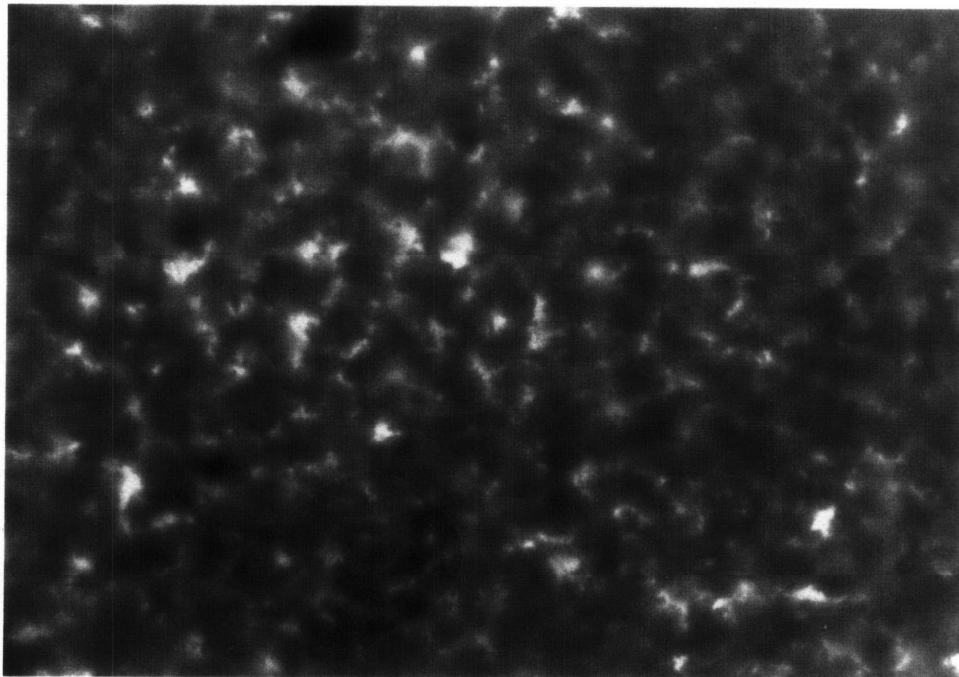
STOCK VOLUME (μ l) @ 0.428 (μ g/ μ l)	GAR-IgG HEAT TREATMENT VOLUME (μ l) @ 0.428 (μ g/ml) TEMP = 83°C TIME (minutes)	R-IgG VOLUME (μ l) @ 0.04 (μ g/ μ l)	RATIO
25	0	25	1:0.1
12.5	12.5	25	1:0.1
12.5	12.5	25	1:0.1

The first entry in Table 4 is the reference or control sample at the 0:0.1 ratio. Figures 23 and 24 are the control photos at 40x and 100x magnification, respectively. In the 5 minute half volume heat treated sample, Figure 25 at 40x, a center region of clustering observed; however, obvious regions of deactivated beads are also seen in the top left and bottom right of the photo. The 100x magnification photo, Figure 26, shows in closer detail the interface between the active (stock) and deactivated (heat treated) beads. The experiment was performed with a heat treatment of 10 minutes for the half bead volume. As seen in Figures 27 and 28, there are again active and deactivated beads but they are not arranged in relatively distinct regions, as seen in Figures 25 and 26. The experiments highlighted the ability for both active and deactivated beads to exist in one sample; thus, demonstrating the specificity of binding of R-IgG to the beads that were not subjected to thermal deactivation. Performing the experiment in 96 well plate utilized the fluid dispersion for ease of agitation to increase the probability of contact between the GAR-IgG beads and R-IgG; however, the active and deactivated regions were intermingled in the fluid. To get selective deposition i.e. distinct regions of thermal deactivation and no thermal deactivation, it was apparent that immobilization of the R-IgG was required.



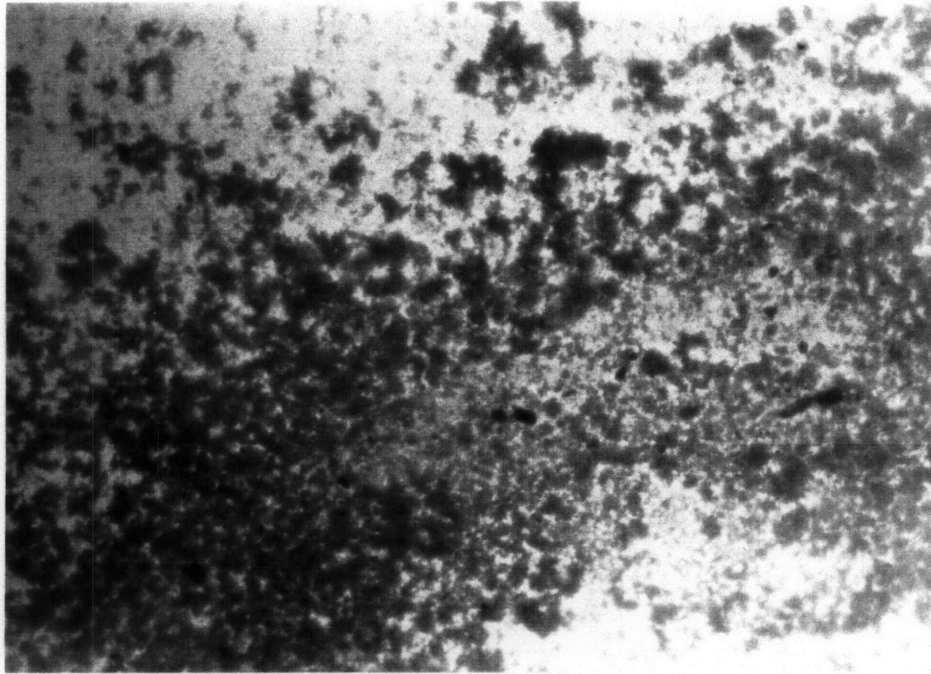
500µm

FIGURE 23 : GAR-IgG BEADS + R-IgG 1:0.1 (50µl); 40x
CONTROL FOR PARTIAL HEAT TREATMENT



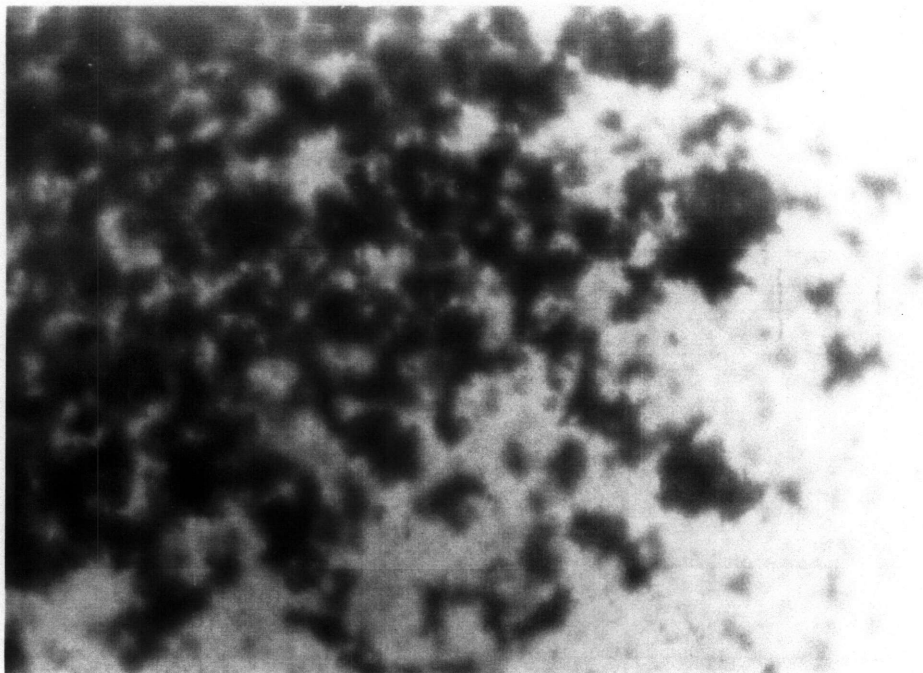
200µm

FIGURE 24 : GAR-IgG BEADS + R-IgG 1:0.1 (50µl); 100x
CONTROL FOR PARTIAL HEAT TREATMENT



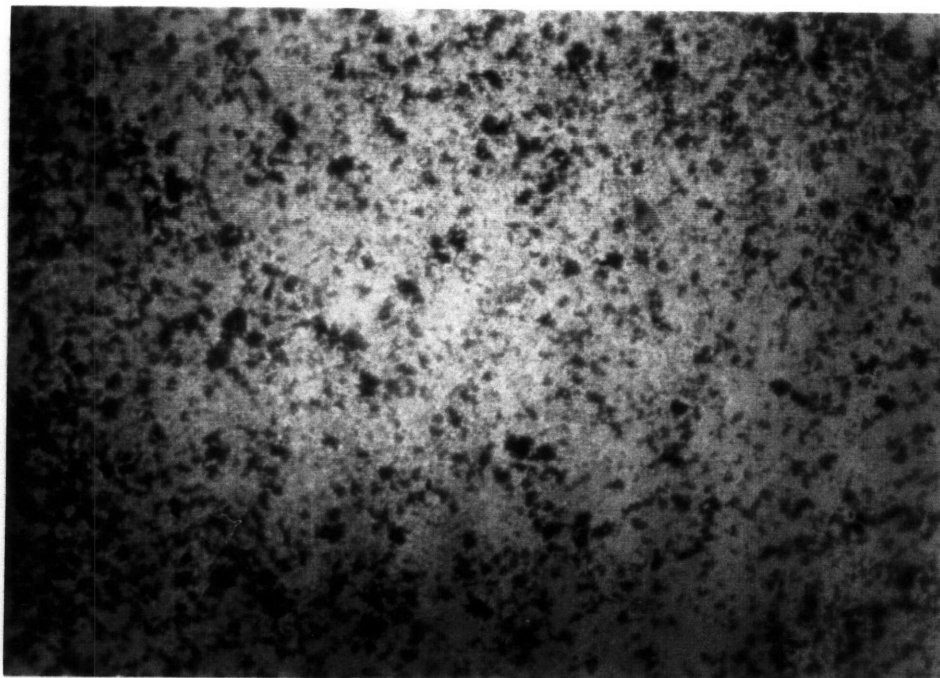
500µm

FIGURE 25 : GAR-IgG BEADS + R-IgG 1:0.1 (50µl); 40x
HALF BEAD VOLUME HEAT TREATMENT 83°C FOR 5 MIN.



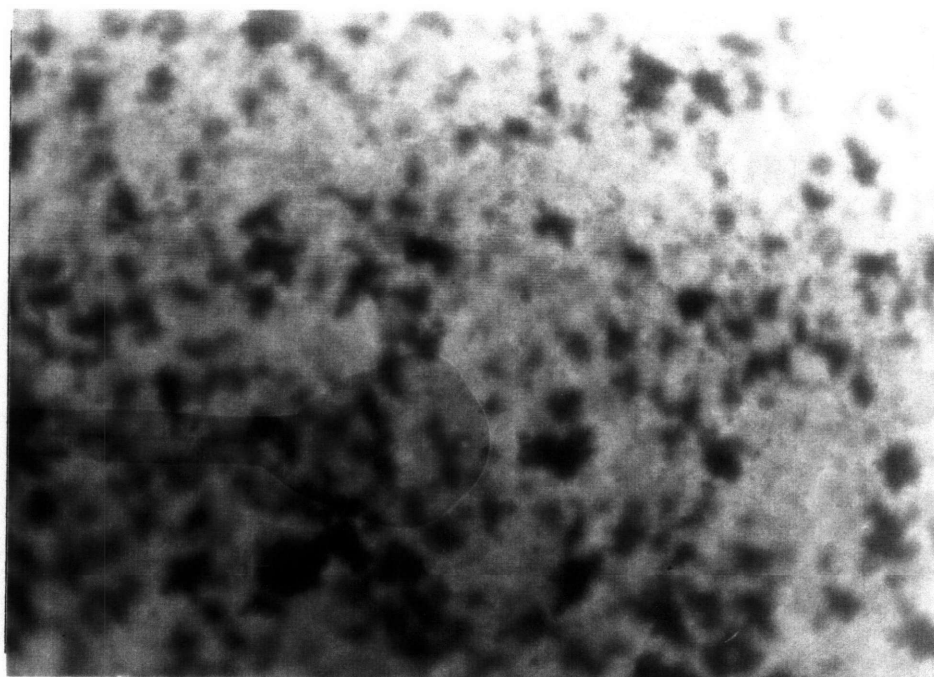
200µm

FIGURE 26 : GAR-IgG BEADS + R-IgG 1:0.1 (50µl); 100x
HALF BEAD VOLUME HEAT TREATMENT 83°C FOR 5 MIN.



500µm

FIGURE 27 : GAR-IgG BEADS + R-IgG 1:0.1 (50µl); 40x
HALF BEAD VOLUME HEAT TREATMENT 83°C FOR 10 MIN.



200µm

FIGURE 28 : GAR-IgG BEADS + R-IgG 1:0.1 (50µl); 100x
HALF BEAD VOLUME HEAT TREATMENT 83°C FOR 10 MIN.

3.3 2D COATING PROCESS

As discussed in the previous section, thermal deactivation was effective in making the agglomeration of R-IgG and GAR-IgG beads selective to only those beads that had not been thermally deactivated. The agglomeration reaction; however, works because it precipitates reactive substrate out of solution but, as seen in Figure 28, does not necessarily make the active and deactivated regions distinct. To get distinct regions of deposition, R-IgG had to be immobilized onto a glass substrate. As discussed in Section 2.2, the immobilization protocol used silane-glutaraldehyde chemistry to attach the R-IgG onto glass.

The glass pieces used to test the effectiveness of the two dimensional (2D) coating procedure were the controls for the thermal deactivation tests. Whenever an array of thermal deactivation experiments was performed, there was always one glass piece not exposed. The unexposed glass was required as a control for comparison and is defined as the R-IgG control. In whatever distribution the beads were placed on the experimental slides, the R-IgG control received the identical treatment; therefore, it was a measure of the effectiveness of the coating procedure as well as a comparative control. The 2D coating process investigation concentrated on establishing a coating protocol and a control deposition standard.

3.3.1 Coating Protocol

The main components of the protocol were to transfer the glass from its storage container into a clean transparent plastic container, add a small amount of PBS designed to maintain hydration of R-IgG and optimize reaction time, pipette beads into the PBS at the air-liquid interface, wait an appropriate time to allow the beads to settle through the PBS level and react with the immobilized R-IgG and wash the glass to remove any unbound beads. The evolution of the protocol was based on addressing these five areas with specific emphasis on the optimization protocol that used microslides to test the effect of varying PBS volume on reaction time.

3.3.1.1 Containment

If the glass is immersed in PBS but the dish was not tailored exactly to the glass dimensions the beads would flow off the slide surface. For all microslide (25mmx75mmx1mm) tests, the PBS was merely pipetted onto the top of the slide because the slide was adequately wetted without the liquid flowing off. This was also true for the 35mmx35mmx3mm black glass pieces but, because of the decreased size of the SEM (150mm²) and 3D layering (20mmx20mmx1mm) pieces, the PBS would not wet the slide without liquid flowing off. In these situations, plastic containers tailored to the glass dimensions were used.

3.3.1.2 Bead Volume

To achieve the maximum coverage of beads onto glass, the total projected area of all the beads should match the surface area of the glass to be covered. Table 6 shows these volume requirements based on the projected area of 1µm diameter beads (0.785µm²).

TABLE 6 : BEAD VOLUMES FOR SURFACE AREA COVERAGE

size	glass	# of beads	volume of GAR-IgG (µl)	
	SA _{glass} (mm ²)		calculated	used
35x35x3	1225	1.56x10 ⁹	68.7	12-15*
25x75x1	1875	2.39x10 ⁹	105	12-15*
20x20x1	400	5.10x10 ⁸	22.4	20
SEM	150	1.91x10 ⁸	8.41	8

* beads applied at regions of interest (i.e. to detect interfaces)

A 25mmx75mmx1mm microslide required 2.39x10⁹ beads or 0.105ml of the total 1ml vial of GAR-IgG beads at around \$100/ml. Given that this is prohibitively expensive for such preliminary work, beads were only placed in regions of interest on the slide and full coverage of the total slide surface area was not attempted. For example, for the continuous hot water jet test, beads would be placed in regions on the slide where the interface was expected. In

this region, 12 to 15 μ l of GAR-IgG beads would be distributed across the width (25mm) of the microslide covering from 8.5mm to 11mm along the length of the slide (Appendix B). For later experiments, SEM and 3D layering, the full coverage bead volume was used because more reasonable sized glass pieces were used. For the optimization tests, 12 μ l of beads were placed at 2 regions on the slides.

3.3.1.3 Washing

The washing of the glass required a water jet that was calibrated to remove unbound beads. Calculations, that are detailed in Appendix B, were based on using data from Cozens-Roberts et al (1990)⁸ in which a Radial Flow Detachment Assay (RFDA) was used to perform quantitative measurement of antibody-antigen bonding force. The resultant force of bonds to the bead required to counter a shearing force and torque imparted on the beads by the passing fluid in the RFDA was determined. Dimensionless expressions for the shearing force and torque were taken from Goldman et al (1967)²⁵ solution of "Slow Viscous Motion of a Sphere Parallel to a Plane Wall - II Couette Flow". Shearing flow was characterized performing mass and momentum balance in the RFDA apparatus. For the referenced system, the bead diameter was 10 μ m. Forces were recalculated for the 1 μ m diameter beads used in the present investigation. The detachment force was calculated to be 1.7x10⁻³ dynes or 1.7x10⁻⁸ N. The detachment velocity was calculated, using a worst case scenario, taking it to be the velocity when the stagnation pressure was equal to the detachment force multiplied by the bead projected area. The detachment velocity was 6.7m/s. The washing apparatus was designed to be safely below this value.

The washing apparatus was a glass bottle with tubing connector at base, 0.25" surgical tubing and connection to 20 gauge (0.035" or 0.889mm) syringe needle. The set up was at an elevation of 27" and a measured flow rate of 0.37ml/s. This is a wash velocity of 0.60m/s which was safely below the 6.6m/s detachment velocity. The washing jet had a laminar portion close to the

outlet and became turbulent as it moves further from the outlet. Care was taken to avoid washing with the turbulent portion of the jet. Generally, for successful washing, a 1mm water level over the slide before washing is desirable and the nozzle should be held at a 45° angle with respect to the slide surface.

3.3.1.4 Protocol Optimization

The protocol optimization test were to determine the best balance between PBS hydration and reaction time. The reaction time was determined by the settling velocity of the polystyrene beads through the height of PBS on the slide surface. As detailed in the Appendix B, the settling velocity was determined by equating the gravitational and buoyancy force balance to the Stokes drag on the spherical particle²⁶.

$$F_{\text{grav}} - F_{\text{buoy}} = D_{\text{Stokes}}$$

$$(\rho_p - \rho_f) \cdot \left(\frac{4\pi a^3}{3} \right) g = 6\pi\mu V_f a \quad \therefore V_f = \frac{2(\rho_p - \rho_f)ga^2}{9\mu}$$

ρ_p = density of the bead = 1.05 g/ml = 1.05x10³ kg/m³

ρ_f = density of liquid = 9.982x10² kg/m³

μ_f = viscosity of liquid = 1.00x10⁻³ kg/m·s

a = radius of bead = 1μm = 1x10⁻⁶ m

g = gravity = 9.81 m/s²

The settling velocity was 1.12x10⁻⁷ m/s. The settling time was determined by dividing the PBS height through which the bead had to settle by the settling velocity. For the microslides, the minimum amount of PBS to add and still cover the whole surface and observe fluid motion was 500μl. Based on the volume of fluid and the surface area of glass to cover, the height of fluid above the slide was determined to be 0.27mm (Appendix B). 40 minutes was calculated to be the settling time for a polystyrene bead to settle down through this height.

Although 500μl was enough to cover the slide it was so minimal that

dehydration was a concern; thus two other PBS volumes were tested:

1ml(0.53mm) and 2ml(1.1mm) with settling times 1 hour and 19 minutes and 2 hours and 44 minutes, respectively.

The extent of reaction was determined by washing the slides at two time intervals : 45 minutes and 2 hours and 30 minutes. The washing was performed using the calibrated nozzle. For all slides, the 45 minute interval was not enough for acceptable deposition. Too many of the beads were disturbed with the pass of the wash nozzle. At the 2 hours and 30 minutes interval acceptable deposition was observed on all samples. To avoid the risk of dehydration, 1 ml PBS volume was selected for the coating protocol. The 500 μ l volume was too minimal to maintain hydration consistently for an extended test time and the 2ml volume was potentially too large and could spill off the side to dehydrate the slide. Because of the varying glass sizes used and the potential for dehydration, the PBS volume requirement was set at a volume that would produce a fluid height of 0.5mm minimum and 1mm maximum. 2 hours was selected because at 2 hours 30 minutes acceptable deposition was observed but the settling time was calculated to be 1 hour 19 minutes, this was a acceptable and easy compromise to reduce test time but still allow for reaction time after the beads had settling to the R-IgG coated glass surface.

3.3.1.5 Protocol

There were 9 basic steps to the coating protocol:

1. Remove the glass from the storage solution
2. Place in a petri dish (25mmx75mmx1mm and 35mmx35mmx3mm) or tailored container (SEM and 20mmx20mmx1mm)
3. Add PBS in volumes to achieve 0.5mm minimum to 1mm maximum fluid height. This requirements are to ensure hydration is easily maintained and to account for meniscus effects in the tailored containers.

25mmx75mmx1mm	1ml
35mmx35mmx3mm	1ml
20mmx20mmx1mm	500 μ l
SEM	100 μ l

4. Add desired amount of beads. Pipette in small amounts too distribute over glass surface. Place pipette tip just into the air -liquid interface.

25mmx75mmx1mm	12-15 μ l at regions of interest
35mmx35mmx3mm	12-15 μ l at regions of interest
20mmx20mmx1mm	20 μ l
SEM	8 μ l

5. Wait 2 hours for settling and reaction. Monitor for dehydration and add additional PBS to the slide if required, care must be taken to rehydrate but not disturb beads.

6. Place into petri dish with distilled water and wash by tipping the dish back and forth 20 times.

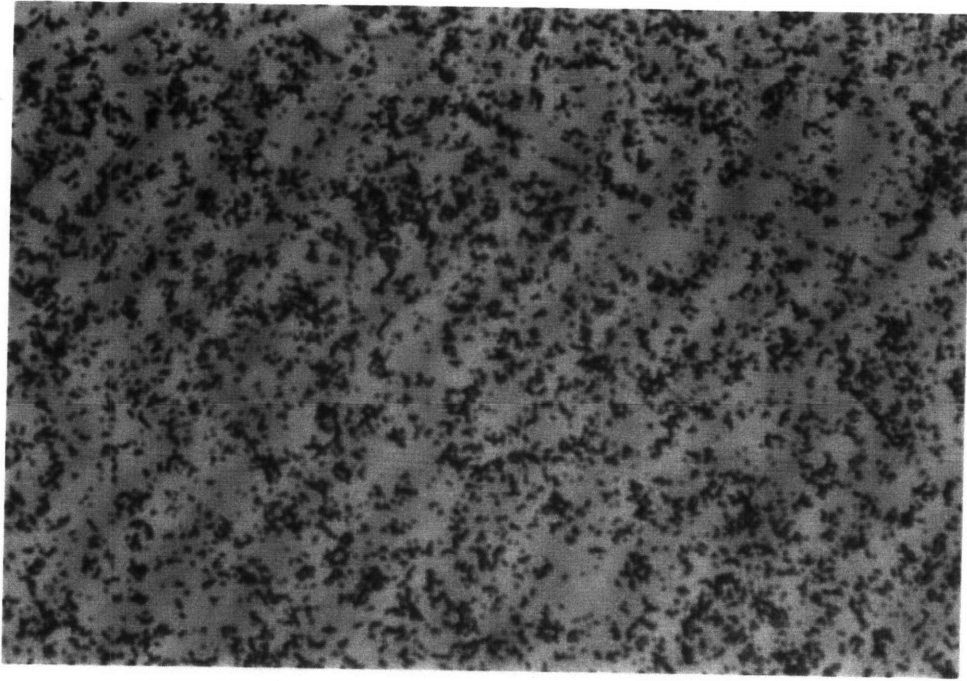
7. Observe in microscope.

8. Wash with distilled water using a nozzle calibrated for unbound bead removal. (20 gauge syringe tip with 0.3-0.4ml/s flow rate)

9. Observe in microscope.

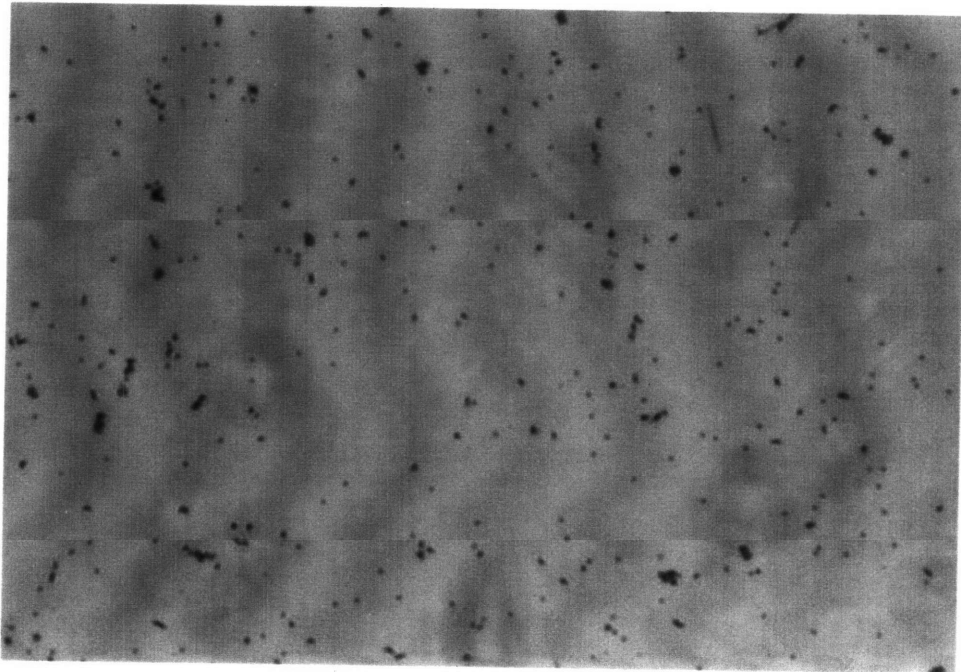
3.3.2 Control Deposition Standard

As detailed previously the R-IgG controls were not only compared with experimentals but were proof that the coating procedure was successful. Figure 29 shows the R-IgG control for the continuous hot water jet experiments. This was a microslide with 19 μ g/cm² surface concentrations and had 12 μ l of beads applied at three regions on the slide. The R-IgG control deposition was the amount of deposition was expected on the active portion of the experimental slides. The deposition was compared to that which occurs when the same amount of beads is applied to a clean glass control, which was a microslide that underwent the only the cleaning portion of the coating protocol. Figure 30 is the glass control and shows the amount of bead deposition expected in deactivated regions of slides. The difference between the glass control and R-IgG control was taken to indicate that a specific reaction had occurred between the immobilized R-IgG and the GAR-IgG beads.



50μm

FIGURE 29 : R-IgG CONTROL; 400x



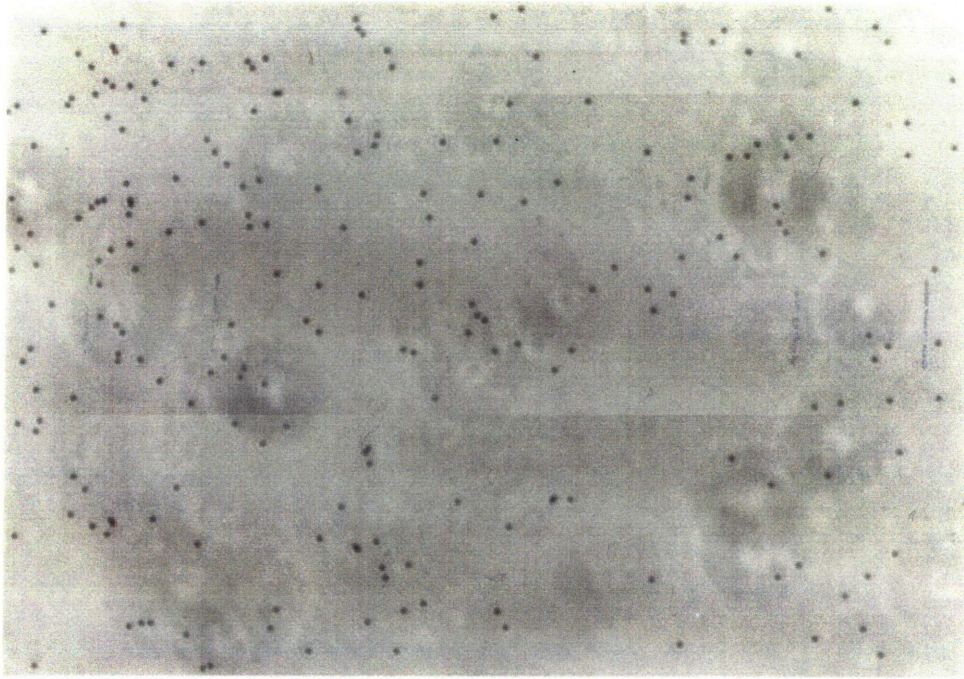
50μm

FIGURE 30 : GLASS CONTROL; 400x

Another series of control tests was to examine the specificity of the GAR-IgG bead reaction with the R-IgG glass surface. The components were both coated and uncoated substrates tested in all possible combinations. The glass substrates were 20mmx20mmx1mm glass pieces where the uncoated glass had undergone the cleaning and buffer storage steps of the protocol and the R-IgG coated glass had undergone the full protocol and attained a surface concentration of $17\mu\text{g}/\text{cm}^2$. The GAR-IgG beads were supplied at 1.25% solids by volume or 2.27×10^{10} beads/ml; the Polybeads[®] were at 2.5% or 4.55×10^8 beads/ml (Appendix A). To achieve maximum coverage, the total bead projected area ($0.785\mu\text{m}^2/\text{bead}$) was targeted to the glass surface area (4.00cm^2). The bead amount selected was 4.54×10^8 beads corresponding to $20\mu\text{l}$ of GAR-IgG stock and $10\mu\text{l}$ of Polybeads[®] stock. The Polybeads[®] were supplied in water and the GAR-IgG beads were supplied in a buffer solution of PBS with 1.0%BSA, 0.1% sodium azide and 5% glycerol. The $10\mu\text{l}$ of Polybeads[®] stock was diluted with $10\mu\text{l}$ of a similar buffer solution, PBS with 1.0%BSA and 0.1% sodium azide. Not only was this step to ensure consistency between the coated and uncoated beads but polystyrene passively adsorbs proteins; thus, the BSA was used to block this reaction. As seen in Figures 31 to 33, the deposition in the cases of BSA passivated Polybeads[®] on uncoated and R-IgG coated glass and GAR-IgG beads on uncoated glass are all similar and minimal. The deposition is substantially greater in the case of GAR-IgG beads on R-IgG glass, Figure 34, which must be a result of a reaction between the GAR-IgG and R-IgG. It follows that any change in the deposition via deactivation is a result of alteration of the GAR-IgG or R-IgG.

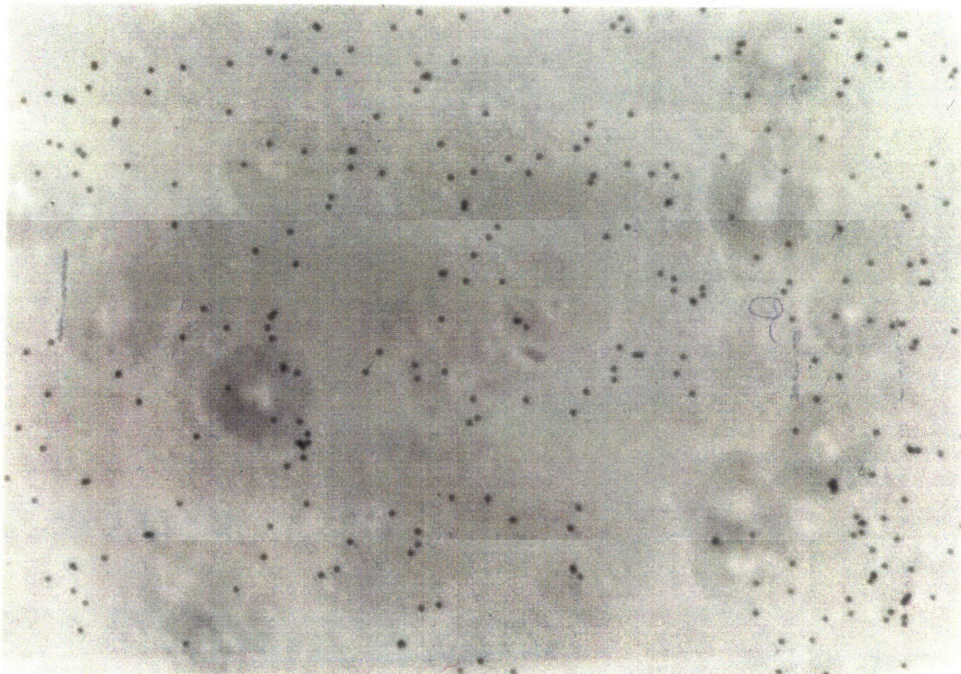
Deposition was abundant enough to reveal specificity and activity of the R-IgG but, ideally, a more uniform and dense deposition was desired. The results of Spitznagel and Clark (1993)²⁷ found that as immobilization loading of a whole antibody (IgA 180000mol.wt.) increased, the binding capacity for large antigen (DNP-Fab 50000mol.wt.) decreased. "These results suggested that at

least some of the immobilized antibody molecules are inactive towards the large antigen due to crowding or orientation effects". In the present investigation, it is possible that the R-IgG antigen (160000mol.wt.) was too crowded on the glass for optimum coverage with the GAR-IgG antibody (160000mol.wt.) coated beads. 20mmx20mmx1mm pieces were used at the original high surface concentration, $17\mu\text{g}/\text{cm}^2$, and a reduced surface concentration, $0.44\mu\text{g}/\text{cm}^2$, to test if decreased crowding would improve the coverage of GAR-IgG beads. Figures 35 and 36 show the results for the two situations. Obviously the improvement is not striking. The desire was that the GAR-IgG deposition would be more uniform and that the void area would be decreased, judging by these criteria the reduced concentration was not an improvement. Higher concentrations were used for the continuous hot water jet tests ($19\mu\text{g}/\text{cm}^2$), laser tests ($16\mu\text{g}/\text{cm}^2$ and $15\mu\text{g}/\text{cm}^2$) but the soldering iron hot water jet tests used both high ($17\mu\text{g}/\text{cm}^2$) and low ($0.44\mu\text{g}/\text{cm}^2$) concentrations.



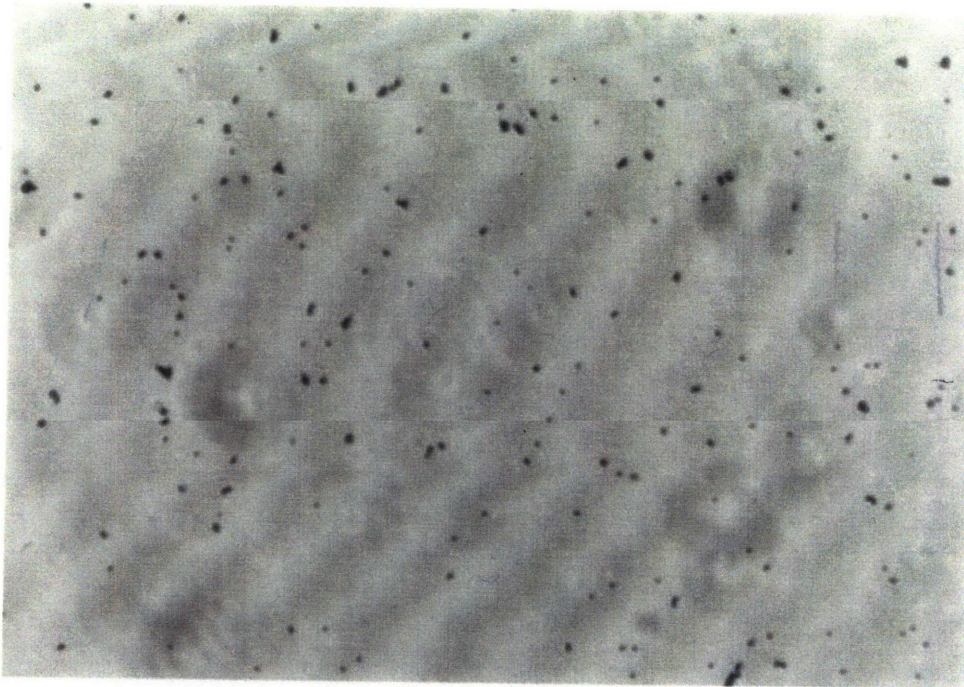
50 μ m

FIGURE 31 : PASSIVATED Polybeads[®] + UNCOATED GLASS; 400x



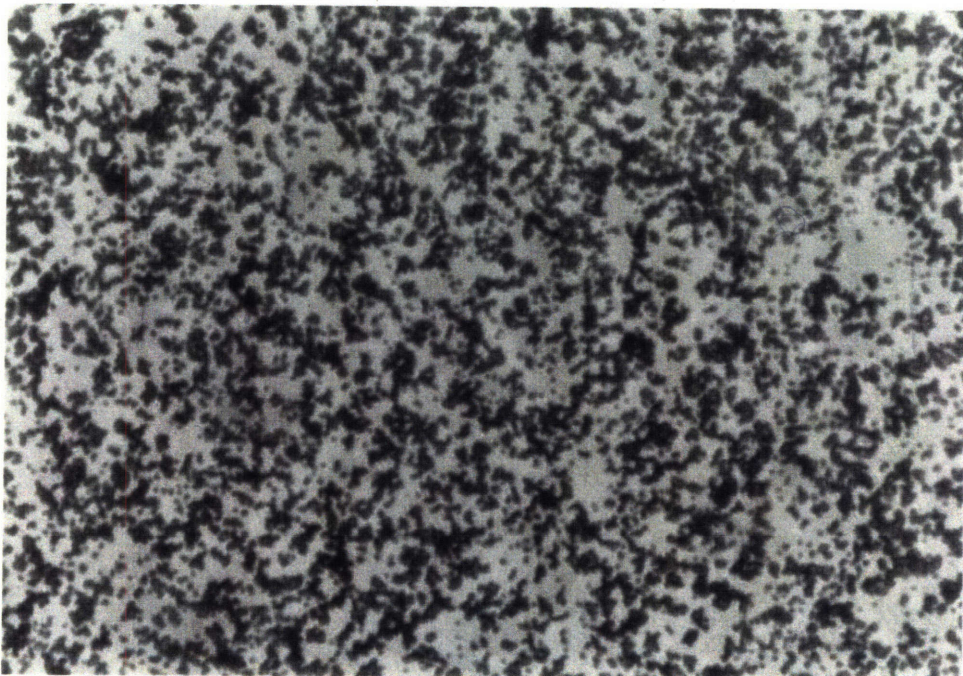
50 μ m

FIGURE 32 : PASSIVATED Polybeads[®] + R-IgG GLASS; 400x



50 μ m

FIGURE 33 : GAR-IgG BEADS + UNCOATED GLASS; 400x



50 μ m

FIGURE 34 : GAR-IgG BEADS + R-IgG GLASS; 400x

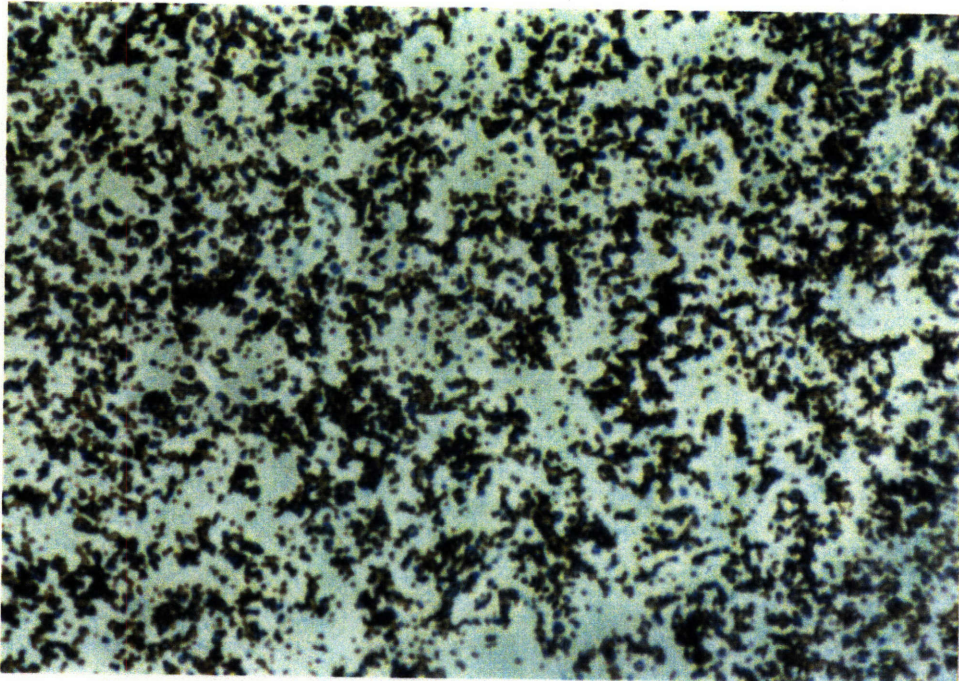


FIGURE 35 : R-IgG CONTROL; 400x
SURFACE CONCENTRATION $17\mu\text{g}/\text{cm}^2$

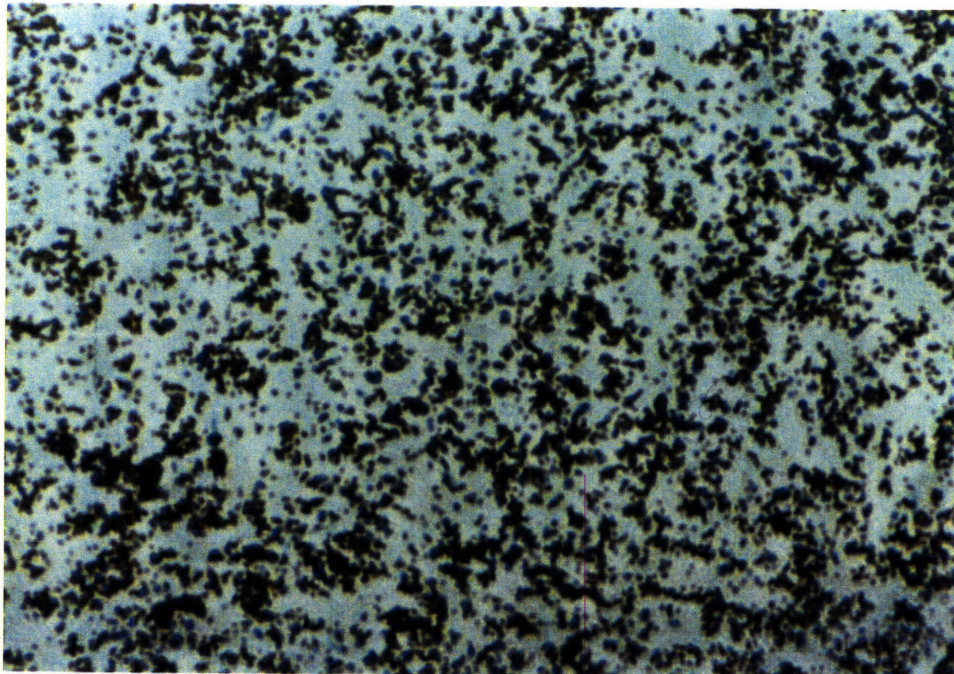


FIGURE 36 : R-IgG CONTROL; 400x
SURFACE CONCENTRATION $0.44\mu\text{g}/\text{cm}^2$

3.4 SELECTIVE DEPOSITION

The goals of the selective deposition investigation were to deactivate the immobilized R-IgG and create local regions of deposition comparable to control depositions.

3.4.1 Immersion

The simple test of the effectiveness of increased temperature on deactivating the immobilized R-IgG was the immersion of half the microslide into a water bath at 98°C. The slide was exposed for 30 seconds keeping the water level at a reference mark on the slide. 13 μ l of GAR-IgG beads were pipetted at the region of interest i.e. the reference mark for the interface. Figure 37 and 38 show the interface of the active and deactivated regions at 20x and 400x, respectively. The active region (Figure 38) is comparable to the R-IgG control (Figure 29) and the deactivated region (Figure 38) is comparable to the glass control (Figure 30). Given this demonstration, the thermal method was successful in deactivating immobilized R-IgG and the focus became to create a thermal delivery method with better resolution and avoid the possibility of secondary steam heating.

3.4.2 Continuous Hot (90°C) Water Jet

The concept of the continuous hot water jet was to directly deliver the hot water to the R-IgG surface constricting the water plume size to create a local deactivated region.

3.4.2.1 Apparatus

The setup for the continuous hot water jet was an elevated 100°C water reservoir taking advantage of gravitational pressure head to force the water through insulated tygon tubing that reduced to a syringe adapter. A variety of tubing diameters and syringe needle gauges were tested in attempts to achieve a 90°C outlet temperature. Requirements were a high enough flow rate so that the temperature did not dissipate but also a small enough outlet so

that the jet plume would not cover the whole surface of the microslide. To achieve a high enough flow rate to maintain water temperature but not drastically increase the outlet flow rate, a T fitting was attached to the tygon tubing immediately before the syringe adapter. In this situation, the water could flow quickly down from its elevated reservoir to the T; thus, maintaining its temperature. Once at the T, the majority of the water bypassed the syringe adapter out the side outlet of the T. In this case, approximately 95°C water entered the syringe adapter.

Now the variable was to select the smallest syringe tip that gave the adequate outlet temperature. Outlet temperature was measured with a thermometer placed in a Styrofoam container that collected the outlet stream. From various preliminary tests at a variety of temperatures, 90°C was determined to be the threshold temperature for adequate deactivation of the immobilized R-IgG. The smallest gauge possible to achieve 90°C was a 16 gauge needle (0.065" or 1.65mm diameter) that produced a plume of approximately 10mm on the 75mm length of the microslide. The 90°C water flow rate was 1.1ml/s which translated into a water velocity of 0.51m/s through the 16 gauge needle (Appendix C).

Although this velocity was well below the detachment velocity for beads, a control experiment was performed observing the effect of this velocity on immobilized R-IgG. A room temperature water jet at the same velocity had no effect on the subsequent deposition of GAR-IgG beads onto the room temperature water jet exposed R-IgG coated slide as seen in Figure 39 and 40. The room temperature water jet control further demonstrates that deactivated regions were produced by thermal and not mechanical mechanisms.

3.4.2.2 Experimental Procedure

The slide was held with forceps, removed from the storage container and subjected to the water stream. The slide was held at a small enough angle to maintain hydration with the residual storage solution of its surface but at a steep enough angle to ensure the water stream ran over and off

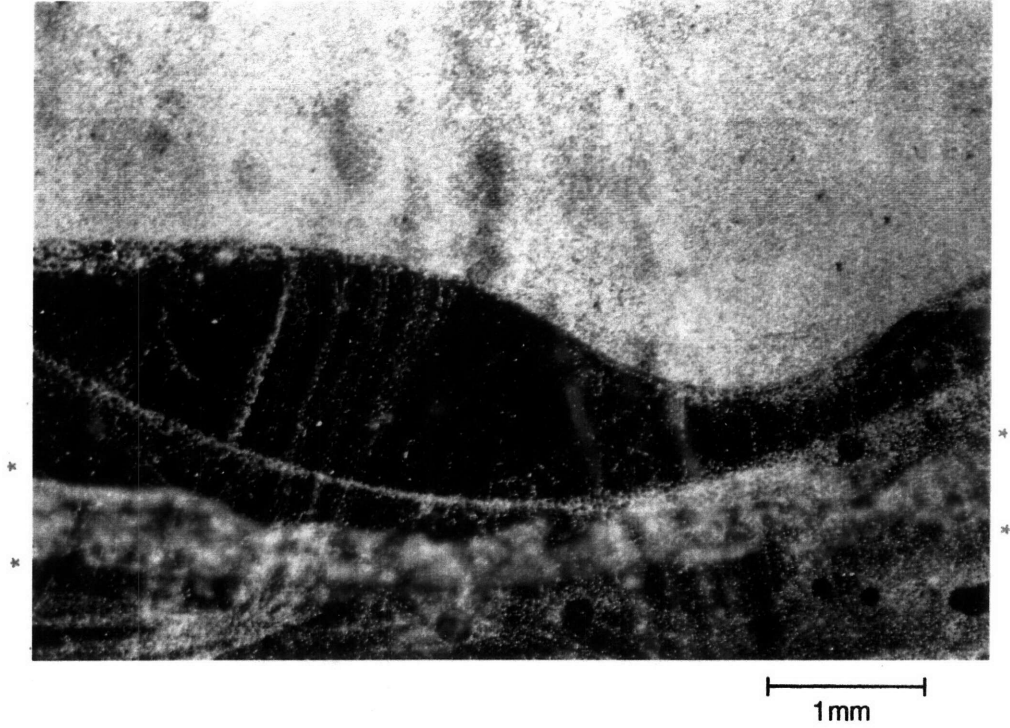


FIGURE 37 : IMMERSION IN 98°C WATER INTERFACE; 20x
EXPOSURE TIME 30 SEC.

* = reference mark (lab marker)

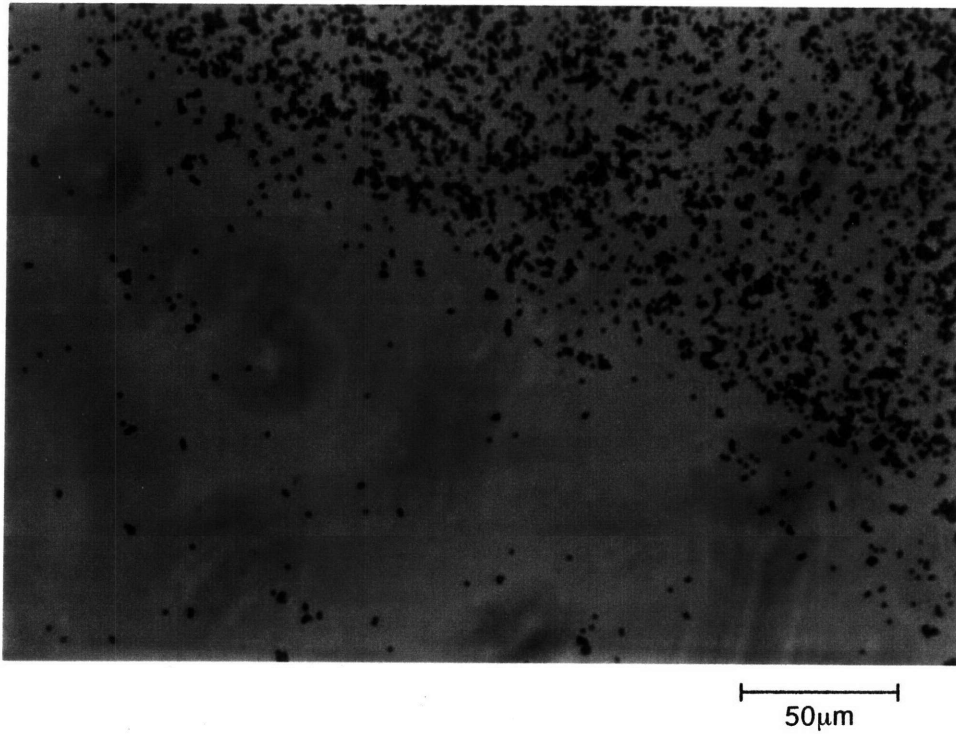
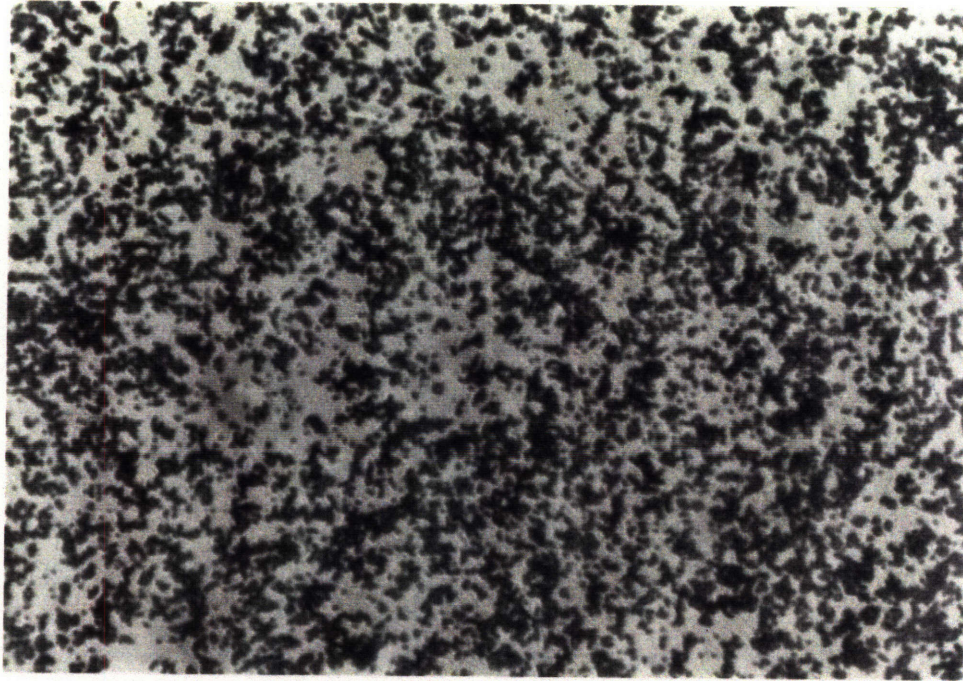
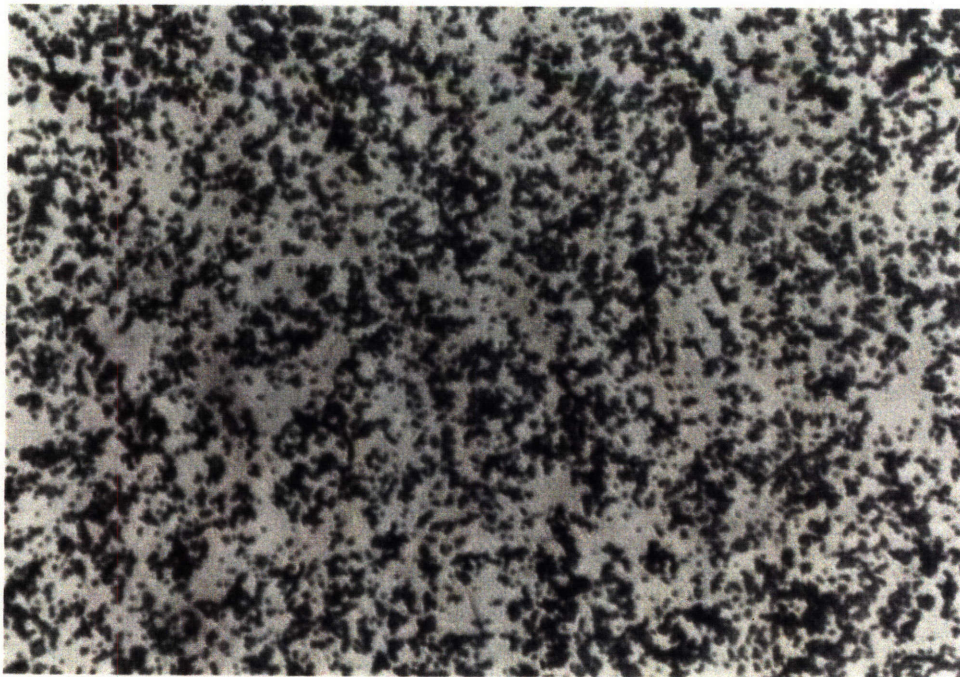


FIGURE 38 : IMMERSION IN 98°C WATER INTERFACE; 400x
EXPOSURE TIME 30 SEC.



50 μ m

FIGURE 39 : CONTINUOUS WATER JET R-IgG CONTROL; 400x



50 μ m

FIGURE 40 : CONTINUOUS WATER JET AT 23°C AND 0.51m/s; 400x
EXPOSURE TIME 1 MIN.

the slide surface. Figure 41 details the steps of the experimental procedure. The coated slide was exposed to the water jet for the desired amount of time; the shaded region represents the extent of the hot water plume and the resulting deactivated region on the microslide. Then, the beads were applied in 12 μ l increments at three regions of interest: (1) right interface, (2) center and (3) left interface. After the 2 hour reaction time, the slide was washed with the calibrated wash nozzle to remove any unbound beads.

3.4.2.3 Results

Figures 42 and 43 show the left interface of a microslide exposed to the 90°C water jet for 1 minute. Similar to the immersion interface, the active region is comparable to the R-IgG control and the deactivated region is comparable to the glass control. Figure 44 and 45 are photos of the deactivated and active regions, respectively, and demonstrate that photos of the distinct active and deactivated regions are equally acceptable proof that deposition is comparable to controls.

The continuous hot water jet tests demonstrated that thermal mechanisms were effective in deactivating R-IgG immobilized to glass. The active and deactivated regions of the glass had GAR-IgG bead deposition comparable to the R-IgG control and glass control, respectively. The performance parameter that required improvement was that the region of temperature increase was not localized enough, plume size was 10mm.

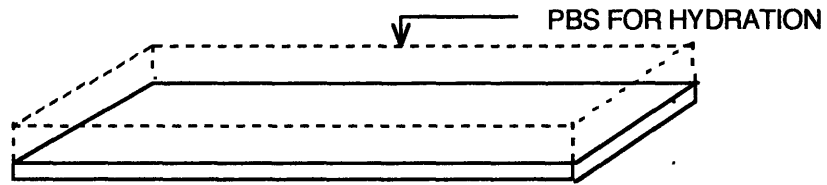
3.4.3 Argon Ion Laser

The laser tests were to reproduce the deposition observed in the continuous hot water jet tests but improve the system resolution to a micron scale.

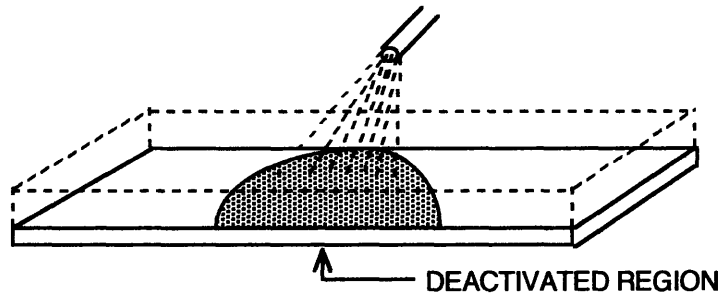
3.4.3.1 Apparatus

As seen in Figure 46, the laser tests were performed using an argon ion laser, SpectraPhysics Stabilite 2016, set for a 488nm wavelength, attenuated to a beam spot size of 12 μ m using a Melles Griot singlet lens.

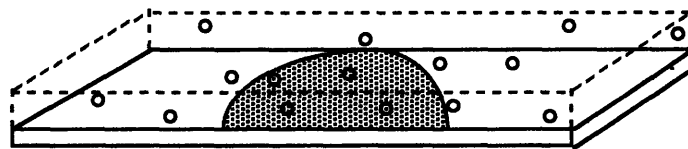
I. COAT SLIDE WITH RABBIT IgG ANTIGEN (R-IgG)



II. LOCALLY HEAT RECEPTOR COATED SLIDE
CONTINUOUS 90°C WATER JET



III. DEPOSIT GOAT ANTI-RABBIT IgG ANTIBODY (GAR-IgG) BEADS



IV. WASH WITH WATER JET CALIBRATED TO REMOVE UNBOUND BEADS

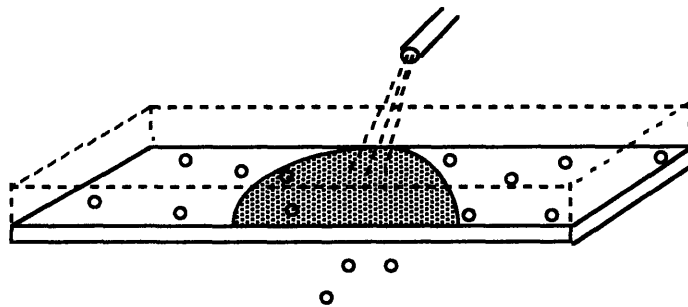


FIGURE : CONTINUOUS 90°C WATER JET
EXPERIMENTAL SCHEMATIC

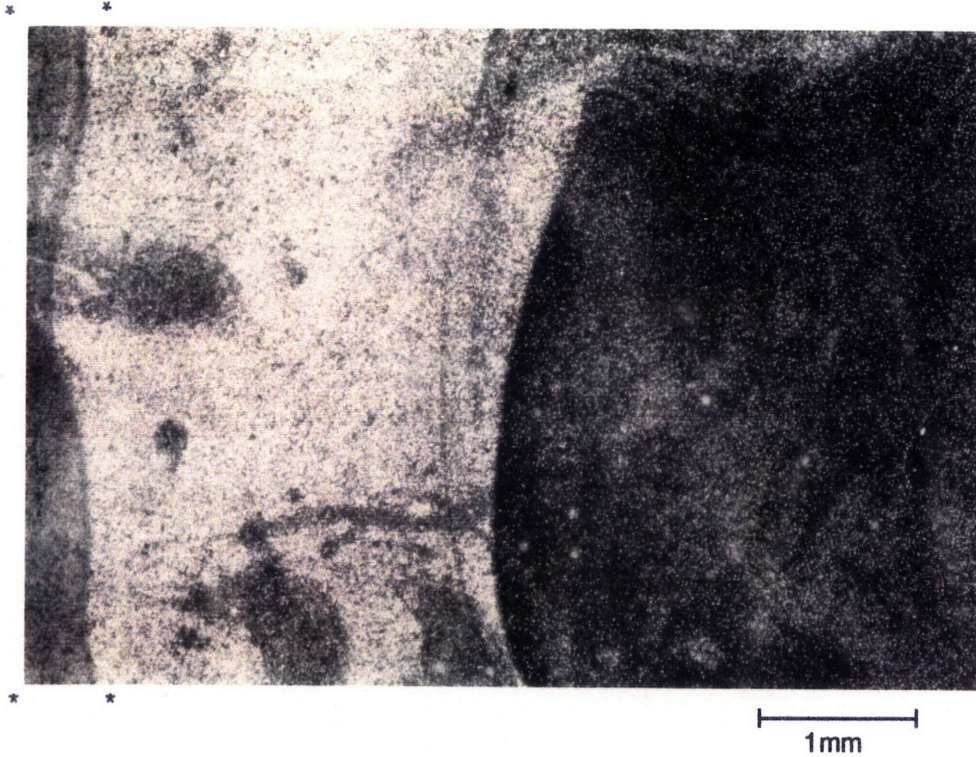


FIGURE 42 : CONTINUOUS 90°C WATER JET DEPOSITION INTERFACE; 20x EXPOSURE TIME 1 MIN. [* = reference mark (lab marker)]

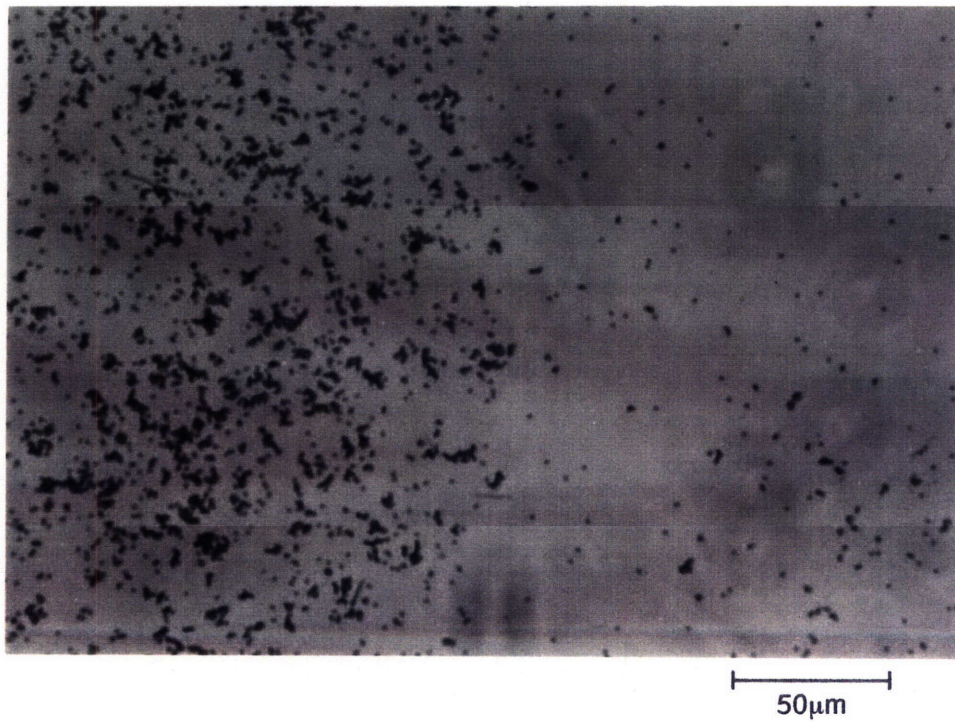
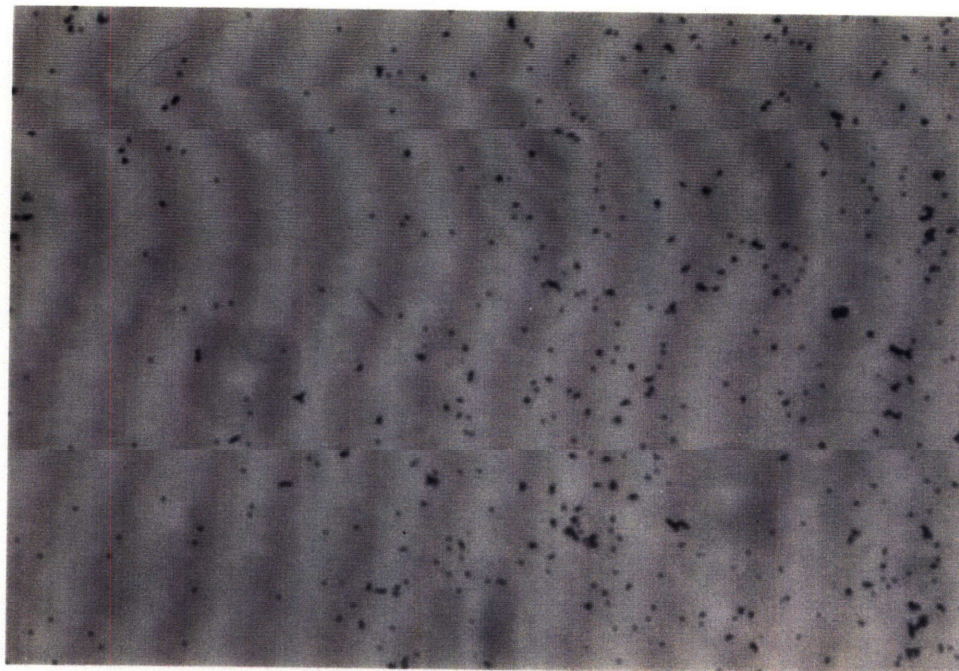
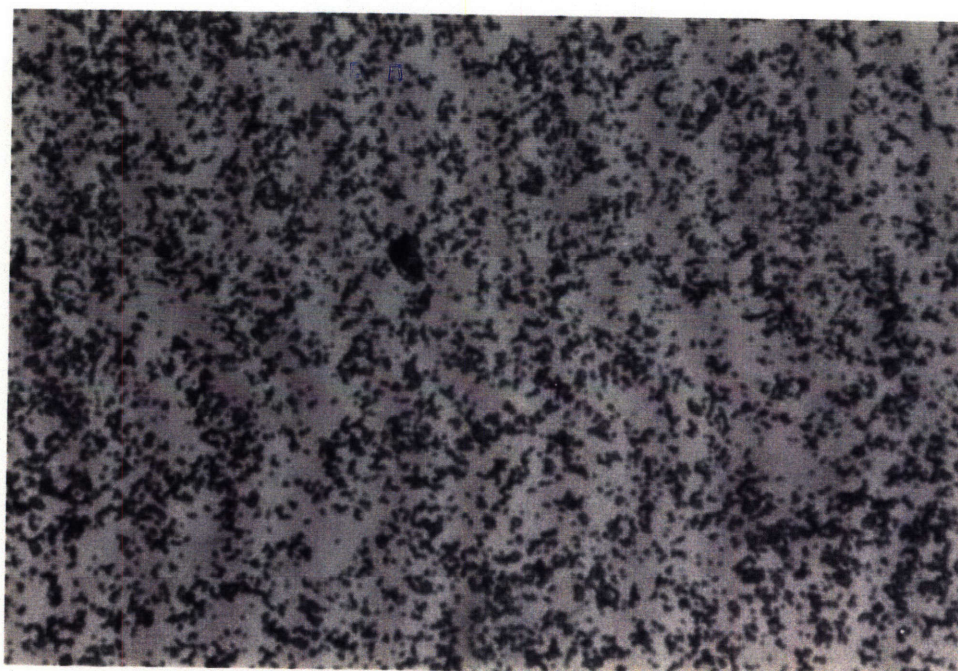


FIGURE 43 : CONTINUOUS 90°C WATER JET DEPOSITION INTERFACE; 400x EXPOSURE TIME 1 MIN.



50 μ m

FIGURE 44 : CONTINUOUS 90°C WATER JET DEACTIVATED REGION; 400x EXPOSURE TIME 1 MIN.



50 μ m

FIGURE 45 : CONTINUOUS 90°C WATER JET ACTIVE REGION; 400x EXPOSURE TIME 1 MIN.

ARGON ION LASER
SpectraPhysics Stabilite 2016
 $\lambda = 488\text{nm}$ and $P_{\text{max}} = 5\text{W}$

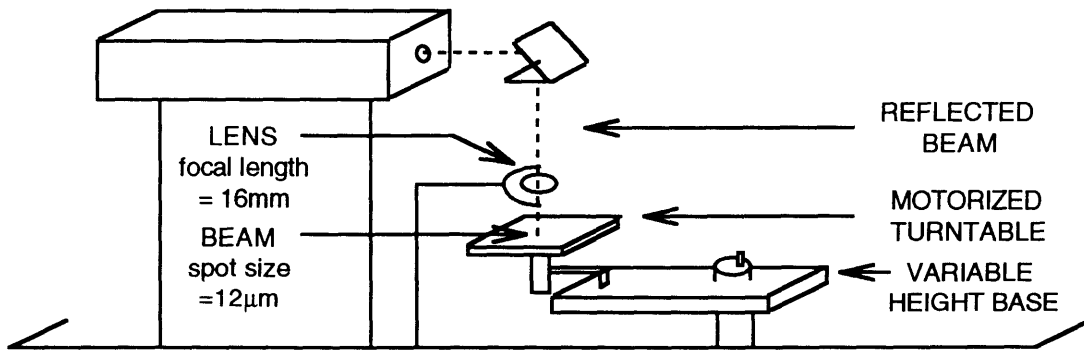


FIGURE 46 : LASER SCHEMATIC

Black glass was used because of its high absorptance of the laser beam; thus, generating the local heating required for the deactivation of the R-IgG. The R-IgG coated 35mmx35mmx3mm or SEM pieces were placed in plastic containers and distilled water was added until a 1mm to 2mm fluid height was visible. The container was then positioned and adhered with double sided tape down to the turntable surface. The turntable was mounted on a variable height base to facilitate the focus operation. Knowing the focal length of the lens to be 16mm, the base was adjusted so that the sample was within the range of focus. The laser was turned on and adjusted to a minimal power setting (0.1W). The height of the sample was adjusted and focus was determined when the beam spot seen on the glass surface looked the brightest. Even with the protective eyewear, the blue-green beam could be seen to become more intense when focus was achieved. The laser was then adjusted to the desired power and focus checked.

3.4.3.2 Experimental Procedure

Glass was traversed under the laser beam at a known speed. Tested speeds were 25 μ m/s, 3cm/s, 6cm/s and 25cm/s. To achieve the 25 μ m/s speed, the sample platform position was adjusted using a micrometer with a motorized rotational attachment. The scan speed was measured timing the micrometer revolutions. The remaining speeds were achieved using a turntable that consisted of a Pitman 19V motor onto which a Plexiglas turntable was fitted. Speed was adjusted using a power supply and the linear speed was calculated based on the rotational speed and the radius at which the beam traversed the glass.

$$V_{lin} = \left[V_{rot} \left(\frac{rev}{s} \right) \right] \cdot \left[2\pi \left(\frac{rad}{rev} \right) \right] \cdot [r(cm)] = \left[1 \left(\frac{rev}{s} \right) \right] \cdot \left[2\pi \left(\frac{rad}{rev} \right) \right] \cdot [4.0(cm)] = 25 \frac{cm}{s}$$

Rotational speed was measured two ways: (1) using a tachometer and (2) timing revolutions. Following exposure with the laser, the R-IgG coated glass was exposed to the GAR-IgG beads and washed following the same procedure used for the continuous hot water jet tests.

3.4.3.3 Results

Laser tests were performed using the 35mmx35mmx3mm black glass samples ($16\mu\text{g}/\text{cm}^2$) and SEM samples ($SA_{\text{glass}} = 150\text{mm}^2$ and $15\mu\text{g}/\text{cm}^2$). The smaller size was required so that the sample could be mounted on the SEM base. Table 6 reveals the array of tests. Power levels and scan speeds were selected to investigate a range of line widths in attempts to achieve micron scale resolution acceptable for a $12\mu\text{m}$ beam spot size. On the 35mmx35mmx3mm samples, line widths were measured using an optical microscope with a calibrated (micrometer) base. The SEM line widths were measured off the SEM photos.

TABLE 6 : LASER TEST SUMMARY

POWER	SPEED	LINE WIDTH (μm)					NOMINAL
		#1 (7/28) 35x35x3	#2 (8/3) 35x35x3	#3 (8/10) 35x35x3	#4 (8/25) SEM	#5(10/28) SEM	
1.9 W	25 $\mu\text{m}/\text{s}$	780 (80)	540 (90)	670			700
	3 cm/s		90		100 \pm 4	97 \pm 5	100
	6 cm/s		50-70				60
	25 cm/s		10 +		27 \pm 2	34 \pm 1 38 \pm 5	40
1.0 W	25 $\mu\text{m}/\text{s}$	340 (70)	N/U (60)	440 (150)			400
	3 cm/s		60		100 \pm 4	110 \pm 5	100
	6 cm/s		20-30				30
	25 cm/s		10 -			19 \pm 1 22 \pm 5	20
0.4W	25 $\mu\text{m}/\text{s}$	100 (10)		500 (90)			100
	3 cm/s		10				10
	6 cm/s		10				10
	25 cm/s		N/V				N/V

N/U = NOT UNIFORM

N/V = NOT VISIBLE

(#) = OUTER LINE WIDTH (INNER LINE WIDTH)

For the 25 $\mu\text{m}/\text{s}$ speed, the majority of the lines has two distinct regions:
 (1) an inner line with minimal deposition and (2) an outer line with greater deposition than the inner line but less than the active region. The 25 $\mu\text{m}/\text{s}$ speed

was not investigated on the SEM samples because of poor resolution 700 μm to 100 μm over the power range.

The 0.4W power level was not high enough for the faster scan speeds. Although 10 μm lines were observed at 3cm/s and 6cm/s, no line was visible at 25cm/s. The 0.4W power level was not further investigated in SEM samples.

In the SEM tests, the parameters investigated were power levels of 1.0W and 1.9W and scan speeds of 3cm/s and 25cm/s. The selected parameters were used to better record results in the tested range and detail the effect of power level and scan speed variation. Whereas the line widths off the 35mmx35mmx3mm samples were measured with the optical microscope and the sample could be kept in the storage buffer, the SEM samples had to be dried to be observed. The SEM samples were washed with the calibrated water nozzle and then stored 24 hours in distilled water. Then the slides were removed from the water and allowed to dry for 24 hours before gold coated for the SEM.

Data listed in the #5 (SEM) column of table were measured off the SEM photos, Figures 47 to 52. At 3cm/s, the system resolution was not as desired; line widths for both 1.0W and 1.9W were on the order of 100 μm : 110 μm (Figure 47) and 97 μm (Figure 48), respectively. However, when the scan speed was increased to 25cm/s, the resolution improved to acceptable levels for a beam spot size of 12 μm : line widths of 19 μm and 34 μm for 1.0W and 1.9W, respectively, measured off 800x magnification photos Figure 50 and 52.

Examining the final column of Table 6, indicating nominal line widths for the tested parameters, the following conclusions can be drawn. At the constant power level, an increase in the scan speed will decrease the line width, except the 3cm/s and 6cm/s line widths remained at 10 μm at 0.4W. At a constant scan speed, a decrease in the power level will decrease the line width, except the 1.0W and 1.9W line widths remained at 100 μm at 3cm/s.



FIGURE 47 : 1.0W AT 3 cm/s; 200x - LINE WIDTH = $110\pm 5\mu\text{m}$

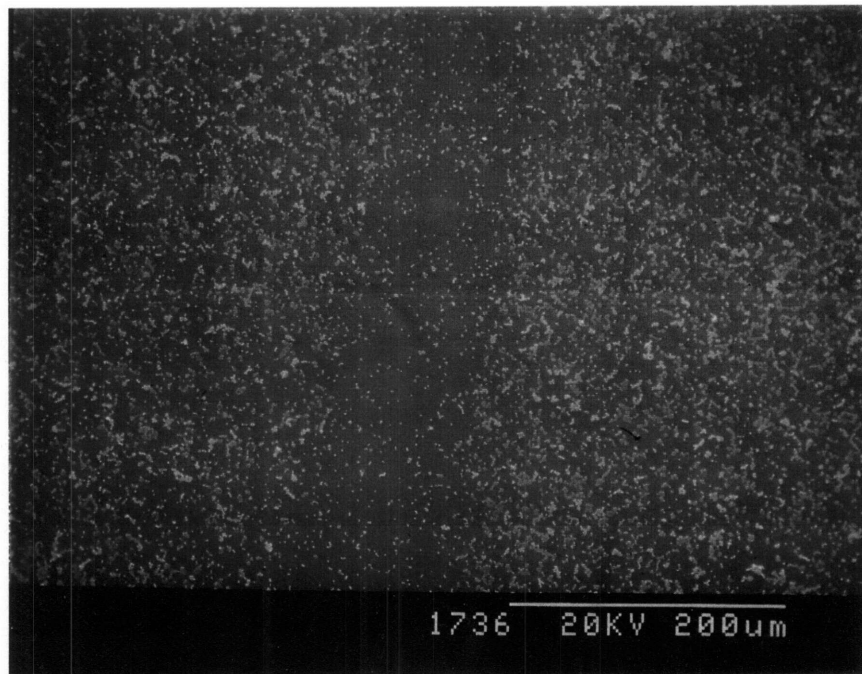


FIGURE 48 : 1.9W AT 3 cm/s; 200x - LINE WIDTH = $97\pm 5\mu\text{m}$

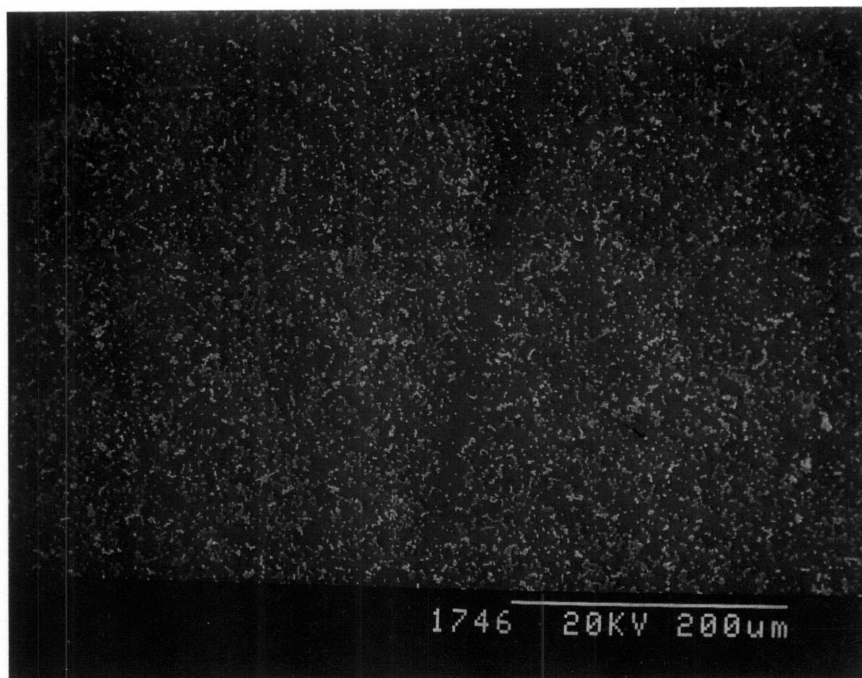


FIGURE 49: 1.0W AT 25 cm/s; 200x - LINE WIDTH = $22\pm 5\mu\text{m}$

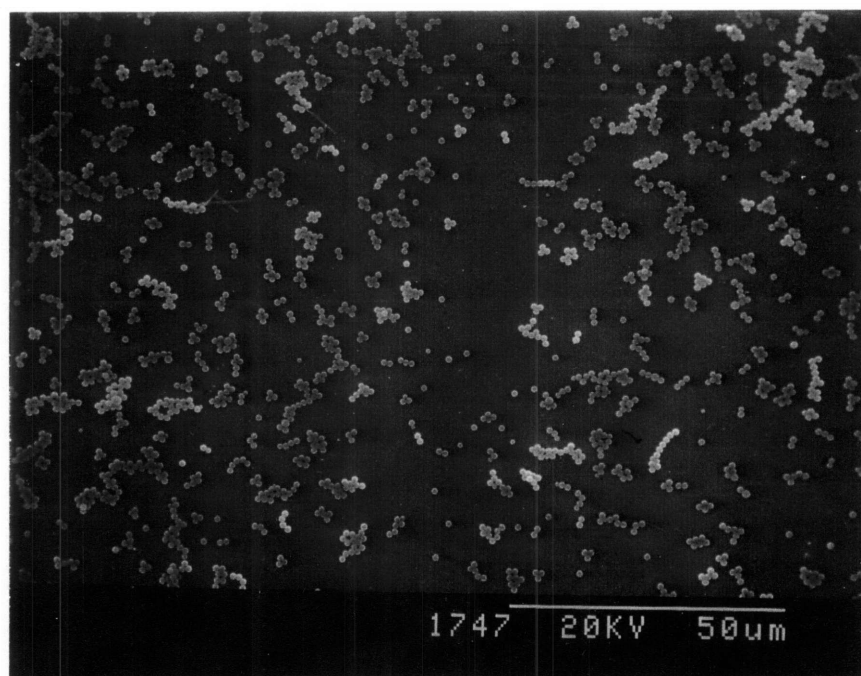


FIGURE 50 : 1.0W AT 25 cm/s; 800x - LINE WIDTH = $19\pm 1\mu\text{m}$

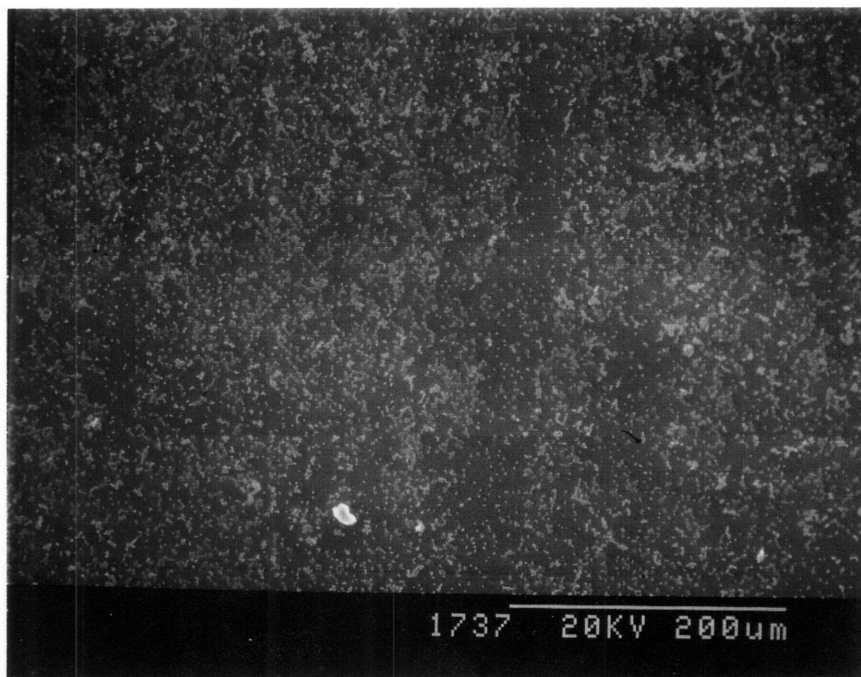


FIGURE 51 : 1.9W AT 25 cm/s; 200x - LINE WIDTH = $38 \pm 5 \mu\text{m}$

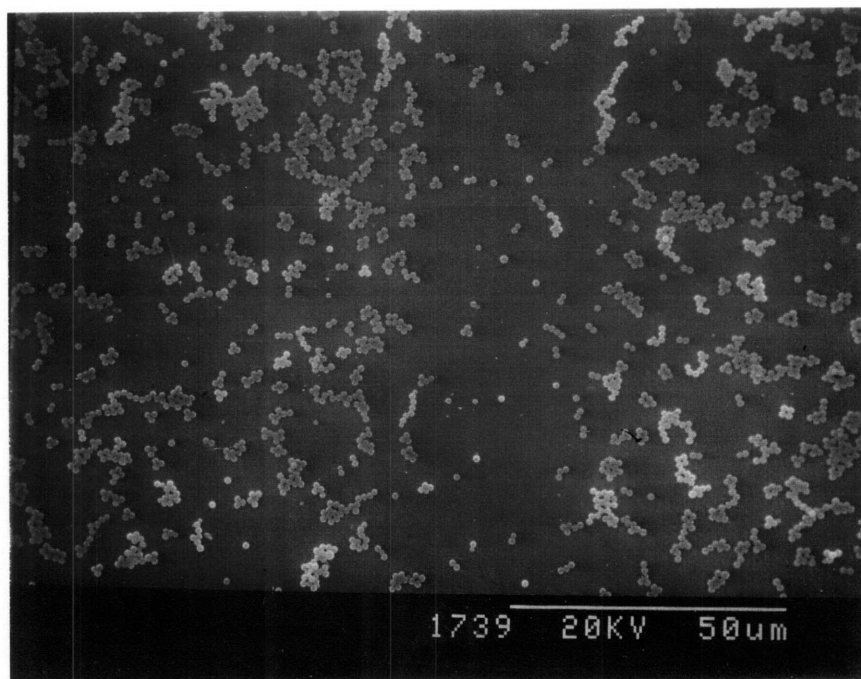


FIGURE 52 : 1.9W AT 25 cm/s; 800x - LINE WIDTH = $34 \pm 1 \mu\text{m}$

The laser tests reproduced the deposition regions observed in the continuous hot water jet tests and demonstrated the system was capable of producing lines with micron scale resolution.

In Tsao (1994)¹, a study that investigated laser induced electroless plating, Photo-Electroforming, used the same laser set up as the present investigation. The author estimated the surface temperature at the laser beam spot and observed a phenomena of microboiling, or generation of hydrogen bubbles. "The estimation shows that the focused laser beam can easily heat up the sample surface to several hundreds of degrees C in less than fractions of a millisecond." As demonstrated by the hot water jet test, only 90°C was required to denature the immobilized R-IgG. As well, the author observed the formation and detachment of hydrogen bubbles with size around 10µm. Because of the potential of microboiling disturbing base layers of beads and the high scan speed required to get ten of microns resolution, the laser thermal deactivation mechanism was not investigated for the production of 3D parts. This in no way suggests that laser thermal or wavelength deactivation methods are ruled out for continuation of the Biolithography process.

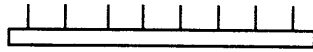
3.5 3D LAYERING PROCESS

The goal of the 3D layering process was to demonstrate the deposition of a second bead layer onto of a first bead layer. Two bead systems were used: (1) both layers of GAR-IgG bead and (2) one layer of GAR-IgG beads and one layer of fluorescent SpA beads.

3.5.1 Goat Anti-Rabbit Immunoglobulin G (GAR-IgG) Second Layer

The two layer parts were constructed using the support of the R-IgG glass base. The 20mmx20mmx1mm glass pieces were used because tailored containers were available to contain the bead volume for maximum coverage. As seen in Figure 53, the concept was to use the R-IgG glass as the base for the first layer of GAR-IgG beads (step 1), then add a second layer of GAR-IgG beads (step 2) and, finally, add R-IgG solution to flow through the layers and link the GAR-IgG beads together (step 3). The other option shown was to add the R-IgG after the first layer (step 2) to bind to the GAR-IgG beads to make them active to bind with the second layer of GAR-IgG beads (step 3).

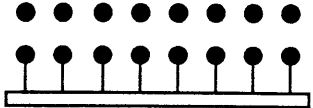
The 20mmx20mmx1mm glass pieces had a surface concentration of $17\mu\text{g}/\text{cm}^2$ which corresponds to 2.56×10^{14} R-IgG on the surface. The next step was the addition of the GAR-IgG beads. To cover the surface area of the piece (400mm^2), 4.54×10^8 GAR-IgG beads were used as detailed in Section 3.3.1.2. Taking the number of beads and multiplying by 6.52×10^4 GAR-IgG per beads, the total number of GAR-IgG was 2.96×10^{13} . The variable in the 3D layering process was the amount of R-IgG to add (Appendix D). The stock R-IgG was an aliquot of $500\mu\text{l}$ at $1\text{mg}/\text{ml}$ which contains 1.88×10^{15} R-IgG. Given that the amount of R-IgG on the slide was 2.56×10^{14} , the R-IgG levels used were approximately 2×10^{15} , 2×10^{14} and 2×10^{13} to get order of magnitude differences. The 2×10^{15} test actually used 1.88×10^{15} R-IgG as this was the amount in one $500\mu\text{l}$ aliquot. For the 2×10^{14} value, $68\mu\text{l}$ was used as this was equal to 2.56×10^{14} R-IgG that was identical to the R-IgG immobilized onto the slide. For the 2×10^{13} value, the amount of GAR-IgG on the beads was considered. The



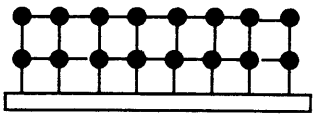
RABBIT IgG COATED GLASS



STEP 1
ADD GOAT ANTI-RABBIT IgG BEADS
LET SETTLE FOR 2 HOURS
WASH WITH CALIBRATED WATER NOZZLE

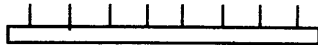


STEP 2
ADD GOAT ANTI- RABBIT IgG BEADS
LET SETTLE FOR 2 HOURS



STEP 3
ADD RABBIT IgG IN SOLUTION
LET SETTLE FOR 2 HOURS
WASH WITH CALIBRATED WATER NOZZLE

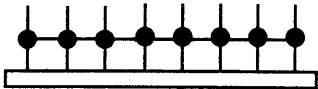
I. STEP 3 ADDITION OF R-IgG



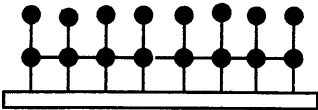
RABBIT IgG COATED GLASS



STEP 1
ADD GOAT ANTI-RABBIT IgG BEADS
LET SETTLE FOR 2 HOURS
WASH WITH CALIBRATED WATER NOZZLE



STEP 2
ADD RABBIT IgG IN SOLUTION
LET SETTLE FOR 2 HOURS



STEP 3
ADD GOAT ANTI-RABBIT IgG BEADS
LET SETTLE FOR 2 HOURS
WASH WITH CALIBRATED WATER NOZZLE

II. STEP 2 ADDITION OF R-IgG

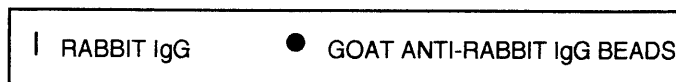


FIGURE 53 : GAR-IgG + GAR-IgG TWO LAYER CONSTRUCTION

GAR-IgG value was 2.96×10^{13} ; however, visualizing the beads, assume half of the GAR-IgG bond to the R-IgG glass and half is available for the second layer. Obviously this neglects the contact area issue that not all GAR-IgG on the beads will be able to reach to surfaces to bind but is acceptable for this volume order of magnitude approximation. Therefore, half of the GAR-IgG amount was 1.48×10^{13} which corresponds to $4 \mu\text{l}$ of the R-IgG stock. The test regimes for the 3D GAR-IgG tests were to test the three orders of magnitude as well as the order of component application, Table 7.

TABLE 7 : TWO LAYER GAR-IgG CONSTRUCTION OPTIONS

ORDER OF MAGNITUDE OF R-IgG	STEP 1	STEP 2	STEP 3
2×10^{15}	GAR-IgG @ $20 \mu\text{l}$	R-IgG @ $500 \mu\text{l}$	GAR-IgG @ $20 \mu\text{l}$
2×10^{14}	GAR-IgG @ $20 \mu\text{l}$	R-IgG @ $68 \mu\text{l}$	GAR-IgG @ $20 \mu\text{l}$
2×10^{13}	GAR-IgG @ $20 \mu\text{l}$	R-IgG @ $4 \mu\text{l}$	GAR-IgG @ $20 \mu\text{l}$
2×10^{14}	GAR-IgG @ $20 \mu\text{l}$	GAR-IgG @ $20 \mu\text{l}$	R-IgG @ $68 \mu\text{l}$
2×10^{13}	GAR-IgG @ $20 \mu\text{l}$	GAR-IgG @ $20 \mu\text{l}$	R-IgG @ $4 \mu\text{l}$

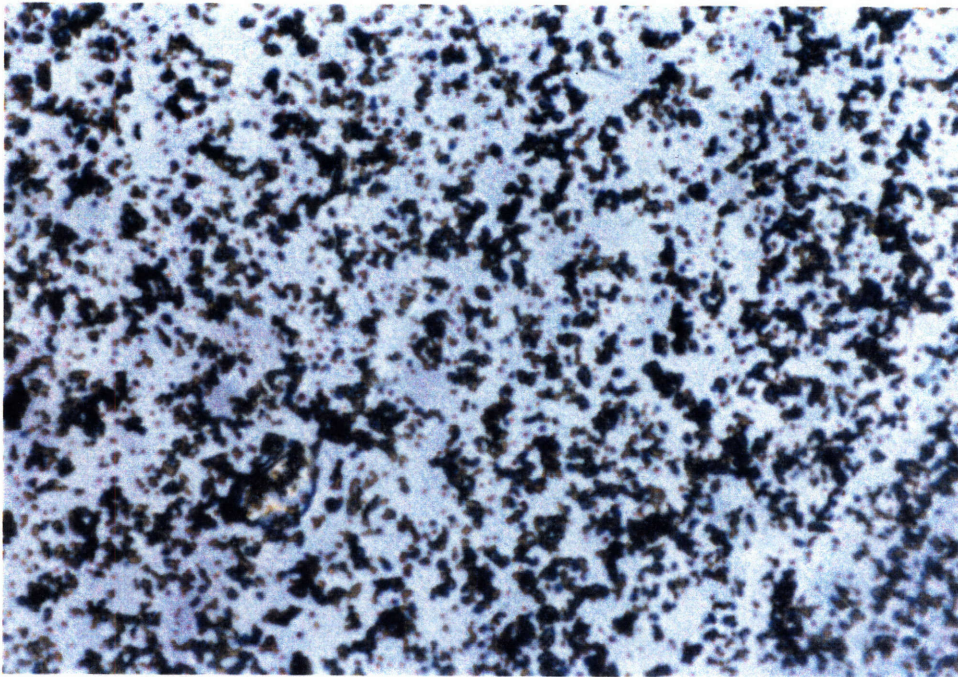
In the tests where the addition of the R-IgG was step 2, Figure 53.II, it was postulated that the R-IgG would bind down to the first layer of GAR-IgG beads and make an active base for the second layer of GAR-IgG beads. Unfortunately, the R-IgG did not bond to the first layer as desired because upon addition of the second layer of GAR-IgG beads clustering of the GAR-IgG beads was visible. With mild movement of the container, it was obvious that the clusters did not bind down. The 2×10^{13} sample had the largest and most mobile clusters and the 2×10^{15} sample had the smallest and least mobile clusters. When the samples were washed, all orders of magnitude had similar deposition that revealed an inadequate second layer had bound down. The 2×10^{13} sample Figure 54 and 55, first layer and second layer, is shown as representative deposition for all magnitude tests with step 2 addition of R-IgG.

The samples where the GAR-IgG second layer was step 2 and the R-IgG flowed through in step 3 produced the best results, Figure 53.I. The 2×10^{13} magnitude produced the best second layer, more deposition than 2×10^{14} . Similar to the agglomeration tests, the lower concentration allowed for better linking. Figures 56 and 57, first layer and second layer, are for the 2×10^{13} sample with step 3 addition of R-IgG. The increases deposition is obvious when compared to the step 2 addition of R-IgG.

Because of the success of the step 3 addition of R-IgG (Figure 57) over the step 2 addition of the R-IgG (Figure 55), step 3 addition of R-IgG was used in all following procedures.

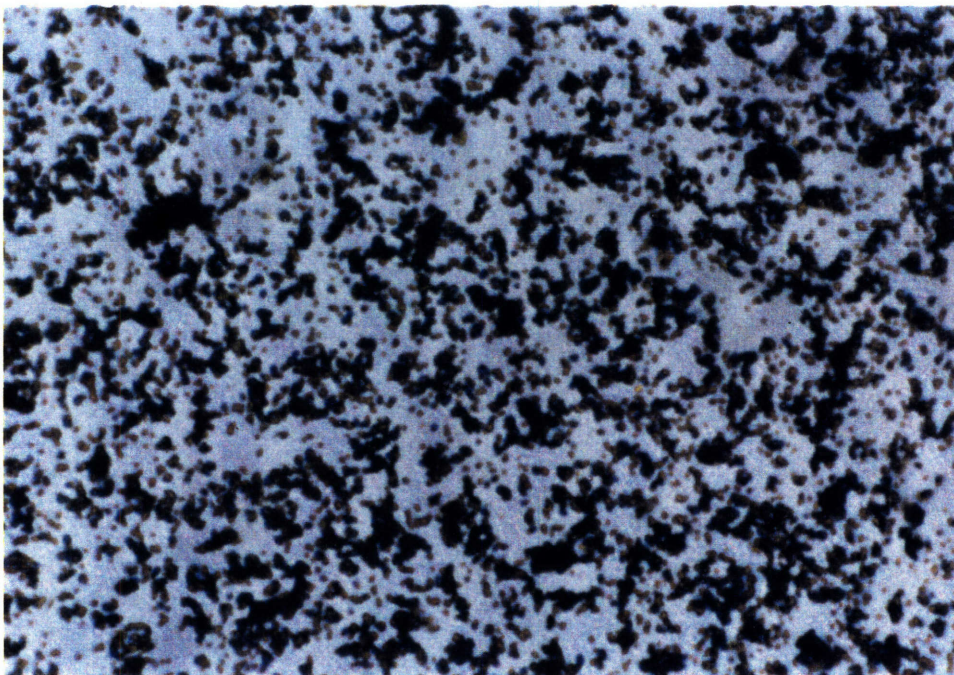
3.5.2 Protein A (SpA) Second Layer

Although the deposition difference was obvious, the judgment of the deposition of a second layer was difficult. For a more instructive test, the second layer added was Fluoresbrite™ SpA beads, Figure 58. In this situation the presence of the fluorescent SpA beads above the blue GAR-IgG beads indicates deposition of the second layer. The SpA second layer was 20 μ l for surface area coverage. Although the SpA and GAR-IgG do react together without the addition of R-IgG, preliminary tests revealed that the addition of R-IgG as a linker between the GAR-IgG and SpA improved deposition. Similar to the GAR-IgG calculation, multiplying number of beads by the protein density per bead (6.30×10^4 SpA/bead), gave the total number of SpA added as 2.86×10^{13} . The SpA value, 2.86×10^{13} was close enough to the GAR-IgG value, 2.96×10^{13} , that the order of magnitude R-IgG volumes were not altered. Table 8 reveals the tested combinations.



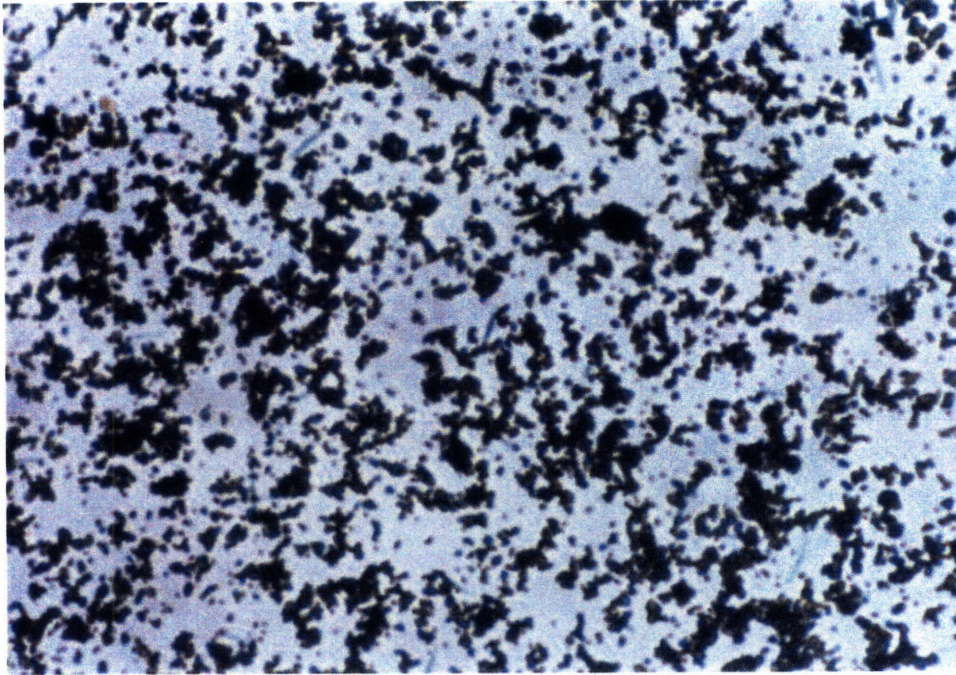
50μm

FIGURE 54 : STEP 2 ADDITION OF R-IgG - FIRST LAYER; 400x



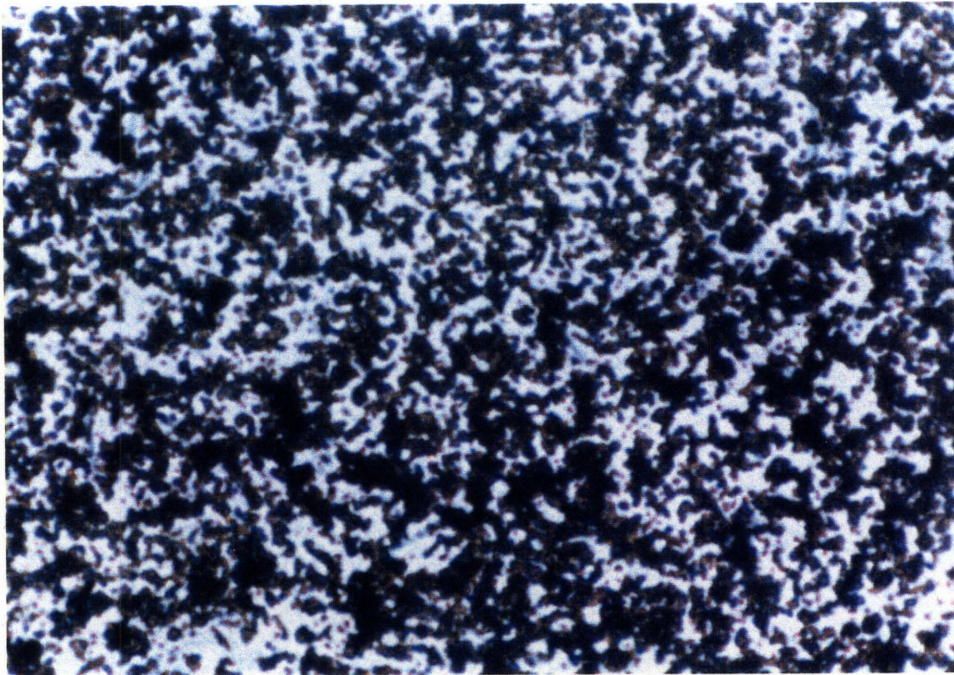
50μm

FIGURE 55 : STEP 2 ADDITION OF R-IgG - SECOND LAYER; 400x



50µm

FIGURE 56 : STEP 3 ADDITION OF R-IgG - FIRST LAYER; 400x

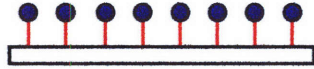


50µm

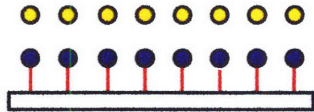
FIGURE 57 : STEP 3 ADDITION OF R-IgG - SECOND LAYER; 400x



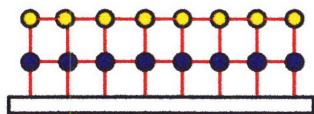
RABBIT IgG COATED GLASS



ADD GOAT ANTI-RABBIT IgG BLUE DYED BEADS
LET SETTLE FOR 2 HOURS
WASH WITH CALIBRATED WATER NOZZLE



ADD PROTEIN A FLUORESBRITE BEADS
LET SETTLE FOR 2 HOURS



ADD RABBIT IgG IN SOLUTION
LET SETTLE FOR 2 HOURS
WASH WITH CALIBRATED WATER NOZZLE

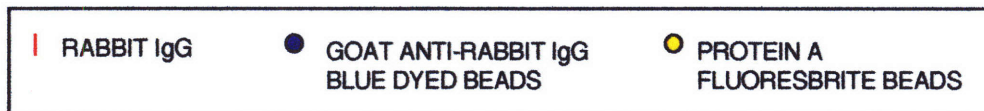


FIGURE 58 : GAR-IgG + SpA TWO LAYER CONSTRUCTION

TABLE 8 : TWO LAYER GAR-IgG + SpA CONSTRUCTION OPTIONS

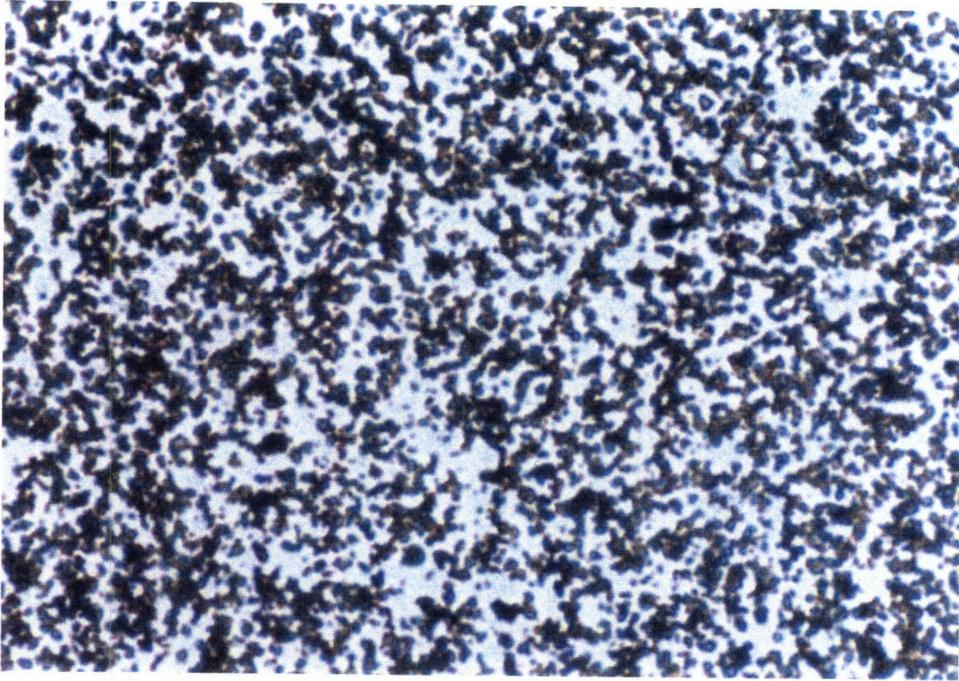
ORDER OF MAGNITUDE OF R-IgG	STEP 1	STEP 2	STEP 3
2X10 ¹³	SpA @ 20μl	GAR-IgG @ 20μl	R-IgG @ 4μl
2X10 ¹³	GAR-IgG @ 20μl	SpA @ 20μl	R-IgG @ 4μl
2X10 ¹⁴	GAR-IgG @ 20μl	SpA @ 20μl	R-IgG @ 68μl

A preliminary test made SpA the first layer to see if the second layer of GAR-IgG would block out the fluorescent SpA as proof of second layer deposition. As seen in Figures 59 to 64, both the 400x and 200x color photos indicate the deposition of GAR-IgG beads but the fluorescent photos do not appear any dimmer. For the SpA second layer, both 2x10¹⁴ and 2x10¹³ magnitudes were tested and found to have similar second layer deposition.

The 2x10¹³ magnitude i.e. when the first GAR-IgG layer was followed by the SpA layer and then 4μl of R-IgG was allowed to flow through and link the GAR-IgG and SpA layer, was selected as the control. Figures 65 and 66 show the 200x magnification color and fluorescent photos for the GAR-IgG first layer. The fluorescent first layer photo shows only black because no fluorescent beads were present. Figures 67 and 68 show quite convincingly the deposition of the Fluoresbrite™ SpA beads. Further documentation of the second layer deposition is shown in the 400x magnification photos, Figure 69 to 71. The arrow indicates a locator landmark to orientate the second layer photos with respect to the first layer photos. The color second layer and fluorescent second layer photos were taken one after the other without moving the sample. The locator and various other landmarks were used to compare the three photos overlaying the first layers landmarks. Taking into account the micron size of the beads and the limits of the method of observation, the encircled region is a sample area that indicate that SpA beads may have deposited on top of previously deposited GAR-IgG beads. Obviously from the first to second layer photos, the SpA beads did deposit in the void areas of the first layer because SpA can bind to R-IgG. However, the SpA does

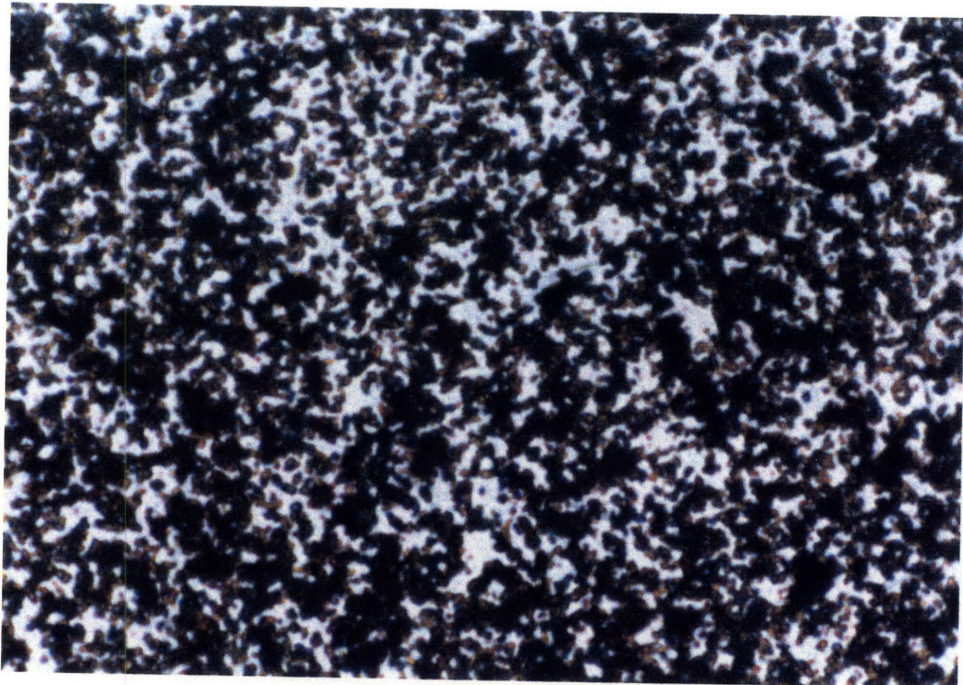
bind to GAR-IgG and the SpA beads could have been orientated to deposit on top of the GAR-IgG beads, as detailed in the encircled regions of Figures 69 to 71. Specifically, SpA beads appear to have deposited on top of the hourglass shaped GAR-IgG bead deposition in the encircled region.

For reference , the deposition shown for the SpA second layer with step 3 addition of 4 μ l R-IgG, Figure 71, is the control deposition for the active regions in all 3D selective definition of geometry parts.



50µm

FIGURE 59 : SpA FIRST LAYER; 400x



50µm

FIGURE 60 : GAR-IgG SECOND LAYER ON SpA FIRST LAYER; 400x

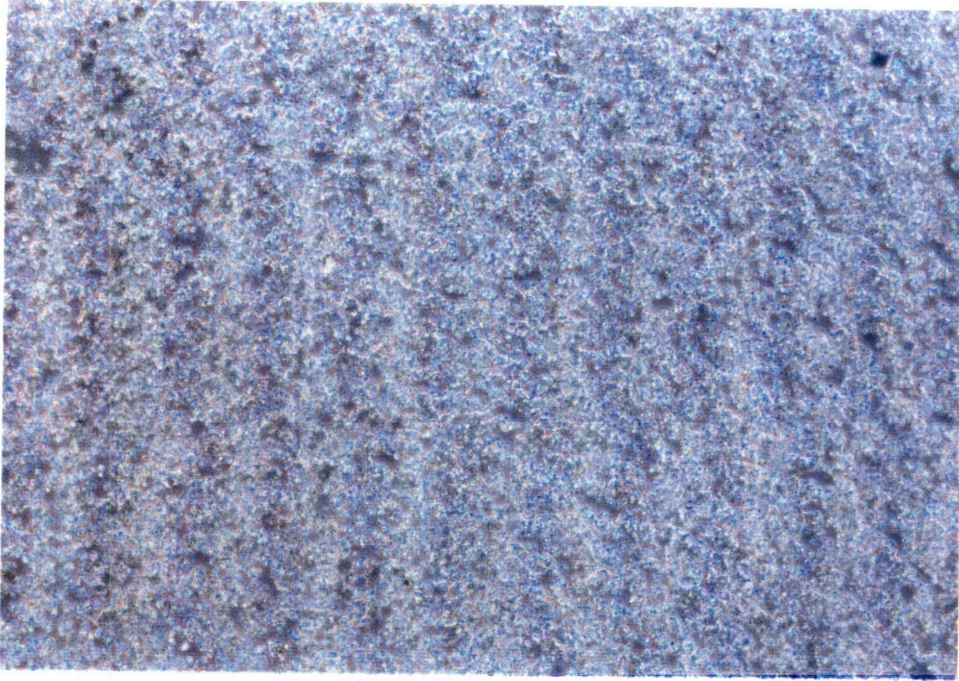


FIGURE 61 : SpA FIRST LAYER; 200x

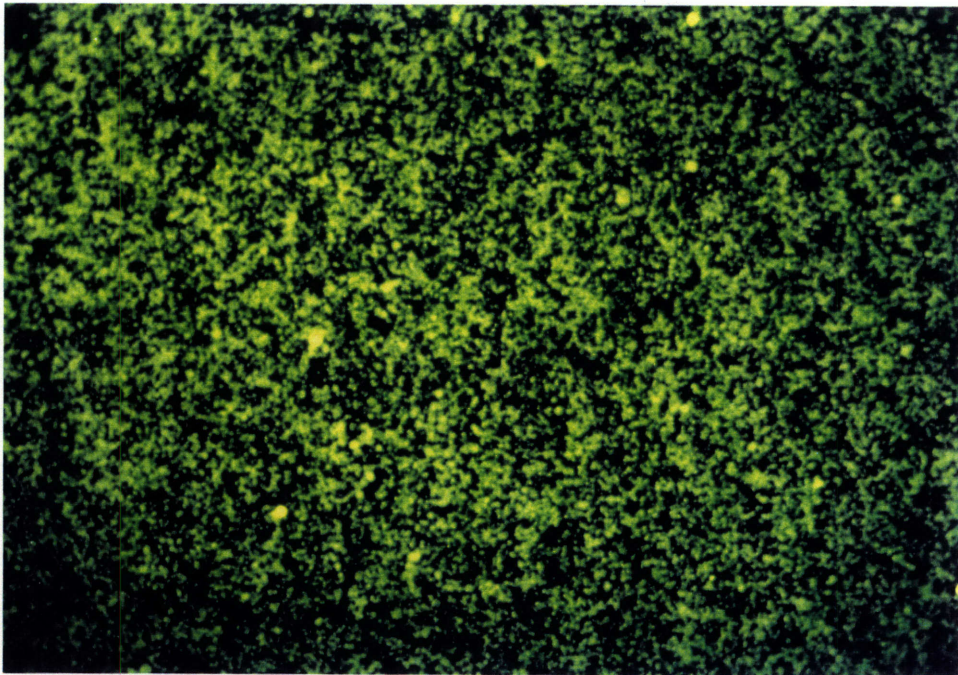
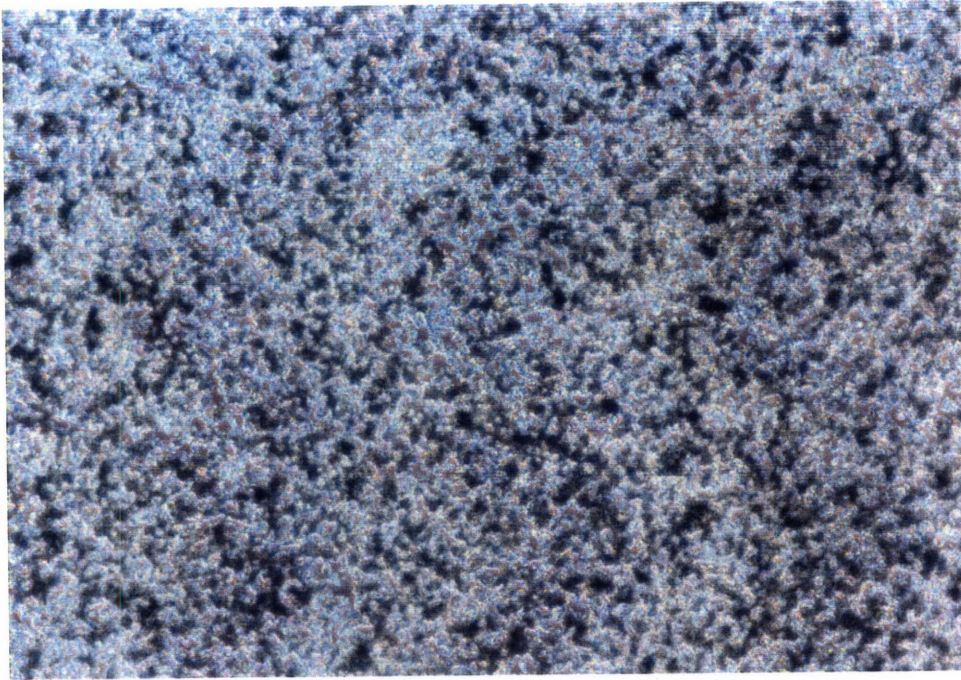
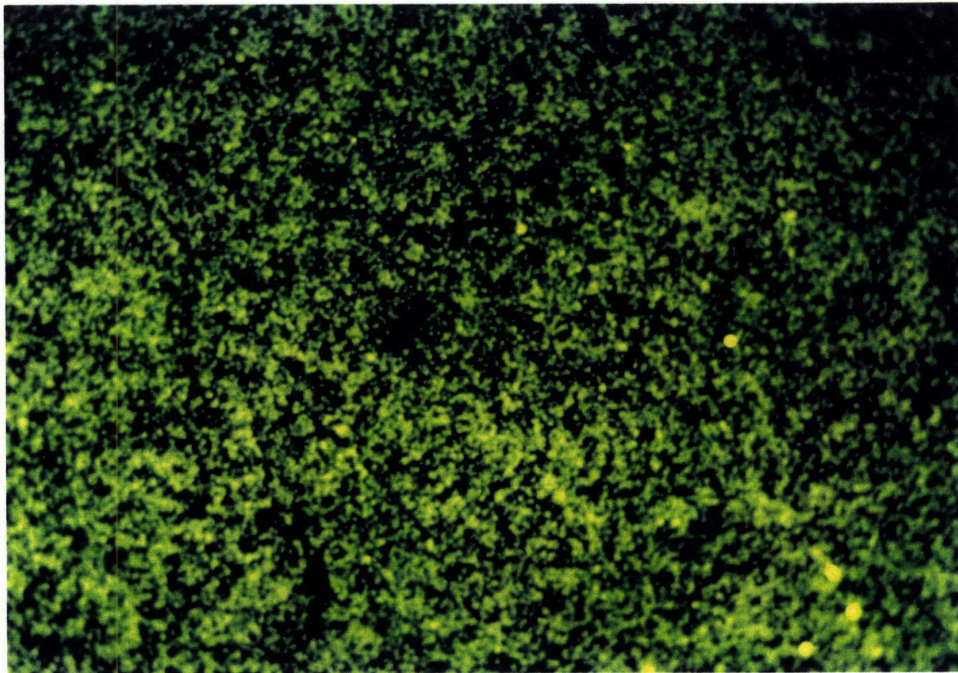


FIGURE 62 : SpA FIRST LAYER; 200x FLUORESCENCE



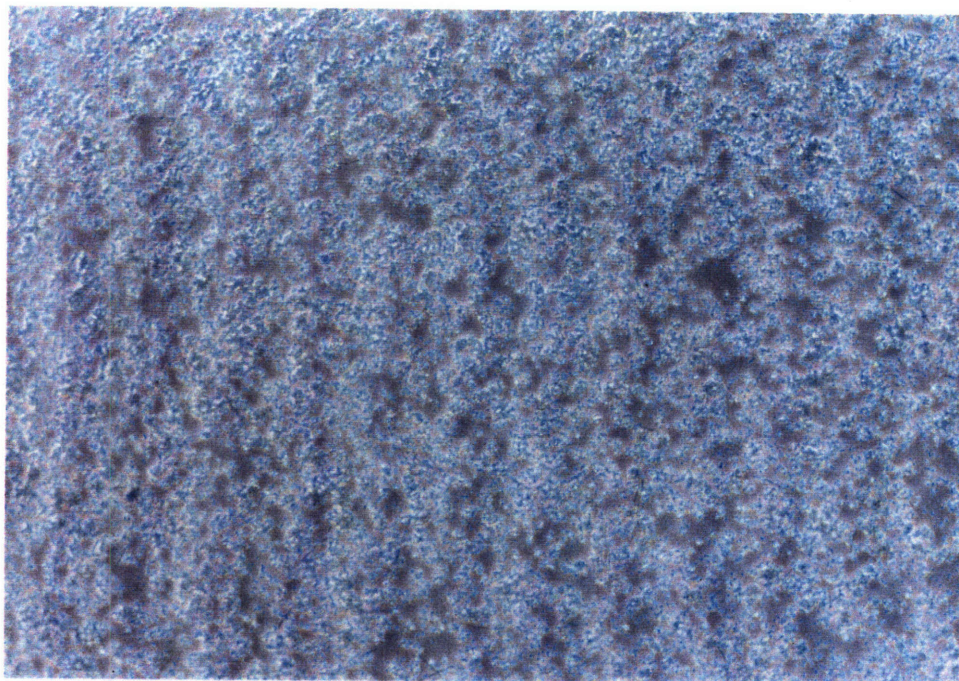
100µm

FIGURE 63 : GAR-IgG SECOND LAYER ON SpA FIRST LAYER; 200x



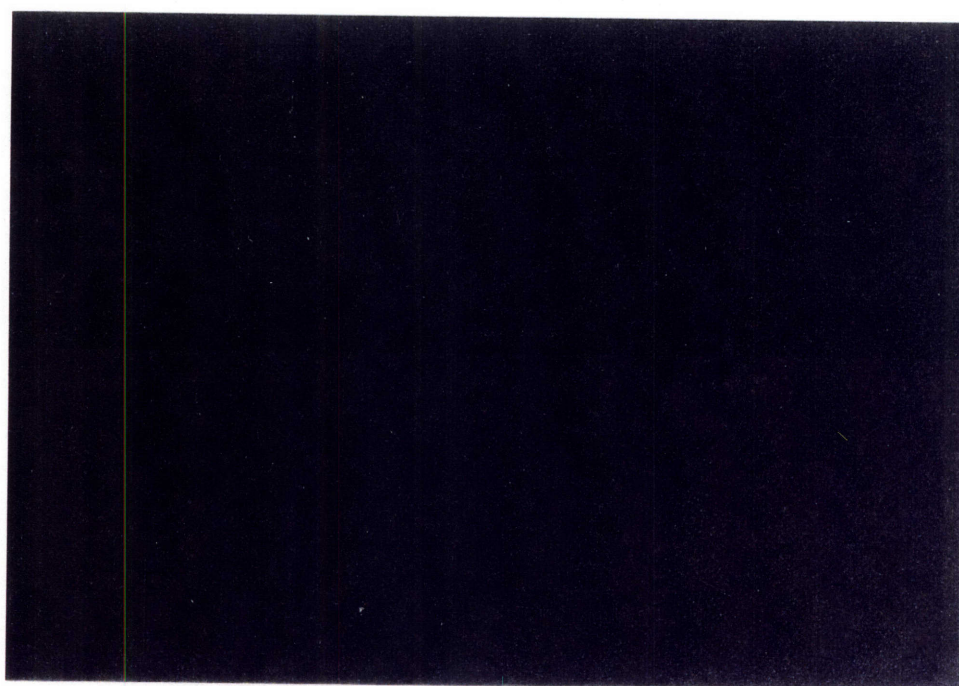
100µm

FIGURE 64 : GAR-IgG SECOND LAYER ON SpA FIRST LAYER; 200x
FLUORESCENCE



100 μ m

FIGURE 65 : GAR-IgG FIRST LAYER; 200x



100 μ m

FIGURE 66 : GAR-IgG FIRST LAYER; 200x FLUORESCENCE

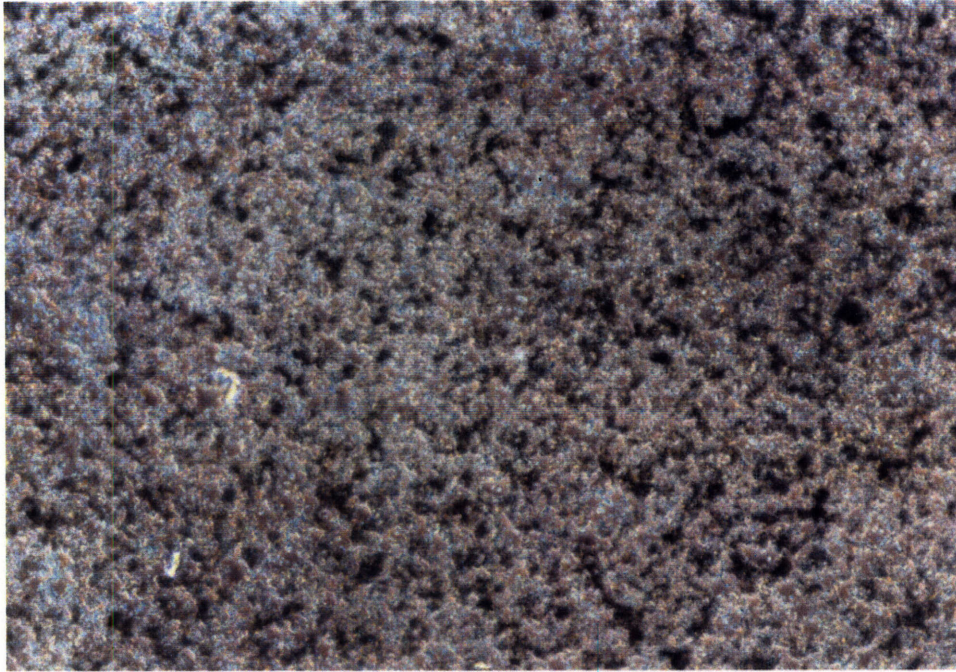


FIGURE 67 : SpA SECOND LAYER ON GAR-IgG FIRST LAYER; 200x

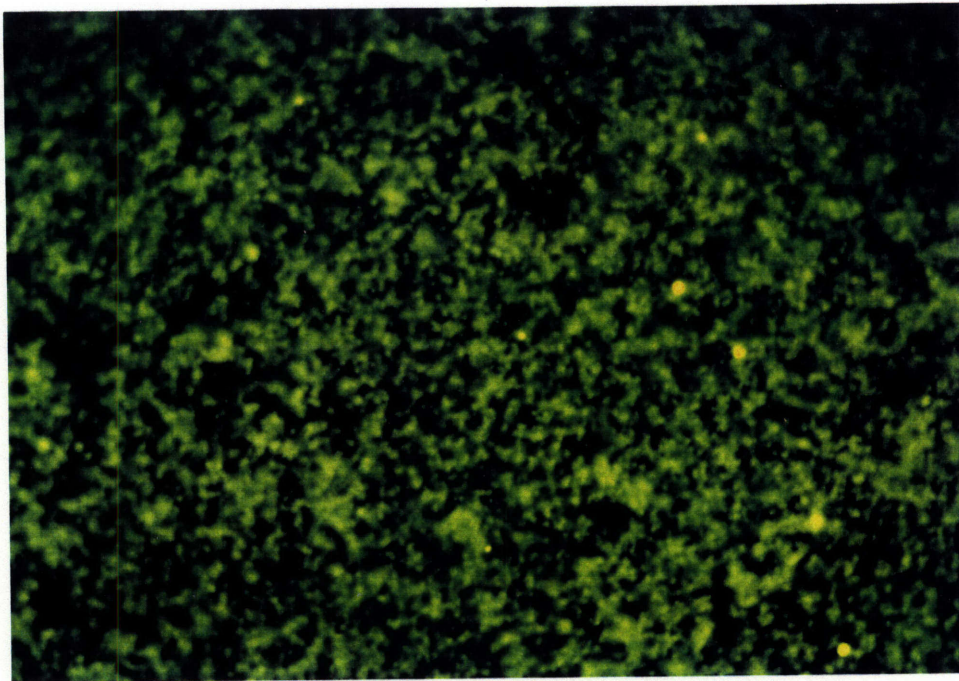
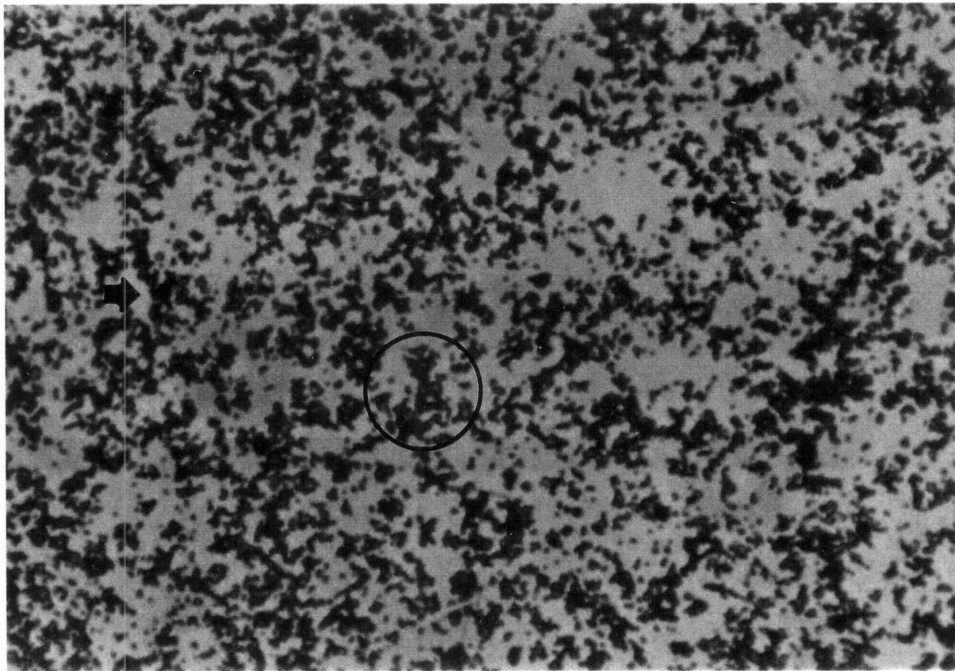
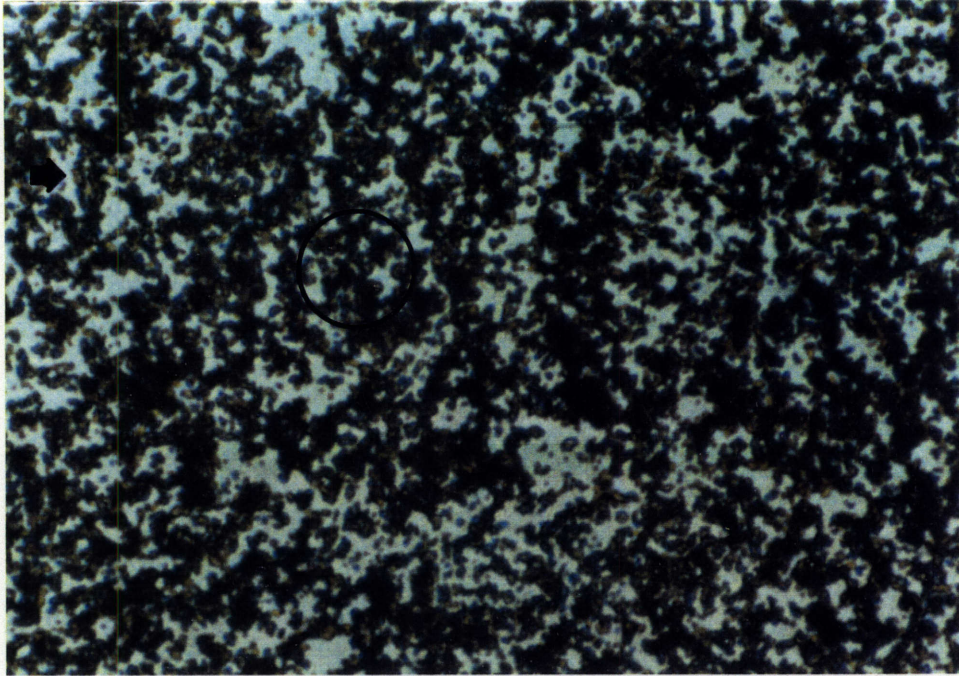


FIGURE 68 : SpA SECOND LAYER ON GAR-IgG FIRST LAYER; 200x
FLUORESCENCE



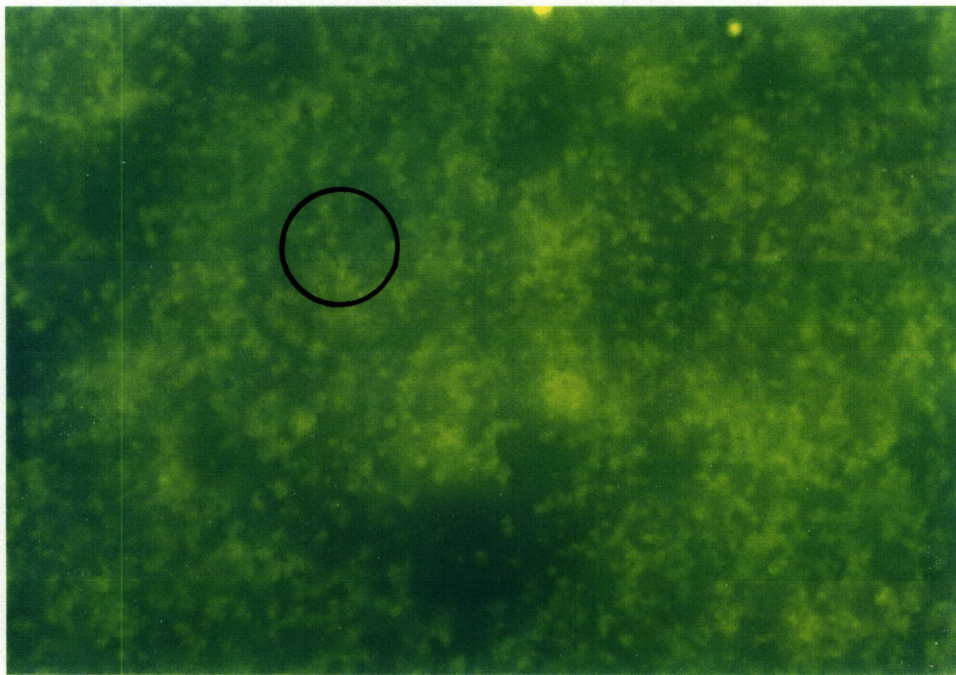
50µm

FIGURE 69 : GAR-IgG FIRST LAYER; 400x



50 μ m

FIGURE 70 : SpA SECOND LAYER ON GAR-IgG FIRST LAYER; 400x



50 μ m

FIGURE 71 : SpA SECOND LAYER ON GAR-IgG FIRST LAYER; 400x
FLUORESCENCE

3.6 SELECTIVE DEFINITION OF GEOMETRY

The objective of selective definition of geometry was to produce multilayered parts with local regions of deposition comparable to controls.

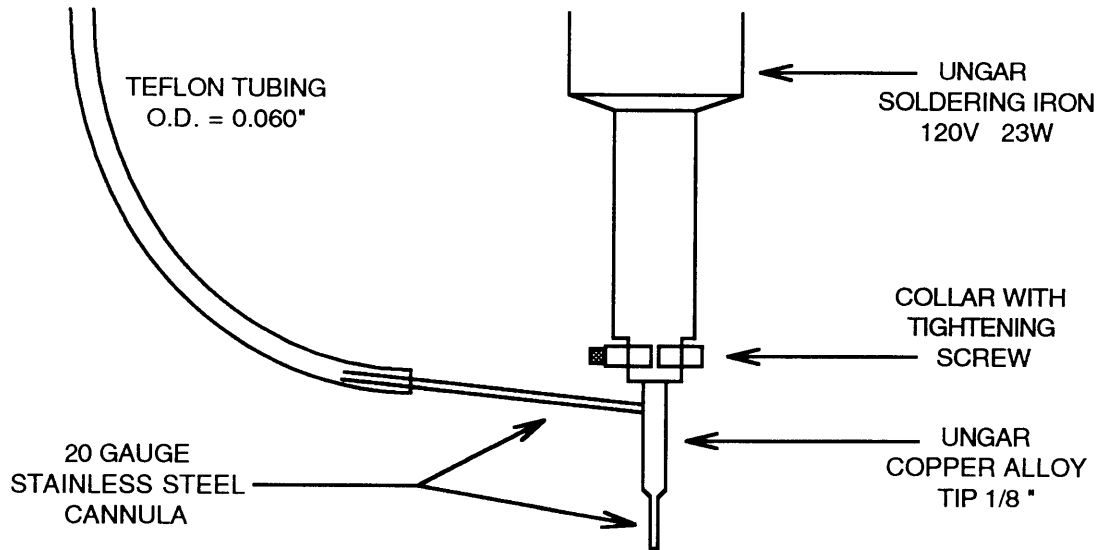
3.6.1 Soldering Iron Hot (90°C)Water Jet

A new thermal deactivation apparatus was required to achieve definition in 3D parts. The laser method provided the desired micron scale resolution; however, with the difficulties with microboiling and excessive temperature increase, the method was set aside. The continuous hot water jet delivered adequate temperature increase but did not provide adequate resolution, deactivated region of approximately 10mm. The principle problem with the continuous hot water jet was the inability to maintain the temperature through the constriction to the syringe needle. The soldering iron (SI) apparatus addressed this problem by heating the nozzle.

The nozzle was a modified copper alloy tip, 1/8", for an Ungar soldering iron as shown in Figure 72.I. The outlet was formed drilling out the center of the tip along the longitudinal axis and the inlet was formed drilling into the side of the tip at an angle ensuring that the hole tapped into the previously drilled outlet hole. The inlet hole was drilled as far from the outlet end as possible to ensure that the length of the tip that water flowed through was maximized, that is the water would be exposed to the heated tip for the longest path possible. Into both holes, 20 gauge stainless steel cannula were fitted and silver soldered into place. The inlet extension was 7cm and the outlet extension was 1cm.

Figure 72.II shows the experimental configuration where the soldering iron was mounted to the guide track to ensure consistent traverse path and nozzle separation distance from the glass sample. The hot plate was used to maintain the reservoir temperature at 100°C. The 100°C reservoir was at a 46cm elevation producing a flow rate of 0.15ml/s and a corresponding velocity through the 20 gauge cannula of 0.24m/s (Appendix C). A Variac was used to control the voltage input to the soldering iron; thus, control the outlet

I. TIP CONFIGURATION



II. EXPERIMENTAL CONFIGURATION

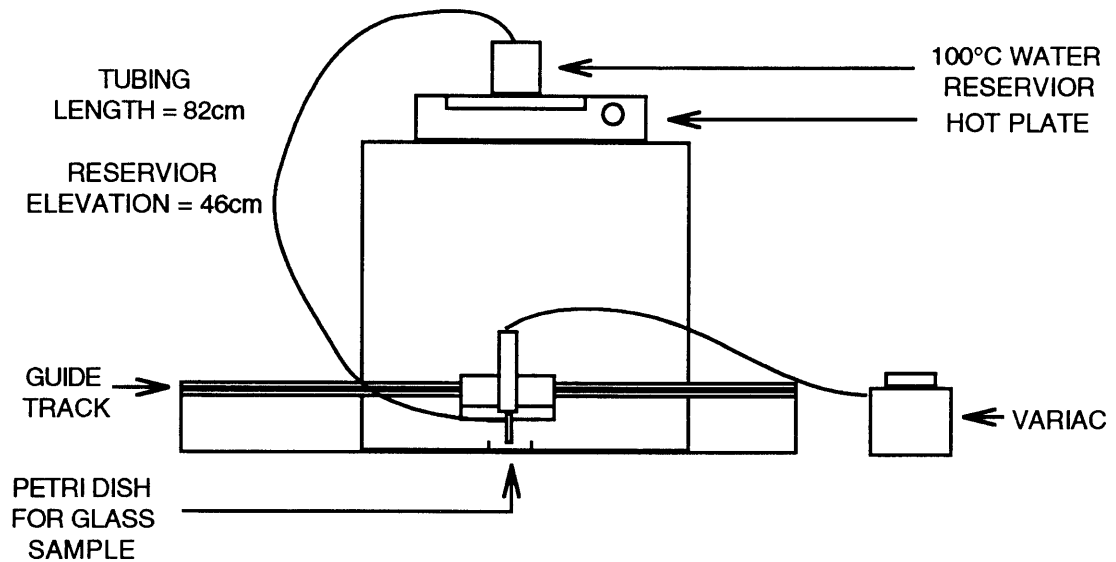


FIGURE 72 : SOLDERING IRON 90°C WATER JET EXPERIMENTAL SCHEMATIC

temperature. Using a thermocouple thermometer, the outlet temperature was measured in two ways: (1) placing the thermocouple in directly the outlet stream and (2) placing the thermocouple in a Styrofoam container collecting the outlet stream. The results agreed so consistently that the direct measurement of the outlet stream was used, because of its convenience, as the judgment of the readiness of the process. Given the continuous hot water jet results, an outlet temperature of 90°C or higher was an indication that the apparatus was ready.

The soldering iron was tested by reproducing the deactivation of the R-IgG coated glass seen in the continuous hot water jet tests. The 20mmx20mmx1mm pieces were removed from the storage container, placed in a petri dish and covered with enough distilled water to keep the samples hydrated before the test. The petri dish was placed under the nozzle and glass to nozzle separation distance of 1mm was checked. The soldering iron jet was traversed at the desired speed. Control tests were performed to ensure that deposition differences were due to the effects of the 90°C water and not the mechanical effects of the water jet. Two tests were performed: (1) room temperature 23°C water in the setup configuration with flow rate of 0.13m/s and (2) 48°C water in the setup configuration with flow rate of 0.24m/s. The slight temperature increase was required to achieve the test flow rate without altering the setup configuration. As seen in Figures 73 to 74, the two control situations did not alter the deposition as compared to the R-IgG control for 20mmx20mmx1mm samples, Figure 35. Therefore, any deposition changes will be a result of thermal and not mechanical mechanisms.

Figure 75 explains the reference markings for the line, deactivated and active regions placed on the samples; these markings are seen in the 20x magnification photos of selective definition of geometry parts. Figure 76 shows the line deactivated when the jet was traversed at 0.17mm/s (20mm in 120s). Figures 77 and 78, the 400x photos of the deactivated and active regions, are comparable to the glass and R-IgG controls, respectively. Figure 79 shows the deactivated line for a 0.33m/s traverse speed. Again, 400x magnification

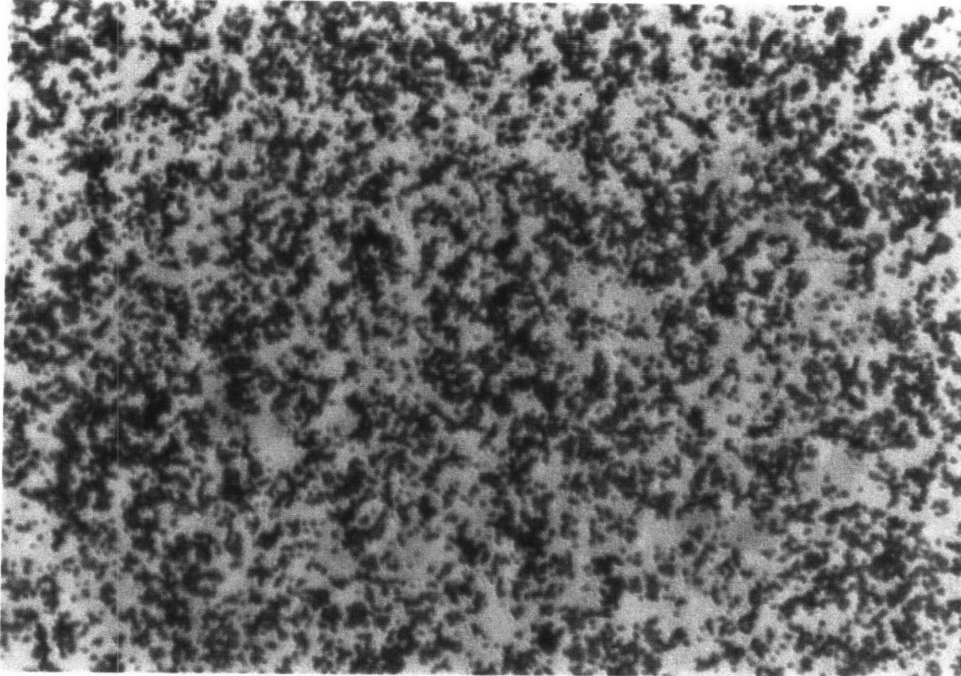
photos, Figures 80 and 81, of the deactivated and active regions are provided for control comparison. The line widths for the 0.17m/s and 0.33m/s traverses were both 1.5mm as measured off the 20x magnification photos. The 400x magnification photos have locator arrows and encircled regions that will be discussed in Section 3.6.2.1 as these samples were used as predeactivated bases for selective definition of geometry. Based on the reproducibility of the deactivation observed in the continuous hot water jet tests, the soldering iron jet was used to produce the deactivated regions in the 3D parts.

3.6.2 Selective Definition in 3D

The test part to determine the effectiveness of the system in producing definition in 3D was two layer part with a deactivated line in the center. Two construction methods were chosen: (1) building up from a predeactivated base and (2) building up on a bound bead base.

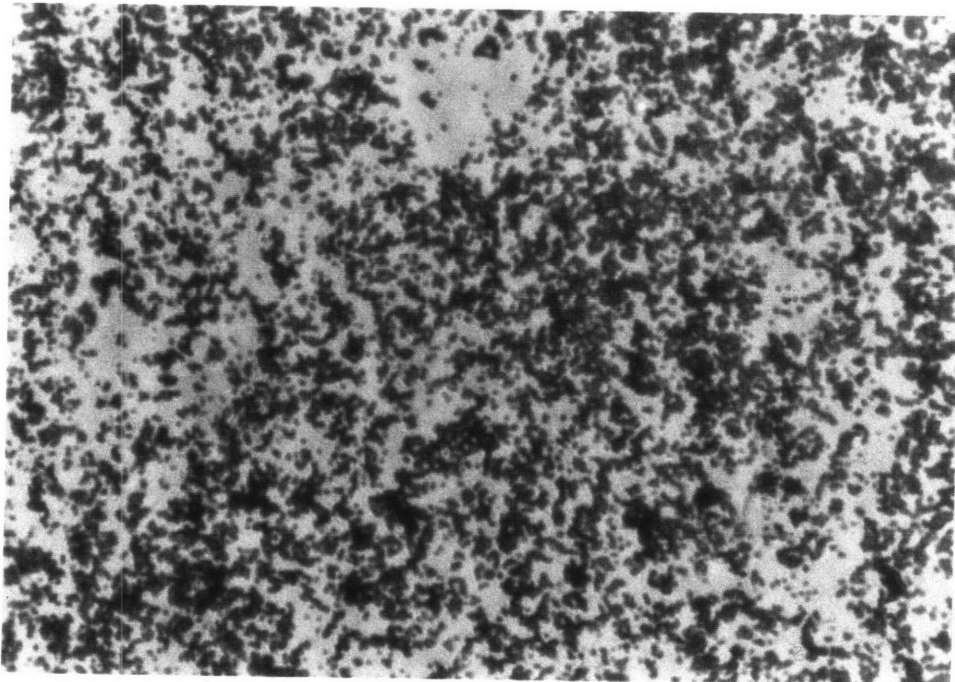
3.6.2.1 Predeactivated base

As seen in Figure 82, the predeactivated base is a R-IgG coated base that had been exposed to the soldering iron jet. Then, GAR-IgG beads were added to reveal the deactivated line; for example, the 1.5mm line produced with a 0.33mm/s traverse, Figure 79. Figures 80 and 81 show the first layer deposition in the deactivated and active regions at 400x magnification. Then, the slide was subjected to the soldering iron jet again, at the same traverse speed, to deactivate the residual beads bound down, Figure 83 and 84. The deactivated region was directly exposed to the jet and as seen, comparing Figures 80 and 83 referencing the locator arrow, no removal of beads was caused by the additional traverse of the 0.24m/s SI jet. In the active region, Figure 84, which had no direct exposure to the SI jet, the encircled region show no net bead removal; however, slight rearrangement of the beads in a few of the small clusters was observed, comparing Figures 81 and 84. This corresponds to a movement on the order of a bead diameter and was not



50 μ m

FIGURE 73 : SOLDERING IRON WATER JET AT 23°C; 400x
FLOW VELOCITY 0.13m/s AND TRAVERSE SPEED 0.17mm/s



50 μ m

FIGURE 74 : SOLDERING IRON WATER JET AT 48°C; 400x
FLOW VELOCITY 0.24m/s AND TRAVERSE SPEED 0.33mm/s

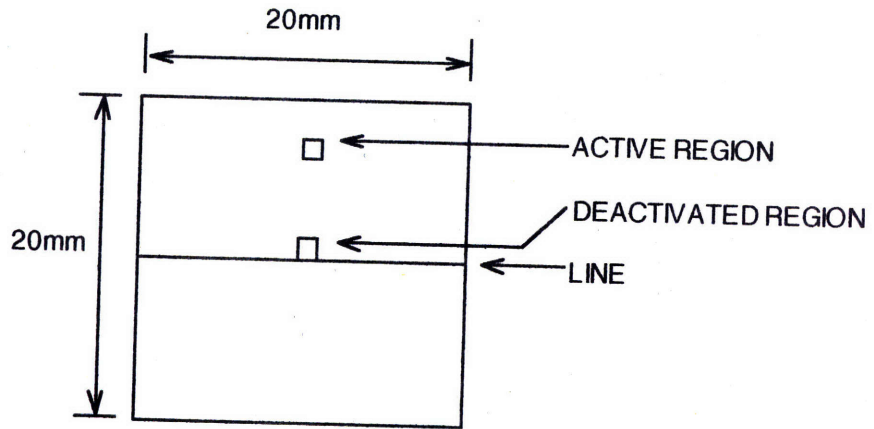
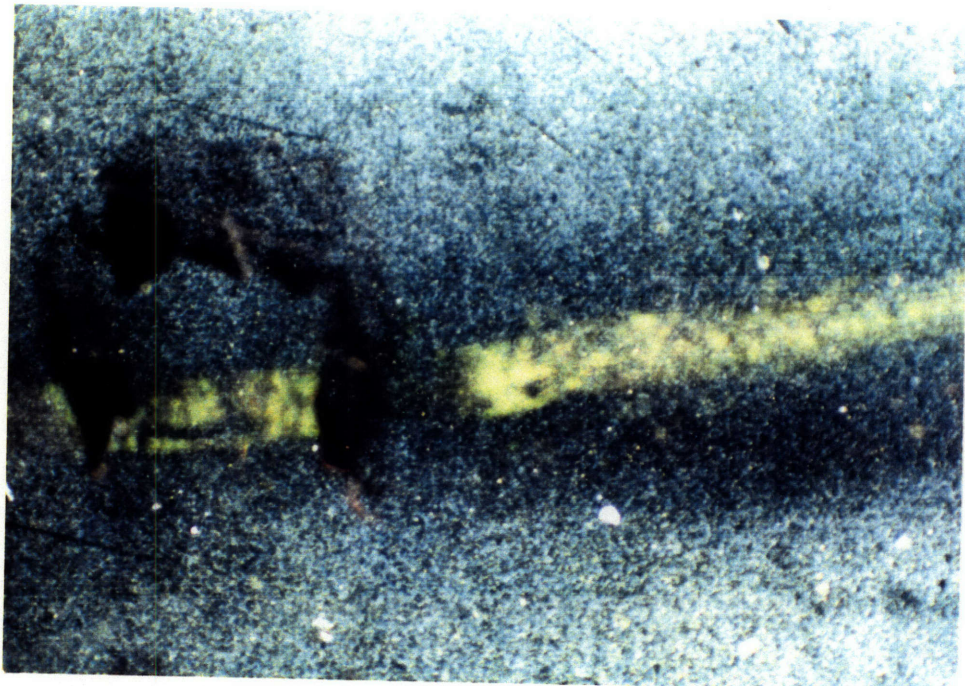


FIGURE 75 : SELECTIVE DEFINITION OF GEOMETRY
3D PART REFERENCE MARKS



1mm

FIGURE 76 : SI JET AT 0.17mm/s; 20x - LINE WIDTH = 1.5mm

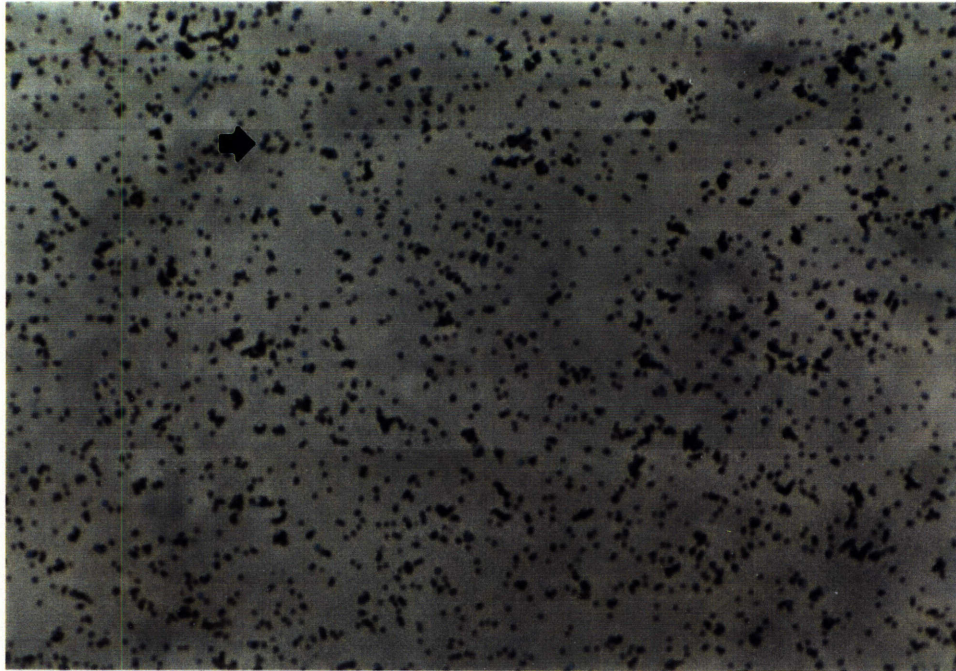


FIGURE 77 : SI JET AT 0.17mm/s; 400x
DEACTIVATED REGION GAR-IgG FIRST LAYER

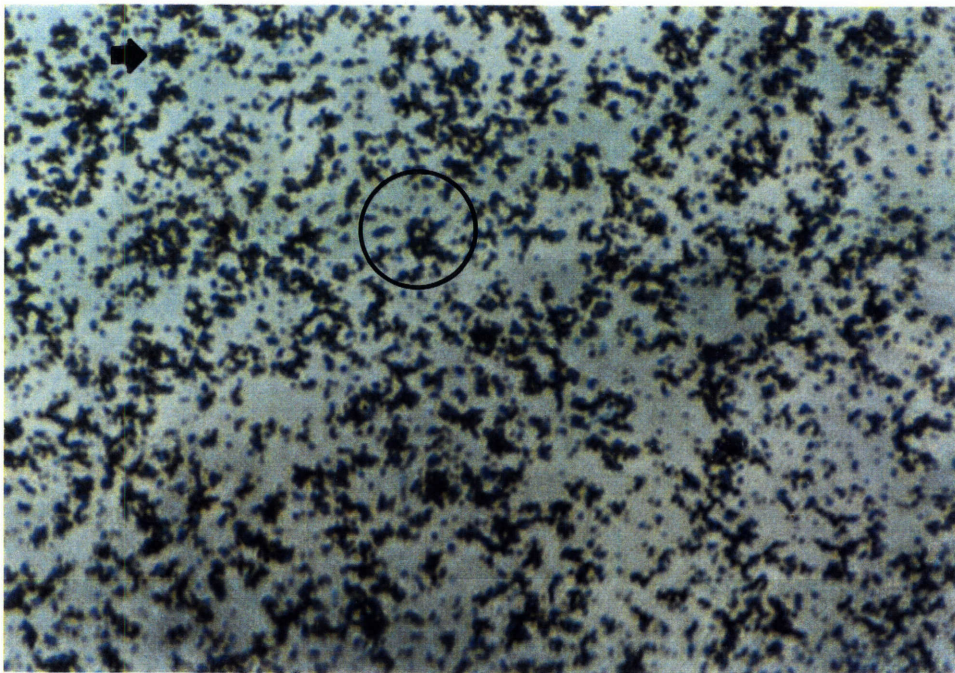
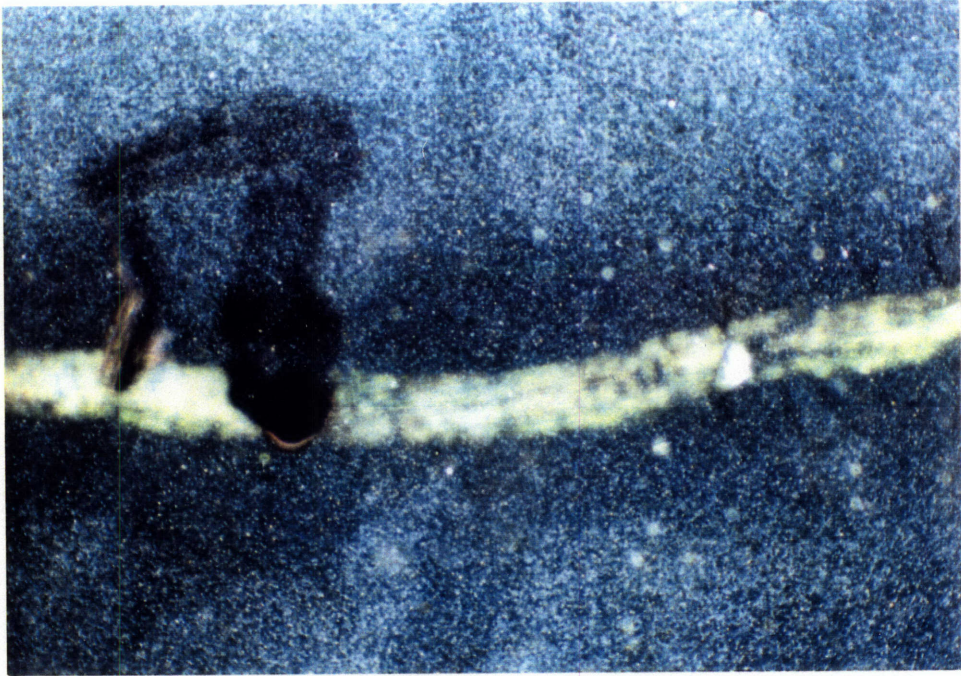


FIGURE 78 : SI JET AT 0.17mm/s; 400x
ACTIVE REGION GAR-IgG FIRST LAYER



1mm

FIGURE 79 : SI JET AT 0.33mm/s; 20x - LINE WIDTH = 1.5mm

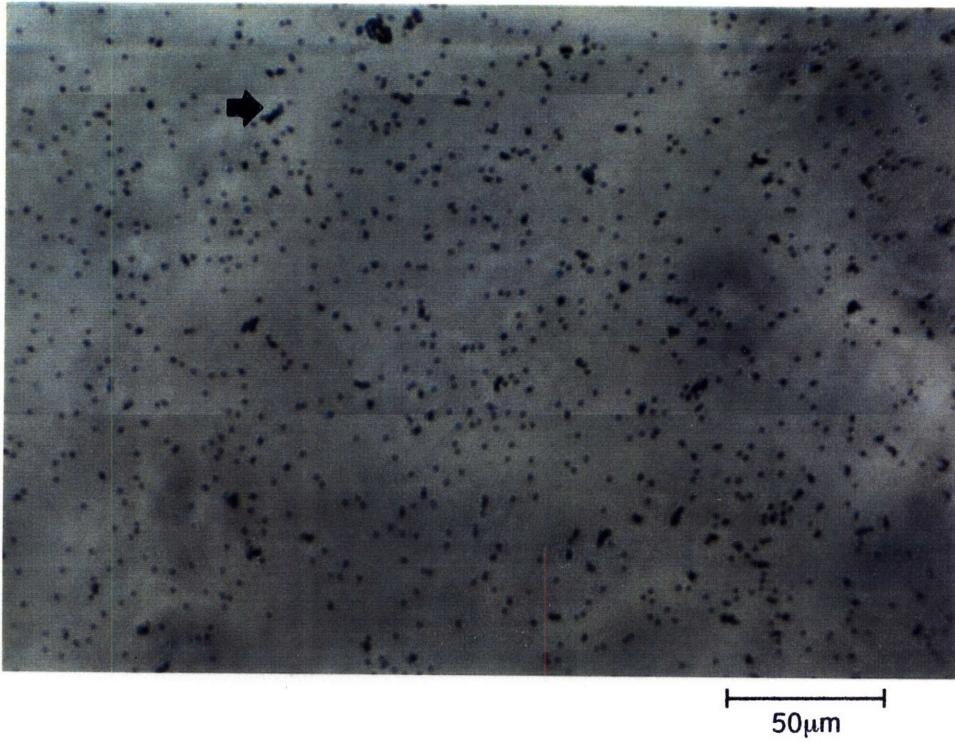


FIGURE 80 : SI JET AT 0.33mm/s; 400x
DEACTIVATED REGION GAR-IgG FIRST LAYER

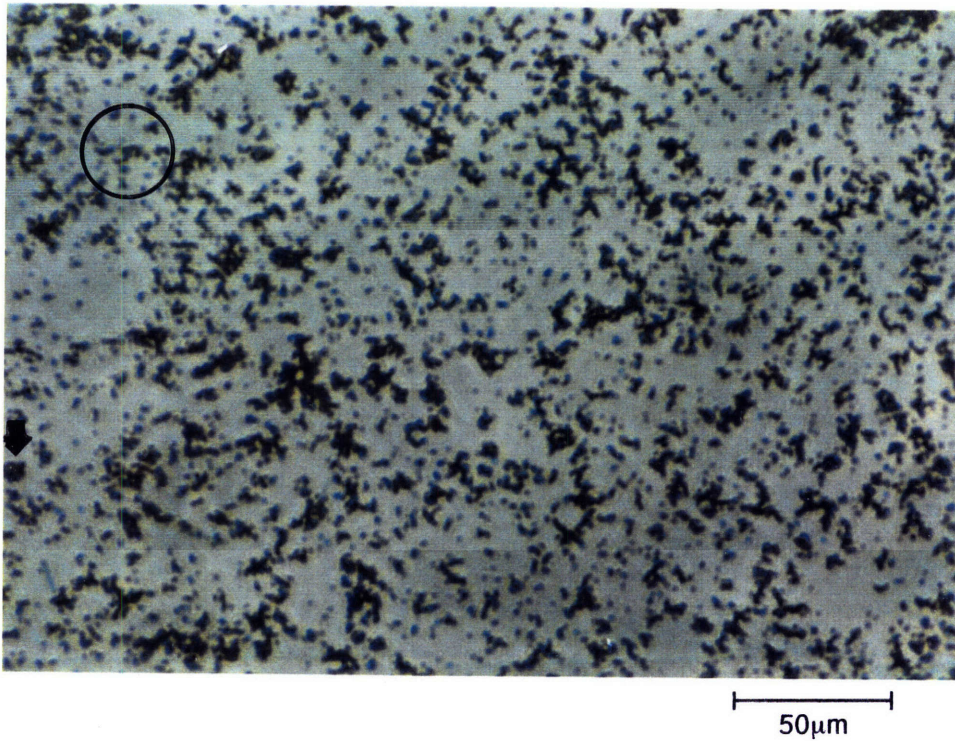
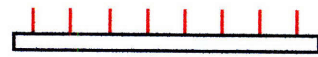
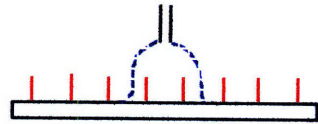


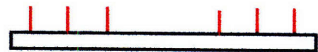
FIGURE 81 : SI JET AT 0.33mm/s; 400x
ACTIVE REGION GAR-IgG FIRST LAYER



RABBIT IgG COATED GLASS



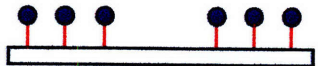
EXPOSE TO 90°C WATER JET



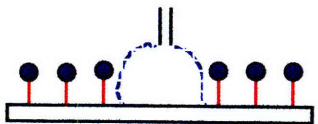
RABBIT IgG DENATURED IN PATH OF JET



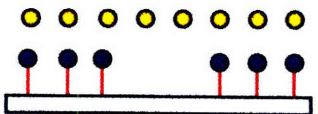
ADD GOAT ANTI-RABBIT IgG BLUE DYED BEADS
LET SETTLE FOR 2 HOURS



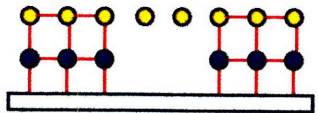
WASH WITH CALIBRATED WATER NOZZLE



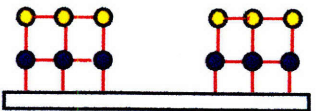
EXPOSE TO 90°C WATER JET



ADD PROTEIN A FLUORESBRITE BEADS
LET SETTLE FOR 2 HOURS



ADD RABBIT IgG IN SOLUTION
LET SETTLE FOR 2 HOURS



WASH WITH CALIBRATED WATER NOZZLE

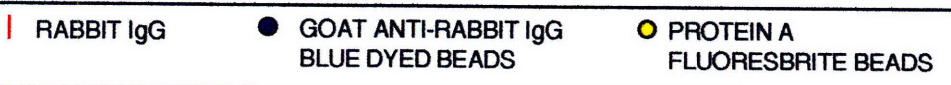


FIGURE 82 : SELECTIVE DEFINITION OF GEOMETRY
PREDEACTIVATED BASE

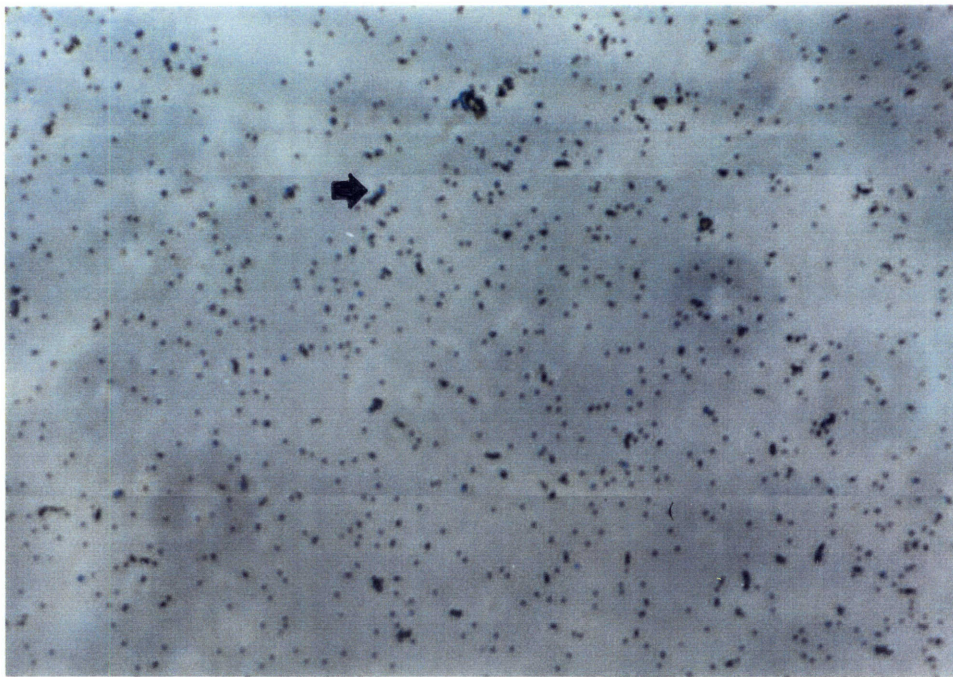


FIGURE 83 : PREDEACTIVATED BASE; 400x
DEACTIVATED REGION GAR-IgG FIRST LAYER
AFTER SECOND PASS OF SI JET AT 0.33mm/s

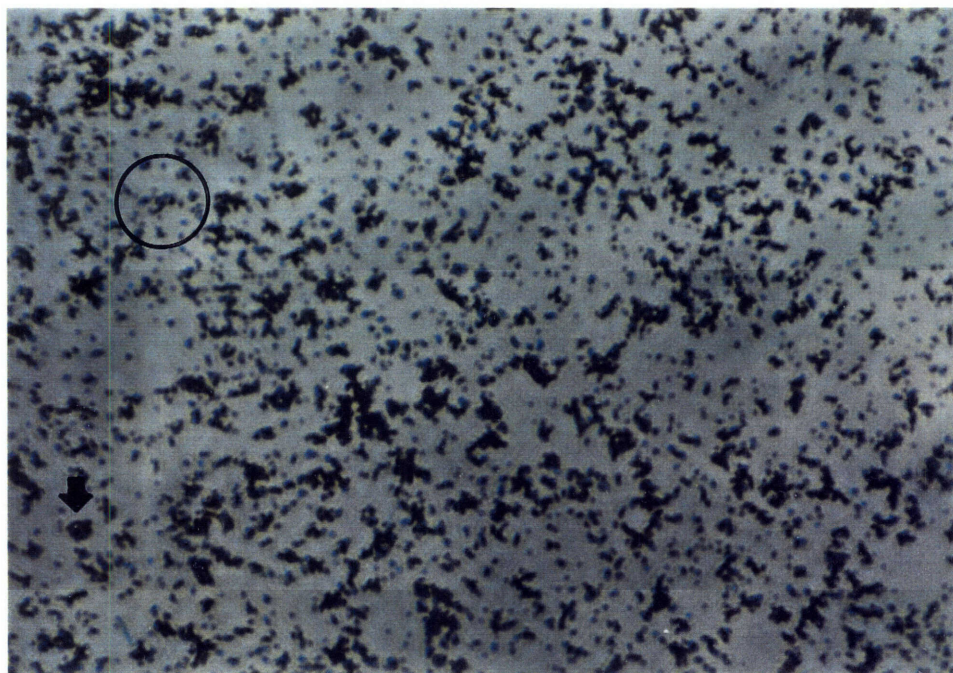


FIGURE 84. PREDEACTIVATED BASE; 400x
ACTIVE REGION GAR-IgG FIRST LAYER
AFTER SECOND PASS OF SI JET AT 0.33mm/s

judged as significant nor a product of the SI jet pass. Then, the SpA beads (20 μ l) were added and then, two hours later, the R-IgG linker (4 μ l) added.

The first sample is the 0.17mm/s traverse speed. Figure 85, at 20x magnification, shows some deposition in the deactivated region versus Figure 76; however a distinct line is still observed. Figure 86, the fluorescence exposure, shows the distinct line at a line width of 1.5mm and a secondary region of increased deposition at a line width of 7.3mm. Figures 87 and 88 are for the deactivated region. Comparing with Figure 77 and 78, first layer, deposition has increased slightly. However, examining the fluorescence photo, Figure 88, the magnitude of SpA deposition was similar to the GAR-IgG deposition on the glass control, Figure 30. The deposition observed was the residual as seen in the glass control. Another contributing factor was the mechanical barrier of the residual GAR-IgG beads preventing removal of neighboring residual SpA beads with the calibrated wash nozzle. Figures 89 and 90 are for the active region. Comparing to Figure 78, first layer, deposition has increased substantially. The magnitude of deposition in Figure 90, fluorescence active region, showed SpA deposition slightly less than the control, Figure 71, but greater than in the deactivated region, Figure 88. The encircled regions indicate that SpA may have deposited on top of the GAR-IgG beads in the first layer; for example in the rightmost region of the circle. Comparing Figures 87 and 89, color deactivated second layer and color active second layer, a total deposition difference was observed. Comparing Figures 88 and 90, fluorescent deactivated second layer and fluorescent active second layer, a SpA deposition difference was observed. Thus, the SI jet was effective in selectively defining the line region on a predeactivated base.

Figures 91 to 96 are the same array of photos for the 0.33mm/s sample. The 20x magnification photos, Figure 91 and 92, are similar to those for the 0.17mm/s sample. The SpA did have some deposition in the deactivated region and this sample also had a secondary deposition region at 5.3mm line width. The deactivated region deposition, Figure 93 and 94, was evident but

minimal enough to be explained by residuals. The 400x active region photos, Figure 95 and 96, show that SpA beads in the square formation have deposited on top of GAR-IgG first layer beads that would be the top of the square. Active region deposition is similar to the 0.17mm/s sample.

The predeactivated base permitted selective definition of geometry. Despite residual deposition in the deactivated region, the deposition differences between the active and deactivated regions were successfully produced by selective thermal deactivation of antigens and antibodies. The analysis of high magnification photos of the active region indicate the possible deposition of SpA beads on top of GAR-IgG beads.

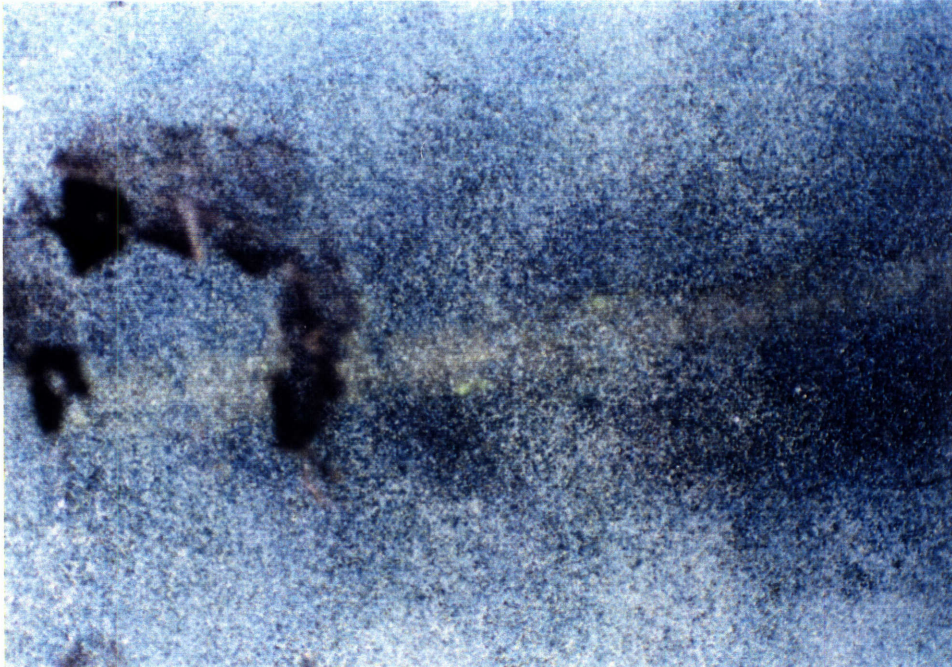
3.6.2.2 Bound Bead Base

In this test the base for drawing the deactivating line was not the R-IgG coated glass but the R-IgG coated glass with GAR-IgG already deposited, Figure 97. The experiment actually tests two possibilities (1) does the hot water jet disturb bound beads and (2) if the beads are not disturbed, do the unbound proteins on the bead surface become deactivated.

Table 9 shows the tested speeds used on the samples with two surface concentrations. As discussed in Section 3.3.2, these concentration were determined to have insignificant deposition differences. The tabular values detail both measurements at eye magnification off parts and 20x magnification off photos.

TABLE 9 : SELECTIVE DEFINITION LINE WIDTHS

SURFACE CONCENTRATION ($\mu\text{g}/\text{cm}^2$)	TRAVERSE SPEED (mm/s)	LINE EYE PART	WIDTH (mm) PHOTO 20x FLUORES	FIGURE
0.44	0.33	10	10.6	98 at 12x
0.44	0.17	3-10	3.8-7.6	99 at 17x
0.44	0.067	3	4.3-5.5	100 at 20x
17	0.22	9	8.5-10.5	
17	0.17	8	4.0	
17	0.067	4-10	5.6	



1mm

FIGURE 85 : PREDEACTIVATED BASE; SI JET AT 0.17mm/s; 20x
AFTER SpA SECOND LAYER - LINE WIDTH = 1.5mm

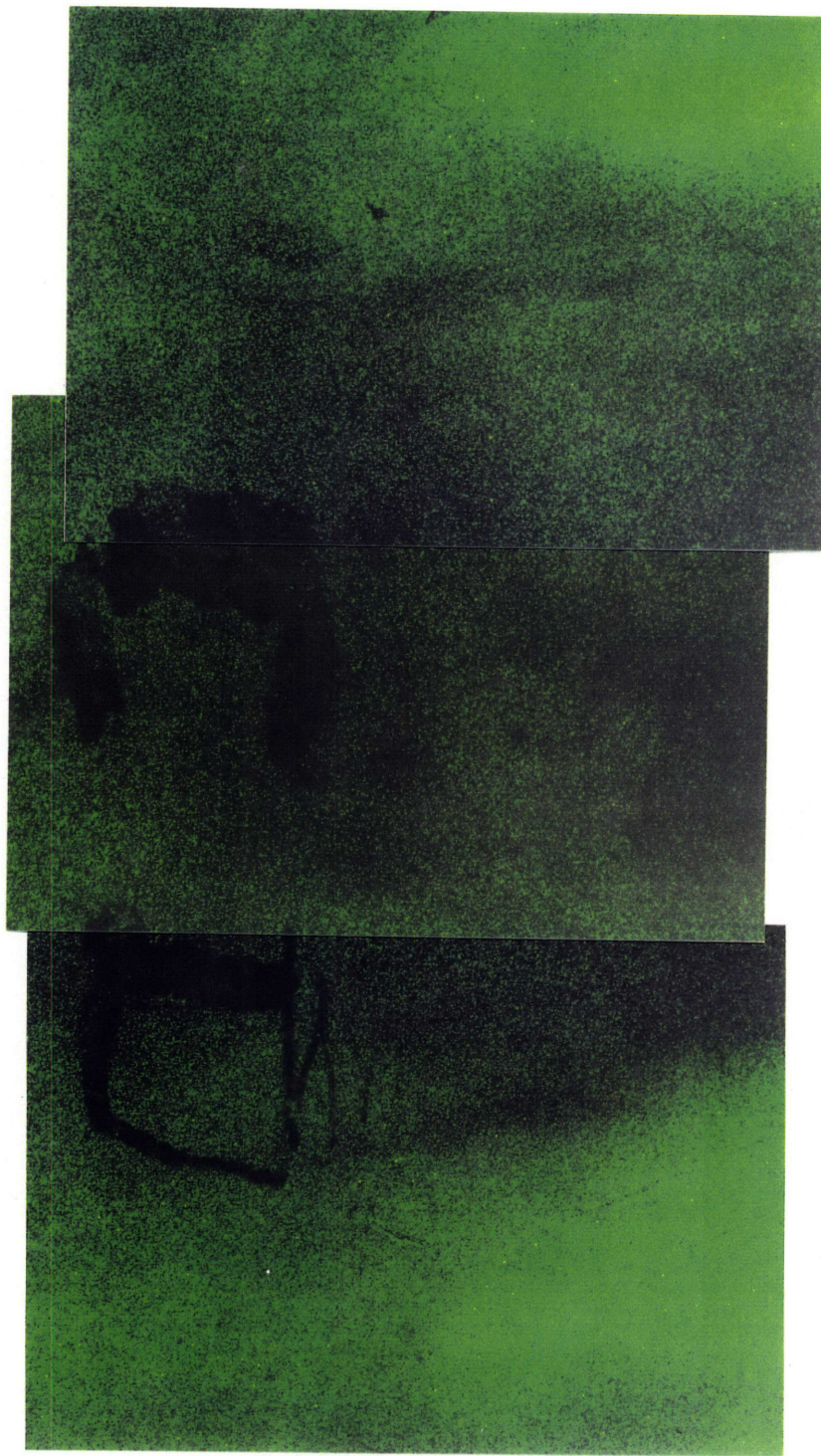
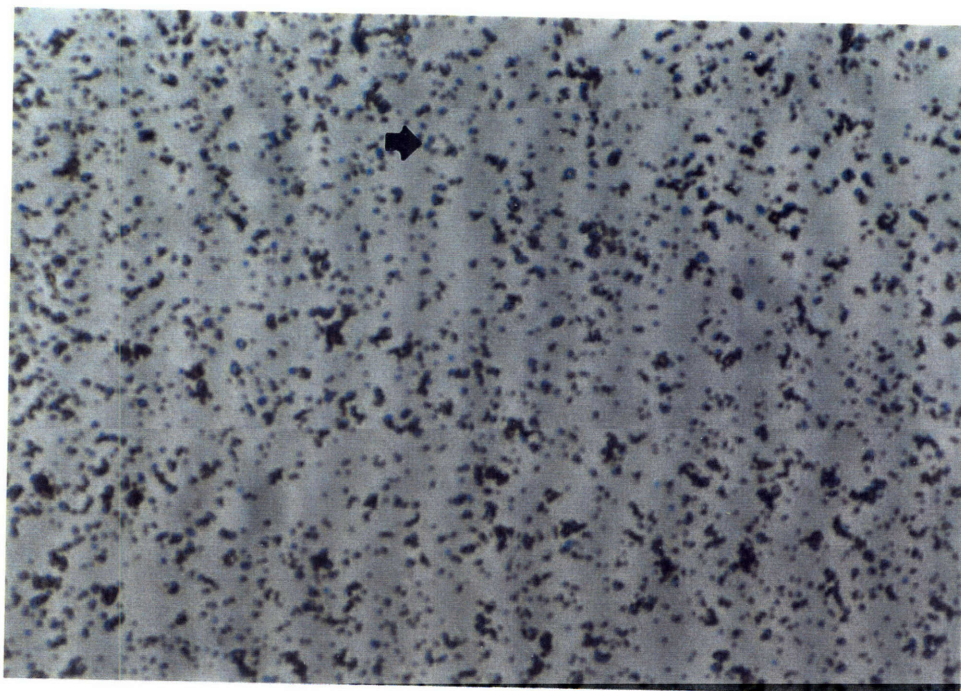
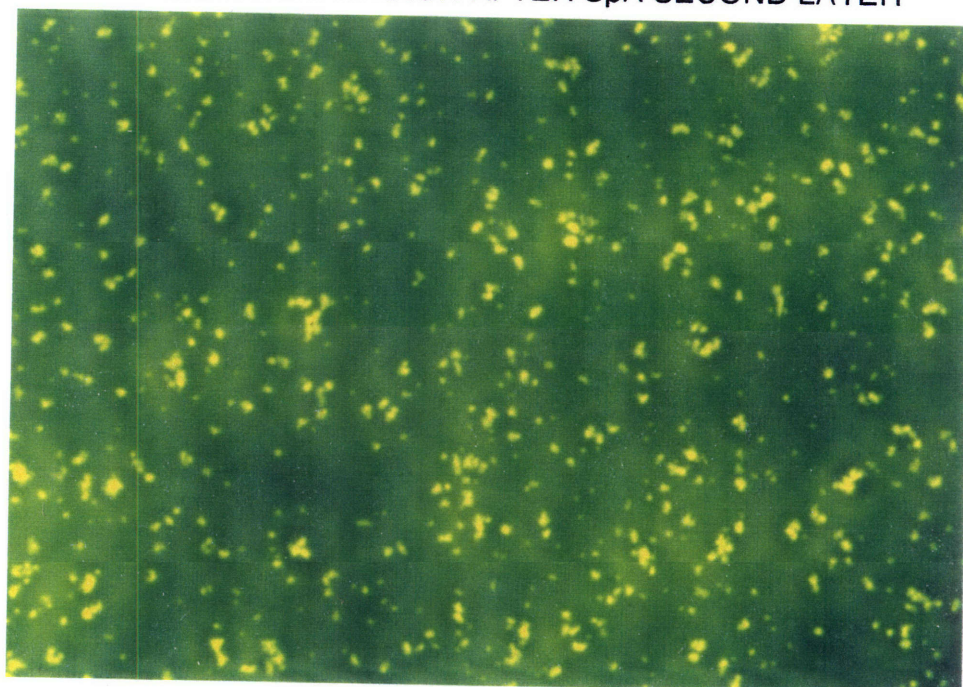


FIGURE 86 : PREDEACTIVATED BASE; SI JET AT 0.17mm/s
AFTER SpA SECOND LAYER - LINE WIDTHS = 1.5mm & 7.3mm
FLUORESCENCE



50 μ m

FIGURE 87 : PREDEACTIVATED BASE; SI JET AT 0.17mm/s; 400x
DEACTIVATED REGION AFTER SpA SECOND LAYER



50 μ m

FIGURE 88 : PREDEACTIVATED BASE; SI JET AT 0.17mm/s; 400x
DEACTIVATED REGION AFTER SpA SECOND LAYER FLUORESCENCE

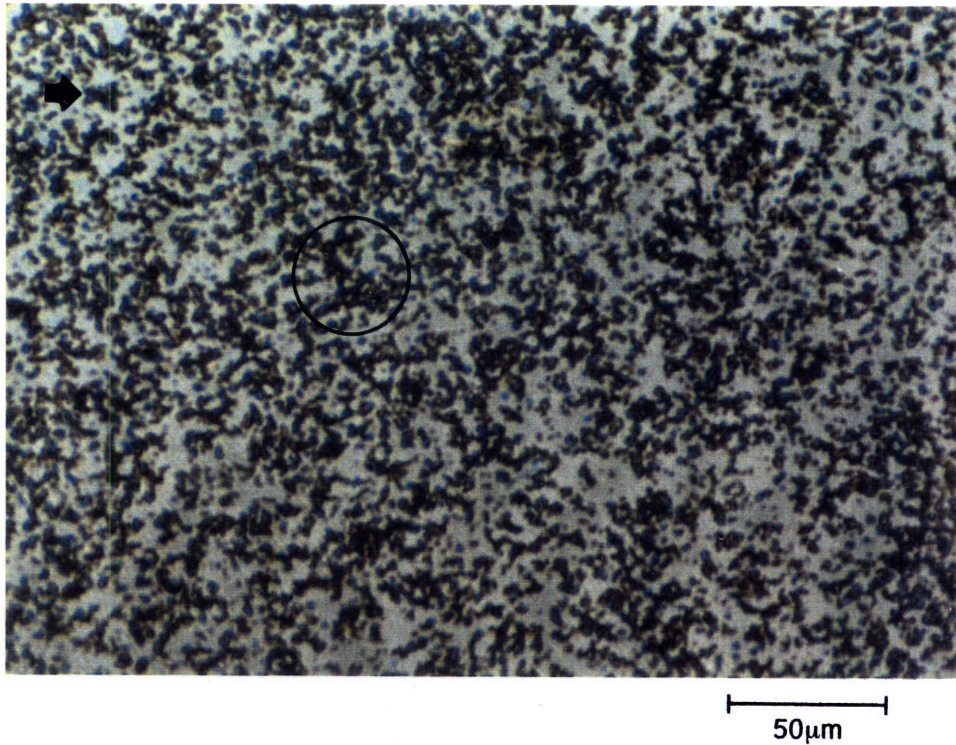


FIGURE 89 : PREDEACTIVATED BASE; SI JET AT 0.17mm/s; 400x
ACTIVE REGION AFTER SpA SECOND LAYER

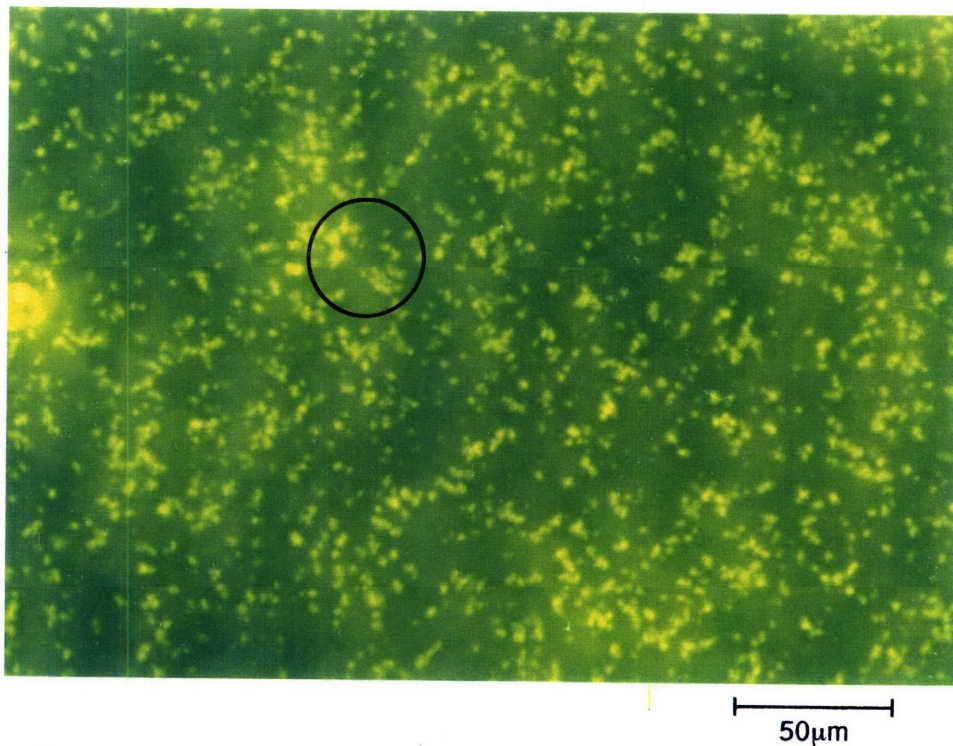
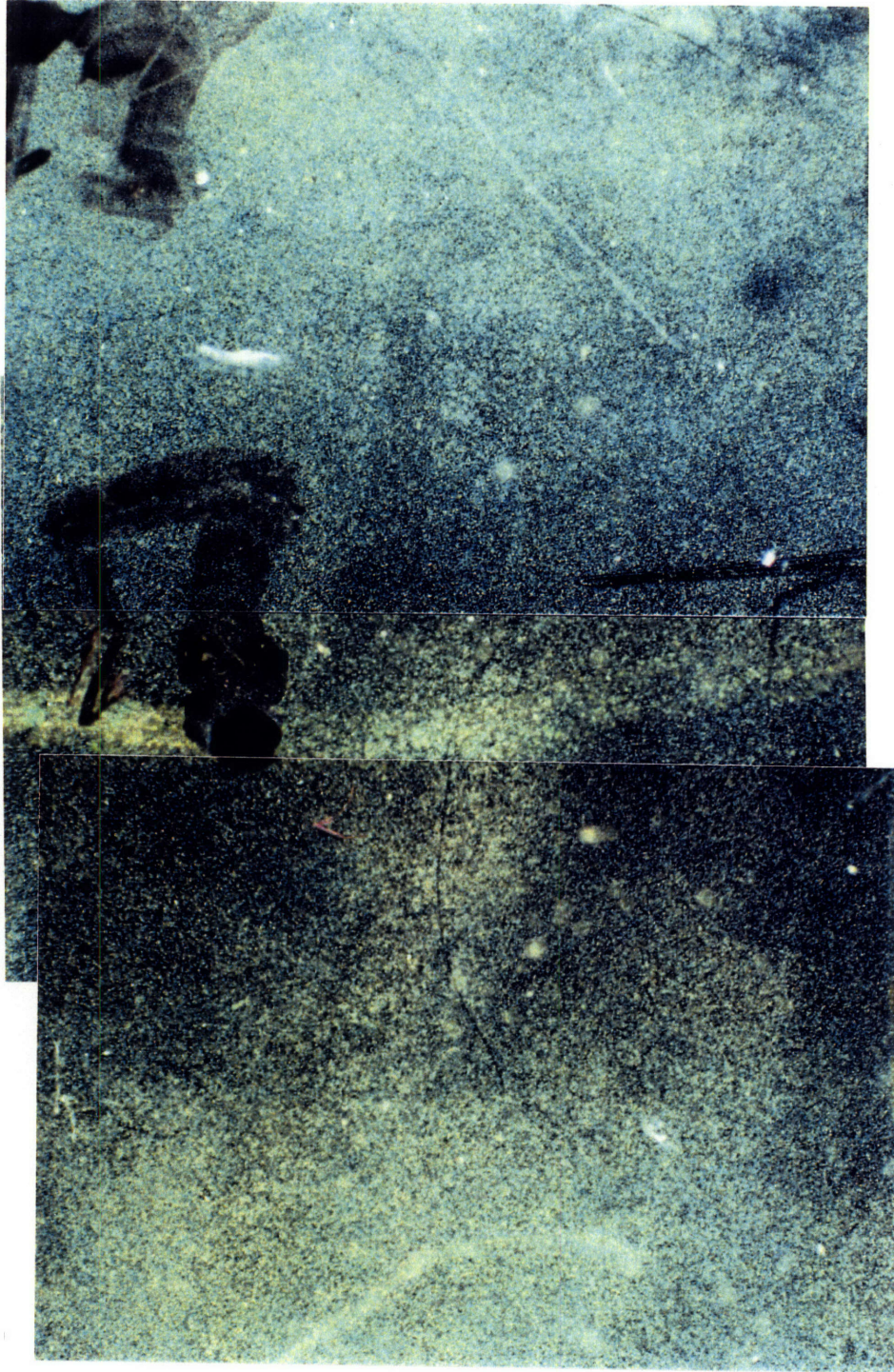
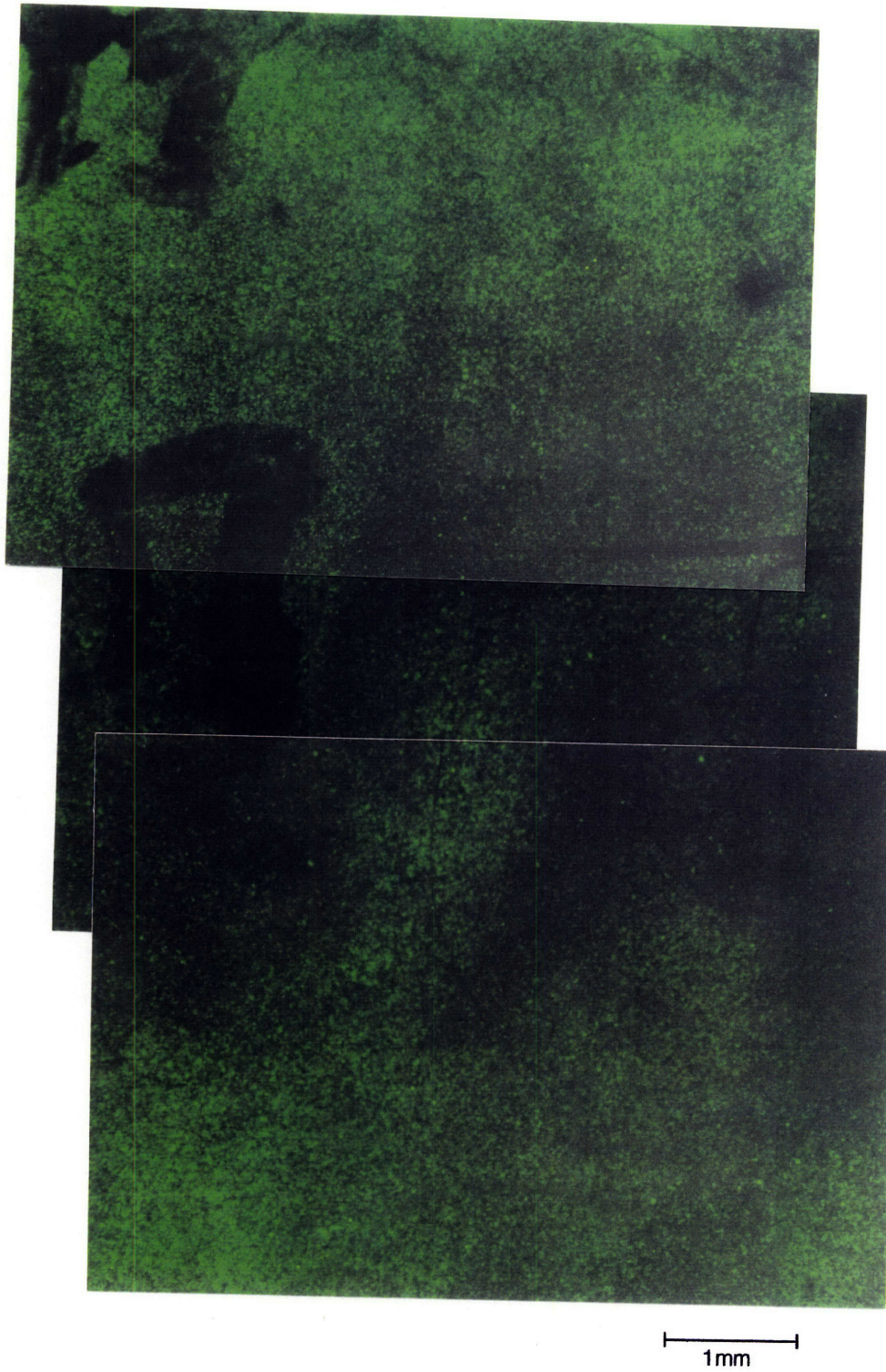


FIGURE 90 : PREDEACTIVATED BASE; SI JET AT 0.17mm/s; 400x
ACTIVE REGION AFTER SpA SECOND LAYER FLUORESCENCE



1mm

FIGURE 91 : PREDEACTIVATED BASE; SI JET AT 0.33mm/s
AFTER SpA SECOND LAYER - LINE WIDTH = 1.5mm



**FIGURE 92 : PREDEACTIVATED BASE; SI JET AT 0.33mm/s
AFTER SpA SECOND LAYER - LINE WIDTHS = 1.5mm & 5.3mm
FLUORESCENCE**

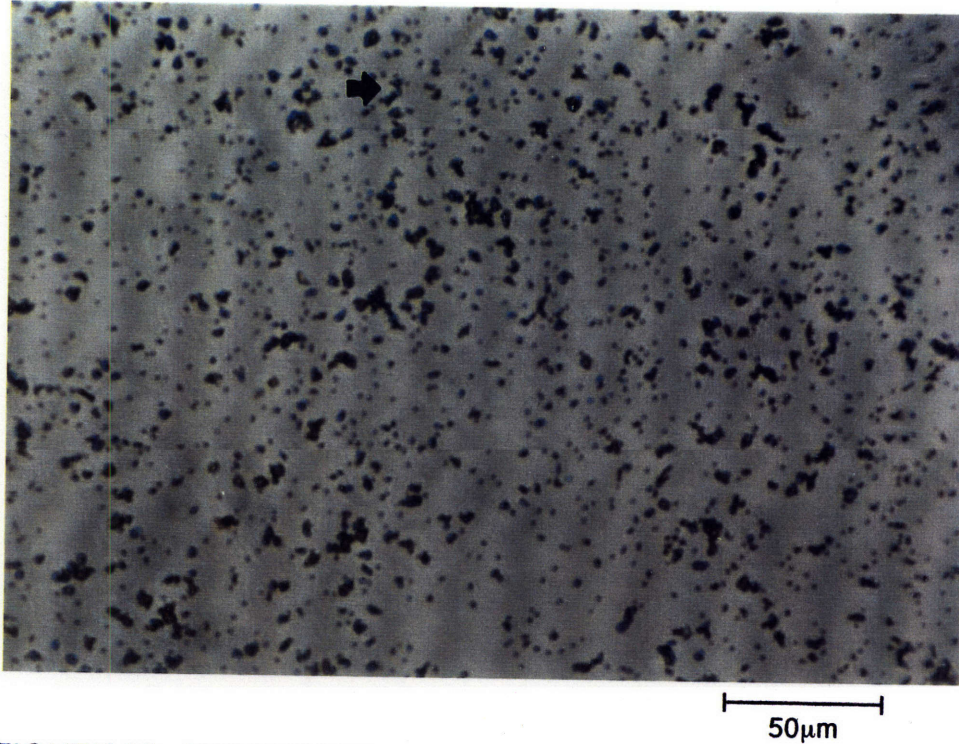


FIGURE 93 : PREDEACTIVATED BASE; SI JET AT 0.33mm/s; 400x
DEACTIVATED REGION AFTER SpA SECOND LAYER

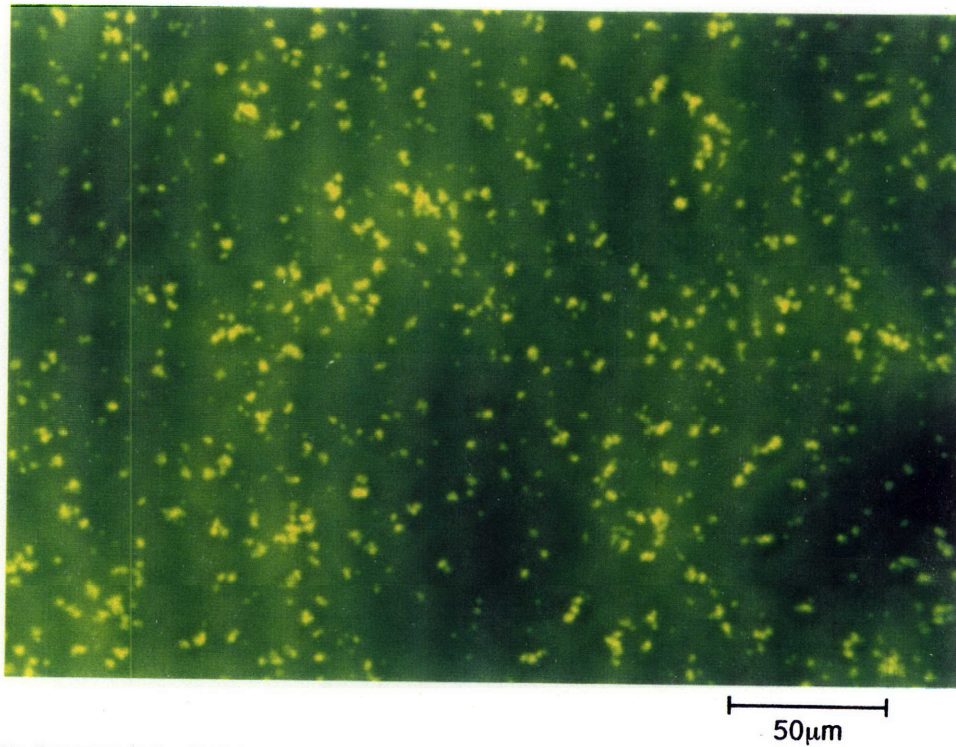


FIGURE 94 : PREDEACTIVATED BASE; SI JET AT 0.33mm/s; 400x
DEACTIVATED REGION AFTER SpA SECOND LAYER FLUORESCENCE

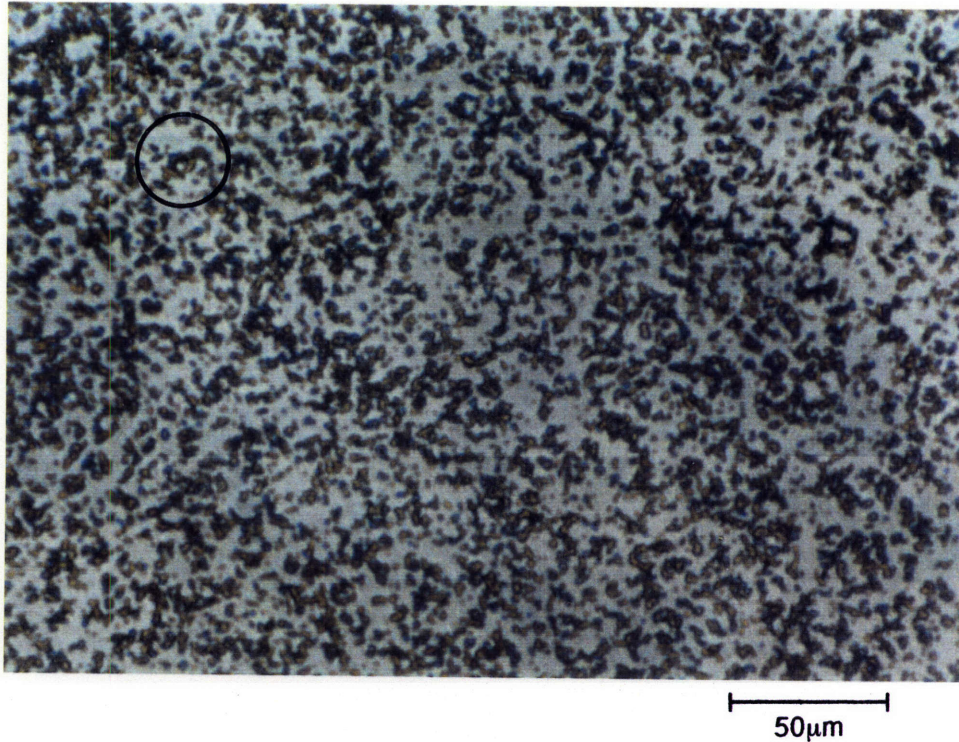


FIGURE 95 : PREDEACTIVATED BASE; SI JET AT 0.33mm/s; 400x
ACTIVE REGION AFTER SpA SECOND LAYER

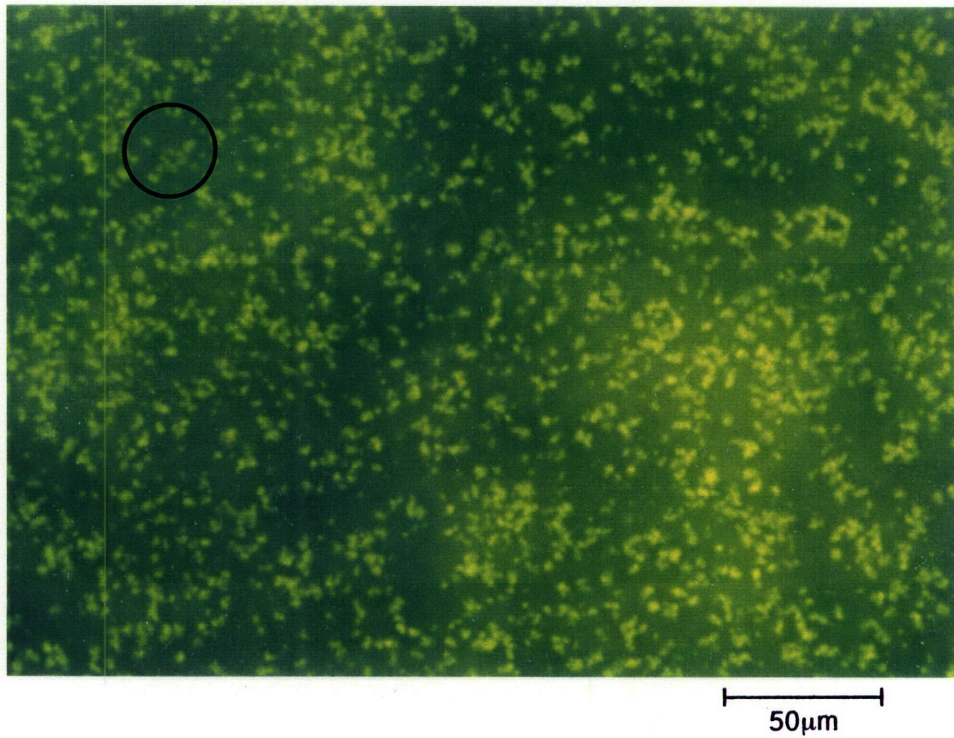


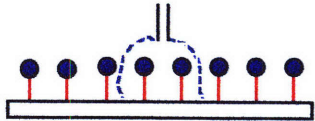
FIGURE 96 : PREDEACTIVATED BASE; SI JET AT 0.33mm/s; 400x
ACTIVE REGION AFTER SpA SECOND LAYER FLUORESCENCE



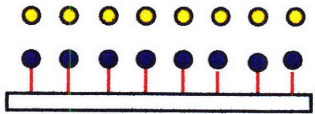
RABBIT IgG COATED GLASS



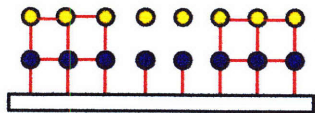
ADD GOAT ANTI-RABBIT IgG BLUE DYED BEADS
LET SETTLE FOR 2 HOURS
WASH WITH CALIBRATED WATER NOZZLE



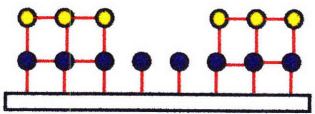
EXPOSE TO 90°C WATER JET
SURFACE GOAT ANTI-RABBIT IgG
DENATURED IN PATH OF JET



ADD PROTEIN A FLUORESBRITE BEADS
LET SETTLE FOR 2 HOURS



ADD RABBIT IgG IN SOLUTION
LET SETTLE FOR 2 HOURS



WASH WITH CALIBRATED WATER NOZZLE

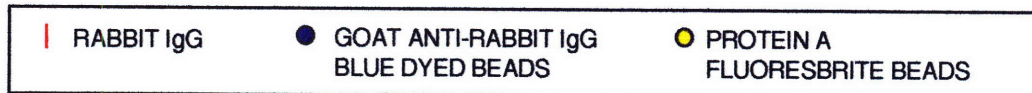
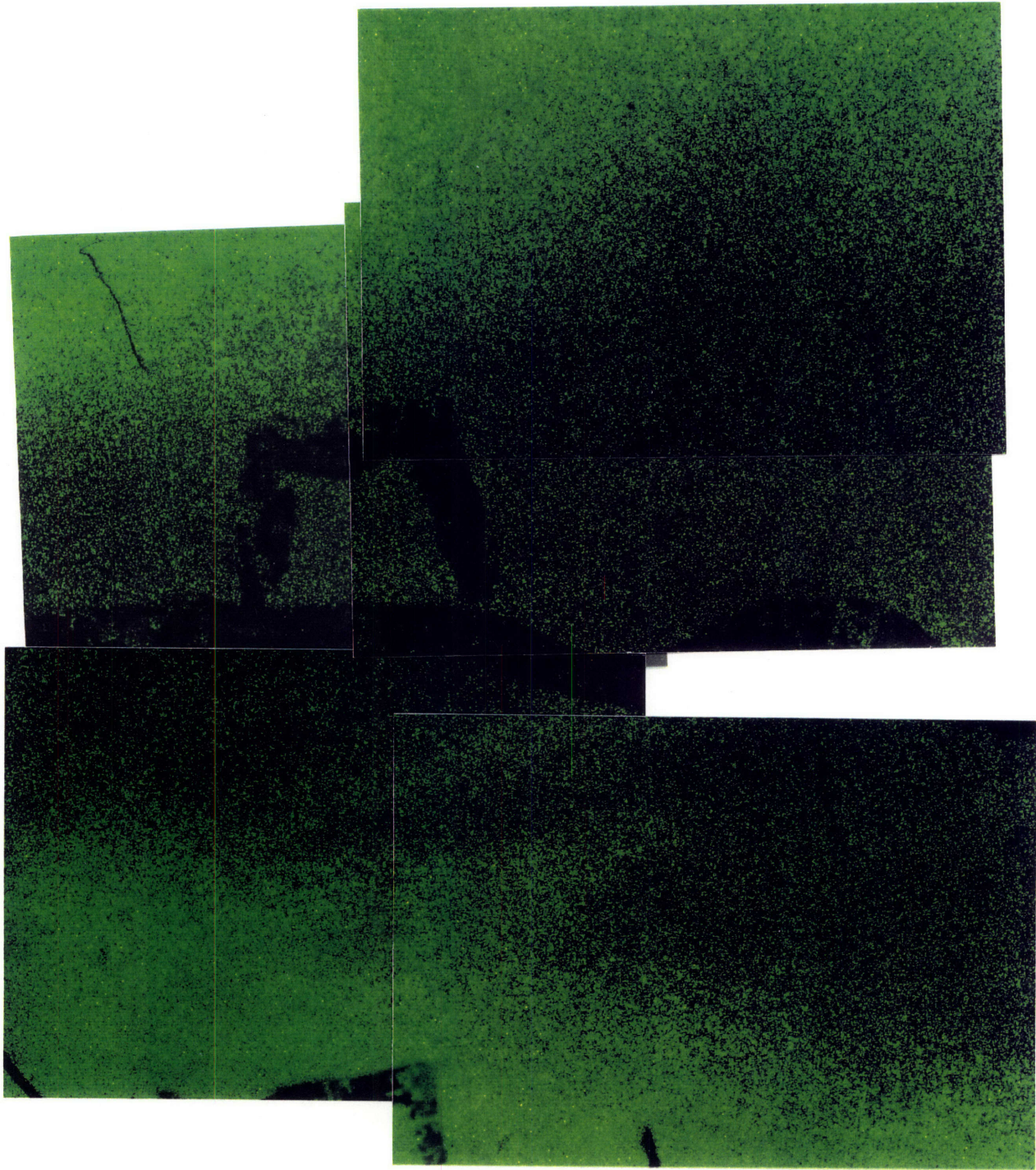


FIGURE 97 : SELECTIVE DEFINITION OF GEOMETRY
BOUND BEAD BASE

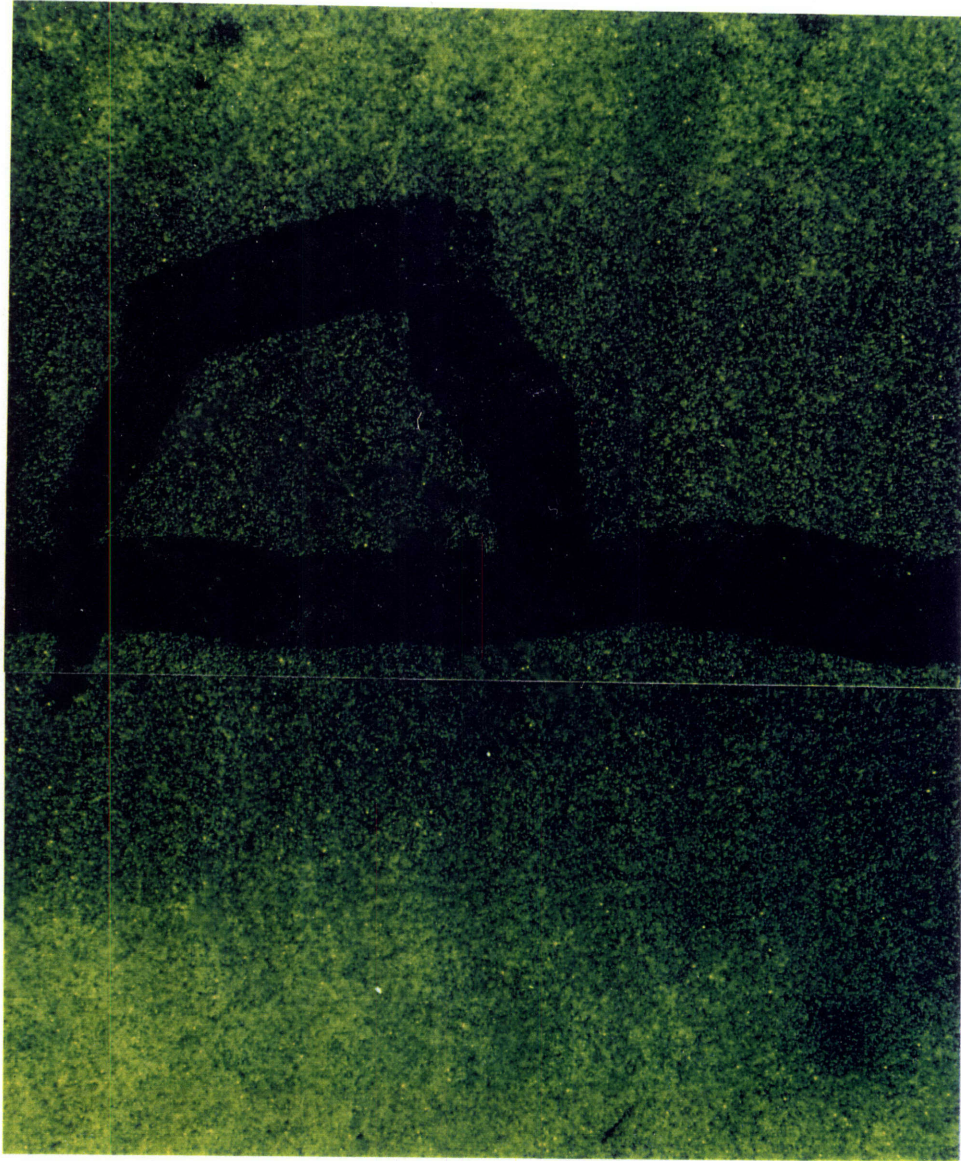


1mm

FIGURE 98 : BOUND BEAD BASE; SI JET AT 0.33mm/s
AFTER SpA SECOND LAYER - LINE WIDTH = 10.6mm
FLUORESCENCE



**FIGURE 99 : BOUND BEAD BASE; SI JET AT 0.17mm/s
AFTER SpA SECOND LAYER - LINE WIDTH = 3.8mm - 7.6mm
FLUORESCENCE**



1mm

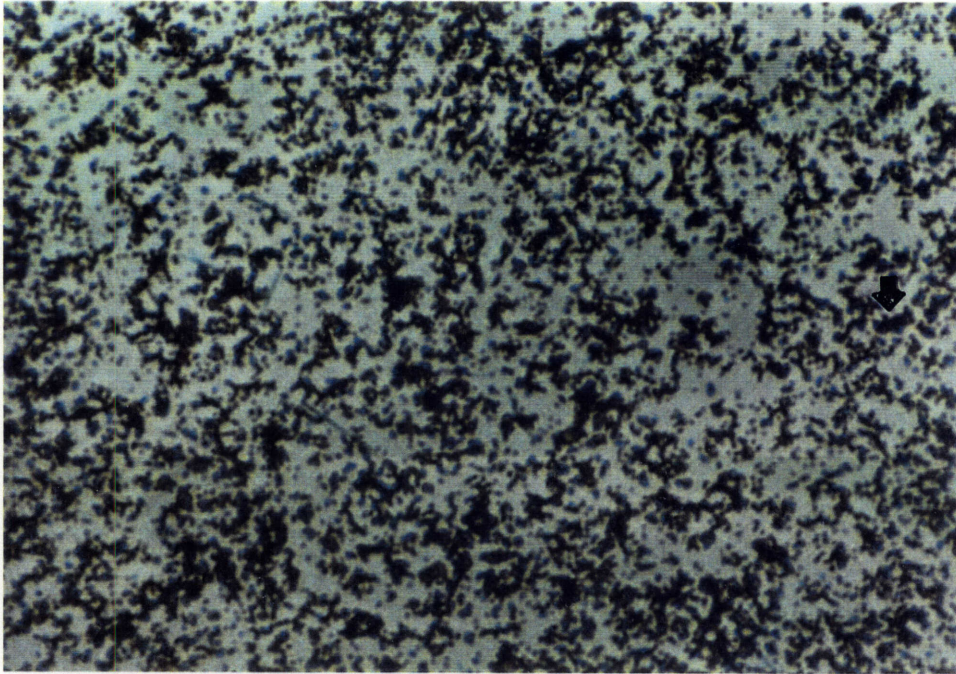
FIGURE 100 : BOUND BEAD BASE; SI JET AT 0.067mm/s; 20x
AFTER SpA SECOND LAYER - LINE WIDTH = 4.3 - 5.5mm FLUORESCENCE

Figures 98 to 100, fluorescence, detail the line widths on the $0.44\mu\text{g}/\text{cm}^2$ samples at the three tested traverse speed. The selective line definition indicates the top surface GAR-IgG of the first bead layer did become deactivated. The line width difference is not judged as a significant correlate with the traverse speed, the more important conclusion is the demonstration of first layer deactivation. The predeactivated base parts had a secondary region of deposition at line widths of 7.3mm for 0.17mm/s and 5.3mm for 0.33mm/s, suggesting additional deactivation in the active region first layer. Thus, the deactivating line width of the SI jet increased from 1.5mm on a R-IgG coated base up to 5 to 10mm on a total or partially bead coated base.

The 0.067mm/s was an extreme heat environment tested when the other traverse speeds did not disturb first layer beads. Figures 101 and 102 are the first layer photos for the 0.067mm/s sample. The first layer photos show deposition comparable to the R-IgG control because the R-IgG coated base was not heat treated. The deactivated and active region assignments are indications of where the SI jet will pass over the first layer. Comparing the first layer deposition to the post SI jet pass photos, Figure 103 and 104, no deposition removal occurred. The traverse of the SI jet over the bound bead base caused no removal of beads for the speed range tested, 0.33mm/s to 0.067mm/s. The relative increase of deposition in the deactivated region (Figure 101, first layer, and Figure 105, second layer) with respect to the active region (Figure 102, first layer, and Figure 107, second layer) show deposition increase in the active region. The fluorescent deactivated region photo, Figure 106, show residual deposition comparable to that of predeactivated base SpA residuals (Figures 88 and 94) as well as glass control residuals (Figure 30). The fluorescent active region photos, Figure 108, shows deposition slightly greater than the predeactivated bases (Figures 90 and 96) and closer to the control (Figure 71) despite photographic contrast differences. The difference between the fluorescence photos detail the selective definition of deactivated and active regions for SpA second layer deposition.

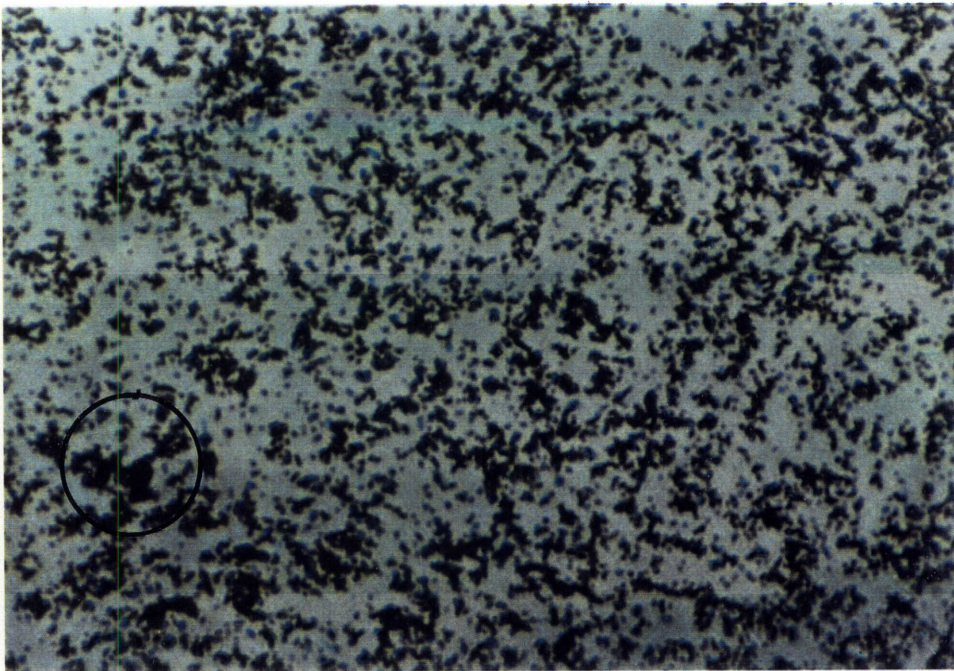
Figure 109 to 114 are the same set of photos for the 0.33mm/s sample provided to demonstrate selective definition reproducibility. Examining the 0.067mm/s and 0.33mm/s deactivated fluorescent photos, Figures 106 and 112, residual deposition is comparable. Active regions for the two scan speeds, Figures 108 and 114, were comparable indicating that deposition was selective to regions unaffected by the extent of the hot water traverse.

The bound bead base 3D parts showed successful selective definition of geometry. The bound beads were not removed by the range of traverse speeds, 0.33mm/s to 0.067mm/s. The GAR-IgG antibodies on the surface of the bound bead layer were deactivated by the SI jet traverse as proven by the selective deposition of the SpA. Deactivated line width increase by almost an order of magnitude going from the R-IgG coated glass base to a bead coated base.



50 μ m

FIGURE 101: BOUND BEAD BASE; 400x
DEACTIVATED REGION GAR-IgG FIRST LAYER



50 μ m

FIGURE 102 : BOUND BEAD BASE; 400x
ACTIVE REGION GAR-IgG FIRST LAYER

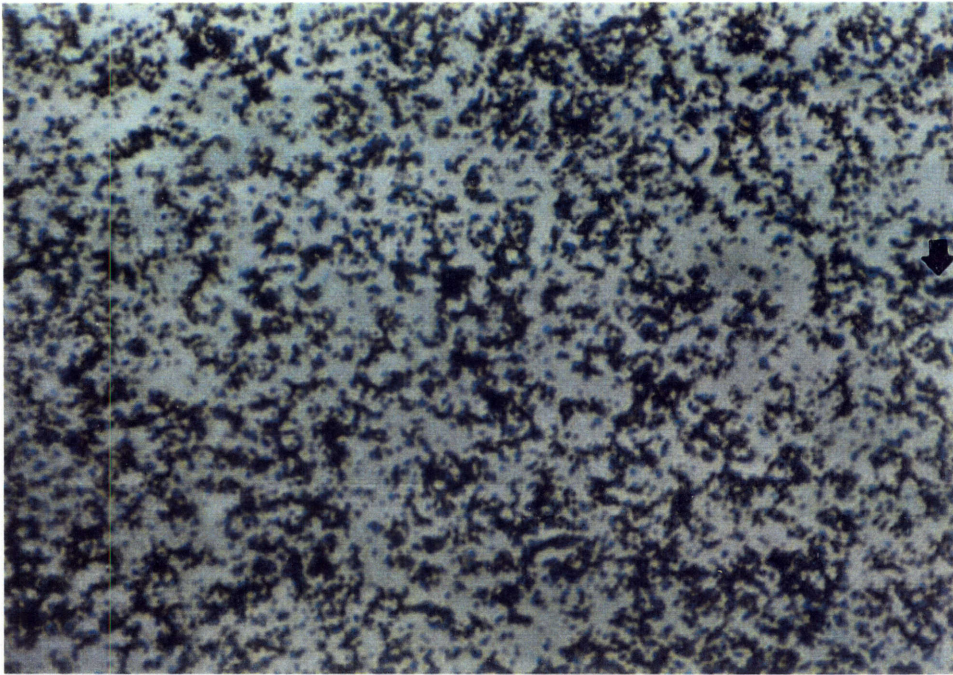


FIGURE 103 : BOUND BEAD BASE; 400x
DEACTIVATED REGION GAR-IgG FIRST LAYER
AFTER PASS OF SI JET AT 0.067mm/s

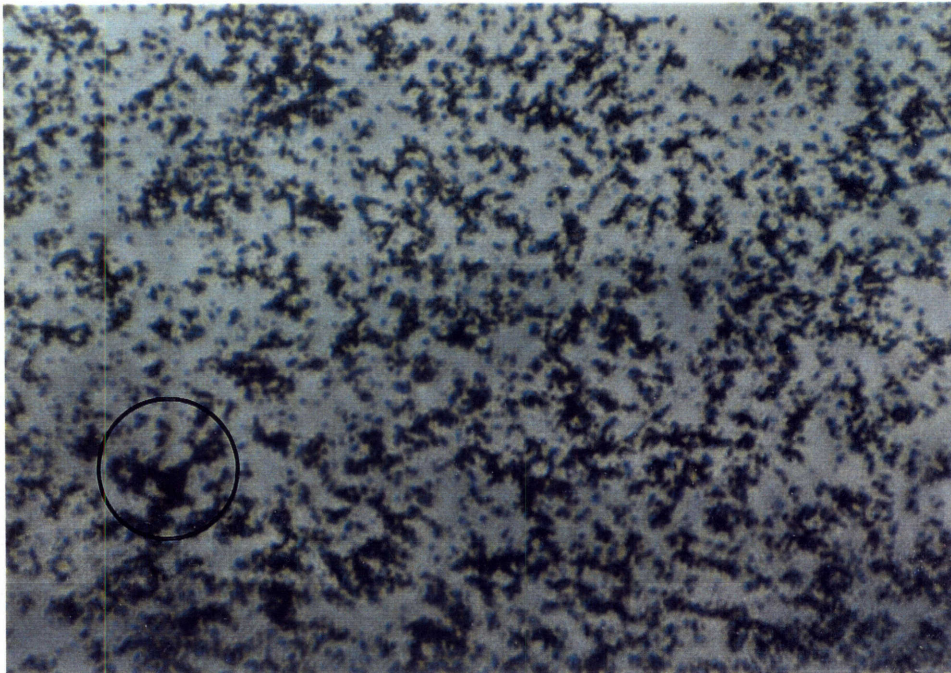
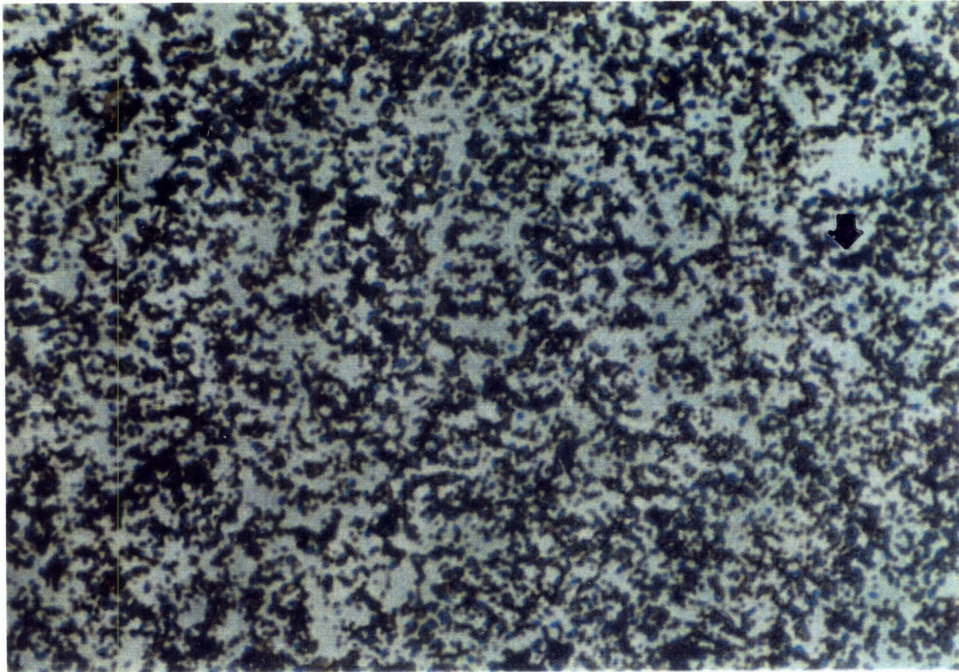
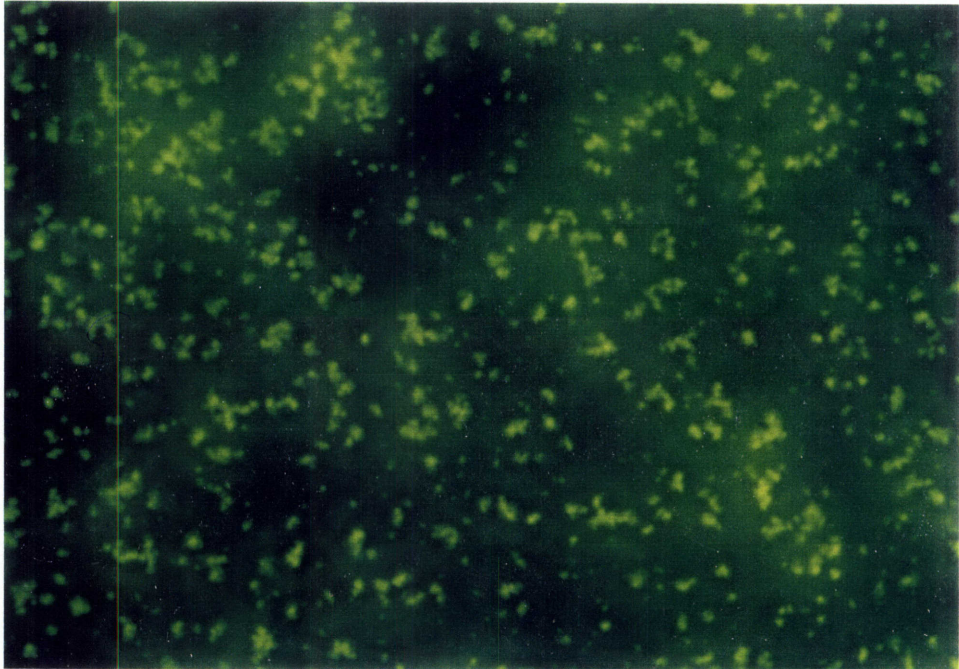


FIGURE 104 : BOUND BEAD BASE; 400x
ACTIVE REGION GAR-IgG FIRST LAYER
AFTER PASS OF SI JET AT 0.067mm/s



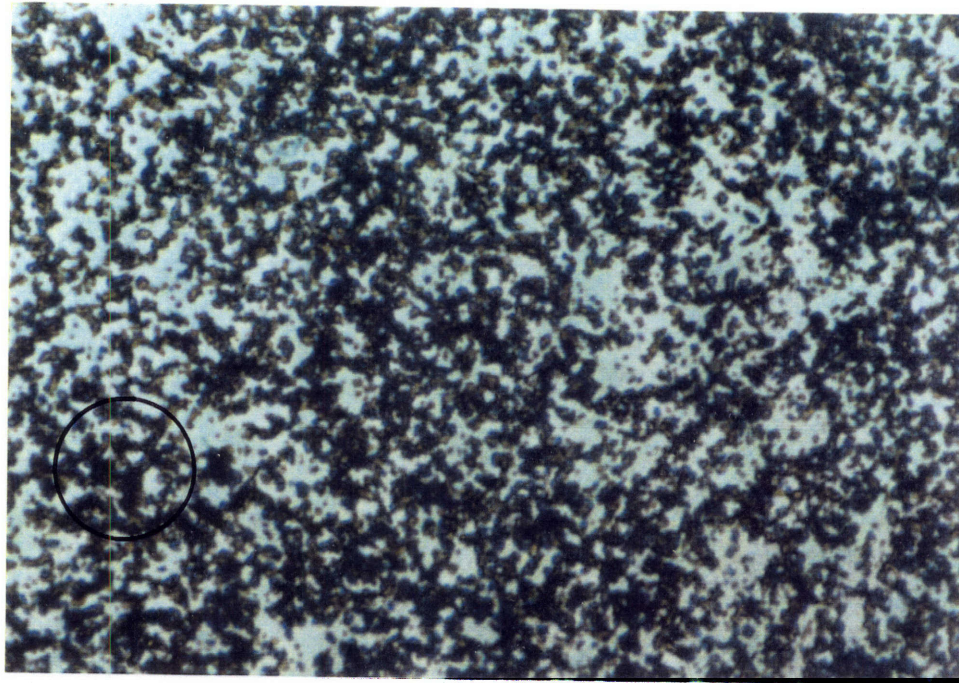
50 μ m

FIGURE 105 : BOUND BEAD BASE; SI JET AT 0.067mm/s; 400x
DEACTIVATED REGION AFTER SpA SECOND LAYER



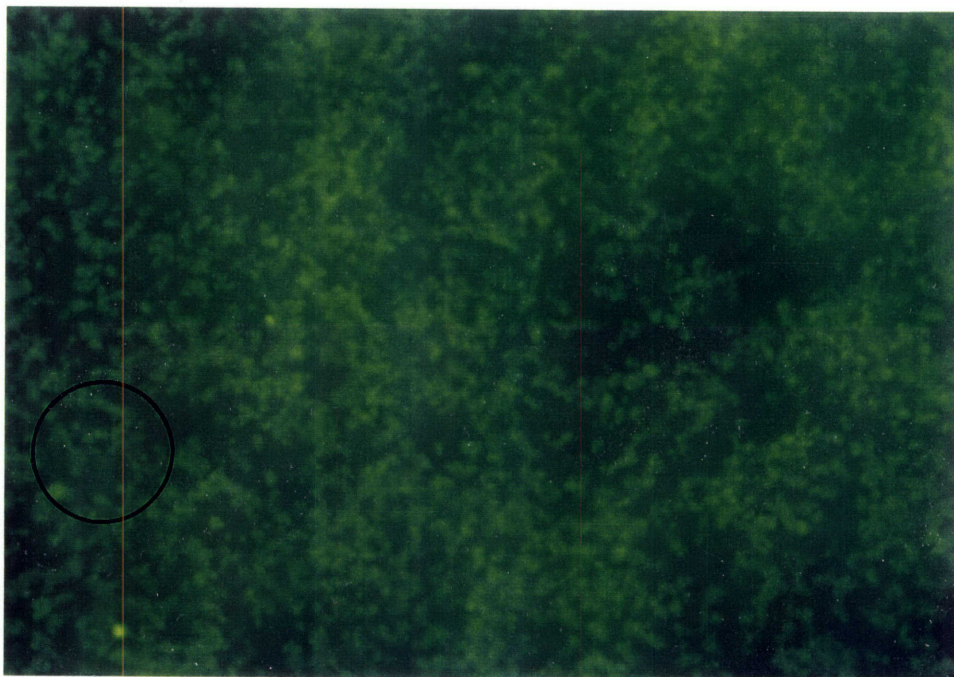
50 μ m

FIGURE 106 : BOUND BEAD BASE; SI JET AT 0.067mm/s; 400x
DEACTIVATED REGION AFTER SpA SECOND LAYER FLUORESCENCE



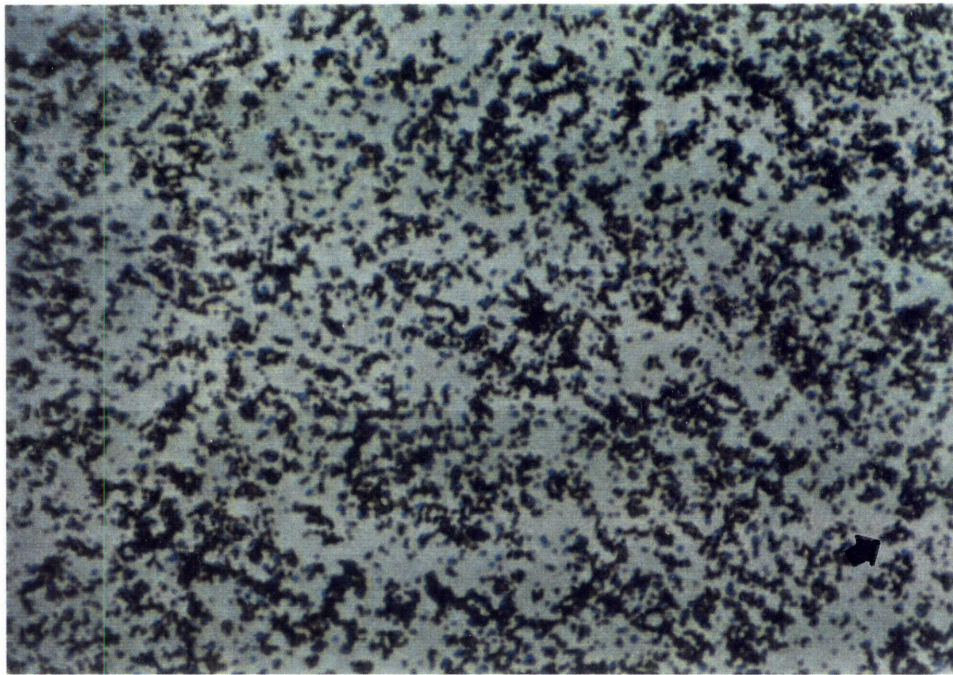
50 μ m

FIGURE 107 : BOUND BEAD BASE; SI JET AT 0.067mm/s; 400x
ACTIVE REGION AFTER SpA SECOND LAYER



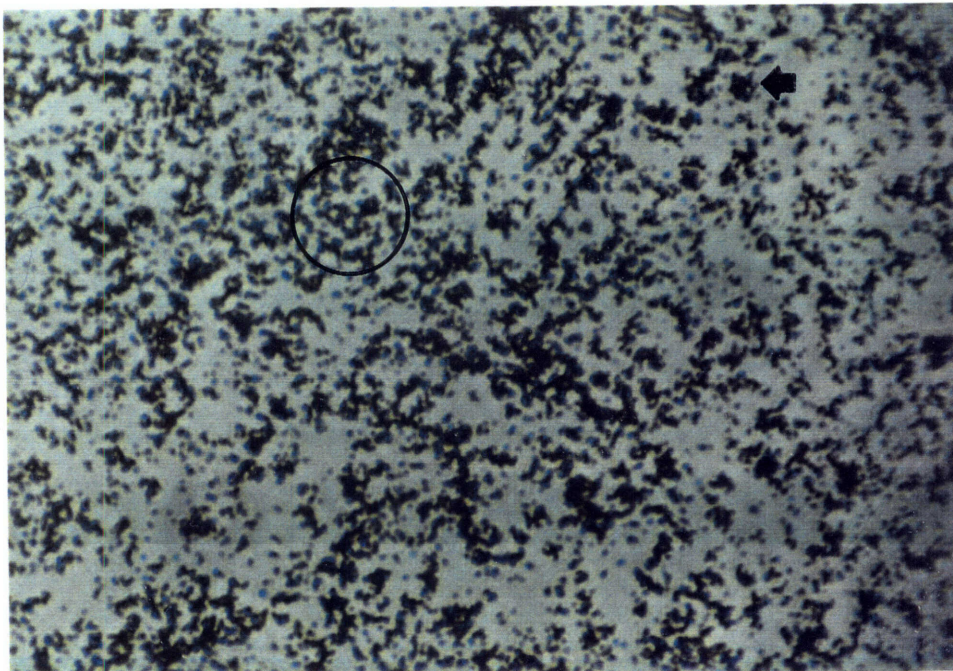
50 μ m

FIGURE 108 : BOUND BEAD BASE; SI JET AT 0.067mm/s; 400x
ACTIVE REGION AFTER SpA SECOND LAYER FLUORESCENCE



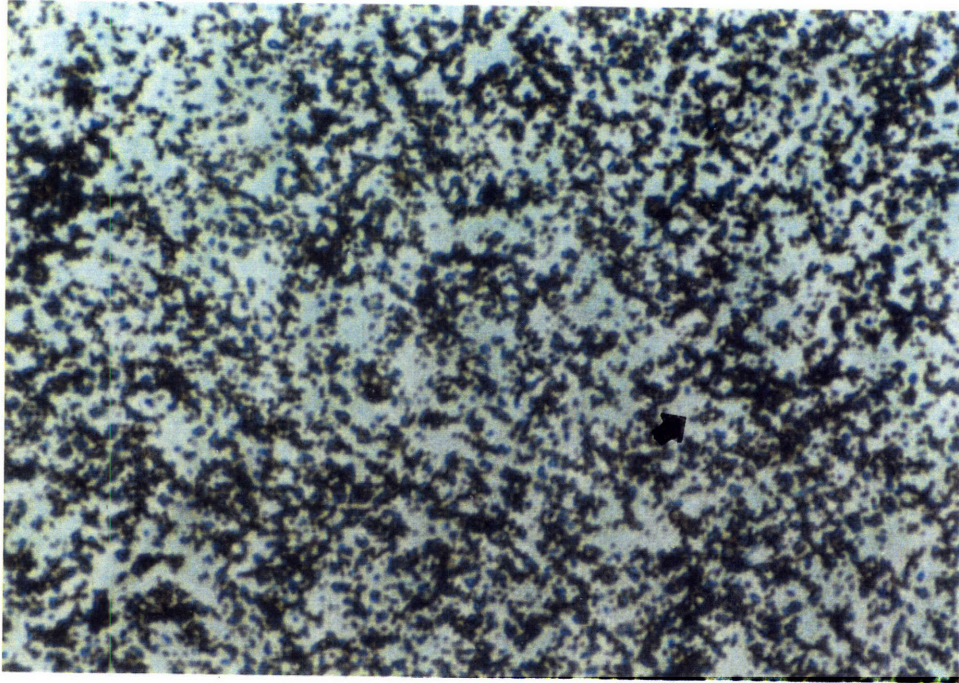
50µm

FIGURE 109 : BOUND BEAD BASE; 400x
DEACTIVATED REGION GAR-IgG FIRST LAYER



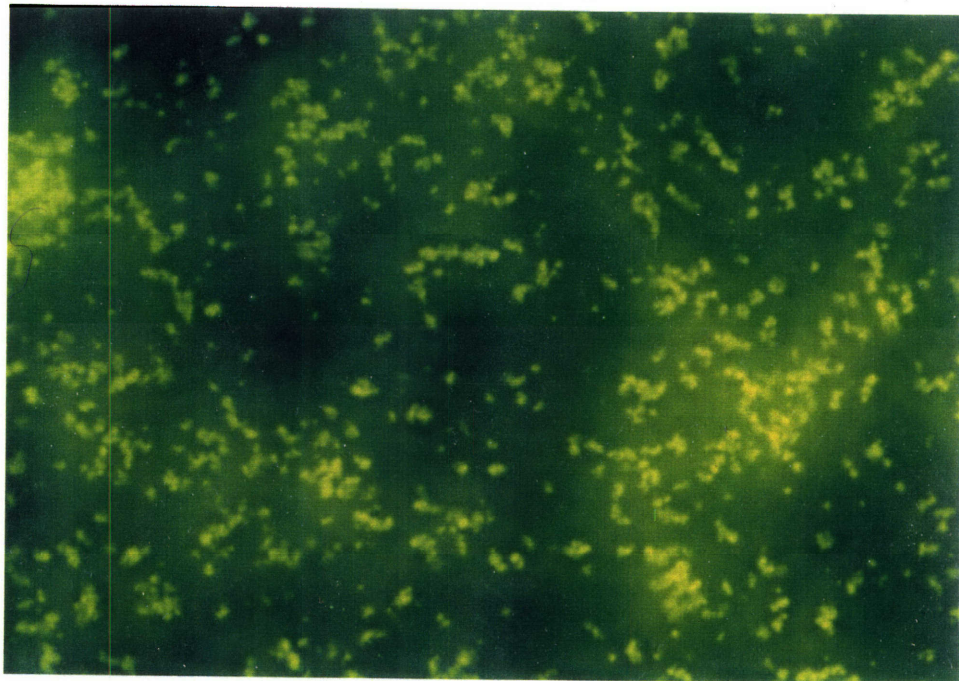
50µm

FIGURE 110 : BOUND BEAD BASE; 400x
ACTIVE REGION GAR-IgG FIRST LAYER



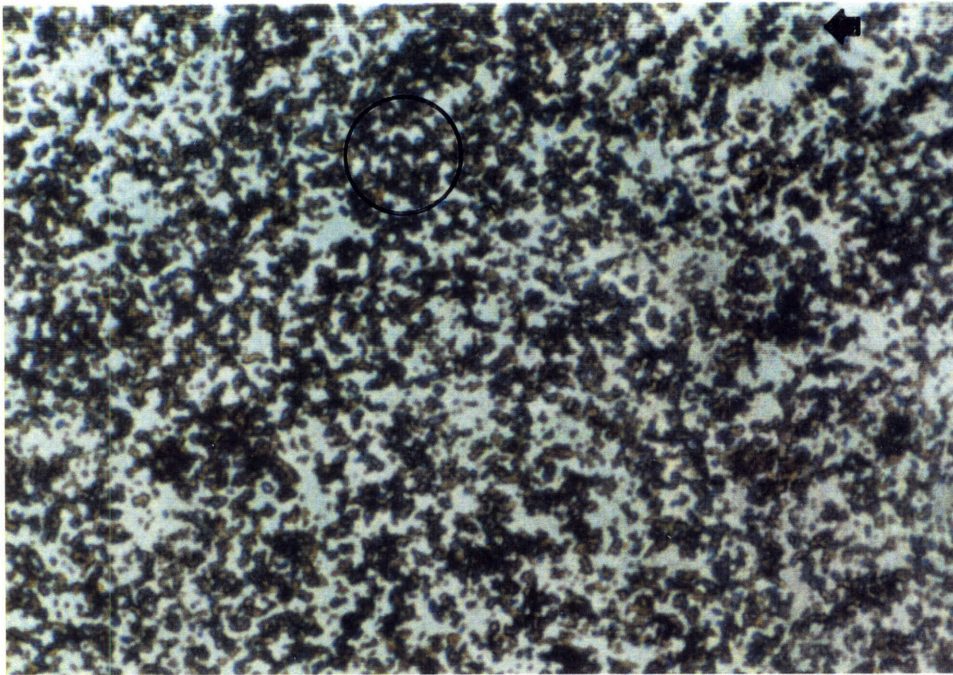
50 μ m

FIGURE 111 : BOUND BEAD BASE; SI JET AT 0.33mm/s; 400x
DEACTIVATED REGION AFTER SpA SECOND LAYER



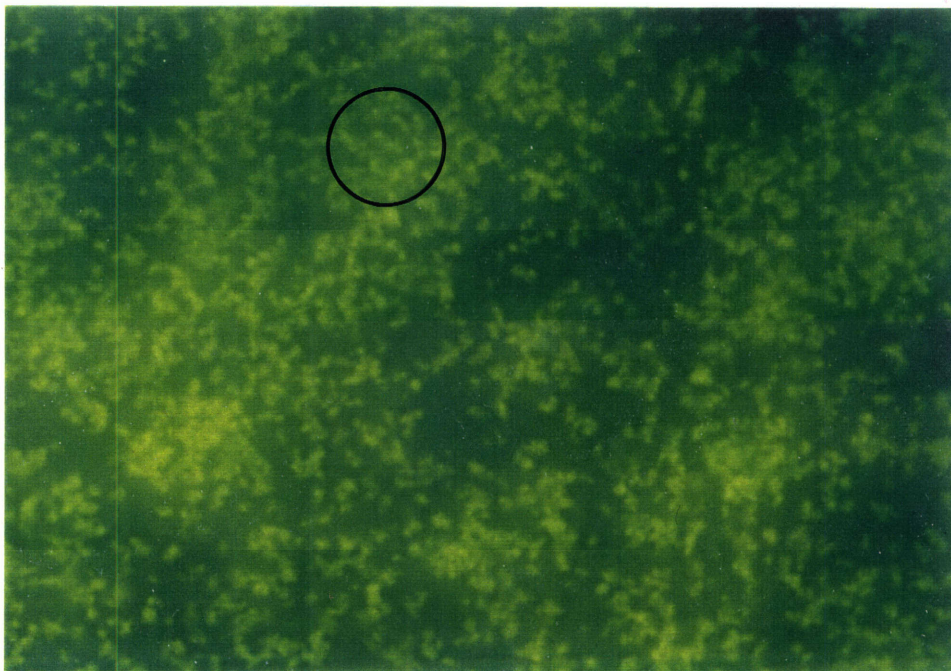
50 μ m

FIGURE 112 : BOUND BEAD BASE; SI JET AT 0.33mm/s; 400x
DEACTIVATED REGION AFTER SpA SECOND LAYER FLUORESCENCE



50 μ m

FIGURE 113 : BOUND BEAD BASE; SI JET AT 0.33mm/s; 400x
ACTIVE REGION AFTER SpA SECOND LAYER



50 μ m

FIGURE 114: BOUND BEAD BASE; SI JET AT 0.33mm/s; 400x
ACTIVE REGION AFTER SpA SECOND LAYER FLUORESCENCE

3.7 PROCESS ISSUES

Bulk strength of Biolithography parts and potential post processing methods are discussed. Suggestions for improvement of deposition uniformity and calculations of production costs are provided.

3.7.1 Bulk Strength

The strength between the bound bead and glass surface was approximated based on calculations from Cozens-Roberts et al (1990)⁸. The detachment force was converted to bead yield strength by dividing by the contact area ($0.13\mu\text{m}^2$), to give $1.4 \times 10^5 \text{Pa}$ (Appendix E). The resulting bead yield strength was converted to a bulk part strength adjusting by a factor for the projection of the contact area in a unit cell (0.13); therefore, the bulk strength was $1.8 \times 10^4 \text{Pa}$. 10^4Pa is approximately equivalent to 1psi; thus, the parts would be able to support their own weight.

Strength is an issue in the post processing of the parts. The majority of the parts were kept in the storage buffer solution, only the SEM samples were dried because of requirements of the microscope. The yield strength between two beads ($1.8 \times 10^5 \text{Pa}$) is close to the capillary stress exerted on two neighboring beads when the part is dried at atmospheric conditions ($2.9 \times 10^5 \text{Pa}$) (Appendix E). A rearrangement study was performed in which it was observed that beads that were 1 to 2 beads diameter apart before drying would be pulled together by capillary stress. The capillary stress however was not enough to actually deform the polystyrene beads that had a tensile strength of 10^7Pa .²⁸ Freeze-drying or lyophilizing of the part would eliminate the rearrangement caused by water evaporation. The moist part is frozen and, under vacuum, the frozen water is converted directly into water vapor and, thus, removed from the part.

Another possibility to improve the strength of the parts is to increase the packing density. For example, as seen in Figure 115, $10\mu\text{m}$ diameter glass beads could be linked together using $1\mu\text{m}$ polystyrene beads. The polystyrene

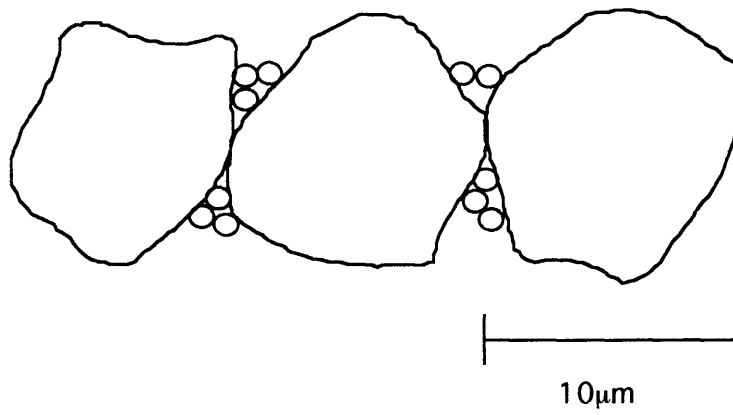


FIGURE 115 : 10µm GLASS + 1µm POLYSTYRENE
BEAD COMPOSITE

beads would fill the voids in the packing density and increase the strength. This material combination provides another post processing option. The part could be fired allowing melted polystyrene to hold the glass beads together.

3.7.2 Deposition Uniformity

In attempts to improve the coverage of the R-IgG coated glass base with the GAR-IgG beads, the R-IgG surface concentration was varied. Unfortunately, as seen in Figures 35 and 36, no elimination of void area or increase in deposition was observed. A problem is the clustering of beads prior to deposition. Despite the covalent attachment of the proteins to the beads, a neighboring bead's protein could become passively adsorbed. The two methods of controlling this problem are now advised: (1) re-passivation of beads with buffer solution containing BSA and (2) agitation of the beads before application to the glass substrate. The other potential problem is the patchy silanization of the glass surface. If the silanization step of the protocol is patchy, it follows that the R-IgG immobilization and subsequent GAR-IgG deposition will also be patchy. Reactivation of the unreacted silanols with amine functionality is a method to improve the uniformity of the immobilization process.

3.7.3 Production Costs

Assume a sample production part is 1cm^3 . Beads, proteins, glass, and time were considerations for the cost estimates. For a 1cm^3 part, the glass base would be 1cm^2 and the bead layers, at $1\mu\text{m}$ per layer, would be added until 1 cm height was achieved, that is, 10000 layers. Based on coverage calculations (Appendix E), 1.27×10^8 beads would be required for each layer. Assuming use of the same components as the present investigation, the beads are already protein coupled with GAR-IgG; however, the linking protein or, in this case, R-IgG need also be considered. Onto the glass base, 6.4×10^{13} R-IgG would be immobilized and 6×10^{12} R-IgG would have to be added to link every layer. The total R-IgG per part would be 6×10^{16} . The cost of the 1cm^2 glass piece and the

immobilization protocol reagents were neglected. The final cost consideration was time. As the process stands, eight hours are required to immobilize R-IgG onto the glass, two hours required to bind down the first layer and four hours for every following layer. Obviously the process can be modified to speed the attachment of each layer. The concepts considered are to make the addition of the R-IgG linker a flow through step so that the solution would be forced into the layer interface and the addition of the bead layer could be forced to settle faster by using flow through or agitating the base. Now the only considerations are the cost of the beads and the proteins.

Based on the bead stock used in the present investigation, at 1.25% solids by volume or 2.27×10^{10} beads/ml, 1.27×10^8 beads per layer equals $6 \mu\text{l}$ per layer or 60ml per part. At \$96.95/ml of the GAR-IgG beads, the bead cost would be \$5817.00. The cost of the linking proteins, 6×10^{16} R-IgG, was taken to be \$39.60 which is the cost for 50mg of R-IgG from Sigma ImmunoChemicals. 50mg of R-IgG is 1.87×10^{17} R-IgG. Using the same components as the present investigation, the cost of a 1 cm^3 part would be \$5856.60. If the protein immobilization onto the beads was performed in house rather than purchasing the beads, the cost per vial would drop to \$10.08/ml to \$4.90/ml. In this case, the part cost would be reduced to \$644.40 to \$333.60.

Further reduction in part cost would required a different selection of biological agents and attachment chemistries. Given that a different micron scale resolution deactivation mechanism, either thermal or wavelength selective, would improve Biolithography parts, alternatives to these components may be desired. All these options are considered for the continued development of the Biolithography process.

4. CONCLUSIONS (EXECUTIVE SUMMARY)

Biolithography is based on selective joining using antibody-antigen reactions. The selectivity is produced by selectively deactivating antigens and antibodies by thermal denaturation.

Antigens and antibodies can react to form clusters because of their multivalency i.e. the multiple binding sites of the antibody are used to link together antigens. Attachment chemistries can be used to couple proteins to polymeric, ceramic and metallic substrates. The antigen could be coupled to a micron sized particle substrate and the multivalent antibody used to link the substrate particles together. The shape of the resulting linked substrate would be altered if the antigens on the surface could not bind. Most proteins denature at high temperatures (greater than 50°C); thus, selective thermal deactivation could be used to define the shape of the linked structure. Based on the ability to immobilize proteins, the use of thermal deactivation to define shape and the selectivity of binding to only active (not deactivated) proteins, Biolithography was proposed.

The evolution of the Biolithography process tested three reactions and the subsequent use of thermal deactivation to create selective joining:

(1) agglomeration reaction and elimination of agglomeration reaction, (2) two dimensional (2D) coating process and selective deposition and (3) three dimensional (3D) layering process and selective definition of geometry.

Agglomeration was produced using antibody coated 1 μ m polystyrene beads and antigen in solution. One multivalent antigen can link together two antibody coated particles. The antibody-antigen system used was produced by immunization. An anti-IgG antibody is produced when a host animal (goat) is immunized with the IgG antigen of a donor animal (rabbit). The antibody was goat anti-rabbit IgG (GAR-IgG) and antigen was rabbit IgG (R-IgG). The IgG molecule has a characteristic Y shape and the tips of the Y are the two binding sites. A successful dilution of GAR-IgG beads to R-IgG solution (1:0.1) was found to produce clusters of 50-100 μ m. The ratio was then tested with beads

that were thermally deactivated in a 83°C oven for 5 minutes and no clustering was observed. Thermal deactivation was effective in eliminating the agglomeration reaction. The specificity of reaction to only active beads was demonstrated using both active and deactivated beads in the same test; however, to get localized deposition, the antigen needed to be immobilized onto a surface substrate.

The 2D coating process tested the deposition of GAR-IgG beads onto a R-IgG coated glass substrate; for example, a piece of microscope slide. Bead amounts to cover the glass were calculated matching the total bead projected area to the glass surface area. A washing jet, calibrated using bead-surface detachment as a guideline, was used to wash unbound beads off the glass surface. Coating reaction time was optimized based on the polystyrene bead settling time through the buffer solution but maintaining buffer hydration of the glass surface. A matrix test of uncoated and coated beads and uncoated and coated glass was performed to demonstrate the specific reaction between the GAR-IgG on the beads and the R-IgG on the glass. Minimal deposition was observed when uncoated beads were placed onto coated and uncoated glass and when coated beads were placed onto uncoated glass. Deposition increased substantially when coated beads were placed onto coated glass. The GAR-IgG beads on the R-IgG glass was the R-IgG control and the GAR-IgG beads on the uncoated glass was the glass control. The attachment of the GAR-IgG bead layer was the successful demonstration of the 2D coating process.

Two methods of thermal deactivation were used to produce local deactivated regions on glass: (1) hot (90°C) water jet and (2) argon ion laser. The same coating protocol was used on the thermally deactivated glass pieces. The continuous hot water jet produced a plume of 1 cm on the surface of the glass. Deposition in this deactivated region was comparable to the glass control. Deposition in the active region was comparable to the R-IgG control. The use of the argon ion laser improved the resolution of the deactivated

region. A variety of scan speeds and powers were tested to achieve micron scale resolution: 1.0W at 25cm/s produced line width of 19 μ m and 1.9W at 25cm/s produced line width of 34 μ m. Selective deposition similar to the continuous hot water jet test was reproduced. Despite the tens of microns resolution, the laser method had some complications that prevented its further investigation: excessive temperatures and micron scale hydrogen bubble production.

A new thermal deactivation system was created to utilize the hot water deactivation mechanism but improve its resolution. A soldering iron (SI) tip was modified to allow for water flow through. Thus, the water was heated as it was constricted through the tip and out a 20 gauge stainless steel cannula. The SI (90°C) water jet apparatus reproduced the continuous hot water jet selective deposition but at a line width of 1.5mm (traverse speeds of 0.33mm/s and 0.17mm/s).

The 3D layering process selectively deposited two bead layers using GAR-IgG beads as a base layer. Although both GAR-IgG and SpA beads were used as the second layer, the use of the SpA was continued because the beads were fluorescent which aided observation of the second layer deposition. The beads were linked together using R-IgG added after the second bead layer had settled. The bead amounts were selected to cover the glass surface area and the R-IgG linker used was an order of magnitude less than the R-IgG immobilized onto the glass. Observed deposition indicated that SpA beads deposited on top of GAR-IgG beads. This deposition was the control deposition for the active region of the 3D selective definition of geometry parts.

The selective definition parts were created working up from two types of bases: (1) predeactivated bases and (2) bound bead bases. The predeactivated bases had active and deactivated regions defined in the first layer. The base was subjected to the SI jet before the addition of the second layer. Deposition in the active regions was slightly less than the two layer control but greater than the deactivated regions. The first layer line widths were

1.5mm and, with the addition of the second layer, an additional secondary line width was observed: 5mm and 7mm for 0.33mm/s and 0.17mm/s, respectively. The bound bead bases had only active regions for the first layer deposition. The bound bead base tests showed thermal deactivation of the surface GAR-IgG on the bound bead base. The SI water jet traverse did not remove the first layer but effectively deactivated a region on the order of 5mm to 10mm for the range of traverse speed tested (0.067mm/s to 0.33mm/s). The bound bead bases had deposition in the active region that was comparable to the two layer control.

Biolithography has successfully demonstrated selective joining based on thermal deactivation of antigens and antibodies. Selective deposition produced deposition of antibody beads selective to regions of active antigens. Deactivation regions on the order of tens of microns were produced with an argon ion laser. Selective definition of geometry demonstrated the selective deposition of two bead layers on both active antigen and antibody bases. Deactivated regions on the order of millimeters were produced with a modified SI hot water jet.

Bulk strength of Biolithography parts is 10^4 Pa which indicates that the parts can support their own weight. Post processing methods are available to increase the part strength. Production costs, deposition uniformity and a higher resolution deactivation mechanism are all issues that can be addressed by modifying biological agents and chemical protocols. These alternatives are being evaluated for the continued evolution of the Biolithography process.

5. REFERENCES

- ¹ Tsao C. (1994). Photo-Electroforming: A New Manufacturing Process for Micro-Electro-Mechanical Systems. Doctor of Philosophy Thesis, MIT.
- ² Kalapakjian, S. (1992). Manufacturing Engineering and Technology, Second Edition. Addison-Wesley, Reading, Ma. pp. 1013-1014.
- ³ Guyton A.C. (1991) Textbook of Medical Physiology. Saunders, Philadelphia. pp. 385-389.
- ⁴ Voet D. and Voet J.G. (1990). Biochemistry. John Wiley & Sons, New York. pp. 1095-1101.
- ⁵ Nossal G.J.V. (1993). Life, Death and the Immune System. *Scientific American*. 269(3):53-62.
- ⁶ Nisonoff A. et al (1975). The Antibody Molecule. Academic Press, New York. pp. 2-3 & 323.
- ⁷ Steward M.W. (1984). Antibodies: Their Structure and Function. Chapman and Hall, London. pp. 21-22.
- ⁸ Cozens-Roberts C. et al (1990). Receptor-Mediated Adhesion Phenomena: Model Studies with the Radial-Flow Detachment Assay. *Biophysical Journal*. 58:107-125.
- ⁹ Bowry T.R. (1984). Immunology Simplified. Oxford University Press, Oxford. pp. 24-29.
- ¹⁰ Clausen J. (1981). Immunochemical Techniques for the Identification and Estimation of Macromolecules. In Laboratory Techniques In Biochemistry and Molecular Biology. Vol. 1 Part 3. Work T.S. and Work E. eds. Elsevier, Amsterdam. pp. 8-14.
- ¹¹ Gergely J. (1988). Multifunctional IgG and IgG Binding Receptors. Elsevier, Amsterdam. 1988. pp.70.
- ¹² Edelman G.M. and Gally J.A. (1964). A Model for the 7S Antibody Molecule. *Proceedings of the National Academy of Science (U.S.A.)*. 51:846-853
- ¹³ Kratky O. et al (1955). Determination of the Shape of Gamma-Globulin by Means of the X-ray Low-Angle Method. *Journal of Polymer Science*. 16:163-175
- ¹⁴ Surolia A. et al (1982). Protein A: Nature's Universal Anti-Antibody. *Trends in Biochemical Sciences*. 7:74-76.
- ¹⁵ Lindmark R. et al (1983). Binding of Immunoglobulins to Protein A and Immunoglobulin Levels in Mammalian Sera. *Journal of Immunological Methods*. 62:1-13.
- ¹⁶ Polysciences, Inc.. 1993-94 Microscopy & Histology Catalog. pp. 19-20.
- ¹⁷ Weetall H.H. (1976). Covalent Coupling Methods for Inorganic Support Materials. In *Methods in Enzymology*. 44:134-148.
- ¹⁸ Polysciences, Inc.. 1995-1996 Particle Catalog. pp10.
- ¹⁹ Kuo S.C. and Lauffenburger D.A. (1993). Relationship between Receptor/Ligand Binding Affinity and Adhesion Strength. *Biophysical Journal*. 65:2191-2200.

- ²⁰ Personal Communication with S.C. Kuo. June, 1994.
- ²¹ Lauffenburger D.A. and Linderman J.J. (1993). Receptors: Models for Binding, Trafficking and Signaling. Oxford University Press, New York. pp. 13 & 274-276.
- ²² Repacholi M.H. et al (1991). Current and Future Applications of Lasers in Medicine. In Grandolfo M. et al. Lights, Lasers and Synchrotron Radiation. Plenum Press, New York. pp. 373-393.
- ²³ Court L.A. et al (1991). Medical Lasers and Biological Criteria and Limits of their Therapeutic Effects. In Grandolfo M. et al. Lights, Lasers and Synchrotron Radiation. Plenum Press, New York. pp. 353-371.
- ²⁴ Brydson J.A. (1989). Plastic Materials. Butterworths, London. pp. 406
- ²⁵ Goldman A.J. (1967). Slow Viscous Motion of a Sphere Parallel to a Plane Wall - II Couette Flow. *Chemical Engineering Science*. 22:653-660.
- ²⁶ Fay J.A. (1994). Introduction to Fluid Mechanics. MIT Press, Cambridge. pp. 300.
- ²⁷ Spitznagel T.M. and Clark D.S. (1993). Surface-Density and Orientation Effects on Immobilized Antibodies and Antibody Fragments. *Bio/Technology*. 11:825-829
- ²⁸ Askeland, D.R. (1989). The Science and Engineering of Materials, Second Edition. PWS-Kent, Boston. pp. 533.

APPENDIX A (SECTION 2.2)

A.1 BEADS

A.1.1 Number of Beads (formula provided by Polysciences, Inc.
1993-94 Microscopy & Histology Catalog)

$$\# \text{ of particles per ml} = \frac{6W \times 10^{12}}{\rho \times \pi \times \varphi^3}$$

W = grams of polymer per ml in latex (0.025g for a 2.5 % latex)

φ = diameter in microns of latex microparticles

ρ = density of polymer in grams per ml (1.05 for polystyrene)

GAR-IgG	lot 435714	1.24% solids	∴ 2.26x10 ¹⁰ beads/ml
GAR-IgG	lot 445454	1.25% solids	∴ 2.27x10 ¹⁰ beads/ml
SpA	lot 443033	1.25% solids	∴ 2.27x10 ¹⁰ beads/ml
SpA	lot 441668	1.25% solids	∴ 2.27x10 ¹⁰ beads/ml
Polybeads [®]	lot 445125	2.5% solids	∴ 4.55x10 ¹⁰ beads/ml

A.1.2 GAR-IgG lot 435714

A.1.2.1 Surface concentration

specified protein concentration = 428μg/ml

surface area of 1μm diameter polystyrene bead (r=0.5μm)

$$SA_{\text{bead}} = 4\pi r^2 = 3.14\mu\text{m}^2$$

surface area of beads/ml = SA_{bead} x number of beads

$$= (3.14\mu\text{m}^2)(2.26 \times 10^{10} \text{ beads/ml}) = 7.09 \times 10^{10} \mu\text{m}^2/\text{ml} = 709\text{cm}^2/\text{ml}$$

$$\text{surface concentration} = \frac{428\mu\text{g/ml}}{709\text{cm}^2/\text{ml}} = 0.604\mu\text{g/cm}^2$$

A.1.2.2 Protein density

molecular weight of IgG 160000mol.wt.

$$\frac{160000 \text{ g/mol}}{6.022 \times 10^{23} / \text{mol}} = 2.66 \times 10^{-19} \text{ g} = 2.66 \times 10^{-13} \mu\text{g}$$

$$\text{protein density} = \frac{0.605 \mu\text{g/cm}^2}{2.66 \times 10^{-13} \mu\text{g}} = 2.27 \times 10^{12} \text{ GAR-IgG/cm}^2$$

proteins per bead =

$$(2.27 \times 10^{12} \text{ GAR-IgG/cm}^2) (3.14 \mu\text{m}^2) \left(\frac{\text{cm}}{10^4 \mu\text{m}} \right)^2 = 7.14 \times 10^4 \text{ GAR-IgG/bead}$$

protein spacing =

$$\sqrt{\frac{1}{2.27 \times 10^{12} \text{ GAR-IgG/cm}^2}} = 6.63 \times 10^{-7} \frac{\text{cm}}{\text{GAR-IgG}} = 6.63 \frac{\text{nm}}{\text{GAR-IgG}}$$

A.1.3 GAR-IgG lot 445454

A.1.3.1 Surface concentration

specified protein concentration = 394 μg/ml

surface area of 1 μm diameter polystyrene bead (r=0.5 μm)

$$SA_{\text{bead}} = 4\pi r^2 = 3.14 \mu\text{m}^2$$

surface area of beads/ml = SA_{bead} x number of beads

$$= (3.14 \mu\text{m}^2) (2.27 \times 10^{10} \text{ beads/ml}) = 7.14 \times 10^{10} \mu\text{m}^2/\text{ml} = 714 \text{cm}^2/\text{ml}$$

$$\text{surface concentration} = \frac{394 \mu\text{g/ml}}{714 \text{cm}^2/\text{ml}} = 0.552 \mu\text{g/cm}^2$$

A.1.3.2 Protein density

molecular weight of IgG 160000 mol.wt.

$$\frac{160000 \text{ g/mol}}{6.022 \times 10^{23} / \text{mol}} = 2.66 \times 10^{-19} \text{ g} = 2.66 \times 10^{-13} \mu\text{g}$$

$$\text{protein density} = \frac{0.552 \mu\text{g/cm}^2}{2.66 \times 10^{-13} \mu\text{g}} = 2.08 \times 10^{12} \text{ GAR-IgG/cm}^2$$

proteins per bead =

$$(2.08 \times 10^{12} \text{ GAR-IgG/cm}^2) (3.14 \mu\text{m}^2) \left(\frac{\text{cm}}{10^4 \mu\text{m}} \right)^2 = 6.52 \times 10^4 \text{ GAR-IgG/bead}$$

protein spacing =

$$\sqrt{\frac{1}{2.08 \times 10^{12} \text{ GAR-IgG/cm}^2}} = 6.94 \times 10^{-7} \frac{\text{cm}}{\text{GAR-IgG}} = 6.94 \frac{\text{nm}}{\text{GAR-IgG}}$$

A.1.4 SpA lot 441668

A.1.4.1 Surface concentration

specified protein concentration = 95 μg/ml

surface area of 1 μm diameter polystyrene bead (r=0.5 μm)

$$SA_{\text{bead}} = 4\pi r^2 = 3.14 \mu\text{m}^2$$

surface area of beads/ml = SA_{bead} x number of beads

$$= (3.14 \mu\text{m}^2) (2.27 \times 10^{10} \text{ beads/ml}) = 7.14 \times 10^{10} \mu\text{m}^2/\text{ml} = 714 \text{cm}^2/\text{ml}$$

$$\text{surface concentration} = \frac{95 \mu\text{g/ml}}{714 \text{cm}^2/\text{ml}} = 0.133 \mu\text{g/cm}^2$$

A.1.4.2 Protein density

molecular weight of SpA 42000 mol.wt.

$$\frac{42000 \text{ g/mol}}{6.022 \times 10^{23} / \text{mol}} = 6.97 \times 10^{-20} \text{ g} = 6.97 \times 10^{-14} \mu\text{g}$$

$$\text{protein density} = \frac{0.552 \mu\text{g/cm}^2}{6.97 \times 10^{-14} \mu\text{g}} = 1.91 \times 10^{12} \text{ SpA/cm}^2$$

proteins per bead =

$$(1.91 \times 10^{12} \text{ SpA/cm}^2) (3.14 \mu\text{m}^2) \left(\frac{\text{cm}}{10^4 \mu\text{m}} \right)^2 = 5.99 \times 10^4 \text{ SpA/bead}$$

$$\text{protein spacing} = \sqrt{\frac{1}{1.91 \times 10^{12} \text{ SpA/cm}^2}} = 7.24 \times 10^{-7} \frac{\text{cm}}{\text{SpA}} = 7.24 \frac{\text{nm}}{\text{SpA}}$$

A.1.5 SpA lot 443033

A.1.5.1 Surface concentration

specified protein concentration = 100 μ g/ml

surface area of 1 μ m diameter polystyrene bead ($r=0.5\mu$ m)

$$SA_{\text{bead}} = 4\pi r^2 = 3.14\mu\text{m}^2$$

surface area of beads/ml = SA_{bead} x number of beads

$$= (3.14\mu\text{m}^2)(2.27 \times 10^{10} \text{ beads/ml}) = 7.14 \times 10^{10} \mu\text{m}^2/\text{ml} = 714 \text{cm}^2/\text{ml}$$

$$\text{surface concentration} = \frac{100\mu\text{g/ml}}{714 \text{cm}^2/\text{ml}} = 0.140\mu\text{g/cm}^2$$

A.1.5.2 Protein density

molecular weight of SpA 42000 mol.wt.

$$\frac{42000 \text{ g/mol}}{6.022 \times 10^{23} / \text{mol}} = 6.97 \times 10^{-20} \text{ g} = 6.97 \times 10^{-14} \mu\text{g}$$

$$\text{protein density} = \frac{0.552\mu\text{g/cm}^2}{6.97 \times 10^{-14} \mu\text{g}} = 2.01 \times 10^{12} \text{ SpA/cm}^2$$

proteins per bead =

$$(2.01 \times 10^{12} \text{ SpA/cm}^2)(3.14\mu\text{m}^2) \left(\frac{\text{cm}}{10^4 \mu\text{m}} \right)^2 = 6.30 \times 10^4 \text{ SpA/bead}$$

$$\text{protein spacing} = \sqrt{\frac{1}{2.01 \times 10^{12} \text{ SpA/cm}^2}} = 7.06 \times 10^{-7} \frac{\text{cm}}{\text{SpA}} = 7.06 \frac{\text{nm}}{\text{SpA}}$$

A.1.6 Polysciences Inc. Protocols



POLYSCIENCES, INC.

Covalent Coupling of Proteins to Amino and Blue Dyed Polystyrene Microparticles by the "Glutaraldehyde" Method*

400 Valley Road, Warrington, Pa 18976-2590, 215-343-6484, 1-800-523-2575, Fax 215-343-0214

Note:

There are many variations used for this procedure. This protocol is offered as a guide and a convenience. Specific situations may require one or more alterations of this protocol. This procedure can be used for coupling proteins to research quantities of microparticles. To use this protocol on a larger scale, increase all volumes in a proportional manner.

Phosphate Buffer Saline (PBS), pH 7.4

First, prepare 0.1 M phosphate buffer, pH 7.4, by adding 0.1 M NaH_2PO_4 to 0.1 M Na_2HPO_4 until pH becomes 7.4. To make PBS, take 200ml of the 0.1 M phosphate buffer, pH 7.4, in a 1 liter volumetric flask. Add 8.77g of NaCl and make up the volume to one liter with DI water. Check the pH of the solution. If necessary, adjust the pH to 7.4 by using diluted HCl or NaOH.

0.5 M Ethanolamine:

Add 0.15ml of ethanolamine (2-aminoethanol) to 4.8ml of PBS, pH 7.4.

Storage Buffer:

Take 20ml of 0.1 M phosphate buffer, pH 7.4, in a 100ml graduated cylinder. Add 0.88g NaCl, 1g bovine serum albumin (BSA), 5ml glycerol, and 0.1g NaN_3 , and make up the volume to 100ml. Check the pH of the final solution. If necessary, adjust the pH to 7.4 by using diluted HCl or NaOH.

Procedure:

1. Transfer 1ml of a 2.5% suspension of beads into an Eppendorf tube (1.5ml - 1.9ml capacity).
2. Fill the tube with phosphate buffered saline (PBS), pH 7.4, and cap the tube.
3. Centrifuge for 5-6 minutes in a micro centrifuge.
4. Remove supernatant carefully using a Pasteur pipette. Discard supernatant.
5. Fill the tube with PBS, cap the tube, and resuspend the beads using a Vortex mixer.
6. Centrifuge for 5-6 minutes.
7. Repeat steps 4, 5, and 6 twice.
8. Resuspend pellet in 1ml of 8% glutaraldehyde (EM Grade) in PBS, pH 7.4.
9. Leave overnight at room temperature with gentle end-to-end mixing.
10. Spin 5-6 minutes and remove supernatant.
11. Wash the pellet three times with PBS (Steps 5 and 6).
12. Resuspend the washed beads in 1ml of PBS, pH 7.4, and add 400-500 μg of protein.
13. Mix gently for 4-5 hours at room temperature by end-to-end mixing.
14. Spin for 10 minutes and save supernatant for protein determination. The amount of protein added in Step 12 minus the amount in the supernatant represents the amount bound to the beads.
15. Resuspend pellet in 1ml of 0.5 M ethanolamine in PBS and mix for 30 minutes at room temperature by end-to-end mixing.
16. Spin for 5-6 minutes and remove supernatant.
17. Resuspend pellet in 1ml of 10mg/ml bovine serum albumin (BSA) in PBS.
18. Mix for 30 minutes at room temperature and spin. Discard supernatant.
19. Resuspend pellet in 1ml of 10mg/ml BSA in PBS and spin.
20. Resuspend pellet in 1ml of PBS, pH 7.4, containing 10mg/ml BSA, 0.1% NaN_3 , and 5% glycerol (storage buffer).

Store at 4°C. **DO NOT FREEZE!**

*Not recommended for microparticles smaller than 0.5 μm .



POLYSCIENCES, INC.

Covalent Coupling of Proteins to Carboxylated Polystyrene Microparticles by the "Carbodiimide" Method*

400 Valley Road, Warrington, Pa 18976-2590, 215-343-6484, 1-800-523-2575, Fax 215-343-0214

Note:

There are many variations used for this procedure. This protocol is offered as a guide and a convenience. Specific situations may require one or more alterations of this protocol. This procedure can be used for coupling proteins to research quantities of microparticles. To use this protocol on a larger scale, increase all volumes in a proportional manner.

Stock Solution:	Prepare using distilled or deionized water unless otherwise indicated.
Carbonate Buffer:	0.1 M Carbonate buffer, pH 9.6 - prepared by adding 0.1 M Na_2CO_3 to 0.1 M NaHCO_3 until pH = 9.6.
Phosphate Buffer:	0.02 M Sodium phosphate buffer, pH 4.5 - prepare by adding 0.02 M Na_2HPO_4 to 0.02 M NaH_2PO_4 until pH = 4.5.
2% Carbodiimide:	2% 1-(3-Dimethylaminopropyl)-3-ethyl carbodiimide hydrochloride dissolved in phosphate buffer (see above). Note: Prepare within 15 minutes of using.
Borate Buffer:	0.2 M Borate buffer, pH 8.5 - use boric acid to prepare this buffer. Adjust pH to 8.5 using 1 M NaOH.
0.25 M Ethanolamine:	Add 20 μl of ethanolamine (2-aminoethanol) to 1.3ml of borate buffer.
Storage Buffer:	First prepare 0.1 M phosphate buffer, pH 7.4, by adding 0.1 M NaH_2PO_4 to 0.1 Na_2HPO_4 until pH becomes 7.4. Take 20ml of 0.1 M phosphate buffer, pH 7.4, in a 100ml graduated cylinder. Add 0.88g NaCl, 1g bovine serum albumin (BSA), 5ml glycerol, and 0.1g NaN_3 , and make up the volume to 100ml. Check the pH of the final solution. If necessary, adjust the pH to 7.4 by using diluted HCl or NaOH.

Procedure:

- Place 0.5ml of 2.5% carboxylated microparticles into an Eppendorf centrifuge tube (1.5 - 1.9ml capacity).
- Add sufficient carbonate buffer to fill tube.
- Centrifuge 5-6 minutes in a micro-centrifuge.
- Carefully remove supernatant using a Pasteur pipette. Discard supernatant.
- Repeat steps 2, 3, and 4 above one more time. To resuspend pellet:
 - fill tube halfway and cap
 - vortex
 - fill tube to capacity
 Note: When term "resuspend pellet" is used, please refer to Step 5 above.
- Resuspend pellet in phosphate buffer.
- Centrifuge for 5-6 minutes.
- Carefully remove supernatant using a Pasteur pipette. Discard supernatant.
- Repeat steps 6, 7, and 8 above two more times.
- Resuspend pellet in 0.625ml of 0.02 M sodium phosphate buffer, pH 4.5.
- Add dropwise 0.625ml of 2% carbodiimide solution.

Note: Carbodiimide solution should be prepared fresh for each procedure and used within 15 minutes of being prepared.
- Mix 3-4 hours at room temperature using an end-to-end mixer (i.e., rocker table, rotary shaker). Do not mix for more than four hours.

*Not recommended for microparticles smaller than 0.5 μ .

13. Centrifuge for 5-6 minutes. Remove and discard supernatant.
14. Resuspend pellet in phosphate buffer.
15. Centrifuge for 5-6 minutes. Remove and discard supernatant.
16. Repeat steps 14 and 15 two more times. These steps get rid of unreacted carbodiimide.
17. Resuspend pellet in 1.2ml of borate buffer.
18. Add 200-400µg of protein to coupled (we have used rabbit anti-goat IgG, IgG fraction).
19. Mix gently overnight at room temperature on an end-to-end mixer.
20. Add 50µl 0.25 M ethanolamine (2-aminoethanol). Mix gently for 30 minutes. This step serves to block unreacted sites on the microparticles.
21. Centrifuge for 10 minutes. Save supernatant for protein determination. The amount of protein added in Step 18 minus the amount in the supernatant represents the amount bound to the beads.
22. Resuspend pellet in 1ml of 10mg/ml BSA solution in borate buffer. Cap and vortex.
23. Mix gently for 30 minutes at room temperature. This step will block any remaining non-specific protein binding sites.
24. Centrifuge for 5-6 minutes. Remove and discard supernatant.
25. Repeat steps 22 and 24 once.
26. Resuspend pellet in 0.5ml of PBS, pH 7.4, containing 10mg/ml BSA, 5% glycerol, and 0.1% NaN₃ (storage buffer).

Store at 4°C. DO NOT FREEZE!

238C pg 2

TOTAL P.06

A.2 GLASS

A.2.1 Glass Composition

For 25mmx75xmmx1mm and 20mmx20mmx1mm pieces:

Becton Dickinson Gold Seal Microslides composition (product number 3050)

Silicon Dioxide	SiO ₂	72.20%
Sodium Oxide	Na ₂ O	14.30%
Potassium Oxide	K ₂ O	1.20%
Calcium Oxide	CaO	6.40%
Magnesium Oxide	MgO	4.30%
Aluminum Oxide	Al ₂ O ₃	1.20%
Ferric Oxide	Fe ₂ O ₃	0.03%
Sulfur Trioxide	SO ₃	0.30%

Personal communication Mike Papps, Erie Scientific Company, 4/4/95

For 35mmx35xmmx3mm and SEM pieces:

Spectrum Black Smooth composition (product number 1009)

Silicon Dioxide	SiO ₂	68.2105%
Sodium Oxide	Na ₂ O	13.3828%
Calcium Oxide	CaO	8.7553%
Potassium Oxide	K ₂ O	2.5176%
Fluorine	F ₂	2.0499%
Manganese Dioxide	MnO ₂	2.0248%
Aluminum Oxide	Al ₂ O ₃	1.5287%
Chromic Oxide	Cr ₂ O ₃	0.6629%
Boric Anhydride	B ₂ O ₃	0.5287%
Nickel Monoxide	NiO	0.1253%
Ferric Oxide	Fe ₂ O ₃	0.0876%
Cobaltous Oxide	CoO	0.0739%
Magnesium Oxide	MgO	0.0391%
Lead Monoxide	PbO	0.0125%
Sulfur Trioxide	SO ₃	0.0003%

Personal communication Lance Britton, Spectrum Glass Company, 4/4/95

A.2.2 Rabbit IgG Glass Protocol

Modified from RFDA Plate Preparation Procedure (Suzanne Kuo)

- | <u>I. Cleaning Glass</u> | <u>TIME</u> |
|---|--------------------|
| 1. Clean with Milli-Q water (distilled water) | |
| 2. immerse glass in hot detergent (Alconox and Milli-Q water) | 30 min. |
| 3. soak in concentrated nitric acid | 15 min. |
| 4. wash in Milli-Q water | |
| 5. soak in 4mM sodium hydroxide (0.0800g/500ml) | 15 min. |
| 6. rinse in Milli-Q water | |
| 7. place in 110-120°C oven | 1 hour |
| 8. Cool at room temp. | |
-
- | <u>II. Coupling alkylamine groups to glass surface</u> | |
|---|---|
| 1. Place glass into 2% v/v 3-aminopropyltriethoxysilane (3-APS) in acetone. | |
| <i>In 1.0ml 3-APS + 49.0ml acetone use:</i> | |
| 1 | 25mmx75mmx1mm microslide |
| 3 | 20mmx20mmx1mm microslide pieces |
| 1 | 35mmx35mmx3mm black glass pieces |
| 6 | average 150mm ² SEM pieces (black glass) |
| <i>Use in combination to use batches of 2.0ml 3-APS + 98.0ml acetone</i> | |
| 2. constantly agitate (RotoMix at lowest speed) | 10 min. |
| 3. aspirate surface to remove contaminants | |
| 4. dip briefly in acetone | |
| 5. place in 110-120°C oven | 1 hour |
| 6. check hydrophobicity with Milli-Q water (compare with clean glass control) | |
-
- | <u>III. Coupling protein via amine group to glass alkylamine group</u> | |
|--|---|
| 1. prepare immediately before use 1.1% v/v glutaraldehyde in Milli-Q water | |
| <i>In petri dish (d=97mm), use 1320μl glutaraldehyde (25% stock) + 28.68ml Milli-Q water for :</i> | |
| 2 | 25mmx75mmx1mm microslide |
| 6 | 20mmx20mmx1mm microslide pieces |
| <i>In petri dish (d=52mm), 440μl glutaraldehyde (25% stock) + 9.56ml Milli-Q water for :</i> | |
| 1 | 35mmx35mmx3mm black glass pieces |
| 6 | average 150mm ² SEM pieces (black glass) |

2. soak in covered petri dish in hood 30 min.
3. aspirate surface
4. wash in Milli-Q water
5. prepare protein solution (use 50µg/ml for maximum coverage)

In petri dish (d=97mm), 1500µl rabbit IgG (500µl @1mg/ml aliquot) + 28.5ml PBS for:

- 2 25mmx75mmx1mm microslide
- 6 20mmx20mmx1mm microslide pieces

In petri dish (d=52mm), 500µl rabbit IgG (500µl @1mg/ml aliquot) + 9.5ml PBS for:

- 1 35mmx35mmx3mm black glass pieces
- 6 average 150mm² SEM pieces (black glass)

6. soak in covered petri dish in 33-35°C oven 2 hours
7. wash glass and petri dish in Milli-Q water
8. soak in 0.2M glycine (3.0028g/200ml) 1 hour
9. wash in Milli-Q water
10. store at 4-6°C in PBS (pH=7.4) with 0.1% sodium azide

USE WITHIN 3 DAYS

Nitric Acid	Mallinckrodt 1409
NaOH	Mallinckrodt 7708
3-APS	Aldrich 11,339-5
Acetone	Mallinckrodt 2443 AR Grade
Glutaraldehyde	Electron Microscopy Sciences EM grade 25% sol'n 16220
Rabbit IgG	SIGMA ImmunoChemicals technical grade I-8140 (500µl @1mg/ml aliquot)
Glycine	Mallinckrodt 7728
PBS	SIGMA ImmunoChemicals P-4417

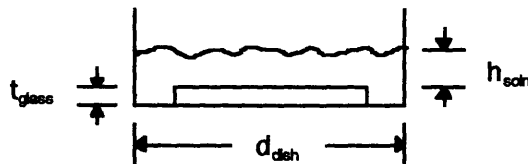
A.2.3 Surface Concentration

$$C_{\text{glass}} \left(\frac{\mu\text{g}}{\text{cm}^2} \right) = \frac{\left[C_{\text{soln}} \left(\frac{\mu\text{g}}{\text{ml}} \right) \right] \cdot [V_{\text{glass}} (\text{ml})]}{[SA_{\text{glass}} (\text{cm}^2)]}$$

where $V_{\text{glass}} (\text{ml}) = [SA_{\text{glass}} (\text{cm}^2)] \cdot [h_{\text{soln}} (\text{cm})]$

- C_{glass} = surface concentration of protein on glass
- C_{soln} = concentration of protein in coating solution
- V_{glass} = volume of coating solution above glass piece
- SA_{glass} = surface area of glass piece
- h_{soln} = height of coating solution above glass piece
(either calculated from volume or measured with ruler)

Example: 35mmx35mmx3mm black glass piece, $t_{\text{glass}} = 3\text{mm}$
 petri dish diameter, $d_{\text{dish}} = 52\text{mm}$
 protein solution volume = 10ml



volume occupied by glass = $(SA_{\text{glass}})(t_{\text{glass}})$
 $= (35\text{mm})^2(3\text{mm}) = 3675\text{mm}^3 = 3.675\text{ml}$

volume of liquid in dish if at $t_{\text{glass}} = \frac{\pi}{4} (d_{\text{dish}})^2(t_{\text{glass}})$
 $= \frac{\pi}{4} (52\text{mm})^2(3\text{mm}) = 6371\text{mm}^3 = 6.371\text{ml}$

remaining volume of liquid to reside above t_{glass}
 $= 10\text{ml} - (6.371\text{ml} - 3.675\text{ml}) = 7.304\text{ml}$

height above glass liquid occupies

$7.304\text{ml} = 7304\text{mm}^3 = \frac{\pi}{4} (52\text{mm})^2(h_{\text{soln}})$ $\therefore h_{\text{soln}} = 3.439\text{mm}$

\therefore calculated $h_{\text{soln}} = 3.439\text{mm}$

measured $h_{\text{soln}} = 3.0\text{mm}$

$$C_{\text{soin}} = 50 \mu\text{g/ml}$$

$$V_{\text{glass}}(\text{ml}) = [SA_{\text{glass}}(\text{cm}^2)] \cdot [h_{\text{soin}}(\text{cm})]$$

$$C_{\text{glass}}\left(\frac{\mu\text{g}}{\text{cm}^2}\right) = \frac{[C_{\text{soin}}\left(\frac{\mu\text{g}}{\text{ml}}\right)] \cdot [V_{\text{glass}}(\text{ml})]}{[SA_{\text{glass}}(\text{cm}^2)]}$$

$$\text{calculated } C_{\text{glass}}\left(\frac{\mu\text{g}}{\text{cm}^2}\right) = \frac{[50\left(\frac{\mu\text{g}}{\text{ml}}\right)] \cdot [12.25(\text{cm}^2)] \cdot [0.344(\text{cm})]}{[12.25(\text{cm}^2)]} = 17 \frac{\mu\text{g}}{\text{cm}^2}$$

$$\text{measured } C_{\text{glass}}\left(\frac{\mu\text{g}}{\text{cm}^2}\right) = \frac{[50\left(\frac{\mu\text{g}}{\text{ml}}\right)] \cdot [12.25(\text{cm}^2)] \cdot [0.30(\text{cm})]}{[12.25(\text{cm}^2)]} = 15 \frac{\mu\text{g}}{\text{cm}^2}$$

TABLE A1 : SURFACE CONCENTRATIONS OF RABBIT IgG

glass(#)	SA _{class} (cm ²)	d _{dish} (mm)	C _{soin} (μg/ml)	h _{soin} (mm) meas'd	h _{soin} (mm) calc'd	C _{class} (μg/cm ²) meas'd	C _{class} (μg/cm ²) calc'd
35x35x3 (1)	12	52	50	3.0	3.439	15	17
25x75x1 (2)	38	97	50	4.0	3.567	20	18
20x20x1 (6)	24	97	50	3.5	3.384	18	17
20x20x1 (6)	24	97	1.3	3.5		0.44	
SEM (6)	9	52	50		2.980		15

Nominal values	35mmx35mmx3mm	16 $\frac{\mu\text{g}}{\text{cm}^2}$
	25mmx75mmx1mm	19 $\frac{\mu\text{g}}{\text{cm}^2}$
	20mmx20mmx1mm	17 $\frac{\mu\text{g}}{\text{cm}^2}$
	20mmx20mmx1mm	0.44 $\frac{\mu\text{g}}{\text{cm}^2}$
	SEM (150mm ²)	15 $\frac{\mu\text{g}}{\text{cm}^2}$

The 15, 16, 17, and 19 $\frac{\mu\text{g}}{\text{cm}^2}$ surface concentration values are not considered significantly different.

A.2.4 Protein density

Example calculation for 35x35x3 peice with

$$C_{\text{glass}} = 16\mu\text{g}/\text{cm}^2 \text{ and } SA_{\text{glass}} = 12.25\text{cm}^2$$

molecular weight of IgG 160000mol.wt.

$$\frac{160000 \text{ g/mol}}{6.022 \times 10^{23} / \text{mol}} = 2.66 \times 10^{-19} \text{ g} = 2.66 \times 10^{-13} \mu\text{g}$$

$$\text{protein density} = \frac{16\mu\text{g}/\text{cm}^2}{2.66 \times 10^{-13} \mu\text{g}} = 6.02 \times 10^{13} \text{ R-IgG}/\text{cm}^2$$

proteins per piece =

$$(6.02 \times 10^{13} \text{ R-IgG}/\text{cm}^2)(12.25\text{cm}^2) = 7.38 \times 10^{14} \text{ R-IgG}/\text{piece}$$

protein spacing =

$$\sqrt{\frac{1}{6.02 \times 10^{12} \text{ R-IgG}/\text{cm}^2}} = 1.29 \times 10^{-7} \frac{\text{cm}}{\text{R-IgG}} = 1.29 \frac{\text{nm}}{\text{R-IgG}}$$

TABLE A2 : DENSITY OF IMMOBILIZED RABBIT IgG

glass(#)	SA _{glass} (cm ²)	C _{glass} (μg/cm ²)	DENSITY R-IgG/cm ²	#/PIECE R-IgG/piece	SPACING nm/R-IgG
35x35x3	12.25	16	6.02x10 ¹³	7.38x10 ¹⁴	1.29
25x75x1	18.75	19	7.15x10 ¹³	1.34x10 ¹⁵	1.18
20x20x1	4.00	17	6.40x10 ¹³	2.56x10 ¹⁴	1.25
20x20x1	4.00	0.44	1.66x10 ¹²	6.62x10 ¹²	7.77
SEM	1.50	15	5.56x10 ¹³	8.47x10 ¹³	1.33

APPENDIX B
(SECTION 3.3)

B.1 COVERAGE OF SLIDES

Example: 20mmx20mmx1mm

$$\text{Projected area of } 1\mu\text{m diameter beads, } PA_{\text{bead}} = \frac{\pi}{4} (1\mu\text{m})^2 = 0.785\mu\text{m}^2 \\ = 7.85 \times 10^{-7} \text{mm}^2$$

Surface area of glass to be covered, $SA_{\text{glass}} = 400\text{mm}^2$

Number of beads required to cover surface area

$$= \frac{SA_{\text{glass}} (\text{mm}^2)}{FA_{\text{bead}} (\text{mm}^2)} = \frac{400\text{mm}^2}{7.85 \times 10^{-7} \text{mm}^2} = 5.10 \times 10^8 \text{beads}$$

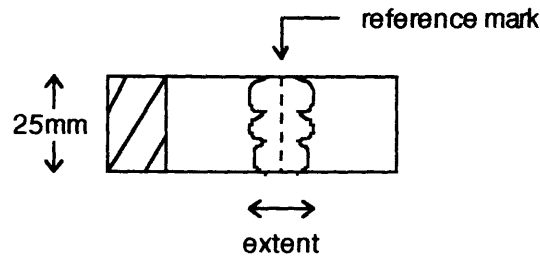
Volume of GAR-IgG beads required

$$= \frac{5.10 \times 10^8 \text{beads}}{2.27 \times 10^{10} \text{beads/ml}} = 0.0224 \text{ml} = 22.4 \mu\text{l}$$

TABLE B1 : BEADS COVERAGE VOLUMES

size	glass	# of beads	volume of GAR-IgG (μl)	
	$SA_{\text{class}} (\text{mm}^2)$		calculated	used
35x35x3	1225	1.56×10^9	68.7	12-15*
25x75x1	1875	2.39×10^9	105	12-15*
20x20x1	400	5.10×10^8	22.4	20
SEM	150	1.91×10^8	8.41	8

* beads applied at regions of interest (i.e. to detect interfaces)



$$\begin{aligned} 12\mu\text{l} &= 2.72 \times 10^8 \text{ beads} = 214\text{mm}^2 = 25\text{mm} \times 8.55\text{mm} & \therefore \text{extent} &= 8.55\text{mm} \\ 15\mu\text{l} &= 3.41 \times 10^8 \text{ beads} = 267\text{mm}^2 = 25\text{mm} \times 10.7\text{mm} & \therefore \text{extent} &= 10.7\text{mm} \end{aligned}$$

The reference mark indicates a region of interest, such as an interface or the path of the soldering iron 90°C water jet. 12-15 μl of beads is added to the region of interest over the 25mm width of the microslide. The extent of the coverage based on the surface area that the bead volume would fully cover is 8.55mm and 10.7mm for the 12 μl and 15 μl volumes, respectively.

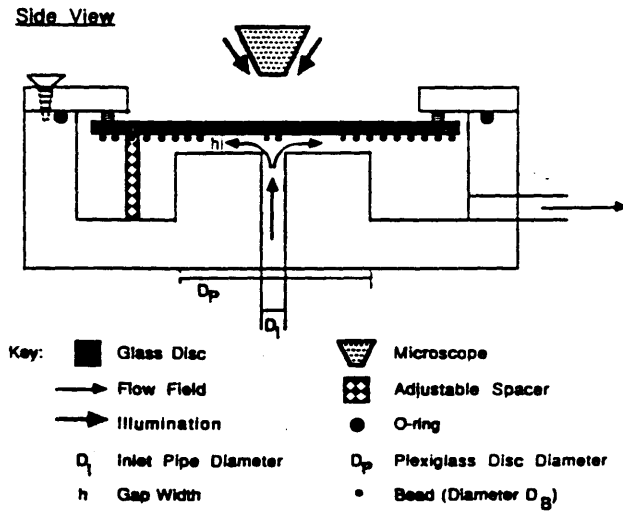
B.2 WASHING NOZZLE

I. MEASUREMENT TECHNIQUE - RADIAL FLOW DETACHMENT ASSAY (RFDA) Provides quantitative measurement of antibody-antigen adhesion force.

Model system was 10 μ m polystyrene beads coated with rabbit anti-goat IgG and glass coated with goat IgG.

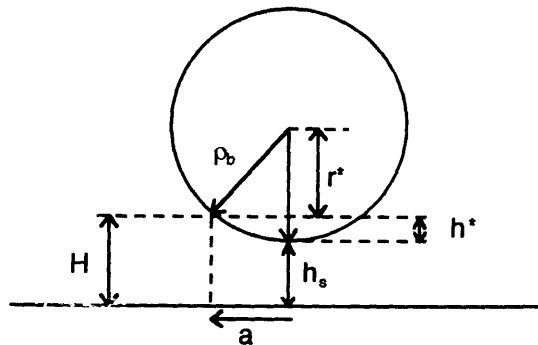
Cozens-Roberts C. et al (1990). Receptor-mediated adhesion phenomena: Model studies with the Radial Flow Detachment Assay. Biophysical Journal. 58: 107-125.

(Additional references provided for specific sections)



RFDA APPARATUS

A. CONTACT AREA - region in which surface to bead bonds will occur



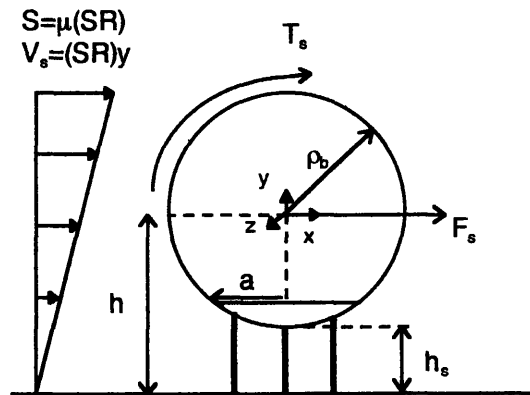
H = maximum separation
 h_s = separation distance between surfaces
 $h^* = H - h_s$
 ρ_b = radius of bead
 $r^* = \rho_b - h^*$
 a = radius of contact area = $\sqrt{(\rho_b)^2 - (r^*)^2}$

From Cozens-Roberts (1990) " The dimensions of IgG are $\sim 19 \times 57 \times 240 \text{ \AA}$;
 therefore, h_s and H are limited to values between ~ 100 and 400 \AA , with $H \geq h_s$."
 For $h_s = 0.010 \mu\text{m}$ and $H = 0.040 \mu\text{m}$, from geometry

$\rho_b = 5 \mu\text{m}$ $a = 0.5 \mu\text{m}$
 $\rho_b = 0.5 \mu\text{m}$ $a = 0.2 \mu\text{m}$

Contact area = πa^2 to $2\pi a^2$ depending on curvature

- A. **FORCE BALANCE** - resultant force must balance the force and torque imparted on the bead by the shearing flow.
 (Hammer D.A. and Lauffenburger D.A. (1987). A Dynamical Model for Receptor Mediated Cell Adhesion to Surfaces. Biophysical Journal. 52:475-487)



BEAD FORCE BALANCE

h_s = separation distance between surfaces
 ρ_b = radius of bead
 $h = h_s + \rho_b$

T_s = torque imparted by the passing fluid
 F_s = shear force imparted by the passing fluid
 (SR) = shear rate

$$S = \text{shear stress} = \mu(\text{SR}) \quad (1)$$

$$V_s = \text{shearing velocity} = (\text{SR})y \quad (2)$$

$$F_x = \text{bonding force in x direction} = F_s \quad (3)$$

$$F_y = \text{bonding force in y direction} = \left(\frac{3\pi}{4a}\right) \cdot (T_s + F_s \rho_b) \quad (4)$$

$$F_t = \text{resultant force} = \sqrt{F_x^2 + F_y^2} = \sqrt{F_s^2 + \left(\frac{3\pi}{4a}\right)^2 \cdot (T_s + F_s \rho_b)^2} \quad (5)$$

B. SHEAR FLOW FORCE AND TORQUE

From Fay J.A. (1994). Introduction to Fluid Mechanics. MIT Press, Cambridge. pp. 299.

Creeping (Stokes) Flow Over a Stationary Solid Sphere

$$\text{Drag Force } F = 6\pi\mu V_s \rho_b \quad (6)$$

Nondimensional solutions (F_s^* and T_s^*)

from Goldman A.J. et al (1967). Slow Viscous Motion of a Sphere Parallel to a Plane Wall - II Couette Flow. *Chemical Engineering Science* 22:653-660.

$$\text{Substituting (2) at } y=h \text{ into (5) gives, } F_s = 6\pi\mu(\text{SR})h\rho_b F_s^* \quad (7)$$

$$\text{Similarly, } T_s = 4\pi\mu(\text{SR})\rho_b^3 T_s^* \quad (8)$$

Substituting (1) into (7) & (8)

$$F_s = 6\pi S h \rho_b F_s^* \quad (9)$$

$$T_s = 4\pi S \rho_b^3 T_s^* \quad (10)$$

Evaluating nondimensional values

$$F_s^* \ \& \ T_s^* = \text{fn} \left(\frac{h}{\rho_b} \right) \quad \text{where } h = h_s + \rho_b$$

From Cozens-Roberts (1990) "The dimensions of an IgG molecule are ~19x57x240A. Hence, the maximum value for h_s is ~2 x 240A (0.048 μm)"

Taking h_s maximum = $0.048\mu\text{m}$, F_s^* & T_s^* are found from tables in Goldman (1967)

$$\rho_b = 5\mu\text{m} \quad \frac{h}{\rho_b} = 1.01 \quad F_s^* = 1.7 \quad T_s^* = 0.94$$

$$\rho_b = 0.5\mu\text{m} \quad \frac{h}{\rho_b} = 1.1 \quad F_s^* = 1.62 \quad T_s^* = 0.95$$

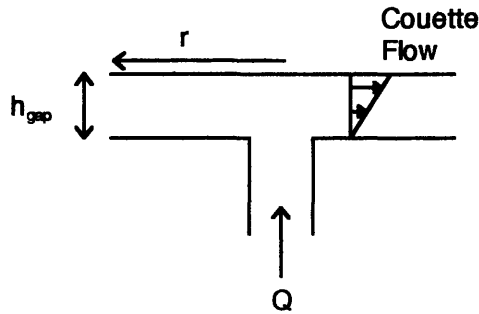
Substituting expressions for F_s (9) and T_s (10), making appropriate selections of a , F_s^* and T_s^* for the ρ_b used and approximating $h = \rho_b + h_s \approx \rho_b$, the expression for F_t (5) becomes,

$$F_t = \frac{110S\rho_b^3}{a} \quad (11)$$

valid for both $\rho_b = 5\mu\text{m}$ and $\rho_b = 0.5\mu\text{m}$

C. RFDA APPARATUS

Mass and momentum balance based on Couette flow given as $S = \frac{3Q\mu}{\pi r h_{\text{gap}}^2}$.



Critical shear stress was examined $S_c = \frac{3Q\mu}{\pi r_c h_{\text{gap}}^2}$ where r_c was measured at the interface between regions of bonded and non-bonded beads.

Flow rate, Q , was varied to obtain different S_c to test for detachment of beads from the glass for the variety of bead and glass surface concentrations investigated. For the referenced system with $\rho_b = 5\mu\text{m}$, the 40 dyne/cm^2 critical shear stress was for glass coated with a coating solution at $20\mu\text{g/ml}$ and beads with surface concentration of 2×10^{12} rabbit anti-goat IgG/cm². For the present

system with $\rho_b = 0.5\mu\text{m}$, the coating solution was $50\mu\text{g/ml}$ rabbit IgG and beads had surface concentration of 2×10^{12} goat-anti rabbit IgG/cm². The concentration parameters were considered equal.

How to determine S_c for an equivalent system except for ρ_b ?

The authors provided a relationship of S_c to ρ_b .

$$S_c = N_L \cdot N_R \cdot \left(\frac{K^\circ}{33e} \right) \cdot \left(\frac{k_B T}{\gamma} \right) \cdot \left(\frac{a}{\rho_b} \right)^3$$

where N_L = ligand concentration

N_R = receptor concentration

K° = receptor-ligand affinity constant

k_B = Boltzman constant

T = temperature

γ = range of interaction

All components taken to be equivalent to the referenced system except for ρ_b ; therefore, expression reduces to

$$S_c = C \cdot \left(\frac{a}{\rho_b} \right)^3 \quad \text{where } C \text{ is the constant of equivalent parameters}$$

Using $\rho_b = 5\mu\text{m}$ ($a = 0.5\mu\text{m}$ and $S_c = 40 \text{ dynes/cm}^2$), the expression can be rearranged to solve for C and this C used to solve for S_c when $\rho_b = 0.5\mu\text{m}$ ($a = 0.2\mu\text{m}$).

$$S_c = \left[\frac{40 \frac{\text{dynes}}{\text{cm}^2}}{\left(\frac{0.5}{5} \right)^3} \right] \cdot \left(\frac{0.2}{0.5} \right)^3 = 2560 \frac{\text{dynes}}{\text{cm}^2}$$

Using (11), F_t for the $\rho_b = 0.5\mu\text{m}$ system can be calculated.

$$F_t = \frac{110 \cdot \left(2560 \frac{\text{dynes}}{\text{cm}^2} \right) \cdot (0.5 \times 10^{-4} \text{ cm})^3}{0.2 \times 10^{-4} \text{ cm}} = 1.7 \times 10^{-3} \text{ dynes} = 1.7 \times 10^{-8} \text{ N}$$

II. WASH VELOCITY

A. Detachment Parameters

$$\text{Detachment force} = 1.7 \times 10^{-3} \text{ dynes} = 1.7 \times 10^{-8} \text{ N}$$

Using the worst case force at stagnation

$$\text{Stagnation pressure } P_o = \frac{1}{2} \rho v^2 \quad \text{and stagnation force } F_o = P_o \cdot PA_{\text{bead}}$$

Solving for the detachment velocity

$$P_o = \frac{F_o}{PA_{\text{bead}}} = \frac{1.7 \times 10^{-8} \text{ N}}{\pi (0.5 \times 10^{-6} \text{ m})^2} = 2.2 \times 10^4 \text{ Pa}$$

$$v = \sqrt{\frac{2P_o}{\rho}} = \sqrt{\frac{2(2.2 \times 10^4 \text{ Pa})}{1000 \frac{\text{kg}}{\text{m}^3}}} = 6.7 \frac{\text{m}}{\text{s}}$$

B. Wash Parameters

The wash velocity (0.60 m/s) used to remove unbound beads is safely less than the detachment velocity (6.7 m/s).

$$\text{wash flow rate, } Q = 0.37 \text{ ml/s} = 3.7 \times 10^{-7} \text{ m}^3/\text{s}$$

$$\text{syringe needle diameter, } d = 0.035'' = 8.89 \times 10^{-4} \text{ m}$$

$$\text{outlet area, } A = \frac{\pi}{4} d^2 = 6.21 \times 10^{-7} \text{ m}^2$$

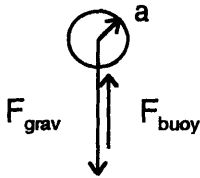
$$\text{wash velocity, } v = \frac{Q}{A} = 0.60 \frac{\text{m}}{\text{s}}$$

B.3 SETTLING TIME

Settling Velocity

From Fay J.A. (1994). Introduction to Fluid Mechanics. MIT Press, Cambridge. pp. 298-103.

Drag on a sphere ... calculation of the steady free fall velocity V_f of a spherical particle of density ρ_p moving downward through a fluid of density ρ_f under the influence of gravity



where a = radius of the particle

$$F_{grav} = \rho_p \left(\frac{4\pi a^3}{3} \right) g$$

$$F_{buoy} = \rho_f \left(\frac{4\pi a^3}{3} \right) g$$

Equate force balance to Stokes Drag

$$(\rho_p - \rho_f) \left(\frac{4\pi a^3}{3} \right) g = 6\pi\mu V_f a \quad \therefore V_f = \frac{2(\rho_p - \rho_f)ga^2}{9\mu}$$

$$\rho_p = 1.05 \text{ g/ml} = 1.05 \times 10^3 \text{ kg/m}^3$$

$$\rho_f = 9.982 \times 10^2 \text{ kg/m}^3$$

$$\mu_f = 1.00 \times 10^{-3} \text{ kg/m}\cdot\text{s}$$

$$a = 1 \mu\text{m} = 1 \times 10^{-6} \text{ m}$$

$$g = 9.81 \text{ m/s}^2$$

$$V_f = 1.12 \times 10^{-7} \text{ m/s}$$

$$\text{valid for } Re \ll 1 \quad Re = \frac{\rho_f V_f a}{\mu} = \frac{\rho_f g^{\frac{1}{2}} a^{\frac{3}{2}}}{\mu} = 0.003 \quad \therefore \text{valid}$$

Settling Time

Example : 1 ml of PBS to cover the 25mmx75mm microslide

The height of PBS on the surface of the slide was determined two ways: (1) observed, h_{PBS} observed and (2) calculated based on volume, h_{PBS} calculated.

h_{PBS} observed < 1 mm

h_{PBS} calculated $1 \text{ ml} = 1 \times 10^3 \text{ mm}^3 = (25 \text{ mm})(75 \text{ mm})(h_{\text{PBS}})$
 $\therefore h_{\text{PBS}}$ calculated = 0.53 mm

Time for beads to settle through 0.53 mm height of PBS

$$t = \frac{d}{V_t} = \frac{0.53 \times 10^{-3} \text{ m}}{1.12 \times 10^{-7} \frac{\text{m}}{\text{s}}} = 4732 \text{ s} = 1 \text{ hour } 19 \text{ minutes}$$

TABLE B2 : SETTLING TIMES

volume PBS (ml)	height PBS (mm) observed	height PBS (mm) calculated	settling time (hours:minutes)
0.5	< 0.5	0.26	0:40
1	< 1	0.53	1:19
2	> 1	1.1	2:44

APPENDIX C
(SECTION 3.4)

C. Thermal Deactivation

C.1 Water Jet Flow Rates

Example calculation for washing jet

flow rate, $Q = 0.37 \text{ ml/s} = 3.7 \times 10^{-7} \text{ m}^3/\text{s}$

nozzle diameter, $d = 20 \text{ gauge} = 0.035'' = 8.89 \times 10^{-4} \text{ m}$

outlet area, $A = \frac{\pi}{4} d^2 = 6.21 \times 10^{-7} \text{ m}^2$

velocity, $v = \frac{Q}{A} = 0.60 \frac{\text{m}}{\text{s}}$

TABLE C1 : WATER NOZZLE VELOCITIES

JET	TEMPERATURE (°C)	FLOW RATE (ml/s)	DIAMETER (gauge)	AREA (m ²)	VELOCITY (m/s)
wash	23	0.37	20	6.21×10^{-7}	0.60
continuous	90	1.1	16	2.14×10^{-6}	0.51
continuous	23	1.1	16	2.14×10^{-6}	0.51
SI	90	0.15	20	6.21×10^{-7}	0.24
SI	48	0.15	20	6.21×10^{-7}	0.24
SI	23	0.08	20	6.21×10^{-7}	0.13

APPENDIX D
(SECTION 3.5)

D. 3D PART CONSTRUCTION

D.1 GAR-IgG + GAR-IgG

D.1.1 R-IgG Coated Glass

From Appendix A (A.2.3 and A.2.4)

20mmx20mmx1mm piece

17 μ g/cm²

6.40x10¹³ R-IgG/cm²

2.56x10¹⁴ R-IgG/piece

D.1.2 GAR-IgG beads

From Appendix A (A.1.3)

lot 445454

0.552 μ g/cm²

2.08x10¹² GAR-IgG/cm²

6.52x10⁴ GAR-IgG/bead

From Appendix B (B.1)

To cover the surface area 20 μ l of beads are used.

Number of beads = (0.020ml)(2.27x10¹⁰ beads/ml) = 4.54x10⁸ beads

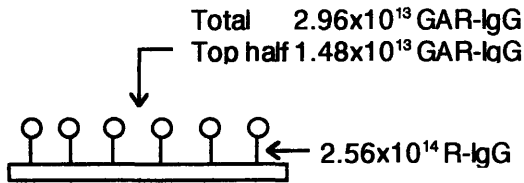
Total Protein = (4.54x10⁸ beads)(6.52x10⁴ GAR-IgG/bead) = 2.96x10¹³ GAR-IgG

D.1.3 R-IgG solution

Aliquot 500 μ l at 1mg/ml = 500 μ g

$$\text{protein} = \frac{500\mu\text{g}}{2.65 \times 10^{-13} \mu\text{g}} = \underline{1.88 \times 10^{15} \text{ R-IgG}}$$

R-IgG solution - select protein values to provide order of magnitude differences



Match the R-IgG solution to the immobilized R-IgG

$$\frac{1.88 \times 10^{15}}{500 \mu\text{l}} = \frac{2.56 \times 10^{14}}{x}$$

$\therefore x = 68 \mu\text{l}$; this is the 2×10^{14} value

The GAR-IgG bead protein value was 2.96×10^{13} . If contact area is neglected then a maximum of half the protein value could be exposed to the second layer, 1.48×10^{13} .

$$\frac{1.88 \times 10^{15}}{500 \mu\text{l}} = \frac{1.48 \times 10^{13}}{x}$$

$\therefore x = 4 \mu\text{l}$; this is the 2×10^{13} value

$500 \mu\text{l}$ from the stock is 1.88×10^{15} ; this is the 2×10^{15} value

Order	Volume
2×10^{15}	$500 \mu\text{l}$
2×10^{14}	$68 \mu\text{l}$
2×10^{13}	$4 \mu\text{l}$

D.2 GAR-IgG + SpA

From Appendix A (A.1.5)

lot 443033
 $0.140 \mu\text{g}/\text{cm}^2$
 2.01×10^{12} SpA/ cm^2
 6.30×10^4 SpA/bead

From Appendix B (B.1)

To cover the surface area 20 μ l of beads are used.

$$\text{Number of beads} = (0.020\text{ml})(2.27 \times 10^{10} \text{ beads/ml}) = 4.54 \times 10^8 \text{ beads}$$

$$\text{Total Protein} = (4.54 \times 10^8 \text{ beads})(6.30 \times 10^4 \text{ SpA/bead}) = \underline{2.86 \times 10^{13} \text{ SpA}}$$

The SpA value was similar enough to GAR-IgG value, 2.96×10^{13} GAR-IgG, that order of magnitude values tested were kept the same.

APPENDIX E
(SECTION 3.7)

E.1 BOND STRENGTH

FROM APPENDIX B.2

$$\rho_b = 0.5\mu\text{m}$$

$$a = 0.2\mu\text{m}$$

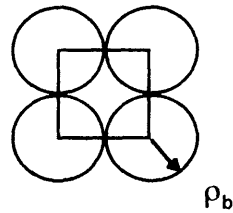
$$\text{Detachment force} = 1.7 \times 10^{-3} \text{ dynes} = 1.7 \times 10^{-8} \text{ N}$$

$$\text{yield strength} = \frac{1.7 \times 10^{-3} \text{ dynes}}{\pi \cdot (0.2 \times 10^{-4} \text{ cm})^2} = 1.4 \times 10^6 \frac{\text{dynes}}{\text{cm}^2} = 1.4 \times 10^5 \text{ Pa}$$

bulk strength

conversion factor

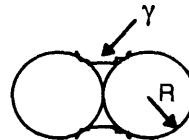
$$\frac{\pi a^2}{(2\rho_b)^2} = 0.13$$



$$\text{bulk strength} = (1.4 \times 10^5 \text{ Pa}) (0.13) = 1.8 \times 10^4 \text{ Pa}$$

E.2 CAPILLARY STRESS

$$\Delta P = \gamma \left(\frac{1}{R_1} + \frac{1}{R_2} \right) = \gamma \left(\frac{2}{R} \right)$$



ΔP = capillary stress

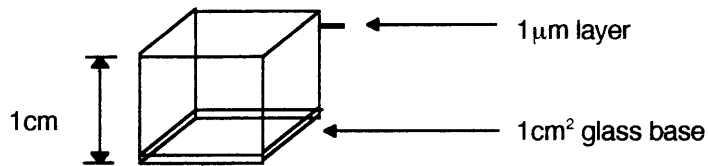
γ = surface tension, for water = 0.073 N/m

R_1, R_2 = principal radii of curvature, in the diagrammed situation, both

$R = 0.5\mu\text{m}$

$$\Delta P = \left(0.073 \frac{\text{N}}{\text{m}} \right) \left(\frac{2}{0.5 \times 10^{-6} \text{ m}} \right) = 2.9 \times 10^5 \text{ Pa}$$

E.3 COST ESTIMATES



1cm³ part with 1cm² base and 1cm height building in 1μm intervals

Building up the 1cm height in 1μm intervals requires 10000 layers.

E.3.1 Beads

To cover 1cm², 1.27x10⁸beads is required; therefore, 1.27x10⁸beads/layer
Assume beads to be at 1.25% solids or 2.27x10¹⁰beads/ml, thus will need 6μl
per layer or 60ml total.

Polysciences 17696 GAR-IgG blue dyed 1μm beads, \$96.95/ml

Cost for part = \$96.95/ml x 60ml = \$5817.00

GAR-IgG beads using Polysciences coupling kit, Polysciences blue dyed beads
and GAR-IgG from Sigma ImmunoChemicals - determine cost per ml

Polysciences 19540 coupling kit for blue dyed beads, for coupling
proteins to at least 50 0.5ml samples (2.5% solids in water) of beads,
\$96.30

Total of 25ml at 2.5% solid or 50ml at 1.25% solids

Polysciences 15712 blue dyed beads at 2.5% solids, 1.0μm, 15 ml,
\$59.45

To make 25ml required 2 x 15ml = 2 x \$ 59.45 = \$118.90

GAR-IgG from lot 445454 0.395mg/ml at 1.25%, will be making 50 ml at
1.25%; thus need 50ml x 0.395mg/ml = 19.75mg of GAR-IgG

GAR-IgG Sigma ImmunoChemicals

R 5506 Rabbit IgG (Whole molecule), Liquid, IgG fraction, host
animal = goat, 2ml @ 1.8mg/ml, \$48.10

(2ml @1.8mg/ml) x 6 = 21.6 mg which costs (\$48.10) x6 = \$288.60

R 1131 Rabbit IgG (Whole molecule), Liquid, Whole Serum, host animal = goat, 2ml @ 15.0mg/ml. \$29.70

2ml @15.0mg/ml = 30 mg which costs \$29.70

Determine cost per vial for the two options which produce 50 ml each

\$ 96.30	\$ 96.30
\$118.90	\$118.90
<u>\$288.60</u>	<u>\$ 29.70</u>
\$503.80	\$244.90
\$10.08/ml	\$4.90/ml

Cost for the part based on the requirement of 60 ml of beads at 1.25% solids

\$604.80	\$294.00
----------	----------

E.3.2 Linker (R-IgG)

Immobilized - Assume glass is at $17\mu\text{g}/\text{cm}^2 = 6.40 \times 10^{13} \text{R-IgG}/\text{piece}$
Solution - Add $6 \times 10^{12} \text{R-IgG} / \text{layer}$

Total - $6 \times 10^{16} \text{R-IgG}$

Sigma ImmunoChemicals I8140 Rabbit IgG Technical Grade
50mg costs \$39.60

50mg = $1.87 \times 10^{17} \text{R-IgG}$ which meets the requirement

R-IgG cost for part = \$39.60

E.3.3 Totals

Polysciences beads + R-IgG
= \$5817.00 + \$39.60 = \$5856.60

Kit beads with GAR-IgG from liquid IgG fraction + R-IgG
= \$604.80 + \$39.60 = \$644.40

Kit beads with GAR-IgG from liquid whole serum + R-IgG
= \$294.00 + \$39.60 = \$333.60

700 ii